

DECEMBER 1985
ENVIRONMENTAL SCIENCE & TECHNOLOGY

ES&T

**The epoch of
acid deposition**
Page 1144

Annual-
Index
1985

REQUEST FOR PROPOSALS ON RESEARCH ON REGIONAL AIR QUALITY PROBLEMS

The Electric Power Research Institute's Energy Analysis and Environment Division is soliciting proposals for conducting exploratory research pertinent to the following aspects of regional air quality:

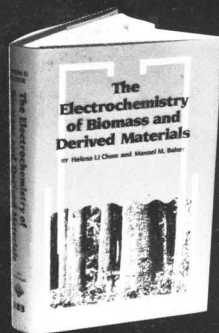
- Long-range transport of atmospheric gases and aerosols
- Preferred chemical pathways for the formation of sulfates, nitrates and oxidants in the atmosphere
- Meteorological influences on the transport and transformation of reactive pollutants
- The magnitude of the random component of air quality variability.

Responses to this solicitation are to be in the form of a clearly stated scientific problem, the research approach, the time schedule and a cost estimate. Proposals from educational institutions involving graduate student participation, and at a total level of effort in the range of one to one and one-half persons-years per year, for a period not exceeding three years, are especially encouraged. The data sets on atmospheric chemistry, meteorology, precipitation chemistry, visibility, emissions, etc., generated by EPRI's Air Quality Control Studies subprogram (SURE, RAQS, UAPSP) are available for these projects.

If you wish to respond to this solicitation, write, requesting RFP1630-25, to Ms. Paulette Fuqua, Electric Power Research Institute, 3412 Hillview Avenue, P.O. Box 10412, Palo Alto, CA 94303.



The Electrochemistry of Biomass and Derived Materials



NEW!

by Helena Li Chum and Manuel M. Baizer

Promotes the successful coupling of two major technologies — biomass conversion and electrochemistry — in making feedstocks for the chemical and fuel industries. Defines and describes various reactions occurring during the electrochemical breakdown of biomass into fuels, fuel components, and valuable chemicals. Covers the basics of electrochemistry, the available forms of renewable resources, and the electrochemical reactions involving carbon dioxide, lignins, hydrocarbons, polysaccharides, and more. Records all the relevant work being done in this ecologically and economically important field and suggests necessary areas of future research and development.

CONTENTS

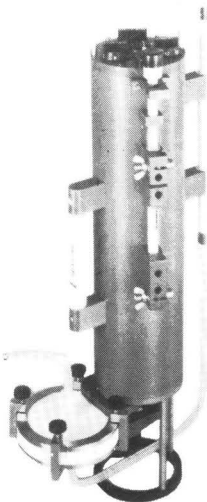
From Biomass, Broadly Defined, to Electrochemical Feedstocks • Introduction to Organic Electrochemistry of Biomass and Derived Materials • The Electrochemistry of Carbon Dioxide • Electrochemistry Involving Nonsaccharidic Alcohols • Electrochemistry of Other Functional Groups • Some Aspects of the Electrochemistry of Monosaccharides • The Electrochemistry of Biopolymers Derived from Biomass • Synthetic Photoelectrochemistry and Other Techniques • Perspectives and Suggestions for Further Work

ACS Monograph No. 183
328 pages (1985) Clothbound
LC 85-1377 ISBN 0-8412-0868-9
US & Canada **\$89.95** Export **\$107.95**

Order from:
American Chemical Society
Distribution Office Dept. 32
1155 Sixteenth St., N.W.
Washington, DC 20036
or CALL TOLL FREE 800-424-6747
and use your VISA, MasterCard,
or American Express credit card.

The SEASTAR IN SITU WATER SAMPLER

- ultra trace extraction of organics, PAH's, PCB's, hydrocarbons and trace metals.
- you select: flow rate, volume, sampling mode
- microprocessor controlled
- large volume extraction
- self powered
- optional filter assembly
- reuseable columns



 **SEASTAR
INSTRUMENTS LTD**

2045 MILLS RD., SIDNEY, B.C., CANADA V8L 3S1
TELEPHONE: (604) 656-0891 TELEX 049-7526

Editor: Russell F. Christman
Associate Editor: John H. Seinfeld
Associate Editor: Philip C. Singer

ADVISORY BOARD

Julian B. Andelman, Marcia C. Dodge, Steven Eisenreich, William H. Glaze, Michael R. Hoffmann, Lawrence H. Keith, Donald Mackay, Jarvis Moyers, Kathleen C. Taylor, Eugene B. Welch

WASHINGTON EDITORIAL STAFF

Managing Editor: Stanton S. Miller
Associate Editor: Julian Josephson

MANUSCRIPT REVIEWING

Manager: Janice L. Fleming
Associate Editor: Monica Creamer
Associate Editor: Yvonne D. Curry
Editorial Assistant: Diane Scott

MANUSCRIPT EDITING

Assistant Manager: Mary E. Scanlan
Assistant Editor: Ruth A. Linville

GRAPHICS AND PRODUCTION

Production Manager: Leroy L. Corcoran
Art Director: Alan Kahan
Designer: Julie Katz
Production Editor: Kate Kelly

BOOKS AND JOURNALS DIVISION

Director: D. H. Michael Bowen
Head, Journals Department: Charles R. Bertsch
Head, Production Department: Elmer M. Pusey
Head, Research and Development Department: Lorrin R. Garson

ADVERTISING MANAGEMENT

Centcom, Ltd.
For officers and advertisers, see page 1162.

Please send *research* manuscripts to Manuscript Reviewing, *feature* manuscripts to Managing Editor. For editorial policy and author's guide, see the January 1985 issue, page 22, or write Janice L. Fleming, Manuscript Reviewing Office, *ES&T*. A sample copyright transfer form, which may be copied, appears on the inside back cover of the January 1985 issue.

Environmental Science & Technology, ES&T (ISSN 0013-936X), is published monthly by the American Chemical Society at 1155 16th Street, N.W., Washington, D.C. 20036. Second-class postage paid at Washington, D.C., and at additional mailing offices. POSTMASTER: Send address changes to *Environmental Science & Technology*, Membership & Subscription Services, P.O. Box 3337, Columbus, Ohio 43210.

SUBSCRIPTION PRICES 1985: Members, \$26 per year; nonmembers (for personal use), \$35 per year; institutions, \$149 per year. Foreign postage, \$8 additional for Canada and Mexico, \$14 additional for Europe including air service, and \$23 additional for all other countries including air service. Single issues, \$13 for current year; \$13.75 for prior years. Back volumes, \$161 each. For foreign rates add \$1.50 for single issues and \$10.00 for back volumes. Rates above do not apply to nonmember subscribers in Japan, who must enter subscription orders with Maruzen Company Ltd., 3-10 Nihon bashi 2 chome, Chuo-ku, Tokyo 103, Japan. Tel: (03) 272-7211.

COPYRIGHT PERMISSION: An individual may make a single reprographic copy of an article in this publication for personal use. Reprographic copying beyond that permitted by Section 107 or 108 of the U.S. Copyright Law is allowed, provided that the appropriate per-copy fee is paid through the Copyright Clearance Center, Inc., 21 Congress St., Salem, Mass. 01970. For reprint permission, write Copyright Administrator, Books & Journals Division, ACS, 1155 16th St., N.W., Washington, D.C. 20036.

REGISTERED NAMES AND TRADEMARKS, etc., used in this publication, even without specific indication thereof, are not to be considered unprotected by law.

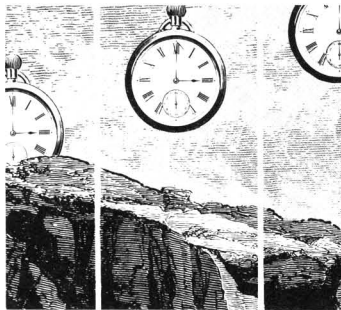
SUBSCRIPTION SERVICE: Orders for new subscriptions, single issues, back volumes, and microfiche and microform editions should be sent with payment to Office of the Treasurer, Financial Operations, ACS, 1155 16th St., N.W., Washington, D.C. 20036. Phone orders may be placed, using Visa, Master Card, or American Express, by calling toll free (800) 424-6747 from anywhere in the continental U.S. Changes of address, subscription renewals, claims for missing issues, and inquiries concerning records and accounts should be directed to Manager, Membership and Subscription Services, ACS, P.O. Box 3337, Columbus, Ohio 43210. Changes of address should allow six weeks and be accompanied by old and new addresses and a recent mailing label. Claims for missing issues will not be allowed if loss was due to insufficient notice of change of address, if claim is dated more than 90 days after the issue date for North American subscribers or more than one year for foreign subscribers, or if the reason given is "missing from files."

The American Chemical Society assumes no responsibility for statements and opinions advanced by contributors to the publication. Views expressed in editorials are those of the author and do not necessarily represent an official position of the society.

ES&T CONTENTS

Volume 19, Number 12, December 1985

FEATURES



1144 Time scales of catchment acidification. A model shows time scales of acidification of surface waters by deposition of sulfuric acid. Bernard J. Cosby, George M. Hornberger, and James N. Galloway, University of Virginia, Charlottesville, Va.; and Richard F. Wright, Norwegian Institute for Water Research, Blindern, Oslo, Norway.



1150 Hazardous wastes in academia. Colleges and universities must solve the problem of disposing of small quantities of many different toxic wastes. Peter C. Ashbrook, University of Illinois, Urbana, Ill.; and Peter A. Reinhardt, University of Wisconsin, Madison, Wis.

REGULATORY FOCUS

1156 EPA drinking-water proposals. Richard Dowd discusses EPA's long-awaited regulatory action on chemical and microbiological contaminants in drinking water.

VIEWS



1157 Jekyll Island meeting report. James Galloway lectures on the comparison of acid deposition in remote areas with that found in industrialized areas.

DEPARTMENTS

- 1139 Editorial
- 1141 Currents
- 1160 Consulting services
- 1161 Classified

1985 INDEX

- 1237 Author Index
- 1242 Keyword Index
- 1247 Front Section Subject Index

UPCOMING

Monitoring airborne toxic materials in New Jersey

Standardizing the management of hazardous waste monitoring data from laboratories

ESTHAG 19(12) 1137-1248 (1985)
ISSN 0013 936X

Cover: Thomas Butler, Cornell University
Credits: p. 1142, courtesy Steel Tank Institute; p. 1143, Todd Gray; p. 1150, courtesy Union Carbide, Harwell Schrader; p. 1152, Ernie Carpenter; p. 1153, Harwell Schrader; p. 1154, General Telephone & Electronics; p. 1159, Thomas Butler

RESEARCH

1165

Characteristics of abiological carbon monoxide formation from soil organic matter, humic acids, and phenolic compounds. Ralf Conrad* and Wolfgang Seiler

Abiological CO formation from soil and humic acids, a thermally sensitized process that follows the Arrhenius equation, is strongly influenced by pH and moisture.

1169

Diffusion and partitioning of hexachlorobiphenyl in sediments. Dominic M. Di Toro,* John S. Jeris, and Daniel Ciarica

A dual-tag experiment directly measures interstitial water diffusion and partitioning.

1176

Gas and aerosol wall losses in Teflon film smog chambers. Peter H. McMurry* and Daniel Grosjean

The effects of aerosol wall deposition on measurements of gas-to-particle conversion in smog chambers are discussed.

1182

Lead cycling in an acidic Adirondack lake. Jeffrey R. White* and Charles T. Driscoll

Results from a sediment trap and water column monitoring program suggest that formation of particulate aluminum contributes to the vertical deposition of lead in an acidic lake.

1188

Rapid consumption of bromine oxidants in river and estuarine waters. Donald A. Jaworske and George R. Helz*

The Patuxent estuary contains about 10^{-5} M substances that react rapidly with bromine at rate constants of 10^7 $M^{-1} s^{-1}$ or higher.

1192

Interference in the bactericidal properties of inorganic chloramines by organic nitrogen compounds. Roy L. Wolfe, N. Robert Ward, and Betty H. Olson*

Nitrogenous organic compounds reduce bactericidal activity of inorganic chloramines by interfering with the formation and subsequent residual measurement of the disinfectant.

1196

Soil sorption of organic vapors and effects of humidity on sorptive mechanism and capacity. Cary T. Chiou* and Thomas D. Shoup

The depression by ambient humidity on organic vapor sorption by a soil is attributed to competitive adsorption by water on soil mineral matter.

1201

Estimation for small normal data sets with detection limits. Alan Gleit

The problem of below-detection-limit data, coupled with small sample size, is studied through computer simulation.

1206

Decomposition of ozone in water in the presence of organic solutes acting as promoters and inhibitors of radical chain reactions. Johannes Staehelin and Jürg Hoigne*

A reaction model is developed and its ability to interpret the kinetic behavior of ozone in natural and wastewaters is tested.

1213

Surface charge and adsorption properties of chrysotile asbestos in natural waters. Roger C. Bales* and James J. Morgan

The relationships between dissolution, adsorption, and surface-charge development for chrysotile asbestos aging in water are studied experimentally.

1219

Studies on microbial and chemical conversions of chlorolignins. Karl-Erik Eriksson,* Marie-Claude Kolar, Pierre O. Ljungquist, and Knut P. Kringstad

Chlorolignins in spent liquors are found to be chemically unstable under some conditions that prevail in receiving-water systems.

1225

Evaluation of the perfluorocarbon tracer technique for determining infiltration rates in residences. Brian P. Leaderer,* Luc Schaap, and Russell N. Dietz

The effectiveness of this simple passive perfluorocarbon tracer technique is evaluated under varied ventilation rates and temperature conditions.

1232

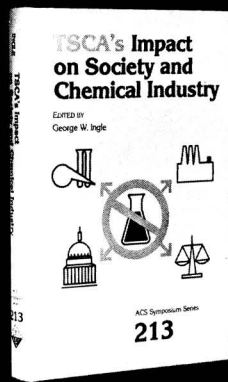
Determination of alkylthoxylated sulfates in wastewaters and surface waters. Thomas A. Neubecker

Alkylthoxylated sulfates are selectively measured in wastewaters and surface waters and shown to constitute only 10% of the nonselective MBAS response.

* To whom correspondence should be addressed.

This issue contains no papers for which there is supplementary material in microform.

TSCA's Impact on Society and Chemical Industry



George W. Ingle, Editor
Chemical Manufacturers
Association

Identifies and evaluates major effects of Toxic Substances Control Act (TSCA) on the chemical industry and on society as a whole. Covers detection and analysis of these effects from a variety of viewpoints. Helps to delineate beneficial and detrimental consequences of this law.

CONTENTS

Background, Goals, and Resultant Issues • Impact on Market Introduction of New Chemicals • Future for Innovation • Harmonizing the Regulation of New Chemicals in US and EEC • Control of Existing Chemicals • Overview After Five Years • Initiatives of Chemical Industry to Modify TSCA Regulations • Management of TSCA-Mandated Information • Impact on Corporate Structure and Procedures • Confidentiality of Chemical Identities • Impact on Reactive Polymer Industry • Effects of TSCA on Metalworking Fluids Industry: Increased Awareness of Nitrosamine Contamination • Impact on Public Health • Quantitative Analysis as Basis for Decisions Under TSCA • Educating the Environmental Chemical Professional • Overall Costs and Benefits • Summary

Based on a symposium jointly sponsored by the ACS Divisions of Industrial and Engineering Chemistry, Chemical Information, Organic Coatings and Plastics Chemistry, Small Chemical Businesses, and the Board Committee on Corporation Associates

ACS Symposium Series No. 213
244 pages (1983) Clothbound
LC 83-2733 ISBN 0-8412-0766-6
US & Canada \$34.95 Export \$41.95

Order from:
American Chemical Society
Distribution Office Dept. 21
1155 Sixteenth St., N.W.
Washington, DC 20036
or CALL TOLL FREE 800-424-6747
and use your VISA or MasterCard.

1/2 (Ethic) = ?

"Ethics in scientific publication." This phrase seems to be gaining attention; even the editors of ACS journals have written guidelines on ethics for authors, reviewers, and editors of scientific publications. But why all the concern when we already know that plagiarism and falsification of data are obvious ethical violations, and that exceptionally few scientists are guilty of these?

Perhaps the concern is for the more subtle ethical violations. These might be compared with not speaking up when one receives change for \$20 instead of \$10, or with driving 65 mph in 55 mph zone. Such mischievous acts occur frequently, as do their counterparts in scientific publishing. Some examples will help illustrate the point.

Type 1 mischief: The misleading statement. Author A writes, "Enclosed is the revised manuscript. We have taken into account all of the reviewers' comments in our revisions." Not so; the authors disagreed with several major reviewer criticisms and these comments were ignored—completely.

Reviewer A says, "I know the review is late. It is being typed and will be mailed in a few days." The truth is that the review has been partially done for two weeks, and it will be finished in a few days, he thinks.

Type 2 mischief: The incomplete statement. Author B writes, "Enclosed is a manuscript I would like you to consider for publication." The omission is that the major thrust of the research project has already been reported in a paper submitted or in press elsewhere. The experimental details and data are presented again so that this paper can stand on its own and look good. Author B wonders how many more publications he can get out of this research project.

Author C writes, "Enclosed is a manuscript I would like you to consider for publication," but fails to say that the paper was published in the proceedings of a major conference. He figures that because the proceedings were not peer reviewed it does not count as a publication. He signs the ACS copyright agreement stating exclusivity of submission, but copyright has previously been assigned to the publisher of the proceedings.

Reviewer B writes, "This work has been previously published." The reviewer does not say when or where the work was published, though.

Reviewer C writes, "The manuscript looks fine." He fails to say he did not feel qualified to review the paper, but he felt compelled to write something.

Type 3 mischief: The irrelevant statement. Reviewer D writes, "This work is valueless. The author obviously needs a refresher course in introductory chemistry." Such a highly charged statement can hardly be termed constructive criticism. We did not ask for a review of the author.

Author D writes, "From the statements he has made, the one reviewer is obviously ignorant. The other two reviewers liked the paper and we agree with their assessments." A blanket claim of reviewer ignorance is hardly a technical reply to the reviewer's comments.

Type 4 mischief: The place for statements. Author E writes in his cover letter, "We have answered all of the reviewers' questions." The difficulty is that the needed clarifications are stated only in the letter. They have not been incorporated into the manuscript.

Reviewer E telephones and says, "The author has made a significant oversight in his study, but I do not want to write it in my review because he is a good friend of mine." The review form is the appropriate vehicle for these expressions, not the telephone.

Type 5 mischief: The poorly timed statement. When called because the review is late, Reviewer F says, "I will not review the article you sent me until you process the paper I submitted to your journal." The review has been deliberately delayed.

Author F calls to say, "Our in-house reviews on the paper we submitted to you five weeks ago have come in, and we need to completely rewrite the results and discussion. Will you please return all of the copies to us?" The reviewers have been wasting their time on the submitted version of this manuscript.

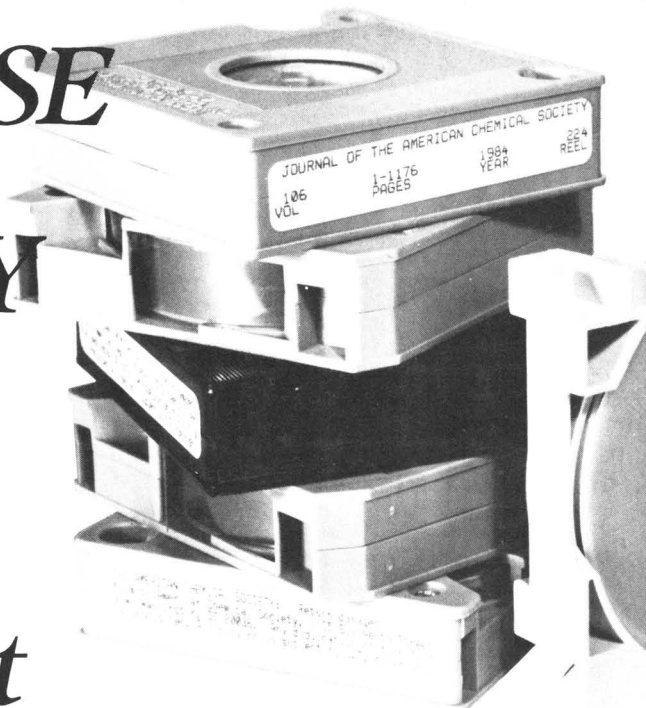
These vignettes depict fairly frequent occurrences in the peer review process. One might argue these infractions are a little disturbing, but seem only partly unethical. Partly unethical? What is one-half of an ethic? Can ethics be divided and compared?

Certainly not. Professional ethics, when practiced and upheld, determine the scientific integrity of our publications. Upon observing the mischievous practices that occur daily it seems appropriate to reacquaint the scientific community with its ethical responsibilities, even as the highway patrolman at the side of the road with his radar reminds us of speed limits. I hope the examples above have served in this regard.

Janice L. Fleming

INCREASE YOUR LIBRARY SHELF SPACE BY 90%

... without adding a single shelf!



When you manage a library these days, you're well aware that space is precious. And, additional shelves for backfiles volumes are expensive.

Well, the American Chemical Society knows your concerns. That's why all the Society's 21 primary publications in the field of chemistry are available in microfilm editions—including complete volumes back to 1879.

If you are setting up a microfilm system, expanding or changing one, or just want to discuss the possibilities—an ACS Sales Representative is ready to work with you. Just give us a call at

800-424-6747, or write to the Sales Office, American Chemical Society,
1155 Sixteenth Street, N.W., Washington, D.C. 20036.



Start Saving Space in Your Chemical Reference Files NOW!

AMERICAN CHEMICAL SOCIETY PUBLICATIONS

Chemical Publishers since 1879.

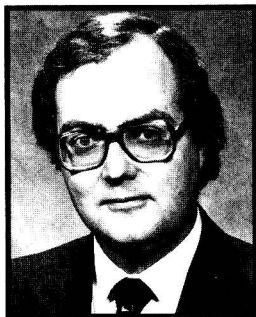
Accounts of Chemical Research
Chemical & Engineering News
Environmental Science & Technology
Inorganic Chemistry
Journal of Medicinal Chemistry
The Journal of Organic Chemistry
The Journal of Physical Chemistry

Analytical Chemistry
Biochemistry
CHEMTECH
Chemical Reviews
Langmuir
Macromolecules
Organometallics

I&EC Fundamentals
I&EC Process Design & Development
I&EC Product Research & Development
Journal of Agricultural & Food Chemistry
Journal of the American Chemical Society
Journal of Chemical Information & Computer Sciences
Journal of Chemical & Engineering Data

ES&T CURRENTS

INTERNATIONAL



Bradley: New funds for acid rain work

Canada's Province of Alberta will spend up to \$4.8 million to study acid deposition from 1985 to 1988, says provincial environment minister Fred Bradley. This expenditure is part of a \$9.5-million acid deposition research program funded jointly by the governments of Alberta, three other western provinces, and the Northwest Territories. Bradley says that although acid deposition levels in Alberta are low, his ministry remains concerned about the problem and supports Canada's aims to reduce SO₂ emissions in central and eastern Canada, where acid deposition is a serious problem. The government of Alberta is also conducting studies on the health effects of SO₂.

The Pacific island nations of Nauru and Kiribati have asked the London Dumping Convention (LDC) to adopt an amendment banning the disposal of all radioactive wastes at sea. They told the LDC's September meeting that nuclear wastes may have detrimental effects on fisheries and other marine resources on which the economies of the two countries depend. Most of the scientific advice on which the countries' proposal is based stems from a paper by Jackson Davis of the University of California at Santa Cruz. He suggested that the disposal of nuclear wastes at sea

could result in more than 13 human casualties/d for 10,000 y. Davis attended the LDC meeting as a member of the Nauru delegation.

FEDERAL

EPA estimates that more than 135 persons have been killed and almost 1500 have been injured in more than 6900 accidents involving toxic chemicals, according to a report released last month. The report covers a period of five years, beginning in 1980, and is incomplete, according to the agency. The study leading to the report was undertaken in response to the accident at Bhopal, India, in which more than 2000 persons died as a result of a leak of methyl isocyanate. In the U.S., most of the harm resulted from fires, explosions, and transportation accidents, rather than from direct contact with hazardous chemicals.

EPA intends to list 1,3-butadiene as a hazardous air pollutant. The agency also will refer to the Occupational Safety and Health Administration for possible regulatory action under the terms of the Toxic Substances Control Act, because 1,3-butadiene, a feedstock for plastics and synthetic rubber, presents an unreasonable health risk in the workplace. EPA will assess the risk from ambient exposure and propose possible controls. The agency concluded that the chemical presents an additional cancer risk over a 70-year lifetime exposure in ambient air of 19 cases/y. In the workplace the risk was put at 0.5-2 extra cases in monomer production, and 1-21 cases in polymerization plants.

EPA-approved revisions to SO₂ emission regulations are legal, according to a report issued by the General Accounting Office. The revisions allowed a 1.5-million-t increase in SO₂ emissions between 1981 and 1983. The Clean Air Act

allows emission increases if national air standards are not violated and if such plans are approved by EPA and the states involved. Still, the August report finds some problems with EPA's decision-making process. It cast some doubts on EPA's modeling methods for assessing long-range transport effects of SO₂ emissions. Also, the models do not satisfactorily project SO₂ transport in areas in which surrounding land is higher than the source's smokestacks, according to GAO.

EPA officials may not enter private premises under the terms of Section 104 of Superfund unless there is an emergency, according to a ruling handed down Sept. 24 by the U.S. Court of Appeals for the Seventh Circuit (Chicago, Ill.). In the case of *Outboard Marine Corporation v. Thomas*, the appeals court decided that there was no imminent or substantial danger to public health or welfare from an actual or threatened release of a hazardous substance, because the substances in question had been present for almost 10 years. The case arose from EPA's proposed cleanup of the harbor of Waukegan, Ill., during which agency workers would have had to occupy six acres of the company's parking lot to contain dredged and excavated materials.

EPA now requires pesticide registrants to notify the agency within 15 working days of learning that their products may endanger public health or the environment. Before the Sept. 17 ruling, registrants had 30 calendar days to make such a notification. In addition, registrants must inform EPA of any evidence of excess residues of pesticides in food and feed, groundwater, and untreated areas. The agency does not require any information previously submitted, nor does it ask for additional research by registrants. EPA acted under Section 6(a)(2) of the Federal

Insecticide, Fungicide and Rodenticide Act.

STATES

The state of New York is conducting a study on radon exposure. The New York State Energy Research and Development Authority and seven other organizations have retained Research Triangle Institute (RTI) to survey radon exposure in single-family homes in the state. Decay products of radon are thought to cause cancer. RTI is seeking 2000 volunteers who will place radon detectors in their homes for 2-12 months. Survey participants also will give data about the size and construction of their homes. In addition to data on radon, RTI will gather information on air infiltration rates and the effects of insulation and indoor contaminants, such as kerosene fumes and tobacco smoke.



Tanks must be registered

During late summer, Maine passed a law establishing a Board of Underground Storage Tank Installers, which administers and enforces a storage tank registration and certification process. To obtain certification for new tanks placed underground, installers must pass a written test on storage tank regulations. Registration and certification fees for the approximately 23,000 existing tanks in the state and increased oil product transfer fees at marine terminals are to provide funds for any necessary cleanups at tank sites.

A waste dump on Stock Island, Fla., may be the cause of high rates of multiple sclerosis (MS) in and near Key West. The MS rate in Key West is about 100 cases/100,000 population; 30 cases/100,000 is considered high risk, and 5 cases/100,000 is considered low risk. The 19-acre, six-story high waste dump has been accumulating wastes, including chemicals, since the 1920s.

The Florida Department of Environmental Regulation has found heavy metal contamination in sediments near the site, and some substances have been leaking into the surrounding ocean. The state Department of Health and Rehabilitative Services is looking into the possibility of a relationship between the wastes and MS, the cause of which is still unknown.

Eighteen drinking-water suppliers in Indiana were cited by EPA in September for failure to meet standards under the Safe Drinking Water Act. Nine did not sample for coliform bacteria, nine violated standards for coliform bacteria, and none of the suppliers notified their customers of the violations. Violators are subject to federal enforcement actions and civil fines.

Cleaning up the Chesapeake Bay and restoring its aquatic life will cost about \$100 million in 1986.

Under the Chesapeake Restoration Plan announced Sept. 20, federal, state, and local governments will improve sewage treatment plant capacity, assist farmers in reducing pollution from agricultural runoff, and enforce toxic pollutant control regulations more stringently. EPA, Maryland, Pennsylvania, Virginia, and the District of Columbia are devising plans to minimize pollution in urban runoff and to preserve wetlands that catch nutrients and topsoil before they enter the bay.

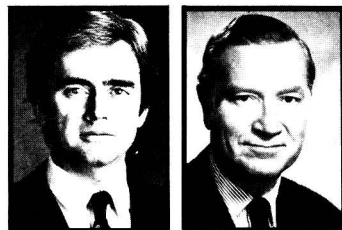
The Rhode Island House Legislative Commission has received a plan to dispose of all of the state's solid waste. Signal Environmental Systems (Hampton, N.H.) will design, build, and operate a 2250-t/d refuse-to-energy facility that would handle Rhode Island's refuse at a lower cost than the state would have to pay to do the job itself, according to Alfred DelBello, president of Signal. He expects that state and local governments will save more than \$80 million in transportation and disposal fees. In addition, the facility would have a waste recycling center.

AWARDS

The Congressional Science and Technology Award went to Jenefir Isbister of Atlantic Research Corporation (Alexandria, Va.). The award is given for "pioneering leadership and achievements in energy and environmental research and development." Isbister, a microbiologist, was recognized for genetically engineer-

ing a microbe that removes up to 47% of the organic sulfur from coal. Sulfur in coal is a major source of SO₂ emissions. The energy content and proportion of volatile materials are not degraded through the process. Bacterial removal of sulfur could become an attractive alternative for SO₂ control, says Rep. Mervyn Dymally (D-Calif.), who presented the award.

ORGANIZATIONS



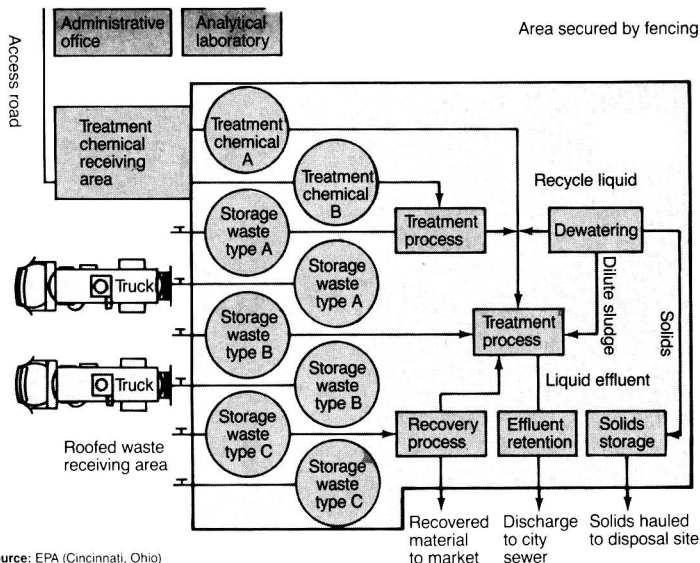
Reilly and Train: A resource pool

The World Wildlife Fund-U.S. and the Conservation Foundation (Washington, D.C.) affiliated formally on Oct. 1, with Russell Train, a former EPA administrator, as chairman and William Reilly as president. The two organizations did not merge. The World Wildlife Fund will continue projects designed to protect living species by promoting a balance between humans and their natural source base. The Conservation Foundation will continue its programs in environmental policy research. The two groups are pooling their intellectual and other resources, and will share office space. Reilly observed that the affiliated organizations are the only group addressing "a whole panoply of problems, including population."

SCIENCE

There is little compelling evidence that acid rain causes forest decline, says John Aber of the University of Wisconsin (Madison). He maintains that acid rain gets the blame because dying forests tend to lie in the path of acid rain. Aber notes that forests in decline are at higher elevations and thus are subject to damage from several pollutants at a time. Soils are thin, and have little capacity to withstand the various chemical assaults. Aber says that research shows that ozone, rather than sulfur, is "forest enemy number one." Second on the list is nitrogen-based air pollutants, and third is heavy metals. Aber blames automobile exhaust for most of the ozone and says that metals—

Central processing facility



Source: EPA (Cincinnati, Ohio)

especially lead—do far more damage than acid rain.

The movement of sediments contaminated with polychlorinated biphenyls (PCBs) in the Hudson River (N.Y.) will be studied under a grant from the Hudson River Foundation (New York, N.Y.). Of interest is the role that fine particles play in the movements of these materials. Thomas Zimmie of Rensselaer Polytechnic Institute (Troy, N.Y.) will study the conditions under which sediments erode and travel downstream. This information will help to determine whether dredging these sediments is necessary to prevent further movement of PCBs in the Hudson River.

TECHNOLOGY

A fast method for the preliminary investigation of volatile organic carbon (VOC) in groundwater is a field-operable gas chromatograph, says Tom Zdeb of Woodward-Clyde Consultants (San Francisco, Calif.). Its function is to provide a quick identification of areas of VOC contamination that will allow monitoring wells to be placed more effectively. The instrument works on the principle that VOC volatilizes from groundwater and moves toward regions of lower concentration in the overlying soil, so that a gas-phase gradient is established. The device Zdeb describes uses the gas-phase gradient to estimate the extent and movement of VOC. Older methods are time consuming and more expensive to use, according to Zdeb.

A centralized facility for treating cyanide and heavy metal wastes

was the subject of an engineering design study by EPA's Water Engineering Research Laboratory (Cincinnati, Ohio). The study concluded that such a facility could be technically and economically feasible if it treats the concentrated wastes of a number of plants. In that case, the cost of treatment and recovery could be substantially reduced, and the replacement of outdated treatment equipment could be economically justifiable. Other advantages include less expensive sources of energy, facilities that recover desired portions of wastes, and centralized laboratory and computing facilities.

Compliance with environmental regulations, including right-to-know laws, could be facilitated with a microcomputer program prepared by Hazox (Wilmington, Del.).

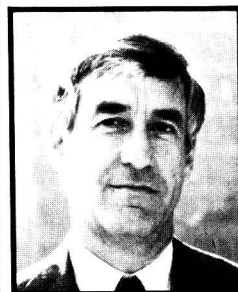
The program provides central computer files on chemical emergency responses, chemical safety data, documentation of chemical incidents, and inspection. Storage tank monitoring and chemical inventories can be included, and functions for inspecting the latest regulatory issues and legislation are also available. The program, known as Toxic Alert, is compatible with a number of standard external programs, including Lotus and dBase III.

BUSINESS

Environmental damage costs Western industrialized nations about 4% of their gross national product

(GNP), says Reinhold Mutke of Deutsche Babcock AG (West Germany). He adds that the same nations spend less than 2% of GNP on environmental protection. Mutke notes that between 1971 and 1980, West German industries spent about \$31.6 billion for environmental protection; West German public expenditures were about the same. Mutke is helping to organize an environmental congress and exposition, ENVITEC 86, to convene in Düsseldorf, West Germany, in mid-February.

"Manage hazardous materials before they become a threat to the environment," counsels the Institute of Scrap Iron and Steel (Washington, D.C.). Institute spokesmen recommend that in the future, metals should be made and used in a manner that makes recycling technically and economically attractive. At present, this is not the normal practice, and many metals are contaminated with materials that render them undesirable or totally useless as scrap. The products then become hazardous waste. Manufacturing metals with a view to future recyclability could help to alleviate some hazardous waste problems, according to the institute.

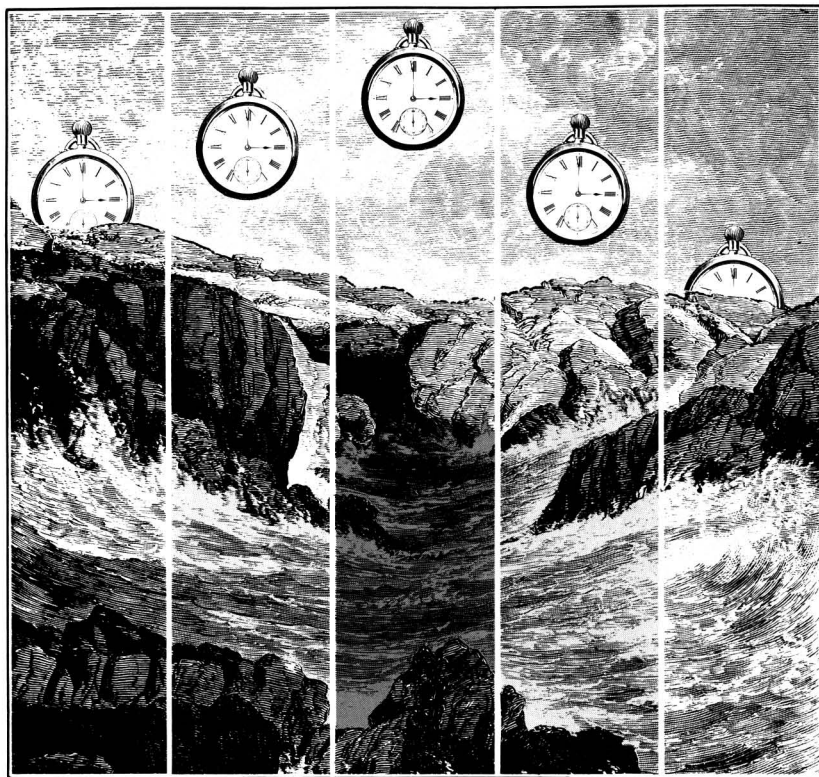


Leal: Legal protection needed

Superfund contractors need protection from undue exposure to legal liability, says George Leal, chief executive officer of Dames & Moore (Los Angeles, Calif.), an engineering firm. Liability risks are so high that many consultants and contractors are hesitant to participate in the Superfund program, and insurance against such risks is difficult to buy. Leal acknowledges, however, that although they did not create hazardous waste problems, engineers and contractors should be held liable for negligent acts. But he adds that the public interest "is best served by allowing creative technological solutions and not by apportioning liability to those who touch the problem during the remedial phase."

Time scales of catchment acidification

*A quantitative model
for estimating freshwater acidification*



Bernard J. Cosby
George M. Hornberger
James N. Galloway
University of Virginia
Charlottesville, Va. 22903

Richard F. Wright
Norwegian Institute for Water
Research
P.O. Box 333 Blindern
Oslo, 3, Norway

by atmospheric deposition of sulfuric acid (1-5). Although the sensitivity of specific regions to potential damage by acid deposition can be defined on a relative scale (6, 7), quantitative predictions have not been made of the time scales of water quality changes under different rates of deposition.

Recent research has focused on certain chemical processes in catchment soils. These processes are probable keys to the responses of surface water quality to acid deposition (1) and include anion retention (e.g., sulfate adsorption), weathering of minerals as a

source of base cations (Ca^{2+} , Mg^{2+} , Na^+ , K^+) and aluminum (Al^{3+}), adsorption and exchange of base cations and aluminum, and alkalinity generation by dissociation of carbonic acid with subsequent exchange of hydrogen ions for base cations. A critical unanswered question, however, is how quickly and to what extent these processes control surface water quality changes in response to changes in atmospheric deposition of sulfuric acid.

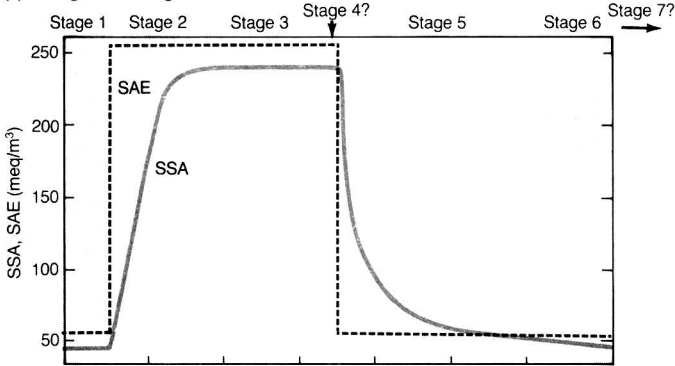
The water quality changes that we are interested in understanding, and ultimately in predicting, occur over sev-

There is empirical and theoretical evidence that surface waters are acidified

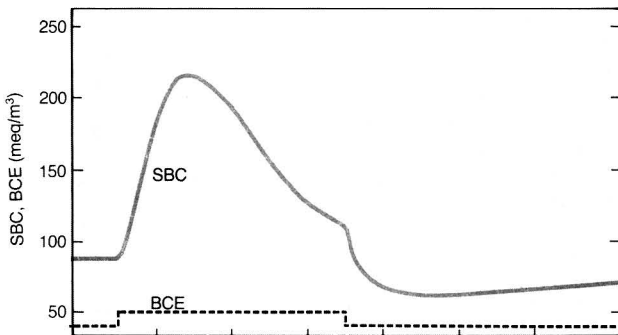
FIGURE 1

Predictions of the model

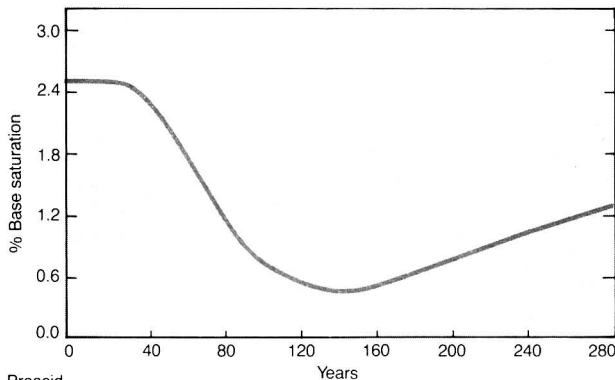
(a) Changes in strong acid anions^a



(b) Changes in base cations^a



(c) Changes in base saturation of the soil



^aCatchment is in steady state with atmospheric inputs only

SSA = Sum of strong acid anion concentrations
 SAE = Sum of atmospheric inputs only
 SBC = Sum of base cation concentration in streamwater
 BCE = Base cation concentration expected

... surface water chemistry is determined by reactions that occur in the soils and rocks within a catchment.

from different soil processes. Acidification is controlled by the sulfate adsorption characteristics of the soil and by the affinity of the soil for adsorbed base cations. Recovery is controlled by the base cation resupply rate from mineral-weathering processes.

The dynamics of sulfate adsorption are perhaps best appreciated by considering the difference between the sum of the strong acid anion concentrations in streamwater (SSA) and the sum of strong acid anion concentrations expected in the streamwater if the system were in steady state with atmospheric inputs (SAE). These dynamics are shown in Figure 1a. The asymmetry of the overall catchment response results from the asymmetry of the sulfate adsorption-desorption dynamics, that is, from the inherent nonlinearity of the sulfate adsorption process (10, 16).

Base cation dynamics are influenced by atmospheric inputs, primarily from weathering, and by the aggregate effects of the various soil equilibrium and exchange processes in the model. As shown in Figure 1b the total base cation concentration in streamwater (SBC) exceeds the concentration that would be expected (BCE) if the catchment were in steady state and if atmospheric inputs were the *only* source of base cations.

The difference between SBC and BCE during the initial steady state (stage 1, Figure 1b) is the result of the primary mineral-weathering inputs of base cations. As base cations are leached from the soil (stages 2 and 3), the base saturation of the soil declines (Figure 1c).

At the beginning of stage 5, as sulfate concentrations begin to decline, fewer base cations are exported by the stream, and the products of the mineral-weathering process begin to replenish the exchangeable base cations in the soil. The prolonged recovery of the catchment (relative to the acidification response to increased deposition) results from the slow replenishment of the soil cation exchange sites.

Taken collectively, the responses provide a consistent picture of catchment response to atmospheric deposition of sulfate. The mobile anion, sulfate, is adsorbed, balanced by base cations leached from the soil, or balanced by

the sequence (9). Estimated background atmospheric deposition at White Oak Run was used for the "off" portion (9, 14).

In this model, background deposition is initially in a steady state. After 20 y, the deposition is assumed to increase in 1 y to currently observed levels and re-

mains "on" at this level for 120 y. The deposition then decreases to background levels and remains "off" for the next 140 y.

Response times

The simulated catchment dynamics for acidification and recovery result

Output of the model: Acidification and recovery

The results of the modeling experiment are divided into the stages of acidification and recovery proposed by Galloway et al. (15) as a convenient means of comparing the time scales of changes in water quality.

Stage 1—Preacidification. This is the steady state prior to the increase in atmospheric deposition of sulfur, represented by the first 20 y of model output. Recovery of the hypothetical catchment after deposition ceases is assessed by the rate at which the water quality variables return to preacidification levels.

Stage 2—Undersaturated sulfate adsorption capacity. During this stage there is a lag in the increase of strong acid anion concentrations (SSA in Figure 2, principally SO_4^{2-}) as the soils adsorb the atmospherically derived sulfur. As anion concentrations slowly increase, base cation concentrations increase and alkalinity decreases (SBC in Figure 2). Given the sulfate adsorption characteristics of the model catchment, 40–50 y must elapse before stream sulfate concentrations stop increasing and the catchment can achieve a sulfur input–output steady state. In this hypothetical catchment the alkalinity is depleted ($\text{Alk} \leq 0$, Figure 2a) after approximately 20 y. The rate of supply of base cations from soil cation exchange reactions reaches a peak after approximately 30 y, as indicated by the plateau and downward turn in base cation concentrations. The response time for the initial acidification of the catchment is 20–40 y.

Stage 3—Saturated sulfate adsorption capacity. Concentrations of anions reach a new steady value as the soil sulfate adsorption sites are filled and the dissolved–adsorbed sulfate equilibrium is reestablished. The flux of high concentrations of anions through the soil continues to deplete the store of exchangeable base cations. Even though the catchment reaches a steady value of sulfate in 45 y (stage 2), base cation concentrations continue to decline for an additional 55 y. The response time of continued acidification of the catchment—when it is no longer accumulating sulfur from atmospheric deposition—is at least 50 y.

Stage 4. New steady state at the higher level of atmospheric deposition. Base cation concentrations should return to preacidification levels because at steady state these levels are controlled only by the primary mineral resupply rate. Stage 4 is not achieved in this example. However, the rates of change of base cation concentrations and alkalinity decrease markedly near the end of stage 3 and appear to approach asymptotic values by year 140 of the simulation. This hypothetical catchment's response to an approximately 10-fold increase in sulfur deposition required about 100 y to complete.

Stage 5—Supersaturated sulfate adsorption capacity. This stage begins when deposition decreases to the initial low level. The rate of decline of streamwater anion concentrations will depend on conditions in the soil because the sulfate adsorbed by the soil must be flushed from the system. As the anion concentrations decrease, the base cation concentrations will also decrease and alkalinity will begin to increase as fewer hydrogen and aluminum ions are needed to balance the strong acid anions. The acidification and recovery curves produced by MAGIC are notably asymmetric. The recoveries estimated by the model are initially rapid but become progressively slower. The model shows a return of strong acid anion concentrations to preacidification levels by year 280, and stage 5 lasts about 100 y. Desorption of the SO_4^{2-} accumulated in the soil takes approximately twice as long as the initial adsorption.

Stage 6—Recovery of soil base saturation. After the anions have returned to their preacidification levels, there is a further lag in the recovery of base cation concentrations and alkalinity. Until the soil base saturation has returned to preacidification levels, recovery of stream base cation concentrations and alkalinity will not be complete. The recovery process appears to take approximately twice as long as the initial acidification. Recovery time for this hypothetical catchment is 150–200 y.

Stage 7—Return to preacidification steady state. This stage in the conceptual model of Galloway et al. (15) is achieved only after an additional 80 y of simulation beyond that shown in Figure 2.

The simulated responses of the pH of streamwater and water that comes into contact with the soil matrix—soil water—(Figure 2b) are also asymmetric. However, the magnitudes of the changes in soil water pH are much smaller than the corresponding changes in surface water pH. Soil water and streamwater pH response times are about decades. As with the other water quality variables, the recovery of pH takes much longer than the initial depression.

Acidification time scales

MAGIC is a simple quantitative model based on the physical and chemical processes in catchment soils. It estimates the orders of magnitude of surface water quality response times to changes in atmospheric deposition. The modeling experiment showed the following results:

- Soils with moderate to high sulfate adsorption capacity and low base saturation (typical of sensitive catchments in the southeastern U.S.) produce acidification response times of a few decades to a century.
- Soils with low sulfate adsorption capacity and low base saturation (typical of sensitive catchments in the northeastern U.S.) produce acidification response times of a few years to a decade.
- Soils with high base saturation or high rates of base cation supply (through mineral weathering or artificial application, for example, in agricultural soils) produce at least century-long acidification response times—regardless of sulfate adsorption capacity.
- In response to decreased deposition, initial recovery rates are relatively rapid compared with initial acidification rates (i.e., the acidification and recovery responses are asymmetric).
- Total recovery times are longer (by a factor of two or more) than total acidification times.
- Catchments in apparent steady state with atmospheric sulfur inputs can continue to be acidified over a period of years to decades.
- Catchments apparently resistant to atmospheric sulfur inputs (sulfate adsorbers) may become acidified before the sulfate adsorption capacity is exhausted.

dissolved aluminum. Adsorbed sulfate cannot contribute to the acidification of fresh waters, and the amount of sulfate adsorbed is soil dependent. Furthermore, the capacity of soils to adsorb sulfate decreases as sulfate loading continues.

The unadsorbed sulfate can be balanced by base cations leached from soil exchange sites. Soils with a large amount of exchangeable base cations will respond to acid deposition by neutralizing essentially all of the atmospherically derived acidity. Soils with a small amount of exchangeable base cations will be able to neutralize little of the atmospherically derived acidity. Thus we would expect to find soils with low exchange capacity in catchments of

Research . . . is beset by problems: first is the paucity of data . . . second is the time scales of the responses that interest us.

streams that have already been acidified by atmospheric sulfur deposition. The response time of these streams should be from one to several years.

On the other hand, we would expect that soils with very high cation exchange capacity (such as most agricultural soils) would be found in catchments with streams that, for all intents

and purposes, are immune to the effects of acidification. The response time in such cases would be much longer ($>> 100$ y).

Long-term modeling

Research on the effects of acid rain on water quality is beset by two severe problems: first is the paucity of data and the time and money required to obtain additional data; second is the time scale of the responses that interest us.

The second problem poses the greater difficulty for modeling. Models—be they empirical or mechanistic, simple or complex—of the effects of acid deposition on catchments are all developed with the implied goal of predicting responses to changes in deposition rates at some point years or decades in the future. Strict verification of these models would require that we wait years or decades to determine whether predictions match observable responses.

Alternatively, the models could be verified by using them to reconstruct historical catchment behavior and comparing that reconstruction with the observed behavior of a catchment. This approach is thwarted by the fact that few, if any, records of catchment water quality extend far enough into the past to provide rigorous tests of the models.

In general, validation of models intended for long-term prediction is problematic (9, 16). Nonetheless, we believe our model provides a simple and effective tool for examining the implications of our assumptions about the processes that control the acidification and recovery of upland catchments.

Acknowledgment

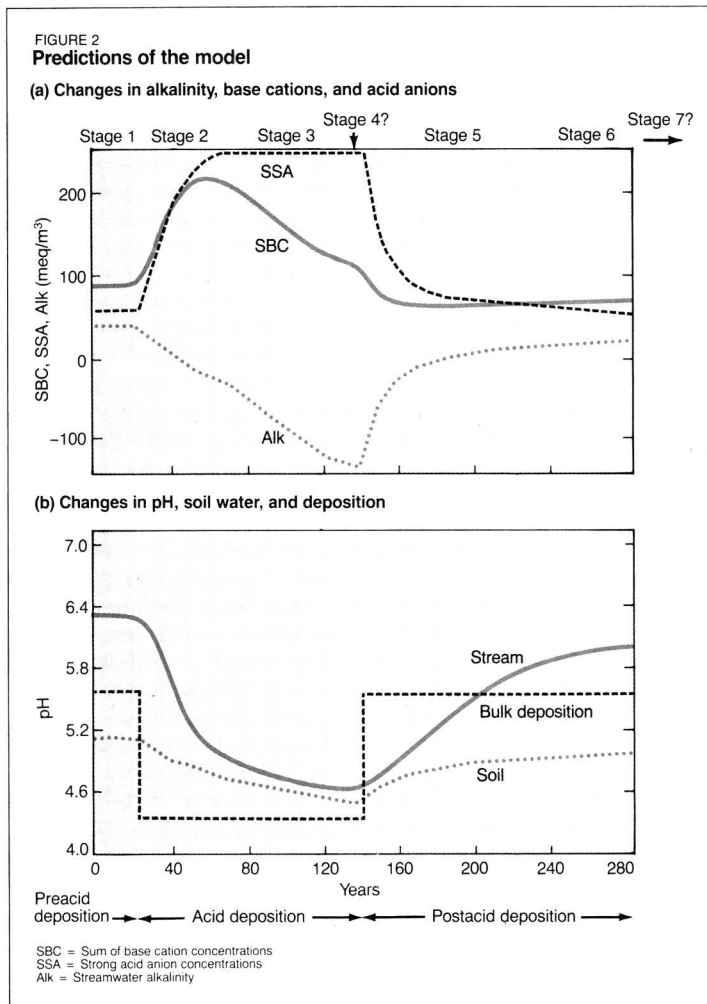
The research described in this article is a contribution to the Shenandoah Watershed Study. Financial support was provided by the National Park Service, EPA, the National Science Foundation (Grant No. CEE-8215914), and the Royal Norwegian Council for Scientific and Industrial Research. D. W. Johnson and J. O. Reuss provided helpful criticism and discussion. Part of this work was accomplished while two of the authors (Cosby and Hornberger) were visiting the Department of Environmental Science, University of Lancaster, Lancaster, U.K. We gratefully acknowledge the support of P. C. Young and his staff.

The research described in this article was funded in part by the EPA/NCSU Acid Precipitation Program, a cooperative agreement between EPA and North Carolina State University. It has not been subjected to EPA's required peer and policy review and therefore does not necessarily reflect the views of the agency; no official endorsement should be inferred. Portions of this research were funded by EPA as part of the National Acid Precipitation Assessment Program.

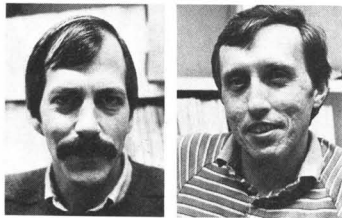
Before publication, this article was reviewed for suitability as an *ES&T* feature by Dale Johnson, Oak Ridge National Laboratory, Oak Ridge, Tenn. 37830; and David W. Schindler, Freshwater Institute, Winnipeg, Manitoba R3T 2N6, Canada.

References

- (1) "Acid Deposition: Processes of Lake Acidification"; National Academy Press: Washington, D.C., 1984.
- (2) "Acid Precipitation, Effects on Forest and Fish"; Overreim, L. N.; Seip, H. M.; Tollan, A., Eds.; SNSF Project Final Report; Sur Nederdørs PÅskog og Fisk: Oslo, Norway, 1980.
- (3) Beamish, R. J.; Harvey, H. H. *J. Fish. Res. Board Can.* **1972**, *29*, 1131-43.
- (4) "Ecological Impact of Acid Precipitation"; Drablos, D.; Tollan, A., Eds.; SNSF Project; Sur Nederdørs PÅskog og Fisk: Oslo, Norway, 1980.
- (5) "Proceedings of the First International Symposium on Acid Precipitation and Forest Systems"; Dochinger, L. S.; Seliga, T. S., Eds.; Technical Report NE-23; U.S. Department of Agriculture, Northeastern Forest Experiment Station: Upper Darby, Pa., 1976.
- (6) Galloway, J. N.; Cowling, E. B. *J. Air Pollut. Control Assoc.* **1978**, *28*, 229-35.
- (7) Burns, D. A.; Galloway, J. N.; Hendry, G. R. *Water Air Soil Pollut.* **1981**, *16*, 277-85.



- (8) Cosby, B. J. et al. *Water Resour. Res.* **1985**, *21*, 51-63.
 (9) Cosby, B. J. et al. *Water Resour. Res.*, in press.
 (10) Cosby, B. J. et al. *Eos* **1984**, *65*, 212.
 (11) Reuss, J. O. *Ecol. Model.* **1980**, *11*, 15-38.
 (12) Reuss, J. O. *J. Environ. Qual.* **1983**, *12*, 591-95.
 (13) Reuss, J. O.; Johnson, D. W. *J. Environ. Qual.* **1985**, *14*, 26-31.
 (14) Galloway, J. N. et al. *J. Geophys. Res.* **1982**, *87*, 8771-86.
 (15) Galloway, J. N.; Norton, S. A.; Church, M. R. *Environ. Sci. Technol.* **1983**, *17*, 541-45A.
 (16) Hornberger, G. M.; Cosby, B. J. In "Proceedings of the 7th IFAC/IFORS Symposium on Identification and System Parameter Estimation"; Pergamon Press: York, U.K., 1985; pp. 229-34.



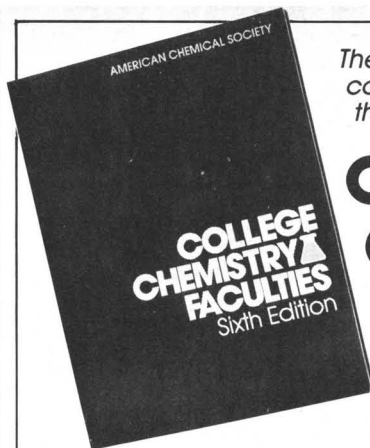
Bernard J. Cosby (l.) is a research assistant professor of environmental sciences at the University of Virginia in Charlottesville. He is a chemical limnologist with particular interests in quantitative analysis and modeling of large-scale environmental systems. He holds a Ph.D. from the University of Virginia.

George M. Hornberger (r.), professor of environmental sciences at the University of Virginia, is a hydrologist with research interests in quantifying the hydrochemical response of catchments and in treating uncertainty in mathematical models of environmental systems. He earned his Ph.D. at Stanford University.



James N. Galloway is an associate professor at the University of Virginia. His research interests include investigating the long-range transport of atmospheric materials, the acidification of fresh waters, and the processes that control the composition of precipitation. He has a Ph.D. from the University of California at San Diego.

Richard F. Wright, a limnologist, is a research scientist at the Norwegian Institute for Water Research, Oslo, Norway. His recent research is on acid deposition to terrestrial systems, including the effects of acidification on fresh waters and vegetation, using monitoring and manipulative experimentation on natural catchments. He received his Ph.D. from the University of Minnesota.



The most complete listing of college chemistry faculties in the U.S. and Canada

COLLEGE CHEMISTRY FACULTIES

SIXTH EDITION



multi-purpose reference, COLLEGE CHEMISTRY FACULTIES is an important tool for researchers, recruiters, industrial chemistry labs, students and teachers as well as college and high school counselors and libraries.

For convenient researching, the directory provides:

1. State-by-state listings of institutions showing degrees offered, staff members and their major fields, department address and phone number.
2. Index of faculty members' names.
3. Index of institutions.

Covering 2,400 two-year and four-year colleges and universities in the U.S. and Canada, COLLEGE CHEMISTRY FACULTIES lists the current affiliations and major teaching fields of over 18,000 faculty members.

State-by-state listings make it easy for students and faculty to find chemistry departments in any area they choose, and for marketers to use the state listings for planning sales and service territories.

Just published, the Sixth Edition of COLLEGE CHEMISTRY FACULTIES is available in time for the fall semester. Order now and keep your information up-to-date. Soft cover, 8 1/2" x 11". 204 pages. . . \$34.00

CALL TOLL FREE 1-800-424-6747

(for credit card orders),
write, or mail coupon below.

American Chemical Society Distribution Office 1155 Sixteenth Street, NW, Washington, DC 20036

Please send _____ copies of **COLLEGE CHEMISTRY FACULTIES** @ \$34.00. On prepaid orders, ACS pays shipping and handling charges.

- Payment enclosed (payable to American Chemical Society)
 Bill me Bill company

Charge my MasterCard VISA Barclay Card ACCESS

Card # _____ Interbank # _____
(MasterCard only)

Expiration Date _____ Signature _____

Name _____

Company/Organization _____

Address _____ Telephone Number _____

Billing Address _____

City _____ State _____ ZIP _____

56170/2504/E710

Hazardous wastes in academia

Colleges and universities are trying to develop ways to manage hazardous wastes

Peter C. Ashbrook
*University of Illinois
Urbana, Ill. 61801*

Peter A. Reinhardt
*University of Wisconsin—
Madison, Wis. 53715*

As do many industries, colleges and universities encounter thorny problems in dealing with hazardous wastes. Industry and academia alike are saddled with the rising cost of waste management and face perpetual liability for costs of waste cleanup. Unlike many industries, however, colleges and universities generate small amounts of waste, most, but by no means all of which is generated in laboratories; almost every operation contributes a certain amount. The wastes consist of nearly every hazardous chemical listed by EPA, including hydrochloric acid, methanol, polychlorinated biphenyls (PCBs), and newly synthesized compounds of unknown toxicity. Moreover, their composition changes with each new research project and experiment.

Liability and cost

An example of academic institutions' perpetual liability is found in a legal proceeding that listed four universities among the parties responsible for cleaning up a Superfund site in Seymour, Ind. In addition, at least one university has an old abandoned disposal site on the Superfund National Priority List (1).

One institution experiencing problems with the dramatically rising costs of hazardous waste management is the University of Illinois. In 1977, the university spent \$2000 to dispose of 100 drums of waste chemicals. By 1982, the cost of disposing of 265 drums had risen to \$46,000, an 87% annual increase in the cost of packaging, trans-

porting, and disposing of the wastes in a landfill. Additional costs are incurred because of the need for adequate space to store waste chemicals pending disposal and because waste chemical management workers must segregate wastes to facilitate disposal (2). At the Davis campus of the University of California, total costs of the hazardous waste management program increased by 113% in five years (2).

We believe that all academic institutions, regardless of size, should develop chemical waste management systems. The environmental benefits of proper management of small quantities of waste chemicals may not be significant in comparison with those derived from managing the larger quantities generated by industry, but there are substantial benefits to be realized in training students in proper management techniques when they begin to work with chemicals. This article explains how colleges and universities are coping with their chemical wastes and discusses what the future holds for hazardous waste management at academic institutions.

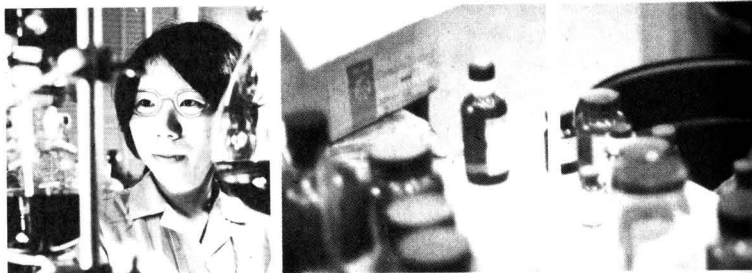
Heterogeneous wastes

Collectively, academic institutions generate less than 1% of the nation's hazardous wastes (Figure 1) (3). Yet the totals at individual institutions can be

surprisingly large. The University of Illinois at Urbana-Champaign disposed of 27,500 kg of waste chemicals in 1984. The University of Wisconsin—Madison generates 36,000 kg/y of chemical wastes. Indeed, hazardous wastes are a problem for any school with a laboratory, regardless of size (4, 5). In 1983, 78 high schools in Minnesota generated an average of 40 kg each of hazardous wastes (6).

The hazardous wastes generated in academic institutions can best be characterized as heterogeneous. A list prepared by the University of Minnesota in 1981 enumerates 1350 frequently used chemicals that can be designated as hazardous wastes (7). At the University of Illinois, 2104 chemicals and chemical mixtures, collected in 7300 containers, were disposed of last year.

Containers typically hold gram to kilogram quantities of wastes, the composition of which often is unpredictable (8). New Mexico State University approached this problem in the following way: On the Part B permit application for its storage facility, required by the Resource Conservation and Recovery Act (RCRA), the university described its wastes by naming every item on EPA's list of hazardous chemicals (9). Actually, certain general patterns in the nature of many academic institutions' wastes can be seen. For instance, un-





Elements of waste chemical management programs

Minimum requirements:

- Collect hazardous wastes, separate from normal trash
- Transport to an on-site storage facility
- Prepare waste chemicals for disposal
- Store safely pending disposal
- Obtain funds for transport, treatment, and disposal

Additional elements, which are highly desirable or may be required by law:

- Permit for storage for more than 90 days
- Education and training of all those producing and handling waste chemicals
- Analytical support
- Facilities and permits for on-site waste treatment
- Computerized record keeping
- Consultation support to laboratories regarding proper handling and disposal methods to provide laboratory workers with information on the proper handling and disposal of waste chemicals

like those from most industries, spent organic solvents account for the largest portion of hazardous wastes generated by academic laboratories (10).

Requirements for waste stream analysis have bedeviled university hazardous waste managers, partly because such analyses are potentially more expensive than the actual disposal of the waste. Expenses can be high if, as some have suggested, each container is analyzed to verify its contents. Some analysis of unlabeled waste is necessary, but it is unlikely that the detailed analysis—in some cases by gas chromatography-mass spectrometry—required by permit writers from EPA or state agencies is necessary to determine a proper method of disposal (11).

Treatment and disposal facility operators, who interpret regulations with great caution, often review lists of wastes to be disposed of without regard for the quantity involved. For example, the disposal of 50 mL of waste acetone would receive the same attention as 50 gal. Moreover, because of the variety of containers and classes of hazards involved, the treatment and disposal of laboratory wastes is a high-risk, low-profit business; willing disposal contractors are difficult to find.

In addition to the heterogeneous nature of the waste stream, there are other unusual aspects of managing waste

chemicals from academic facilities. Educational institutions are usually open to the public, so it is difficult to restrict access to areas in which hazardous materials are used and stored. Intersecting public roads and noncontiguous boundaries between university property and other land, which are typical of educational institutions' layouts, make interpretation of the regulations difficult and compliance with the law costly. For example, many academic institutions transport waste chemicals along city streets—often for only a few blocks—without EPA manifests and without the packaging required by the Department of Transportation (DOT).

Moreover, the need for a well-designed chemical waste management program is not always apparent to academic administrators, especially when the disposal of chemical wastes has not previously been perceived to be a problem. Many researchers believe that the chemicals with which they work are not hazardous or that the substances are easily rendered nonhazardous before they are discarded. These researchers also believe they have the expertise to dispose of their chemical wastes properly. According to this reasoning, there are few waste chemicals generated, and a good control program can be set up with relative ease.

A more typical situation, however, is

that if a chemical disposal service is available, clean-outs of laboratories and storerooms are prompted, and waste chemicals start accumulating in much larger quantities than expected (12). Reducing the improper discarding of chemicals in sewers and dumpsters also may add to the large amounts of wastes suddenly requiring disposal.

Some solutions

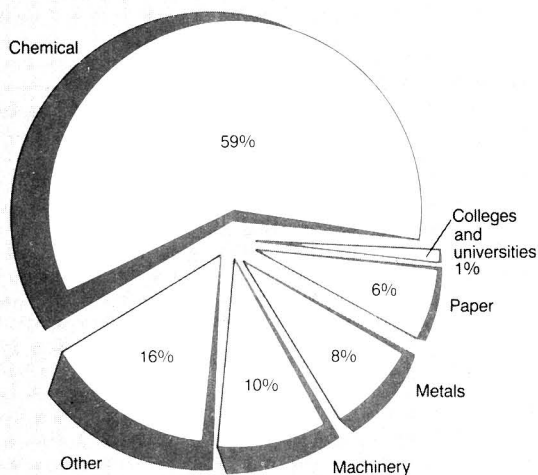
Hazardous waste management strategies for academia are no different from those used by industry. In practice, however, academic producers rely on landfills more heavily than industry does. Academic institutions frequently use the labpack, a 55-gal drum filled with liquid- and solid-waste containers surrounded by absorbent material. These labpacks are usually disposed of in a secure landfill. This method is the most convenient and, if the potential for future legal liability is not considered, the least costly.

Academic institutions are beginning to adopt alternative management practices because of the rapidly escalating cost of sending labpacks to landfills. Other factors responsible for the new approach include regulations that restrict the use of landfills, the fear of future liability, and the availability of other options that are more desirable from an environmental and safety standpoint. A review of the efforts of several institutions illustrates the benefits of several approaches.

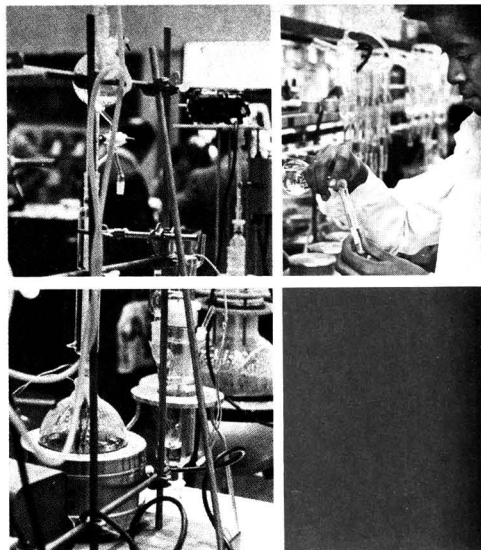
Waste reduction. Waste reduction is the most attractive answer to the problem of hazardous waste generation (13). This approach encompasses two basic options: the purchase and use of smaller quantities of chemicals and the substitution of less hazardous chemicals in laboratory work. The best results are achieved at the point of generation of wastes, because the user is the person most familiar with the required quantities and properties of chemicals used.

The amount of wastes generated in laboratory course work can be reduced. According to a recent survey by the American Chemical Society (ACS), 116 of 155 academic laboratories ran experiments using smaller amounts of chemicals to reduce hazardous waste generation (14). One example is micro-scale organic laboratory courses, such

FIGURE 1
Hazardous waste generators*



Source: Reference 3



must be publicized. The financial benefits, more than \$20,000 annually at the University of Wisconsin, come much more from avoiding chemical purchases than from saving on chemical disposal costs.

Reclamation. With the possible ex-

as those taught at Bowdoin College (15), in which extremely small amounts of chemicals are used. Such efforts not only reduce quantities of hazardous wastes, but they are safer and more economical.

The use of less hazardous materials is encouraged at the University of Wisconsin, where premixed chromic acid cleaning solutions are no longer readily available from the chemical supply stores; nonchromium alternatives are offered instead. Constraints on the acquisition of certain chemicals, however, can be expensive to administer and are seen as a burden to teachers and

researchers. Also, the use of less hazardous materials does not necessarily reduce the amount of waste, although it might simplify waste handling.

Source separation. Once waste chemicals are collected, their amounts can be reduced by segregating wastes according to their properties. Flammable liquids can be combined in 55-gal drums for incineration, rather than placed in labpacks, which are limited by DOT regulations to 15 gal/drum of waste. This approach not only reduces the amount of chemicals disposed of in landfills and the cost of such disposal, but substitutes a more desirable disposal method.

The segregation of chemicals also allows the removal of nonhazardous chemicals from those that must be disposed of as hazardous wastes. These simple, logical procedures often are not carried out because of shortages in the amount of staff available or because of inadequacies in storage and handling facilities.

Such materials as aqueous solutions of heavy metals can be evaporated to reduce their volume. Southern Illinois and Iowa State Universities have used this method with good results (12, 16).

Recycling. Interlaboratory recycling of unwanted bottles of stock chemicals has been successful at the University of Wisconsin and other schools (17). To make such a program work, criteria for suitable chemicals must be established, storage space must be made available, and the availability of the chemicals

National Research Council recommendations

Some changes have been suggested for EPA regulations that cover academic laboratories and other such generators of small quantities of chemical wastes. They appear in "Prudent Practices," published by the National Research Council (20).

- Encourage consistency and integration among federal, state, and local regulations and uniformity with EPA rules as states assume regulatory authority.
- Reduce the detail required for waste characterization, reporting, shipping, and disposal by describing wastes according to seven classes of waste.
- Create a special uniform manifest for labpacks.
- Simplify record keeping by using aggregate waste units—labpack units for wastes taken off-site and class units for wastes kept on-site.
- Continue to regard laboratory hazard reduction methods as an unregulated activity and the products of these methods as nonhazardous, unless proven otherwise.
- Provide for the design and operation of small-scale incinerators that are purchased pretested and approved for operation below 25 kg/h for ignitable, listed, and up to 5% acute wastes.

Wastes generated in colleges and universities

Major laboratory wastes:

- spent solvents
- spent acids and bases
- unwanted stock chemicals

Minor laboratory wastes:

- spent toxic metals
- degraded stock chemicals
- contaminated laboratory apparatus
- chemicals that react with air or water
- potentially explosive chemicals
- cyanides and sulfides
- pesticides
- polychlorinated biphenyls
- small gas cylinders



All forward thinking environmental scientists depend on ES&T. They get the most authoritative technical and scientific information on environmental issues—and so can you! *Have your own*

subscription delivered directly to you each month!

YES! Enter my own subscription to *ENVIRONMENTAL SCIENCE & TECHNOLOGY* at the rate I've checked below: 1985

One Year	U.S.	Mexico & Canada	Europe	All Other Countries
ACS Members*	<input type="checkbox"/> \$ 26	<input type="checkbox"/> \$ 34	<input type="checkbox"/> \$ 40	<input type="checkbox"/> \$ 49
Nonmembers—Personal*	<input type="checkbox"/> \$ 35	<input type="checkbox"/> \$ 43	<input type="checkbox"/> \$ 49	<input type="checkbox"/> \$ 58
Nonmembers—Institutional	<input type="checkbox"/> \$149	<input type="checkbox"/> \$157	<input type="checkbox"/> \$163	<input type="checkbox"/> \$172

Payment Enclosed (Payable to American Chemical Society)
 Bill Me Bill Company Charge my: VISA MasterCard

Card No. _____

Exp. Date _____ Interbank # _____ (Mastercard Only)

Signature _____

Name _____

Title _____ Employer _____

Address _____

City, State, Zip _____

Employer's Business: Manufacturing, type _____

Academic Government Other _____

*Subscriptions at these rates are for personal use only.

All foreign subscriptions are now fulfilled by air delivery. Foreign payment must be made in U.S. currency by international money order, UNESCO coupons, U.S. bank order through your subscription agency. For nonmember subscription rates in Japan, contact Maruzen Co., Ltd.

Please allow 45 days for your first copy to be mailed. Redeem until December 31, 1985.

— MAIL THIS POSTAGE-PAID CARD TODAY! 3144P



All forward thinking environmental scientists depend on ES&T. They get the most authoritative technical and scientific information on environmental issues—and so can you! *Have your own*

subscription delivered directly to you each month!

YES! Enter my own subscription to *ENVIRONMENTAL SCIENCE & TECHNOLOGY* at the rate I've checked below: 1985

One Year	U.S.	Mexico & Canada	Europe	All Other Countries
ACS Members*	<input type="checkbox"/> \$ 26	<input type="checkbox"/> \$ 34	<input type="checkbox"/> \$ 40	<input type="checkbox"/> \$ 49
Nonmembers—Personal*	<input type="checkbox"/> \$ 35	<input type="checkbox"/> \$ 43	<input type="checkbox"/> \$ 49	<input type="checkbox"/> \$ 58
Nonmembers—Institutional	<input type="checkbox"/> \$149	<input type="checkbox"/> \$157	<input type="checkbox"/> \$163	<input type="checkbox"/> \$172

Payment Enclosed (Payable to American Chemical Society)
 Bill Me Bill Company Charge my: VISA MasterCard

Card No. _____

Exp. Date _____ Interbank # _____ (Mastercard Only)

Signature _____

Name _____

Title _____ Employer _____

Address _____

City, State, Zip _____

Employer's Business: Manufacturing, type _____

Academic Government Other _____

*Subscriptions at these rates are for personal use only.

All foreign subscriptions are now fulfilled by air delivery. Foreign payment must be made in U.S. currency by international money order, UNESCO coupons, U.S. bank draft, or order through your subscription agency. For nonmember subscription rates in Japan, contact Maruzen Co., Ltd.

Please allow 45 days for your first copy to be mailed. Redeem until December 31, 1985.

— MAIL THIS POSTAGE-PAID CARD TODAY! 3144P



(800) 424-6747 (U.S. only)



NO POSTAGE
NECESSARY
IF MAILED
IN THE
UNITED STATES

BUSINESS REPLY CARD

FIRST CLASS PERMIT NO. 10094 WASHINGTON D.C.

POSTAGE WILL BE PAID BY ADDRESSEE

American Chemical Society

Periodicals Marketing Dept.
1155 Sixteenth Street, N.W.
Washington, D.C. 20036



(800) 424-6747 (U.S. only)



NO POSTAGE
NECESSARY
IF MAILED
IN THE
UNITED STATES

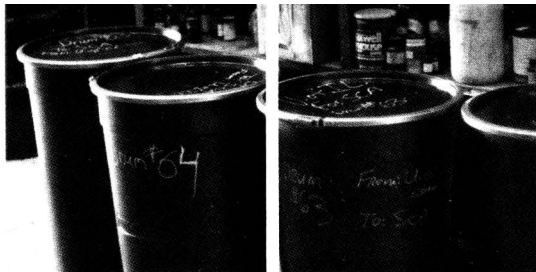
BUSINESS REPLY CARD

FIRST CLASS PERMIT NO. 10094 WASHINGTON D.C.

POSTAGE WILL BE PAID BY ADDRESSEE

American Chemical Society

Periodicals Marketing Dept.
1155 Sixteenth Street, N.W.
Washington, D.C. 20036



ceptions of mercury and some organic solvents, few wastes can be reclaimed economically. Nevertheless, the University of Minnesota and other schools have reclaimed silver from photographic wastes (7). Ohio State University has recycled paint thinner from which contaminants have precipitated and has redistilled ethanol (18). Turning chemical wastes over to commercial recyclers is normally infeasible; they are interested in volumes of waste that are far larger than academic institutions normally generate.

Chemical treatment. Chemical treatment has great potential because the necessary expertise and facilities already exist at most academic institutions. Neutralization is the easiest method, but numerous other options are available for the treatment of reactive materials, cyanides, and other toxic agents (19, 20). The University of Wisconsin's hazardous waste program, for example, will not accept waste acids and bases; they must be neutralized in the laboratory and disposed of through the sewer. Other chemicals also can be treated in the laboratories where the wastes are generated; researchers can carry out the necessary procedures.

Another approach is to bring wastes to a central facility for treatment by specialized personnel, thereby relieving researchers of the responsibility for treatment. This method takes advantage of economies of scale and avoids liability that could be incurred as a result of disposal by untrained persons. Each school decides on what approach to use according to its resources and priorities. But many schools, particularly smaller ones, cannot bear the expense of a treatment facility, properly trained personnel, or the hazardous waste permits that are required in many cases.

None of these management strategies should be considered a panacea applicable to all waste chemicals, although the landfilling of labpacks has been viewed as such. Instead, a sound management program combines these strategies, as appropriate, with the goal of minimizing the generation of wastes.

Current needs

Managers of waste chemicals at academic institutions will benefit most

from increased awareness of the nature of the hazardous waste problem; this will motivate them to develop policies, services, and technologies to deal with the wastes generated. The most thorough discussion of these problems is found in the National Research Council's book, "Prudent Practices" (20). Its authors recommend certain changes in EPA regulations and describe a number of useful developments that deserve encouragement.

In April 1984, ACS petitioned DOT for a simplification of the shipping requirements for labpacks (21). Although other organizations have lobbied for regulatory changes most academic institutions consider themselves to be small-quantity generators and have not given much attention to hazardous waste disposal rules. Managers of academic institutions should note that the new definition of small-quantity generators in the law reauthorizing RCRA brings many more schools into the hazardous waste regulatory system.

The following is a short list of topics that merit consideration and discussion by academic hazardous waste managers, hazardous waste disposal companies, and regulatory agencies:

Hazard assessment procedures for chemicals not specifically regulated by EPA. By focusing on industrial wastes, EPA regulates only a small fraction of the millions of chemicals in existence. Although some general guidelines have been prepared, determining whether a chemical or chemically contaminated material can be safely disposed of in an ordinary trash container or sanitary sewer may be extremely difficult (20).

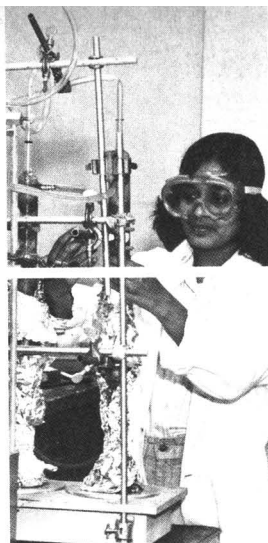
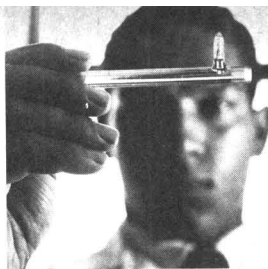
Small, or *de minimis* quantities or concentrations of hazardous wastes, considered exempt from regulation. The lack of agreement on what constitutes a *de minimis* amount leaves colleges and universities liable for record keeping, management, and disposal of all sizes of containers, even those of the frequently encountered gram and milliliter capacities. More schools will be concerned about regulatory requirements for small containers of waste chemicals, since the small-quantity generator limit has been lowered from 1000 kg/mo to 100 kg/mo by the law reauthorizing RCRA.

Standard tests for the identification of unknown contaminants. These tests would clarify a generator's responsibility and liability. They are needed because wastes with deteriorated, cryptic, or missing labels are common in academic institutions. Contractors charge anywhere from a few dollars to several hundred dollars per sample for analysis and disposal of wastes of unknown composition.

Acutely hazardous wastes. Because the accumulation of an acutely hazardous waste, such as a cyanide compound, is subject to much tighter regulations than those covered by the small-quantity provisions of RCRA, almost all academic institutions should be prepared to comply with the stringent generator rules. Alternative regulations are suggested for minimizing this regulatory burden; for instance, the shipment of 1 kg every 90 d (in the extreme case) is an inappropriate requirement for small schools.

One-time generation. The unclear regulatory status of infrequent generators of hazardous waste discourages schools that have adopted waste reduction procedures from cleaning existing chemical stockrooms. Because of the uncertain regulatory status, these infrequent generators often are required to spend an inordinate amount of time learning the regulatory requirements that apply to larger generators.

Simplification of record keeping. Current requirements for record keeping on waste generation, storage, transport, and disposal focus on each chemical entity separately and multiply disproportionately for the many different wastes that academic institutions produce (22). Academic institutions should be allowed to simplify this record keeping. For example, rather than specifying that a drum of commingled



solvents contains 1 L of one solvent and 10 L of another, it could be specified that the drum contains nonhalogenated flammable solvents.

Access to services. Because the volume of hazardous wastes from colleges and universities is small, companies in the hazardous waste business do not find it profitable to serve academic institutions. Therefore, when they are called upon to do so, these companies charge high prices. Also, the diversity of waste composition presents a major problem for contractors; some have refused to serve academic institutions because of this problem (23). Commercial facilities for the incineration of nonsolvent wastes, such as organic solids or contaminated laboratory apparatus, generally will not handle the relatively small quantities academic institutions have. Few companies offer appropriate services, such as chemical treatment and solvent recycling, for the quantities typically generated by academic institutions.

One way of reducing costs may be through cooperative efforts, following the examples of the University of Minnesota and some municipalities (6). We believe that cooperative ventures aimed at meeting the hazardous waste disposal needs of small-quantity generators are worthy of encouragement.

Small-scale incineration. As an alternative preferable to landfilling, some schools have considered the use of existing incinerators that normally burn pathological (usually infectious) wastes for destroying solvents and other waste chemicals. Most existing on-campus incinerators, however, are not designed to destroy chemical wastes as efficiently as EPA requires.

Moreover, a waste stream that constantly changes in chemical composition is difficult and expensive to test. Although a test burn may cost as little as \$10,000, EPA estimates the usual cost of a trial burn to be \$50,000-\$100,000 (24). Exacerbating this is the possibility of incurring large expenses in complying with current regulations and in improving equipment. The high costs, combined with the lack of availability of small-scale incinerators, have made on-campus incineration an impractical option for almost all institutions (25).

The alternative of using some waste

solvents as a fuel supplement in boilers may become restricted by the RCRA amendments of 1984. In any event, the fuel supplement approach is suitable for only some of the wastes.

Several developments could lead to the availability of an off-the-shelf, small-scale (<25 kg/h) incinerator that could be granted an EPA permit for the destruction of certain chemicals. These include EPA's acceptance of a trial burn of surrogate principal organic hazardous compounds rather than a burn of specific wastes (26), a generic permit application, and reduced siting procedures and instrumentation requirements for small treatment facilities. Given that the quantities of waste involved are relatively small, it might be reasonable for EPA to relax the 99.99% destruction efficiency standards for small-scale incinerators.

Standard methods for destruction of potentially explosive materials. Degraded picric acid and compounds that can form peroxides are serious laboratory hazards that are usually found in larger amounts than the gram quantities recommended for laboratory treatment procedures. Off-campus help has come from local bomb squads, but they often ignore DOT transportation rules and EPA regulations for thermal treatment facilities. Moreover, contractors that handle shock-sensitive materials are almost impossible to find, and those few that render this service charge up to \$500/lb to dispose of these wastes. Standard procedures for siting, containment during detonation, and monitoring for residuals are needed.

Uncertain future

We have identified some, but by no means all, of the difficult issues of managing hazardous wastes at academic institutions. There are other

newer problems, such as those with leaking underground storage tanks, that arise all too frequently.

It is unlikely that EPA or the waste disposal industry will soon address the hazardous waste problems of colleges and universities. The few large firms that dominate the hazardous waste management industry do not need the business of such a small economic sector. Because of the prohibitive cost of liability insurance, hazardous waste management is not a field suited to small businesses that might otherwise be interested in the academic market.

Many treatment technologies have been investigated, but the simplest, incineration, is bogged down by requirements for siting, testing, and permitting. As a result, some wastes will be stored until appropriate methods of disposal or destruction become available.

We believe that the answer for most academic generators is self-sufficiency in all aspects of hazardous materials management, from waste reduction and recycling to laboratory scale treatment. This approach may become the model for all hazardous waste generators.

Acknowledgment

Before publication this article was reviewed for suitability as an *ES&T* feature by Stanley Pine, California State University, Los Angeles, Calif. 90032; and Fay Thompson, University of Minnesota, Minneapolis, Minn. 55455.

References

- (1) *Fed. Regist.* 1984, 49, 40328.
- (2) Holdstock, R. S. In "Forum on Hazardous Waste Management at Academic Institutions, Western and Midwestern Regional Meetings"; American Chemical Society: Washington, D.C., 1983; pp. 6-10.
- (3) "Technical Environmental Impacts of Various Approaches for Regulating Small Volume Hazardous Waste Generators"; Office of Solid Waste and Emergency Response, EPA: Washington, D.C., 1979; Vol. 1.
- (4) Francis, W. M. In "Forum on Hazardous Waste Management at Academic Institutions, Western and Midwestern Regional Meetings"; American Chemical Society: Washington, D.C., 1983; pp. 1-5.
- (5) Garin, D. L.; Hickerson, J. L. In "Forum on Hazardous Waste Management at Academic Institutions, Western and Midwestern Regional Meetings"; American Chemical Society: Washington, D.C., 1983; pp. 23-28.
- (6) Thompson, E. M. In "Abstracts of Papers"; 186th National Meeting of the American Chemical Society, Washington, D.C., Aug. 1983; American Chemical Society: Washington, D.C., 1983; ACSC 7.
- (7) "Hazardous Chemical Waste Management: A Guidebook for Lab Personnel"; University of Minnesota: Minneapolis, Minn., 1981.
- (8) Kinslow, M. In "Forum on Hazardous Waste Management at Academic Institutions, Western and Midwestern Regional Meetings"; American Chemical Society: Washington, D.C., 1983; pp. 29-32.
- (9) Bean, S. In "Forum on Hazardous Waste Management at Academic Institutions, Rocky Mountain Regional Meeting"; American Chemical Society: Washington, D.C., 1984; pp. 1-12.

- (10) Heliotis, F. D.; Reinhardt, P. A. *J. Environ. Sci. Health* **1984**, A19(7), 757-74.
- (11) Shaw, R., Washington State University, personal communication, 1984.
- (12) Meister, J. F. In "Waste Management in Universities and Colleges"; Region V, EPA: Chicago, Ill., 1980; pp. 2-1 to 2-25.
- (13) "Less Is Better"; American Chemical Society: Washington, D.C., 1985.
- (14) American Chemical Society Department of Public Affairs, personal communication, 1984.
- (15) Rawls, R. *Chem. Eng. News* **1984**, 63(6), 20.
- (16) Mitchell, L., Iowa State University, personal communication, 1984.
- (17) Willhoit, D. G. In "Management of Hazardous Chemical Wastes in Research Institutions"; Research Safety Monograph Series; National Institutes of Health, Public Health Service: Bethesda, Md., 1981; Vol. 5, pp. 35-45.
- (18) Schultz, R., Ohio State University, personal communication, 1984.
- (19) Armour, M. A.; Browne, L. M.; Weir, G. L. "Hazardous Chemicals Information and Disposal Guide," 2nd ed.; University of Alberta: Edmonton, Alta., Canada, 1984.
- (20) National Research Council. "Prudent Practices for Disposal of Waste Chemicals from Laboratories"; National Academy Press: Washington, D.C., 1983.
- (21) Niederhauser, W. D., personal communication, 1984.
- (22) Berkowitz, J. B. In "Management of Hazardous Chemical Wastes in Research Institutions"; Research Safety Monograph Series; National Institutes of Health, Public Health Service: Bethesda, Md., 1981; Vol. 5, pp. 75-82.
- (23) Orendorff, R. R. In "Waste Management in Universities and Colleges"; Region V, EPA: Chicago, Ill., 1980; pp. 2-31 to 2-33.
- (24) "A Burning Answer to a Difficult Question," *EPA J.* **1982**, 8(4), 16.
- (25) Rogers, H. W. In "Waste Management in Universities and Colleges"; Region V, EPA: Chicago, Ill., 1980; pp. 4-26 to 4-28.
- (26) Waterland, L. R. Acurex Final Report. Acurex: Mountain View, Calif., 1983.



Peter C. Ashbrook (l.) is the head of the hazardous waste management program at the University of Illinois at Urbana-Champaign. He has a master's degree in environmental health from the University of Minnesota and a bachelor's degree in chemistry from Carleton College. Ashbrook has participated in and organized a number of symposia on hazardous waste management at various universities.

Peter A. Reinhardt (r.) supervises the hazardous waste program at the University of Wisconsin—Madison, which manages that university's chemical, radioactive, and infectious wastes. He also serves as an adviser on hazardous waste to the National Committee for Clinical Laboratory Standards. He is an instructor for the university extension program's course on infectious waste management.

FREE!

New Catalog!



From the
American
Chemical Society

- Introduces 18 brand new courses
- Covers a wide range of subjects
- Features courses taught by renowned authorities
- Offers the ACS money-back guarantee

Choose from a variety of effective learning methods

- Audio Courses
- Short Courses
- Computer Courses
- Audio-Teleconference Courses
- Video Courses
- In-House Courses

Write, use the coupon, or call TOLL FREE 800-424-6747 to receive your ACS catalog covering all continuing education services.

Yes! Please send me a free copy of the new ACS Professional Development Courses Catalog.

Name _____

Title _____

Organization _____

Address _____

City, State, Zip _____

Mail coupon to:

American Chemical Society
Distribution Office
1155 Sixteenth Street, N.W.
Washington, DC 20036

EPA drinking-water proposals: Round one



Richard M. Dowd

Last month in the *Federal Register* EPA proposed a long-awaited series of actions on drinking water. This package of proposed rules, recommendations, and goals is perhaps as important for its potential effects beyond the regulated drinking-water supply community (i.e., public water supply systems) as for its direct requirements.

The drinking-water program operates through a two-step standard-setting process. Initial recommended maximum contamination limits (RMCLs) serve as program goals. RMCLs are restrictions on levels of contamination in drinking water that are judged desirable but not proposed as enforceable standards. Next, maximum contamination limits (MCLs) are set. These are enforceable standards. MCLs are set as close as feasible to RMCLs, based on factors such as health effects, treatment technology, and cost.

In these actions, EPA has promulgated goals and proposed enforceable standards for eight volatile chemical compounds. The agency also proposed RMCLs for 37 other chemicals and four microbiological contaminants potentially found in drinking water. In addition, EPA announced "health advisories," which are neither binding standards nor goals, but rather informational reports to public water suppliers on the status of information about selected chemicals. These advisories cover 28 chemicals for which RMCLs were proposed and 11 for which no RMCLs have been suggested.

Protecting groundwater

The implications (beyond those for public water suppliers) relate to the

desire of various regulatory bodies around the country for a federally sanctioned, health-related basis on which to anchor their own judgments about contaminant levels in waters other than public drinking supplies. In particular, concern has been growing over the contamination of groundwater.

The linkage of groundwater concerns with these drinking-water actions was made explicit in EPA Administrator Lee M. Thomas's statement that EPA's intent in the action "is to control current contamination of groundwater and prevent future contamination."

Thus, although the RMCLs and MCLs directly apply only to public water systems that draw their supplies from surface water and groundwater, these values will tend to be interpreted as benchmarks for other decisions about the cleanliness of groundwater. This could pose a number of scientific and public policy problems.

EPA regulates chemicals in three groups, based on risk. The groups are known or probable human carcinogens, possible human carcinogens, and non-carcinogenic substances. The RMCLs for all probable human carcinogens are proposed to be zero. "Zero," as all who are in the measurement game know, is a very small number.

An immediate question arises: How does a goal of zero translate into a binding level? EPA has, in effect, called for this translation in setting a number of RMCLs at zero, for example, for chlordane, dibromodichloropropane, ethylene dibromide, polychlorinated biphenyls, and toxaphene.

The agency has further declared that the MCLs will be based on evaluation of three areas:

- the availability and performance of analytical methods,
- the availability and performance of technology, and
- the cost of applying technology to achieve contamination levels as close as feasible to RMCLs.

The analytical methods for MCLs that EPA has approved for the volatiles include gas chromatography and gas

chromatography-mass spectrometry techniques.

Regulation by analytical chemistry

In setting the standards, EPA is concerned with the limit of detection for regulatory purposes; the practical quantitation limit (PQL). For the proposed MCLs, the PQLs are set at a level such that volatile organic compounds can be measured with an accuracy of $\pm 40\%$.

These PQLs have been established at 5 ppb for trichloroethylenes, carbon tetrachloride, 1,2-dichloroethane, and benzene; 1 ppb for vinyl chloride; 7 ppb for 1,1 dichloroethylene; 200 ppb for 1,1,1-trichloroethane; and 750 ppb for *p*-dichlorobenzene. Thus, a regulation is being established that will require the clean-up of drinking water to levels of contamination that are as low as is practicable—i.e., to detectable levels—using standard analytical techniques. Regulation by analytical chemistry has arrived.

In addition, EPA has established monitoring requirements for 51 chemicals potentially found in public water system supplies. Implementation of this requirement should identify levels of contamination actually occurring in these supplies.

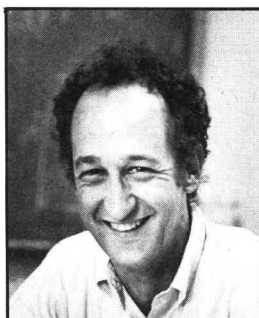
Public comment has been invited on these proposals; the record will remain open for 90 days on the proposed MCLs and for 120 days on the proposed RMCLs. The Health Effects Committee of EPA's Science Advisory Board will be convening a session on the proposed health advisories. There are, however, no current plans for the Science Advisory Board to review the RMCLs or the MCLs.

A substantial portion of the *Federal Register* notice addresses questions concerning the technologies of aeration and granular activated carbon. More on this later.

Richard M. Dowd, Ph.D.; is a Washington, D.C., consultant to Environmental Research & Technology, Inc.

Jekyll Island meeting report

James Galloway compares acid deposition in remote areas with that found in industrialized areas



James Galloway

In May 1985, the 15th Annual Symposium on the Analytical Chemistry of Pollutants convened in Jekyll Island, Ga. As part of the meeting, a series of lectures on acid deposition was presented. In the past two months, we have reported on the lectures given by Courtney Riordan of EPA and George Hidy of the Desert Research Institute. This month, we conclude this series of Views with a report of the lecture given by James Galloway of the University of Virginia.

Galloway was one of five scientists chosen in 1983 to advise the White House staff on the problems of acid rain. His involvement in this field goes back to his days of postgraduate research at Cornell in 1974. While there, his task was to develop new analytical techniques or use existing ones to measure inorganic and organic acid concentrations in precipitation in representative areas of the U.S.

In his opening remarks, Galloway said that a paper in *Science*, written by John O. Frohlinger and Robert Kane, came to his attention in 1975 (1). The paper's thesis was that acid deposition can be attributed to a phenomenon of weak acids, including carbonic acid. Galloway found as part of his own research that nitric acid and sulfuric acid were in fact the primary contributors, but that carbonic acid, ammonium ion, and to a certain extent organic acids also contribute to the total acidity of precipitation. The ecological impact of weak acids, according to his work, was insignificant.

More questions

Galloway pointed out that there are a number of questions attendant to the

study of acid precipitation. For instance, although we know that the trends for the past 30 years show that strong acids and, to a lesser extent, organic acids are the causes of free acidity, it might be useful to know what the composition of precipitation was a century ago. What, in fact, is the natural component of acid in precipitation?

The questions go on: What is the exact mixture of acids in precipitation? Is it the same all over the world? How can analytical chemistry be used to help find answers? We know that North American acid deposition is a largely anthropogenic phenomenon caused by the emission of sulfur dioxide and nitrogen oxides to the atmosphere. But does everything that is emitted over the continent fall here? How does North America contribute to the global atmosphere?

Since 1979, Galloway and his colleagues at the University of Virginia, in conjunction with Gene Likens of the New York Botanical Garden, have been collecting precipitation at remote sites—such as the southern part of Chile and at Cape Point in South Africa—with two questions in mind: What are the processes that control precipitation in remote areas, and how does the acid composition compare with that found in eastern North America? Gal-

loway said, "Using data from these sites and data from other parts of the world, we were able to determine the rate of [wet and dry] deposition of sulfur and nitrogen compounds to remote continental areas."

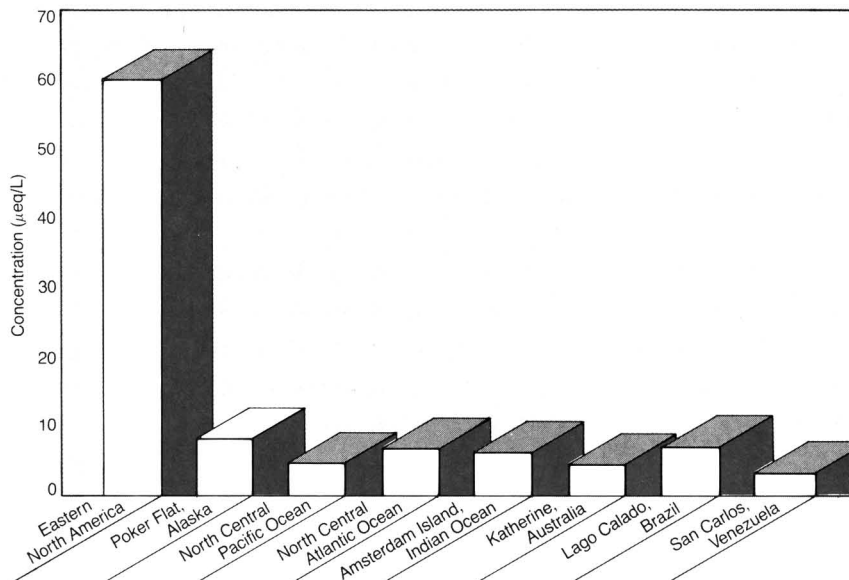
Wet deposition appears to control the removal of excess sulfur from the atmosphere. It appears that emission of dimethyl sulfide from the oceans is the primary source of marine excess sulfur. Galloway said, "In the case of the continents, sulfur precipitation is controlled by emissions of hydrogen sulfide and dimethyl sulfide; each of these gases will be converted to sulfuric acid in the atmosphere."

Developments in analytical chemistry have increased our understanding of how sulfur and nitrogen move through remote areas. Galloway said that he is confident that wet deposition figures are good to about a factor of two, but that dry deposition figures may be off by as much as an order of magnitude. There are two kinds of errors involved with dry deposition measurements. Galloway said, "We don't know how fast something comes out of the atmosphere—this is a microphysical problem—and we don't know the species and their concentrations. Further, for some species we don't have the sensitivity to measure naturally occurring concentrations."

How bad is acid rain in eastern North America? How does it compare with that in remote areas? According to Galloway, it is clear from the data that there is a substantial difference in the composition of precipitation between eastern North America and other parts of the world (Figure 1).

Another interesting aspect of these

FIGURE 1

Sulfate precipitation from eastern North America and seven remote sites^a

^aMean concentration of non-sea salt (excess) sulfate. North American data are from the MAP3S program; remote data except for those from Brazil are from Galloway's global precipitation project. Brazilian data are courtesy John Melak of the University of California at Santa Barbara

data is that throughout the world the concentration of excess sulfate in precipitation is remarkably similar. The mean concentration of sulfate is $5.5 \mu\text{eq/L}$, and the standard deviation is $1.5 \mu\text{eq/L}$. Galloway explained that he and two colleagues published research in 1984 showing that average annual concentrations of sulfate in precipitation are about 16 times greater in developed areas than in remote areas (2).

Surprising finding

During the course of their investigations and analyses of precipitation from remote areas, the researchers made an interesting—if accidental—discovery. Galloway said that when the project was being designed, he and Gene Likens published a paper "that said you don't need to add a biocide to precipitation to maintain its chemical composition [3]. Why? Because in eastern North America, the precipitation is stable in composition because of the high acidity. But we were not sure of the composition of the remote areas. Just to be on the safe side, we added chloroform to an aliquot of precipitation." The protocol for the site operator in the remote areas being studied was to take a rain sample using clean collectors, to divide the sample in two aliquots, and to put chloroform in one aliquot. These samples were then returned to the researchers for chemical analysis.

Galloway said, "When we looked at the data for the chloroform samples, the laboratory pH measurements in all cases were identical to pH measurements made at the field collection site, within 0.2 pH units. But for the samples without the chloroform addition, the field pH was lower than the lab pH. When we started looking at the data, we found that the ion balances of the samples without chloroform were always very good; the cations equaled the anions."

Although there was no change in pH for the chloroformed samples between the field and lab analyses, the ion balances were always off; there were always more cations than anions. Galloway said, "We began to wonder what could be happening. William Keene of our laboratory came up with the hypothesis that there is some activity in the sample"; something that was biologically useful was being consumed. The candidate was organic acids. "We discovered that formate and acetate were in the rain samples. We also found that there were enough of these organic acid anions in the chloroformed samples to account for any changes in pH."

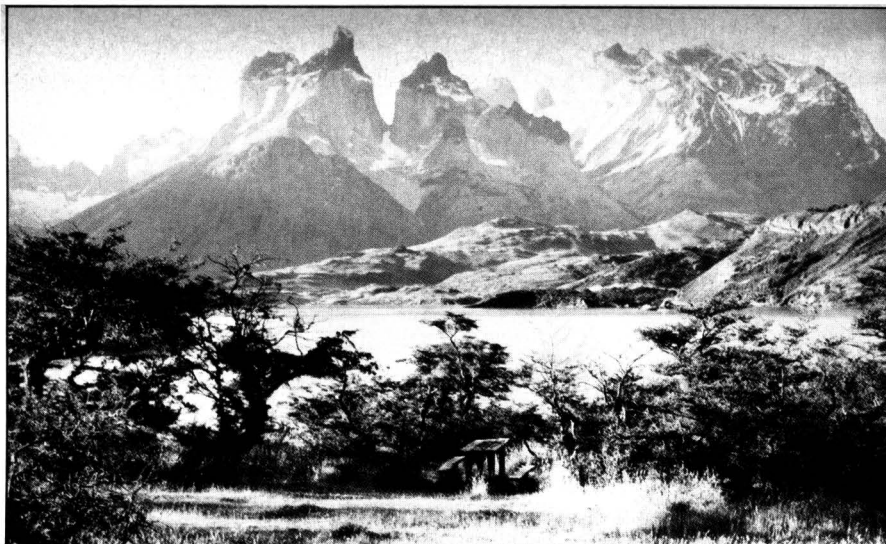
The researchers began a series of lab experiments to see whether biological activity could account for losses of formate and acetate in rain samples. This was the definitive experiment for the chloroform samples.

This observation, in addition to other experiments on the stability of formate and acetate with and without chloroform, proved that microbial activity was causing the decrease in formate and acetate and the increase in pH.

Role of organic acids

Galloway then turned his discussion more to the issue of organic acids. He said, "I view myself as a detective using chemical clues. And this organic acid contribution to the acid deposition story is in fact a detective story. We made some initial analytical chemical measurements on environmental samples. We noted the discrepancy between pH in the field and laboratory samples. Either we were doing something wrong or there was something about the natural system that we did not understand. Using analytical chemistry, we discerned the importance of organic acids and resolved the problem."

Galloway explained that the researchers' aim was to understand the connection between the composition of precipitation and its effects on various receiving systems. He said, "We need to understand the linkage between the chemical and the biological." For the past two years, Galloway and his co-workers have been studying microorganisms in the atmosphere and in precipitation to see whether they could pinpoint the role of bacteria and fungi



The acid deposition at this site in southern Chile comes mainly from organic acids

in oxidizing organic acids. Another intriguing possibility is that perhaps the microorganisms are in themselves producing organic acids. Galloway said, "I have this vision of clouds being little biochemical factories that both produce and consume organic acids. Therefore, let's not forget the biology when we deal with the chemistry."

Galloway once again referred to Frohlinger and Kane's paper showing that organic acids were not a factor in the increasing acidity of precipitation in North America (1). Recent analyses of North American precipitation confirm that research. Although the concentrations of organic acids in North America and remote areas are about the same, in remote areas, organic acids can control pH, but in the northeastern U.S. H_2SO_4 and HNO_3 control the pH of precipitation because of their much higher concentrations.

Where it comes down

Galloway then turned the focus of the discussion to the dispersion of acid in the atmosphere. He said that the stack of the copper and nickel smelter in Sudbury, Ont., Canada, is, at 1400 ft, the tallest stack in the world, and it emits a few percent of the world's sulfur to the atmosphere. Galloway said, "This brings up the topic of long-range transport. From an atmospheric sulfur budget that Doug Whelpdale, an atmospheric physicist at the Canadian Atmospheric Environmental Service, and I analyzed, we found two things." First, the total of North American sulfur emissions (U.S. and Canadian) is about 16 teragrams. This quantity is several orders of magnitude higher than the natural contribution of sulfur to the atmosphere of eastern North America. Second, of the anthropogenic sulfur

emitted to the atmosphere, only 50% falls in eastern North America. Galloway stated that this figure was arrived at as a result of the Western Atlantic Ocean Experiment in 1981, which studied the flux of sulfur out of eastern North America by atmospheric transport (4). The study sought to answer several questions: Where does the sulfur go? How much falls over the ocean? How much goes to Europe? How much exchanges with the Southern Hemisphere?

Several sampling platforms were used in the study to determine the transport of sulfur eastward from North America. They included cruise ships of the Home Lines, which travel weekly between New York, Bermuda, and Nassau. For the past four years, researchers have been studying rain collected on board the ships. They have measured its chemical composition and gathered data on deposition over the western Atlantic Ocean. Other platforms are National Oceanic and Atmospheric Administration (NOAA) research aircraft. Last spring NOAA's *King Air* was used to collect gases and aerosols between North America and Bermuda. In January they will use the *King Air* and the NOAA P3 to investigate transport of gases and aerosols eastward from North America.

Galloway said that about 4.3 teragrams of sulfur is ejected from North America to the atmosphere over the Atlantic Ocean. He said, "From our measurements in Bermuda and on board the ships and aircraft, we estimate that the wet deposition of sulfur to the western Atlantic Ocean is about 1.2 teragrams. Dry deposition is 0.1 teragrams."

Natural emission of sulfur to the atmosphere in the western Atlantic Ocean is about 0.1 teragrams. That

leaves about 3.1 teragrams unaccounted for. This amount is being ejected to the east of Bermuda. A site on the western coast of Ireland has been established to investigate the trans-Atlantic transport of North American sulfur.

Finally, Galloway touched on the matter of nitrogen. "We don't know how much nitrogen is lost from North America by atmospheric transport because we cannot measure it," he said. "Until we get analytical instrumentation that measures nitrogen dioxide, PAN-peroxyacetyl nitrate, and ammonia at the part-per-trillion level, we will not be able to determine the effect of North American emissions on the global atmosphere."

Prognosis


Until scientists can provide convincing data, and explain them, policy makers will be reluctant to make regulations concerning acid deposition. This may be reasonable because although we know how much controls will cost, we are not really sure how effective they will be in reducing sulfur and nitrogen.

Meanwhile, 20 countries, not including the U.S., have subscribed to a "cleaner air convention," under which they agree to reduce SO_2 levels by at least 30% by 1993 or 1995. Not until SO_2 emissions are reduced in all developed nations can the acidification phenomenon be reversed.

References

- (1) Frohlinger, J. O.; Kane, R. *Science* **1975**, *189*, 455-57.
- (2) Galloway, J. N.; Likens, G. E.; Hawley, M. E. *Science* **1984**, *226*, 829-31.
- (3) Galloway, J. N.; Likens, G. E. *Limnol. Oceanogr.* **1979**, *24*, 427.
- (4) Galloway, J. N. et al. *Atmos. Environ.* **1981**, *16*, 1677-1700.

professional consulting services directory




TRADITIONAL SOURCE SAMPLING

- Air Emissions Testing and Compliance Determination for Particulate and Gases
- Control Device Evaluation
- Particle Sizing Studies
- Resistivity Studies
- Specialized Analysis
- Method 1 Alternative
- 3-D Air Flow Studies

D. James Grove, P.E., Director
 PO Box 12291, Research Triangle Park, NC 27709 (919) 781-3550 or 1-800-ENTROPY

ENTROPY
 ENVIRONMENTALISTS INC.




SPECIALIZED SAMPLING

- (RCRA) Incinerator Testing
- Volatile Organic Compound (VOC) Testing
- Vapor Recovery Unit Compliance/Performance Testing
- Specialized Hydrocarbons Testing
- Testing of High Temperature and Pressure Sources

Walter S. Smith, P.E., Director
 PO Box 12291, Research Triangle Park, NC 27709 (919) 781-3550 or 1-800-ENTROPY

ENTROPY
 ENVIRONMENTALISTS INC.



CONTINUOUS EMISSIONS MONITORING (CEM)/ENGINEERING

- Performance Specification Tests of Opacity, SO₂, NO_x, O₃, CO, CO₂ and TRS CEMS
- Stratification Tests (All Pollutants)
- CEM Performance Audits (RAA and CGA)
- Real-time Measurements Using Transportable CEM System — Boiler Tuning (NO_x)
- FGD Performance Evaluation — Combustion Efficiency Studies
- Performance Tests of Gas Turbines (Method 20)

James W. Peeler, Director
 William G. DeVees, Associate Director
 PO Box 12291, Research Triangle Park, NC 27709 (919) 781-3550 or 1-800-ENTROPY

ENTROPY
 ENVIRONMENTALISTS INC.

A Cost Effective On-Site Biodegradation Process That Is Working!
SOIL AND GROUNDWATER CONTAMINANTS CLEANED-UP AT COSTS OF LESS THAN 1¢ PER GALLON!

How Does It Work?

The proprietary system is based on accelerating Nature's own process of biodegradation by utilizing naturally occurring microorganisms. This on-site process eliminates contamination in both soil and groundwater.

Why Is It Cost Effective?

The complete system operates at your facility. There are no contaminants materials, soil or water to be hauled away to other locations.

Let KG BIO-TECHNOLOGIES EASE YOUR CONCERNS ABOUT YOUR WASTE DISPOSAL. AFTER EVALUATING CONTAMINANTS, WE GUARANTEE TO CLEAN YOUR WASTE, IN MOST CASES WITHIN WEEKS. PLEASE CALL 214-690-9451 Or 9478.

KG BIO-TECHNOLOGIES
 1303 Columbia Dr., Suite 221
 Richardson, Texas 75081-2936



COMPLETE ANALYTICAL SERVICES GC/MS CAPABILITIES

- Screening & Analysis of Industrial & Hazardous Waste.
- Superfund & RCRA Requirements.
- Sampling to EPA Protocols.
- Toxicity Studies.

(516) 334-7770
 75 URBAN AVE, WESTBURY, NY 11590
NYTEST ENVIRONMENTAL INC.

Cenref Labs

BRIGHTON, CO (303) 659-0497
 LIBERAL, KS (316) 624-4292

ENVIRONMENTAL TESTING

Priority Pollutants • PCB's
 RCRA Hazardous Waste Analyses
 Drinking Water • Wastewater
 Pesticides • Sludge
 Engine Emission Monitoring

ROUX ASSOCIATES INC. CONSULTING GROUND-WATER GEOLOGISTS

ROUX

- RCRA Monitoring
- Superfund Response
- Site Evaluation
- Aquifer Clean-Up
- Resource Development

11 STEWART AVENUE
 HUNTINGTON NEW YORK 11743 516-673-7200
 1503 N GRAVEL PIKE
 PERKIOMENVILLE PA 18074 215-234-4900

BML COMPLETE ANALYTICAL SERVICES

- Gas Chromatography/ Mass Spectrometry
- Trace Metal Analyses - ICAP, AA, GFAA
- Drinking Water Analyses
- Industrial Hygiene Services
- Research and Development
- Environmental Field Sampling
- EPA Priority Pollutant Analyses

Brochure and/or fee schedule available on request
BARRINGER MAGENTA LTD.
 304 Carlingview Drive Rexdale Ont Canada (416) 675-3870
 US Office Denver CO 80401 (303) 232-8811

ENVIRODYNE ENGINEERS

a consulting engineering and sciences firm

- environmental engineering
- analytical chemistry
- priority pollutant analyses
- environmental monitoring and assessment
- hazardous waste monitoring
- hazardous waste management
- transportation engineering
- energy engineering
- construction management

12161 Lackland Road
 St. Louis, Missouri 63146
 (314) 434-8960

Baltimore / Chicago / New York

THE CONSULTANTS' DIRECTORY

UNIT	Six Issues	Twelve Issues
1" X 1 col.	\$55	\$50
1" X 2 col.	110	100
1" X 3 col.	160	140
2" X 1 col.	110	100
2" X 2 col.	200	180
4" X 1 col.	200	180

Jay Francis
 ENVIRONMENTAL SCIENCE & TECHNOLOGY
 25 Sylvan Road South
 P.O. Box 231
 Westport, CT 06881
 Or call him at (203) 226-7131

ENVIROMED LABORATORIES, INC.

Sampling, Testing, & Consulting Services

- Priority Pollutants GC/MS, GC, AA
- RCRA-Hazardous Waste
- Animal Toxicity & Bioassay Studies
- Wastewater, Water & Sewage Analysis
- Permit Preparation, Audits
- TOX, TOC
- PCB and Chlorinated Hydrocarbon Analysis
- Industrial Hygiene & Ambient Air Monitoring
- Ground Water Monitoring

414 W. Calif., Ruston La. 71270 (318) 255-0060
 1874 Dallas Dr. Baton Rouge, La. 70806 (504) 928-0232
 La. Toll Free 1-800-421-2993

NATION'S BEST PRICE/PERFORMANCE GC/MS FACILITY

nanco labs, inc.
 "The complete testing laboratory"

- EPA APPROVED AS A CONTRACT LABORATORY
- N.Y., N.J., CT—APPROVED
- DATA ACCEPTABLE FOR LEGAL DOCUMENTATION

UNITY STREET & ROUTE 376, P.O. BOX 10
 HOPEWELL JUNCTION, NY 12533
 NY (914) 221-2485 ELSEWHERE (800) 55NANCO

GERAGHTY & MILLER, INC.
 Ground-Water Consultants

The North Shore Atrium
 6800 Jencho Tpke., Syosset, NY 11791
 (516) 921-6060

AIKEN, SC
 ANNAPOLIS, MD
 BATON ROUGE, LA
 DENVER, CO
 HACKENSACK, NJ
 HOUSTON, TX
 MILWAUKEE, WI
 NEWTOWN, PA
 OAK RIDGE, TN
 PALM BEACH, FL
 TAMPA, FL
 WASHINGTON, DC

CLASSIFIED SECTION

ATMOSPHERIC CHEMIST: A Research Chemist position to develop a research program in atmospheric chemistry in collaboration with atmospheric chemists and physicists presently within the Institute is available immediately in the Research and Development Division of the New Mexico Institute of Mining and Technology. A Ph.D. in Chemistry is required, with preference given to individuals with analytical, inorganic, and/or physical chemistry backgrounds. Post-doctoral experience preferred. This position will carry adjunct status with the Department of Chemistry. The facilities at the Langmuir Laboratory for Atmospheric Research, the instrumented Schweizer aircraft capable of penetrating thunderstorms, the Chemistry Department Laboratories, and a separate Chemistry Laboratory within the Research Division will be made available. The Research Division collaborates closely with the College Division at the Institute, and individuals will be expected to work with students, both at the undergraduate and graduate levels and may teach a course in his/her specialty area. The Chemistry Department presently offers degrees through the masters degree and is in the process of obtaining approval to offer the Ph.D. degree. Submit resume, names of three references, and a description of interest in atmospheric chemistry to: Chairman, Atmospheric Chemistry Search Committee, c/o Personnel Office, New Mexico Institute of Mining and Technology, Socorro, NM 87801. An Equal Opportunity/Affirmative Action Employer.

SCIENTISTS/ ENGINEERS

\$23,170-\$41,105 per annum

The U. S. Nuclear Regulatory Commission has positions available in the Division of Waste Management, Silver Spring, MD. These positions are:

- Environmental Science
- Health Physics
- Hydrology
- Geochemistry/Geophysicist
- Geoscience
- Project Management
- Technology and Public Policy
- Systems Engineering/Systems Analysis
- Materials Science
- Geotechnical Engineering
- Mining Engineering

For immediate consideration send Federal Employment Application Form (SF-171) or resume with salary requirements to:



U.S. Nuclear
Regulatory Commission
Division of Personnel
SPE: NMSS/ES/DEC
Washington, DC 20555

An Equal Opportunity Employer M/F/H
U.S. Citizenship Required

ENVIRONMENTAL CHEMIST

Research Planning Institute is seeking to add an environmental chemist to a diversified and growing staff of consulting scientists. Duties will include technical consulting and support in broad-based activities including pollutant fate and effects in marine, groundwater and soil environments. This position requires an M.S. level with 0-2 years experience and excellent communication skills. RPI offers competitive salary, profit sharing, benefits and relocation. Submit resume to: **Victor Owens, Research Planning Institute, Inc., P.O. Box 328, Columbia, SC 29202.** EOE.

DIRECTOR ATMOSPHERIC CHEMISTRY PROGRAM

San Francisco Bay Area

SRI International (formerly Stanford Research Institute) is seeking a Director for its research activities in atmospheric chemistry, which include field studies, laboratory analyses, and simulation modeling, emphasizing air quality and global tropospheric chemistry research. Qualified candidates should possess at least 10 years of progressively responsible experience in atmospheric chemistry research. A Ph.D. in atmospheric chemistry, chemical engineering, or a related field is highly desirable.

The Atmospheric Chemistry Program is part of SRI's Atmospheric Science Center, which also has active programs in meteorology, atmospheric physics, air-quality analysis, and remote sensing. This multidisciplinary work environment provides excellent opportunities for professional growth; SRI's location in the beautiful San Francisco Bay area offers ideal living conditions. Please send resume to: **Michael Patrick, Professional Staffing, Dept. EST-12, SRI International, 333 Ravenswood Ave., Menlo Park, CA 94025.** An EEO employer. U.S. Citizenship is required.



WATER POLLUTION RESEARCH SCIENTIST

Betz Laboratories, a leader in the engineered treatment and control of industrial water, wastewater and process systems, has an immediate opening for a creative Research Scientist in its Water Waste Research Group.

The qualified candidate will be a recent Ph.D. in Environmental, Physical or Biophysical Chemistry. Industrial or Postdoctoral experience in a related field is highly desirable. The individual will be responsible for establishing research programs leading to new products and technology for solving water pollution problems.

This is a highly visible career development position and offers an attractive base salary plus a full package of corporate benefits.

Candidates are invited to submit a detailed resume outlining their education, work experience and salary requirements to: Dept. DD, Betz Laboratories, Inc., 4636 Somerton Road, Trevose, PA 19047. An Equal Opportunity Employer M/F/H/V.

BETZ LABORATORIES

CLASSIFIED SECTION

UNIVERSITY OF ARIZONA

Immediate opening: faculty position in aquatic chemistry, assistant professor, Department of Hydrology and Water Resources. Tenure track position. Ph.D. required with strong background in hydrogeochemistry or analytical methods applied to aquatic chemistry. Successful candidate will develop strong research program, work with graduate students, offer graduate seminars, and develop courses. Deadline for application is Dec. 15, 1985. Letter of interest, resumé, and names and telephone numbers of at least three references to be sent to: **Search Committee, Dept. of Hydrology & Water Resources, University of Arizona, Tucson, Arizona 85721.** The University of Arizona is an affirmative action and equal opportunity employer.

SENIOR STACK TESTER

Applicants must be experienced in all EPA Methods and continuous monitoring. Lab and GC experience helpful. Send resumé to: Pape & Steiner Environmental Services, 5801 Norris Road, Bakersfield, California 93308.

EOE/MF

USE THE CLASSIFIED SECTION

ENGINEERS (NUCLEAR PLANT)

UNC Nuclear Industries, a prime operating contractor to the U.S. Department of Energy at Richland, WA, is embarking upon a major multi-year program to upgrade the N Reactor. We are looking for a few select professionals to join our top notch technical team.

The following positions require an appropriate technical degree plus specific experience:

• Nuclear Safety

Requires experience in the independent oversight of nuclear facility operations from a safety perspective. Responsibilities include independent safety appraisal of operations and activities; review of safety evaluations and proposed plant modifications; support to independent safety oversight committee; operations readiness review. Other positions require experience in safety analysis related to the performance of probabilistic risk assessment or reliability analysis for nuclear power plants.

• Process Engineering

Emphasis in physics and thermodynamics. Experience areas should include nuclear reactor, start-up administration and operation. Requires heavy interface with engineering and operation, review of procedures, design changes, plant tests and project review for nuclear safety. Knowledge of DOE requirements is desirable.

• Environmental Engineering

At least 3 years of applicable professional environmental experience in the control of airborne and liquid effluents. Experience must include familiarity with RCRA, CERCLA, and TSCA regulations.

If the above describes your background and you are interested in being considered, please send resumé, salary history and salary requirements, in confidence to: K.A. Bresnahan, Dept. DB, UNC Nuclear Industries, P.O. Box 490, Richland, WA 99352.

U.S. citizenship required (DOE security clearance preferred).

Equal employment opportunity is our pledge and our practice.



**UNC NUCLEAR
INDUSTRIES**

INDEX TO THE ADVERTISERS IN THIS ISSUE

ADVERTISERS

PAGE NO.

EPRI IFC
Sobel Knight Advertising

Seastar Instruments Ltd. IFC

Advertising Management for the
American Chemical Society Publications

CENTCOM, LTD.

President

Thomas N. J. Koerwer

Executive Vice President Senior Vice President

James A. Byrne Benjamin W. Jones

Alfred L. Gregory, Vice President

Clay S. Holden, Vice President

Robert L. Voepel, Vice President

Joseph P. Stenza, Production Director

25 Sylvan Road South

P.O. Box 231

Westport, Connecticut 06881

(Area Code 203) 226-7131

Telex No. 643310

ADVERTISING SALES MANAGER

James A. Byrne, VP

ADVERTISING PRODUCTION MANAGER

Jay S. Francis

SALES REPRESENTATIVES

Philadelphia, Pa. . . . Patricia O'Donnell, CENTCOM, LTD., GSB Building, Suite 725, 1 Belmont Ave., Bala Cynwyd, Pa 19004 (Area Code 215) 667-9666

New York, N.Y. . . . Dean A. Baldwin, CENTCOM, LTD., 60 E. 42nd Street, New York 10165 (Area Code 212) 972-9660

Westport, Ct. . . . Edward M. Black, CENTCOM, LTD., 25 Sylvan Road South, P.O. Box 231, Westport, Ct 06881 (Area Code 203) 226-7131

Cleveland, Oh. . . . Bruce Poorman, CENTCOM, LTD., 325 Front St., Berea, OH 44017 (Area Code 216) 234-1333

Chicago, Ill. . . . Michael J. Pak, CENTCOM, LTD., 540 Frontage Rd., Northfield, Ill 60093 (Area Code 312) 441-6383

Houston, Tx. . . . Michael J. Pak, CENTCOM, LTD., (Area Code 312) 441-6383

San Francisco, Ca. . . . Paul M. Butts, CENTCOM, LTD., Suite 1070, 2672 Bayshore Frontage Road, Mountainview, CA 94043. (Area Code 415) 969-4604

Los Angeles, Ca. . . . Clay S. Holden, CENTCOM, LTD., 3142 Pacific Coast Highway, Suite 200, Torrance, CA 90505 (Area Code 213) 325-1903

Boston, Ma. . . . Edward M. Black, CENTCOM, LTD., (Area Code 203) 226-7131

Atlanta, Ga. . . . Edward M. Black, CENTCOM, LTD., (Area Code 203) 226-7131

Denver, Co. . . . Paul M. Butts, CENTCOM, LTD., (Area Code 415) 969-4604

United Kingdom:

Reading, England—Technomedia, Ltd. . . .
Wood Cottage, Shurlock Row, Reading
RG10 0QE, Berkshire, England 0734-343302

Lancashire, England—Technomedia, Ltd. . . .
c/o Meconomics Ltd., Meconomics House,
31 Old Street, Ashton Under Lyne, Lanca-
shire, England 061-308-3025

Continental Europe . . . Andre Jamar, Rue Mallar 1,
4800 Verviers, Belgium. Telephone (087) 22-
53-85. Telex No. 49263

Tokyo, Japan . . . Shuji Tanaka, International Media
Representatives Ltd., 2-29, Toranomon 1-
Chrome, Minatoku, Tokyo 105 Japan. Tele-
phone: 502-0656

Now and take advantage of all the programs and activities planned for 1986.

ACS Membership Application 1986

American Chemical Society • 1155 Sixteenth Street, N.W., Washington, D.C. 20036
(202) 872-1600

Applicant

Mr., Mrs. _____
 Dr., Miss, Ms. _____ (Please type or print) Family Name First Middle
 Mailing Address _____
 _____ Number and Street Office
 _____ Telephone Home
 City State Zip Code/Country

Academic Training

Name of College or University (Including current enrollment)	City and State	Curriculum Major	Years of Attendance	Title of Degree(s) Received or Expected	Date Degree Received or Expected

Courses Completed

Not required of those with a bachelor's, master's or doctor's degree in a chemical science or those with a doctor's degree in a science closely related to chemistry with demonstrated significant experience in the practice of a chemical science. Please list completed courses (by title) in the chemical sciences (Attach separate sheet or transcript if more space is needed.)

Quarter hour credits should be multiplied by two-thirds. If school did not use a credit hour system, please estimate credits on basis of 15 lecture clock hours or 45 laboratory clock hours as equivalent to one semester hour credit.

Course Title	Semester Hours	Course Title	Semester Hours	Course Title	Semester Hours

Nomination

Although nomination by 2 ACS members is required by ACS bylaws, if this presents difficulty, we suggest you contact the Washington office. In any case, such nomination is not necessary for former members (student affiliation does not constitute membership).

We recommend _____ for membership in the American Chemical Society.
 (Name of Applicant)

ACS Member: _____
 (Signature) (Printed Name)

ACS Member: _____
 (Signature) (Printed Name)

This space for use of:
ADMISSIONS COMMITTEE

1 2 3 4 N

Local Section/Division Commission Claim

Statistical Information

Mr., Mrs. _____
Dr., Miss, Ms. (Please type or print) Family Name First Middle

Mailing Address _____
Number and Street

City State Zip Code/Country

Date of Birth _____ Sex F M Telephone _____
(Information needed for statistical purposes) Office _____
Home _____

Previous Membership

I have have not previously been a member.
I have have not previously been a student affiliate.

Office Use Only

AMC _____
MJR _____
DEL _____
MED _____
CSD _____
PNI 8398B _____
CLD _____
CNS _____
CNR _____
TEC _____
WTD _____

Professional Experience

Employer	Job Title	Functions	% Time on Chemical Work	Inclusive Dates of Employment (Mo. & Yr.)

Dues/Subscriptions/Divisions

There are four start dates for membership: 1 January, 1 April, 1 July, and 1 October. We are anxious to begin your membership as soon as possible and will therefore enroll you immediately upon approval of your application by the ACS Admissions Committee. Dues for 1986 are \$72.00. If you subscribe to publications, the amount will be prorated, unless you indicated that you wish the full year's subscription. Your membership will begin at the nearest quarter and you will be billed accordingly. Those entering 1 October will be billed for three months of the year plus the full dues for the following year (or 15 months dues) or at the new member's option, may pay for the final three months of the current year only. Former members who did not resign will be assessed a \$10.00 reinstatement fee. *Please send no money now.*

Student Dues

If you are a student majoring in the chemical sciences a 50% reduction on membership is available. To apply you must be registered for at least six credit hours as an undergraduate or be enrolled as a full-time graduate student.

I am an undergraduate student enrolled as described above.
 a graduate student enrolled as described above.

Name of College or University

National Affiliation

National affiliates pay three-quarters dues (i.e. \$54.00) and likewise will receive a prorated bill based on the quarter national affiliation begins.

Husband/Wife Dues

If you are the spouse of a member receiving C&EN, 25% (or the prorated amount) will be deducted from your bill. This is the portion that is allotted for C&EN. If you are eligible, please give the name of your spouse and his/her membership number.

Spouse's Name

Membership Number

If you wish to subscribe to an ACS publication or join an ACS division please list the publication(s)/division(s) below.

Remember, send no money now.

Agreement

I agree to restrict for my own personal use all publications to which I subscribe at member rates. I understand that membership dues are payable annually unless my signed resignation is received by the Executive Director before January 1 of the year for which the resignation is to take effect.

(Date)

(Signature of Applicant)

IUPAC Affiliation

Beginning in 1986, the International Union of Pure and Applied Chemistry (IUPAC) is offering individual Affiliation to members of national chemical societies. Recognized by all the sciences and by the national level academies of science as the international representative body for chemistry, IUPAC is the authority on chemical nomenclature, terminology, symbols, atomic weights, and related topics. IUPAC Affiliate Dues for ACS members residing in the U.S. are \$15.00 and include a subscription to *Chemistry International* magazine.

IUPAC Affiliation \$15.00 (U.S. members only)

CIRCLE 20 ON READER SERVICE CARD →

Characteristics of Abiological Carbon Monoxide Formation from Soil Organic Matter, Humic Acids, and Phenolic Compounds

Ralf Conrad* and Wolfgang Sellaer

Max-Planck-Institut für Chemie, D-6500 Mainz, Federal Republic of Germany

■ The abiological CO formation from soil and humic acids is a thermally sensitized process following the Arrhenius equation. The magnitude of the Arrhenius constant (activation entropy) and the activation energy decreased with increasing moisture content and pH, i.e., conditions favoring the solubilization of the humic acid polymers. CO was also formed from various phenolic compounds provided that water or preferably alkali was added. The CO formation was stimulated by an oxygen atmosphere but was not inhibited by the addition of chemicals quenching singlet oxygen, superoxide, or hydroxyl radicals.

Introduction

It is well established that soils contain microorganisms which are able to oxidize CO (1-5). Some of these microorganisms have such a high affinity for CO that they are able to utilize atmospheric CO (6, 7) and thus provide a removal mechanism for the CO that is produced by natural and anthropogenic processes (8, 9). However, little attention has been paid to the fact that CO not only is consumed but is also produced in soil (3). Under arid conditions, e.g., in deserts or savannahs, CO production rates often exceed CO consumption rates so that these soils even act as a net source of atmospheric CO (10, 11). CO formation in soil was shown to be an abiological process (3, 10). It was shown by field measurements that CO emission from soil into the atmosphere was dependent on soil temperature, soil moisture, and organic carbon content and that most of the emitted CO was produced in the upper soil layers by a light-independent reaction (11).

The intention of this work was to characterize the abiological CO-producing reaction in soil by laboratory experiments. We present data on temperature dependence of CO formation in soils which were treated in different ways, as well as in purified quartz sand to which humic acids and other phenolic compounds were added.

Materials and Methods

Soil samples were taken from the top 10-cm layer of different field sites which were under arid conditions. The field sites and the characteristics of their soils have already been described (11-13). The soil samples were passed through a 4-mm mesh screen and stored in polyethylene bottles at ambient temperature for several months. NaOH, HCl, NaN₃, L-alanine, and D-mannitol were obtained from Merck (Darmstadt), humic acid (*M_n*, 600-1000) was from Fluka (Switzerland), and all the other chemicals were from Aldrich (EGA Chemie, Steinheim). N₂ (99.99%) and

technical O₂ were purchased from Linde, Germany.

Soil (100 g) was filled in 1-L glass flasks which were placed in a water bath kept at a constant temperature (± 0.5 °C). The flasks were gassed with air, N₂, or O₂ which was purified from traces of CO by passing the gas stream over Hopkalit catalyst (Dräger Werke, Lübeck). The gas stream was moistened by passing it through an H₂O bubbler kept at the temperature of incubation. After 15 min of temperature adaptation, the flasks were pressurized to 1.3 bar and closed. Gas samples were taken from the flasks at 5-min intervals for a total of 30-45 min and analyzed immediately for CO by using an instrument based on the HgO-to-Hg vapor conversion technique (9, 14). CO production rates were determined from the linear temporal increase of the CO mixing ratio (vol/vol) in the headspace of the flask. When 100 g dry weight (d.w.) of soil was used, the lower detection limit was 0.05 nL of CO h⁻¹ g⁻¹ d.w. Maximum rates of <600 nL of CO h⁻¹ (g d.w. of soil)⁻¹ were sometimes observed. These rates resulted in CO mixing ratios of <23 ppm (volume) (10⁻⁶ vol/vol) after a 30-min incubation of 100 g d.w. of soil.

Temperature dependence of CO production was determined by incubation of the soil samples at increasing temperatures (20, 30, 40, 50, 60, and 70 °C). The activation energy and the Arrhenius constant of CO production were determined by using the logarithmic form of the Arrhenius equation

$$\ln P = \ln A - (E_A/R)(1/T) \quad (1)$$

with *P* = CO production rate, *A* = Arrhenius constant, *E_A* = activation energy, *R* = gas constant, and *T* = incubation temperature (K). *A* and *E_A* were calculated from a linear regression of $\ln P$ to $1/T$. The regression coefficients (*r* ≥ 0.98) indicated significant regression at the 1% level for each experiment. The CO production rates at 20 and 60 °C were calculated from eq 1 by using the values of *E_A* and *A* obtained from the regression of the experimental data.

CO production from humic acid was assayed by adding 2 g of humic acid to 100 g of quartz sand (Merck, Darmstadt). CO production from phenolic compounds was assayed at 60 °C by mixing 0.5 g of the crystalline compound into 20 g of quartz sand and adding either 4 mL of H₂O or 4 mL of 0.25 N NaOH. Controls with quartz sand to which only water or NaOH were added did not show any CO production at 60 °C.

Results

Field studies have shown that both production and destruction of CO occur in soils (10, 11). However, when

Table I. CO Production in Different Arid Soils

location	soil type	pH	H ₂ O, %	org. C, %	E _A , kJ (mol of CO) ⁻¹	A, nL h ⁻¹ g ⁻¹ d.w.	CO production rates, nL h ⁻¹ g ⁻¹ d.w., at	
							20 °C	60 °C
Waldthausen (Germany)	eolian sand, rendzina	7.3	1.8	3.9	110	2 × 10 ¹⁹	0.45	100.13
Transvaal (S. Africa)	sandy loam, mispah formation	5.0	2.9	1.2	80	2 × 10 ¹³	0.13	6.93
Andalusia (Spain)	loamy sand, reddish-brown soil	7.4	1.7	0.5	87	2 × 10 ¹⁴	0.05	3.64
Karoo (S. Africa)	sand, sierozem	7.0	0.6	0.5	97	4 × 10 ¹⁵	0.03	2.43

the soil samples were stored in dry condition for several months, they no longer showed any CO uptake activity when tested at CO mixing ratios of 1–3 ppm (volume). CO uptake activity could not be reestablished by wetting the soil with water, indicating that the originally present CO-oxidizing microorganisms apparently had been inactivated during the storage of the soil. CO formation activity, however, was observed in all of the soil samples studied.

CO release from the soil into the headspace of the incubation vessel was linear with time. The rate of CO release was not affected by previous evacuation or repeated flushing with CO-free air. Even flushing with CO-free air at elevated temperatures for up to 5 h did not result in a decrease of the CO release rates at lower temperature. These observations demonstrate that the release of CO was due to production processes and not to reequilibration with the CO-free atmosphere of CO adsorbed to soil matter. The rates of CO increase in the gas headspace were proportional to the amount of soil; i.e., the CO production rate (*P*) per gram of soil was the same for different amounts of soil (up to 150 g d.w.) tested. Autoclaving of the soil sample for 1 h at 121 °C did not inactivate CO formation but rather resulted in CO production rates that were enhanced by a factor of ~1.8 at 20 and 60 °C, demonstrating that CO formation must be an abiological process. The rates of CO production (*P*) increased exponentially with the incubation temperature (20–70 °C) and were significantly correlated to the Arrhenius equation.

Table I summarizes the data obtained from soils taken at different field sites with different pHs and different organic carbon contents. The soils had been sampled at arid field conditions with soil moisture contents of only 0.6–2.9% H₂O. CO production rates ranged between 0.03 and 0.45 nL h⁻¹ (g dry weight of soil)⁻¹ at 20 °C and between 2.43 and 100.13 nL h⁻¹ g⁻¹ d.w. at 60 °C, reflecting the relatively high activation energies of the CO-forming processes. The values of *E_A* and *A* ranged between 80 and 110 kJ (mol of CO)⁻¹ and between 10¹³ and 10¹⁹ nL of CO h⁻¹ g⁻¹ d.w., respectively. The amount of CO formed per hour was less than 10⁻⁶ of the soil organic carbon content so that soil organic carbon would be sufficient to sustain CO production for >100 years, even at a temperature of 60 °C. The activation energies and the Arrhenius constants apparently were not related to the soil organic carbon content, indicating that the formation of reactive compounds releasing CO depends on the quality rather than on the quantity of the soil organic compounds and depends on the other physicochemical soil conditions. The CO formation process was then further characterized with sandy loam soil which was sampled in a broad-leafed savannah in Transvaal.

Figure 1 illustrates the temperature dependence of the CO formation processes at low (0.6% H₂O) and high (>15% H₂O) soil moisture contents. The diagram presents the data in a plot according to the linearized logarithmic form of the Arrhenius equation. The values of *E_A*, *A* and the production rates at 20 and 60 °C were calculated from

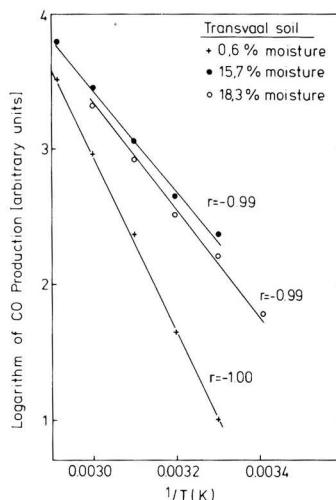


Figure 1. Arrhenius plot of temperature-dependent rates of CO production in dry and moist soil.

Table II. Influence of Moisture on CO Production in Transvaal Soil

	soil water, %	E _A , kJ (mol of CO) ⁻¹	A, nL h ⁻¹ g ⁻¹ d.w.	production rate, nL h ⁻¹ g ⁻¹ d.w., at	
				20 °C	60 °C
H ₂ O	0.6	129	2 × 10 ²¹	0.03	11.82
	15.7	70	3 × 10 ¹²	1.06	33.02
	18.3	76	3 × 10 ¹³	0.72	29.92
D ₂ O ^a	18.3	75	2 × 10 ¹³	0.66	25.84

^a 66.5% D₂O.

the linear regression of the data according to eq 1 and are shown in Table II. CO production was enhanced at high soil water contents. The enhancement was mainly due to a decrease of the activation energy from 129 kJ (mol of CO)⁻¹ at 0.6% H₂O to 70–76 kJ mol⁻¹ at 15–19% H₂O and was not compensated by the simultaneous decrease of the Arrhenius constant from 10²¹ to 10¹³ nL of CO h⁻¹ g⁻¹ d.w. Addition of D₂O instead of H₂O resulted in almost identical values of *E_A*, *A*, and the CO production rates.

Table III shows the influence of the pH on the CO formation. The pH of the soil was changed by adding NaOH or HCl. CO production rates were strongly stimulated by alkali due to a strong decrease of the activation energy from 70 kJ (mol of CO)⁻¹ in the control of 51 kJ mol⁻¹ under alkaline conditions. The Arrhenius constant, on the other hand, decreased only slightly from 10¹² to 10¹⁰ nL of CO h⁻¹ g⁻¹ d.w. Addition of acid, on the other hand, resulted in an increase of the activation energy to 96 kJ

Table III. Influence of pH on CO Production in Transvaal Soil^a

addition	pH ^b	E _A , kJ (mol of CO) ⁻¹	A, nL h ⁻¹ g ⁻¹ d.w.	CO production rate, nL h ⁻¹ g ⁻¹ d.w., at	
				20 °C	60 °C
NaOH ^c	9.3	51	5 × 10 ¹⁰	37.5	469.2
H ₂ O	5.0	70	3 × 10 ¹²	1.1	33.0
HCl ^c	2.4	96	1 × 10 ¹⁷	0.9	102.9

^a Soil moisture was 15.7% (grams of H₂O per 100 g d.w.). ^b pH was measured in a mixture of soil and H₂O (1:2). ^c 7.5 mmol g⁻¹ d.w.

Table IV. CO Production from Humic Acid

humic acid, 2 g	E _A , kJ (mol of CO) ⁻¹	A, nL h ⁻¹ (g of humic acid) ⁻¹	CO production rate, nL h ⁻¹ (g of humic acid) ⁻¹ , at	
			20 °C	60 °C
dissolved ^a + 16 mmol of NaOH (pH ~11)	32	9 × 10 ⁹	17875	86515
dissolved ^a (pH ~7)	60	3 × 10 ¹³	640	12449
dissolved ^a + 16 mmol of HCl (pH ~1)	64	1 × 10 ¹³	48	1109
particulate ^b + H ₂ O (pH ~5)	79	8 × 10 ¹⁴	8	413
particulate	83	6 × 10 ¹⁴	1	91

^a Humic acid (2 g) was dissolved in 13 mL of 0.5 NaOH and mixed into 100 g of quartz sand. NaOH, H₂O, or HCl was added to give a total of 15 mL of H₂O. ^b Humic acid (2 g) was mixed into 100 g of quartz sand; 15 mL of water was added.

mol⁻¹ but also in a relatively strong increase of the Arrhenius constant to 10¹⁷ mL of CO h⁻¹ g⁻¹ d.w. so that CO production rates were only enhanced at high temperatures (60 °C) but not at low ones (20 °C).

Humic acids make up a major fraction of soil organic matter and thus may be considered as model compounds were studied in an artificial system composed of quartz sand and commercial humic acids. By use of this system, temperature-dependent CO formation was observed from humic acids under similar conditions as from native soil samples (Table IV). Control experiments with quartz sand but without humic acids did not result in any CO formation. Activation energies increased and CO production rates decreased with increasing acidity of the humic acids system, but the Arrhenius constants did not exceed values of 10¹³ nL of CO h⁻¹ (g of dry humic acid)⁻¹ which is lower than the values observed in native Transvaal soil. The activation energies, on the other hand, were also lower with humic acids than with native soil. Particulate humic acid displayed much higher activation energies and much lower CO production rates than dissolved humic acid. This behavior was only partially reverted by addition of water.

Table V compares CO production rates at 60 °C in Transvaal soil treated in different ways. Compared to an air atmosphere, CO production was enhanced under an oxygen atmosphere and was reduced under a nitrogen atmosphere. This observation indicates that CO formation is an oxidative process in which molecular oxygen is involved. The lifetime of singlet O₂ is 10 times longer in D₂O than in H₂O (15). However, D₂O did not enhance CO production, indicating that the oxidative process is not mediated by free singlet O₂. This conclusion was con-

Table V. Influence of Oxygen and O Radical Quenching Chemicals on CO Production in Transvaal Soil

treatment of 100 g of soil	CO production rate, % of control
control in air	100
oxygen ^a	312
nitrogen ^a	39
D ₂ O (66.5%) ^b	86
1,4-diazabicyclooctane (1 g) ^b	10400
1,3-diphenylisobenzofuran (0.25 g) ^c	151
NaN ₃ (750 μmol) ^b	254
hydroxylamine (15 μmol) ^b	109
mannitol (750 μmol) ^b	168

^a Dry soil (100 g) (H₂O = 0.6%) was incubated at 60 °C. ^b Aqueous solution (15 mL) of the indicated amounts of the chemicals was mixed into 100 g of dry soil and incubated at 60 °C. The control was treated with 15 mL of H₂O. ^c 1,3-Diphenylisobenzofuran was dissolved in methanol and mixed into the soil. The methanol was evaporated under an air stream at room temperature, and then 15 mL of H₂O was added to the dried soil mixture.

Table VI. CO Production from Phenolic Compounds^a

compound	solubility in water (20 °C), %	CO production, μL h ⁻¹	
		H ₂ O	NaOH
phenol	8.2	0	2.70
catechol	31.1	0.54	36.06
resorcinol	63.7	0	3.78
hydroquinone	6.7	0.08	70.48
pyrogallol	38.5	1.90	95.81
gallic acid	0.94	0.08	3.77
phloroglucinol	1.12	0.20	0.61
L-alanine	0.16	0	0
L-tyrosine	0.45	0	0.37
coumaric acid	1.3	0	0.07
coniferyl alcohol		0.07	5.68

^a A total of 0.5 g of the compound was mixed into 20 g of quartz sand, and 4 mL of either H₂O or 0.25 N NaOH was added.

firmed by the observation that CO production was not inhibited in the presence of 1,4-diazabicyclooctane, 1,3-diphenylisobenzofuran, and NaN₃ which are chemicals quenching singlet O₂. CO production was also not inhibited when the soil was treated with compounds quenching superoxide radicals (i.e., hydroxylamine) or quenching hydroxyl radicals (i.e., mannitol), indicating that reactive oxygen radicals either were not involved in CO formation or emerged only in close vicinity to the reaction site so that they could not be quenched by external compounds. Several of the added quenchers even stimulated CO production. Tests using aqueous solutions of 1,4-diazabicyclooctane or mannitol mixed into quartz sand showed only marginal CO production rates, indicating that the quenchers were not acting as CO-generating substrates on their own. The same is true for NaN₃ which does not contain carbon. Hence, the stimulatory effect of some of the oxygen radical quenchers on CO production can only be explained by reactions involving soil organic compounds as well as the quenching compounds.

Since humic acids are composed of phenolic compounds (16), we tested several simple phenolic compounds as models for CO formation. Table VI shows the CO production rates at 60 °C in the presence of water and alkali from the different phenolic compounds including tabulated data on their solubility in water. No CO was formed when the dry crystalline compounds were tested. However,

significant amounts of CO were produced from many of the phenolic compounds when water was added although the solubility of some of these compounds is very low so that the added crystals were not dissolved completely. After addition of alkali, CO was produced from every phenolic compound tested. No CO was formed from L-alanine which constitutes the side chain of the phenolic ring in L-tyrosine. Since tyrosine is a CO-forming compound, CO apparently is formed from the ring and not from the side chain.

Discussion

The results of this study confirmed earlier observations (3, 10) that CO is produced by abiological reactions in soil. They further established that phenolic compounds present in humus can serve as substrates for the CO formation. It has been known since 1864 (17) that CO is formed during autoxidation of alkaline pyrogallol solution. Autoxidative CO production has also been observed in alkaline solutions of other phenolic compounds (18). Here, we showed that CO may even be produced from mixtures with water, although the solubility of some of the compounds is very low. Hence, phenolic compounds may be responsible for the CO production in soil.

The reaction mechanism leading to CO formation from phenolic compounds is still unknown. CO production rates were especially high from those compounds which had a second hydroxy group (or methoxy group, e.g., in coniferyl alcohol) in ortho or para position to the first hydroxy group. CO production was especially low from coumaric acid which has an alkene function in para position to the hydroxy group. These observations indicate that CO formation may be enhanced if high electron density is established by mesomeric effects at the ring carbon atom with a hydroxy function.

Since the base-catalyzed autoxidation of phenolic compounds seems to involve radical formation (19), it is likely that the CO-forming reaction is also based on a radical mechanism. A radical mechanism of CO formation is also likely for reactions involving humic acids which are known to stabilize radicals that most probably play an important role in polymerization-depolymerization reactions (20). Radical formation most probably is initiated by reactions with molecular oxygen which by itself has a radical nature. Recently, it has been shown that singlet O₂ is generated in a photosensitized reaction at the soil surface (21) and that superoxide anion and singlet oxygen are photochemically generated in humic waters (22, 23). In fact, CO is produced in ocean and freshwater environments by photochemical reactions (24, 25). In soil, however, the CO formation reactions occur in darkness and are thermally rather than photochemically sensitized. Our experiments do not support the assumption that reactive oxygen species such as singlet O₂, superoxide, or hydroxy radicals were involved as free species in the CO formation since CO production was not inhibited by chemicals with quenching activity. This does not disclude, however, that other radicals, e.g., stabilized by the humic acid polymer, are involved in CO formation or that oxygen radicals emerge in such a close vicinity to the CO-generating substrates that quenching by added chemicals is not possible.

CO production from humic acid as well as from native soils is a dark reaction that is stimulated by heat. Therefore, the CO production rates are greatly influenced by the magnitude of the activation energy. The most important factor influencing the activation energy apparently is the physicochemical state of humic acid. Less activation energy was necessary if humic acids were allowed to dissolve and dissociate in alkaline solution.

Compared to particulate humic acid, less activation energy was necessary, if the humic acid was freshly precipitated out of an alkaline solution by adding acid. We believe that the required activation energy increases with the increasing size of the humic acid particles and decreases with increasing solubilization. Swelling and partial solubilization of the humic acid polymers most probably are also the reasons why the activation energies of CO formation decreased at high soil moisture contents. The activation energy of CO formation was higher in native soils than in commercial humic acids, suggesting differences in quality or physicochemical state.

The physicochemical state of humic acids also influenced the Arrhenius constant of the CO-forming reactions. The Arrhenius constant gives a measure of the activation entropy. Our results indicate that the activation entropies decreased when humic acid was solubilized and increased when humic acid was precipitated. A relatively strong enhancement of the Arrhenius constant was observed in native soil when HCl was added. This increase most probably not only was due to precipitation of humic acid but possibly was in addition due to making additional substrates susceptible for CO formation. The existence of additional substrates for CO formation may also be deduced from the observation that the Arrhenius constants on a gram basis were lower for pure humic acids than for native soil. An alternative explanation would be the assumption of a different status of the native humic acid as compared to the commercial substance resulting in different activation entropies.

The magnitudes of the activation energies and entropies apparently change parallel to each other when soil conditions are changing. Both are decreasing when conditions favor the solubilization of soil humic acids. In fact, it seems to be a rule that the Arrhenius constants are high and thus stimulative for CO production, when at the same time the activation energies are also high and thus restrictive for CO formation at moderate temperatures. The values of both constants finally determine the CO-forming behavior of soil at varying temperatures. More soil types have to be tested in order to determine whether a relationship exists between quality and quantity of soil organic matter on one side and the activation energy and the Arrhenius constant on the other. At the moment, activation energy and Arrhenius constant seem to be related to each other in a way that the resulting CO production rates show an apparent increase with increasing soil organic matter content.

Care must be taken when extrapolating laboratory data to CO emission rates under field conditions. In this case, the extent of the CO emission from soil into the atmosphere is dependent not only on the rates of abiological CO production but also on the activity of microbial CO utilization. In arid soils, where microorganisms are inactive or localized in deeper soil layers, CO production in upper soil layers is not balanced by oxidation (11). Therefore, significant quantities of CO are emitted into the atmosphere from regions with arid climate. On a global basis, however, the source strength of soils for atmospheric CO is most probably less than 30 Tg year⁻¹ and, thus, is considerably smaller than the total sink strength of 190–580 Tg year⁻¹ due to CO-consuming microorganisms (11).

Acknowledgments

We thank Carsten Köbbeman for technical assistance.

Registry No. CO, 630-08-0; O₂, 7782-44-7; phenol, 108-95-2; catechol, 120-80-9; resorcinol, 108-46-3; hydroquinone, 123-31-9; pyrogallol, 87-66-1; gallic acid, 149-91-7; phloroglucinol, 108-73-6;



ES&T

Order *your own* subscription to ES&T and be among the first to get the most authoritative technical and scientific information on environmental issues.

Yes, I want my own subscription to **ENVIRONMENTAL SCIENCE & TECHNOLOGY** at the rate I've checked:

One Year	ACS Members		Nonmembers	
	U.S.	Personal	Personal	Institutional
U.S.	<input type="checkbox"/> \$ 26	<input type="checkbox"/> \$ 35	<input type="checkbox"/> \$ 149	<input type="checkbox"/> \$ 157
Mexico & Canada	<input type="checkbox"/> \$ 34	<input type="checkbox"/> \$ 43	<input type="checkbox"/> \$ 157	<input type="checkbox"/> \$ 172
Europe	<input type="checkbox"/> \$ 40	<input type="checkbox"/> \$ 49	<input type="checkbox"/> \$ 58	<input type="checkbox"/> \$ 172
All Other Countries	<input type="checkbox"/> \$ 49	<input type="checkbox"/> \$ 58	<input type="checkbox"/> \$ 67	<input type="checkbox"/> \$ 172

Payment Enclosed (Payable to American Chemical Society)
 Bill Me Bill Company Charge my: VISA MasterCard

Card No. _____
Exp. Date _____ Interbank # _____
(Mastercard Only)

Signature _____
Name _____
Title _____
Employer _____
Address _____
City, State, Zip _____

Employer's Business: Manufacturing, type _____
 Academic Government Other _____

*Subscriptions at these rates are for personal use only.
All foreign subscriptions are now fulfilled by air delivery. Foreign payment must be made in U.S. currency by international money order, UNESCO coupons, U.S. bank draft, or order through your subscription agency. For nonmember subscription rates in Japan, contact Maruzen Co., Ltd. Please allow 45 days for your first copy to be mailed. Redeem until December 31, 1985.

MAIL THIS POSTAGE-PAID CARD TODAY!



**CALL
TOLL
FREE**

(800) 424-6747 (U.S. only)



NO POSTAGE
NECESSARY
IF MAILED
IN THE
UNITED STATES

BUSINESS REPLY CARD

FIRST CLASS PERMIT NO 10094 WASHINGTON D C

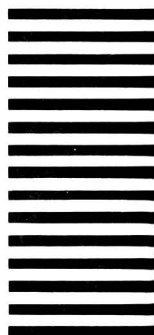
POSTAGE WILL BE PAID BY ADDRESSEE

American Chemical Society

Periodicals Marketing Dept.

1155 Sixteenth Street, N.W.

Washington, D.C. 20036



L-tyrosine, 60-18-4; coumaric acid, 25429-38-3; coniferyl alcohol, 458-35-5.

Literature Cited

(1) Bartholomew, G. W.; Alexander, M. *Appl. Environ. Microbiol.* **1979**, *37*, 932-937.
 (2) Bartholomew, G. W.; Alexander, M. *Environ. Sci. Technol.* **1982**, *16*, 300-301.
 (3) Conrad, R.; Seiler, W. *Appl. Environ. Microbiol.* **1980**, *40*, 437-445.
 (4) Ingersoll, R. B.; Inman, R. E.; Fisher, W. R. *Tellus* **1974**, *26*, 151-159.
 (5) Meyer, O.; Schlegel, H. G. *Annu. Rev. Microbiol.* **1983**, *37*, 277-310.
 (6) Conrad, R. In "Current Perspectives in Microbial Ecology"; Klug, M. J.; Reddy, C. A., Eds.; American Society for Microbiology: Washington, DC, 1984; pp 461-467.
 (7) Conrad, R.; Seiler, W. *Arch. Microbiol.* **1982**, *132*, 41-46.
 (8) Liebl, K. H.; Seiler, W. In "Production and Utilization of Gases"; Schlegel, H. G.; Gottschalk, G.; Pfennig, N., Eds.; Goltze KG: Göttingen, Federal Republic of Germany, 1976; pp 215-229.
 (9) Seiler, W. In "Environmental Biogeochemistry and Geomicrobiology"; Krumbein, W. E., Ed.; Ann Arbor Science Publishers: Ann Arbor, MI, 1978; Vol. 3, pp 773-810.
 (10) Conrad, R.; Seiler, W. *Geophys. Res. Lett.* **1982**, *9*, 1353-1356.
 (11) Conrad, R.; Seiler, W. *J. Geophys. Res.* **1985**, *90*, 5699-5709.
 (12) Seiler, W.; Liebl, K. H.; Stöhr, W. T.; Zakosek, H. Z. *Pflanzenernähr. Bodenkd.* **1977**, *140*, 257-272.

(13) Slemr, F.; Conrad, R.; Seiler, W. *J. Atmos. Chem.* **1984**, *1*, 159-169.
 (14) Seiler, W.; Giehl, H.; Roggendorf, P. *Atmos. Technol.* **1980**, *12*, 40-45.
 (15) Merkel, P. B.; Kearns, D. R., *J. Am. Chem. Soc.* **1972**, *94*, 7244-7253.
 (16) Stevenson, F. J. "Humus Chemistry"; Wiley: New York, 1982; pp 195-220.
 (17) Calvert, F.; Cloez, S.; Boussingault, M. *Justus Liebigs Ann. Chem.* **1864**, *130*, 248-249.
 (18) Miyahara, S.; Takahashi, H. *J. Biochem. (Tokyo)* **1971**, *69*, 231-233.
 (19) Nanni, E. J., Jr.; Stallings, M. D.; Sawyer, D. T. *J. Am. Chem. Soc.* **1980**, *102*, 4481-4485.
 (20) Choudhry, G. G. In "The Handbook of Environmental Chemistry"; Hutzinger, O., Ed.; Springer: Berlin, Federal Republic of Germany, 1984; Vol. 1C, pp 1-24.
 (21) Gohre, K.; Miller, G. C. *J. Agric. Food Chem.* **1983**, *31*, 1104-1108.
 (22) Baxter, R. M.; Carey, J. H. *Nature (London)* **1983**, *306*, 575-576.
 (23) Haag, W. R.; Hoigné, J.; Gassman, E.; Braun, A. M. *Chemosphere* **1984**, *13*, 641-659.
 (24) Conrad, R.; Seiler, W. *FEMS Microbiol. Lett.* **1980**, *9*, 61-64.
 (25) Conrad, R.; Seiler, W.; Bunse, G.; Giehl, H. *J. Geophys. Res.* **1982**, *87*, 8839-8852.

Received for review December 27, 1984. Accepted May 7, 1985. This work was financially supported by Bundesministerium für Forschung und Technologie (KBF 68).

Diffusion and Partitioning of Hexachlorobiphenyl in Sediments

Dominic M. Di Toro,* John S. Jerls, and Daniel Clarcia

Environmental Engineering and Science Program, Manhattan College, Bronx, New York 10471

■ The diffusion coefficient and partition coefficient of hexachlorobiphenyl (HCBP) in a sediment are determined by using a dual radio-tag experiment that extended over 2 years. Essentially constant coefficients were observed. An independent measurement of the diffusion coefficient for a nonsorbing chemical (tritiated water) allows an estimate to be made of the interstitial water-sediment partition coefficient. The result is in close agreement with that predicted from hydrophobic sorption correlations based upon sediment organic carbon and HCBP octanol-water partition coefficient. It also corresponds to the low particle concentration limit of the partition coefficients found when batch equilibrations of dilute suspensions of the same sediment were used.

Introduction

The fate of persistent hydrophobic chemicals in natural bodies of water is greatly influenced by the transport mechanisms between sediments and the overlying water: particle transport (settling and resuspension) and interstitial water diffusion. An analysis of each of these mechanisms is required if rational mass balance calculations of chemical fate are to be made. The purpose of this paper is to present an experimental investigation of the latter mechanism. It is designated to evaluate the diffusive mass transport and partitioning of a highly sorbed chemical, hexachlorobiphenyl (HCBP), in undisturbed sediments.

Conventional reversible sorption theory predicts that the apparent diffusion coefficient of total chemical, D_s^* (cm^2/day), is (1)

$$D_s^* = \frac{D_s}{1 + m\rho_s/\phi} \quad (1)$$

where D_s is the aqueous diffusion coefficient (cm^2/day) in the interstitial water for nonadsorbing chemicals, m is the sediment solids concentration $m = \rho_s(1 - \phi)$, π is the adsorption-desorption partition coefficient (L/kg), and ϕ is the porosity. For this equation to apply, adsorption and desorption are assumed to be described by a linear reversible isotherm.

The initial concern was what would the effect of non-reversible HCBP adsorption-desorption, which has been observed in agitated suspended sediment experiments (2), be on the rate of diffusion in sediments. Nonreversible behavior may inhibit migration as has been observed for soil column leaching experiments (3). The importance of the question is related to the burial of chemical by sedimentation. If contaminated sediment is buried by uncontaminated sediment faster than interstitial water diffusion can contaminate the newly deposited layer, then sedimentation in the absence of bioturbation provides an ultimate sink for sorbed chemical.

A second, and more puzzling, question relates to the effect of particle concentration on the measured partition coefficient in agitated suspensions. It has been observed by using conventional batch experiments (4) that both the adsorption and reversible partition coefficient for HCBP decrease with increasing particle concentration, m . The question was which partition coefficient describes sorption in stationary sediments.

The experiment is not without its practical difficulties. If l is the distance from the initially contaminated sedi-

Table I. Sediment Properties for Saginaw Bay Station 50 (<75- μ m Fraction)

organic matter, %	7.6
organic carbon fraction, %	2.8
surface area, m ² /g	12.8
size fractions, μ m	% total weight
1-2	4
2-10	15
10-30	20
30-75	61

ment layer, then the time, t , to reach this distance is on the order of

$$l \sim \sqrt{2D_s * t} \quad (2)$$

For example, if $m/\phi = 1$ kg/L, $\pi = 10^5$ L/kg, and $D_s = 1$ cm²/day, then after 1 day, the concentration is predicted to migrate a distance of $l = 0.045$ mm, and after 100 days, the distance is increased only 10-fold. Thus, it is necessary to be able to measure changes of concentration in distances on the order of 0.1 mm and to be able to wait for time periods on the order of 10² days (5, 6).

Materials and Methods

The experimental vessel is a hypodermic syringe from which the top assembly is removed. A layer of uncontaminated sediment is deposited and allowed to settle, and the supernatant is removed. A layer of HCBP-contaminated sediment is added and allowed to settle, and the supernatant is removed. A final layer of uncontaminated sediment is added and settled, the supernatant is removed, and the syringe is capped.

After a specified period of time has elapsed for migration to take place, the syringe is mounted on a device that is equipped with a screw-driven mechanism that advances the syringe plunger in small (0.125–0.25 mm) increments. The exuded sediment slices are carefully removed and analyzed for radioactivity. Thus, it is possible to examine the profile of HCBP in fractions of millimeter increments throughout the sediment column.

The initial design involved only HCBP-tagged sediment. However, it was soon discovered that ambiguous results could be obtained since it is not possible to exclude the possibility that, initially, the interface regions between tagged and untagged sediment were not exactly perpendicular (to within ~ 0.2 mm) to the syringe axis. As a consequence, the horizontal slices through a tilted interface would give the false impression of migration.

The solution to the problem was a double-tag experiment. A small quantity of an absolute particle tracer, [¹⁴C]graphite particles, was added to the tritiated HCBP tagged sediment. The liquid scintillation counter can distinguish between the tritium and carbon-14. The migration of the HCBP is then unambiguously monitored since if it appears in a sediment slice in excess of the [¹⁴C]graphite concentration, the only possibility is that aqueous phase diffusive transport has occurred.

The sediment used in these experiments was obtained from Saginaw Bay (station 50) (see ref 4 for station location and sediment properties). The sediment was wet sieved through a no. 200 sieve (75 μ m) to remove the coarse material which would interfere with the slicing. Table I lists the sieved sediment characteristics. The preparation of the dual-tag sediment began with the transfer of the contents of an ampule containing 40 μ Ci of [³H]HCBP into a 250-mL Erlenmeyer flask. This [³H]HCBP was a con-

centrated stock solution of custom synthesized 2,4,5,2',4',5'-hexachlorobiphenyl in acetone with a high specific concentration (38.2 Ci/mmol; New England Nuclear Corp.). The ampule was rinsed twice with acetone and the rinse placed into the flask. The acetone was evaporated by purging the flask with a moderate flow of nitrogen which first passes through a distilled water trap. To prevent atmospheric contamination, the exit gas was passed through octanol and amyl alcohol traps.

After the acetone was evaporated, 25 g of wet sediment (approximately 20 ml) and 10 mL of distilled water were added to the flask to make the sediment less viscous. The flask was placed on a wrist action shaker and allowed to shake for 4 days. At this point, samples were removed from the flask and analyzed for ³H radioactivity. The final step was the addition of 2 μ Ci of [¹⁴C]graphite particles (10 mCi/mmol; New England Nuclear Corp.) to the flask which was then shaken overnight. The weight fraction of added graphite was insignificant. The flask contents were allowed to settle for 24 h, and 9 mL of supernatant was withdrawn with a syringe. The remaining sediment mixture containing both [¹⁴C]graphite and sorbed [³H]HCBP was used as the stock sediment for the dual isotope experiments. The concentration of sorbed HCBP was 23 ng of HCBP/g of dry sediment.

Disposable plastic syringes (3 mL, 0.8 cm i.d., Benton Dickenson), with their tips removed by using a lathe to assure a parallel cut, were the experimental vessels. Approximately 0.4 mL of untagged sediment was added to the syringe, and the sediment was allowed to settle for approximately 1 week. Any overlying water was carefully removed. Approximately 0.3 mL of tagged sediment was added in the same manner and allowed to settle for 4 days. Overlying water was removed and 0.3 mL of untagged sediment added. Stoppers were placed in the top of the reaction vessel syringes and the vessels placed in the humidifier.

Reaction vessels were removed from the humidifier at the appropriate time and placed in the extraction device. The plunger of the reaction vessel syringe was moved slowly and accurately by using an unconfined compression machine (Soiltest). The proving ring normally used in this device was removed and replaced with a stationary mounting block. Displacement was measured by a strain gage connected to the mounting block. A single-edged safety razor was used to slice the sediment. Glass tracks, mounted on the top of the block, were used to guide the cutting razor across the top of the reaction vessel. The upper end of the syringe was positioned flush with the glass tracks and clamped securely. A slice was taken by the raising the platform the desired slice thickness and slowly moving the razor along the glass tracks perpendicular to the mounting block. The sediment slice, which adheres to the razor, was carefully jetted with water into a 20-mL liquid scintillation counting vial by using a 1-mL syringe with 1 mL of distilled water, 10 mL of Aquasol was added, and this was mixed by using a vortex mixer for 15 s. The vial was counted for 2 min on a liquid scintillation counter using the carbon-14 window. The vial was then centrifuged at 6000g for 15 min in order to remove both the [¹⁴C]graphite and sediment particles. The toluene-base Aquasol extracts the HCBP into the liquid phase, which was decanted into another vial, and then this phase was counted for 2 min by using the tritium window to measure the concentration of [³H]HCBP in the slice. The extraction efficiency was typically greater than 80%.

Identically prepared syringes were used to measure the diffusion coefficient of tritiated water. To a 3-mL syringe

Table II. Tritiated Water Diffusion Experiment

porosity in syringe	$\phi = 0.75$
solids density, g/cm ³	$\rho_s = 2.65$
solid-liquid phase ratio, kg/L	$m/\phi = \rho_s(1 - \phi)/\phi = 0.883$
sediment volume, μL	$v_2 = 1400$
diffusion coefficient, cm ² /day	$D_{s,H_2O} = 1.5$

Overlying Water Volume

t, min	$v_1, \mu\text{L}^a$
0	330
30	290
120	255
180	255

^a Volume is linearly interpolated between the tabulated values.

containing 1.4 mL of consolidated sediment were added 300 μL of distilled water and, after 1 h, 30 μL of ³H₂O. Samples of this overlying water (5 μL) were taken at prescribed intervals and were counted for radioactivity.

Analysis of Tritiated Water Diffusion

An independent measurement of the interstitial water diffusion coefficient can be made with a nonadsorbing substance. Tritiated water is an ideal choice since its presence does not significantly alter the ionic composition of the interstitial water as would be the case if, for example, high concentrations of a major cation or anion were introduced.

The conventional method (e.g., see ref 7) is to introduce a quantity of tracer into the water overlying the sediment and, after the passage of a suitable length of time, to measure the depth distribution of the tracer. The problem with this approach when applied to the syringe experimental design is that a considerable time is required to slice the sediment and, during this time, the tracer continues to diffuse within the progressively shortening sediment column. Although it is possible to numerically compute the spatial distribution of tracer to be expected for this situation, the method lacks a directness which can be achieved by simple modification.

Instead of relying on the depth distribution of the tracer at a fixed time, it is possible to measure the decline of tracer concentration in the overlying water with time as the tracer diffuses into the sediment (e.g., see ref 8). If the volume ratio of overlying water to interstitial water is suitably small so that the decline is appreciable, and the tracer measurement is sufficiently sensitive so that only small volumes need to be removed from the overlying water, then the analysis of this experiment is direct.

Let l_1 be the depth of the overlying water and l_2 be the depth of sediment. Let $C_{T1}(t)$ and $C_{T2}(z,t)$ be the tracer concentrations in the overlying and interstitial water, respectively, at time t and depth z , positive downward. The mass balance equation for the overlying water is

$$l_1 A \frac{dC_{T1}}{dt} = D_s A \left. \frac{\partial(\phi C_{T2})}{\partial z} \right|_{z=0} \quad (3)$$

where A is the interfacial area. This equation states that the time rate of change of tracer in the overlying water is due to the diffusive flux of tracer into the sediment. The mass balance equation in the sediment is

$$\frac{\partial(\phi C_{T2})}{\partial t} - D_s \frac{\partial^2(\phi C_{T2})}{\partial z^2} = 0 \quad 0 < z < l_2 \quad (4)$$

The boundary conditions correspond to continuity of fluid tracer concentration at $z = 0$

$$C_{T1}(t) = C_{T2}(0,t) \quad (5)$$

and a zero flux condition at the sediment bottom:

$$\left. \frac{\partial C_{T2}(z,t)}{\partial z} \right|_{z=l_2} = 0 \quad (6)$$

The solution of these equations is known to be (9)

$$C_{T1}(t) = \frac{C_{T1}(0)}{1+k} \left[1 + 2k(k+1) \sum_{i=0}^{\infty} \frac{\exp(-\alpha_i^2 T)}{P_i} \right] \quad (7)$$

$$C_{T2}(z,t) = \frac{C_{T1}(0)}{1+k} \times \left[1 + 2k(k+1) \sum_{i=0}^{\infty} \frac{\exp(-\alpha_i^2 T) \cos(\alpha_i^2(1-z/l_2))}{P_i \cos(\alpha_i)} \right] \quad (8)$$

where

$$k = l_2 \phi / l_1 \quad (9)$$

$$P_i = \alpha_i^2 + k(k+1) \quad (10)$$

$$T = D_s t / l_2^2 \quad (11)$$

and α_i values are the positive roots of

$$k \tan \alpha_i + \alpha_i = 0 \quad (12)$$

For small times a fairly large number of roots are required for accurate solutions, but no computational problems arise. The solution is easily checked at $t = 0$ to determine the maximum number of terms required in the sums. Note that at $t \rightarrow \infty$, the solutions conserve mass

$$l_1 C_{T1}(0) = l_1 C_{T2}(\infty) + l_2 \phi C_{T2}(z,\infty) \quad (13)$$

as they should.

One refinement is required to account for the effect of sample withdrawal on the volume and therefore the depth, l_1 , of the overlying fluid. Initially $v_1 = l_1 A = 330 \mu\text{L}$, whereas at the end of the experiment, $v_1 = 255 \mu\text{L}$. This is a large enough change to influence the computations. However, instead of solving this problem directly, the following approximation is employed. At each time, t , the average depth

$$\bar{l}_1(t) = (1/t) \int_0^t l_1(t) dt \quad (14)$$

is computed, and this is used in eq 7-12 for C_{T1} . While this is not a rigorously correct solution, it appears to be a reasonable approximation. One check is to compare the actual tracer mass lost via sampling to that removed from the computation by using $\bar{l}_1(t) = A(l_1 - \bar{l}_1(t))C_{T1}(0)$ at each sampling time. The average absolute error for the volume ratio employed in this experiment is 17%. Errors are positive during the early periods (more mass lost than computed) and negative in the latter stages. However, the approximation appears reasonable and simple to apply.

The results of the analysis are shown in Figure 1A, for two replicate experiments. The coefficients and relevant parameters are listed in Table II. The apparent sediment diffusion coefficient is found to be $D_{s,H_2O} = 1.5 \text{ cm}^2/\text{day}$.

As a confirmation of this result, a spatial profile that resulted after an exposure time of 2.5 h is shown in Figure 1B. Beyond the first few slices, the flattening of the data profile due to the increased dispersion during the slicing is evident. Nevertheless, the data are in reasonable agreement with the diffusion coefficient estimated from the penetration experiment.

The apparent sediment diffusion coefficient found from these experiments can be compared to empirical correlations found for natural sediments. The relationship be-

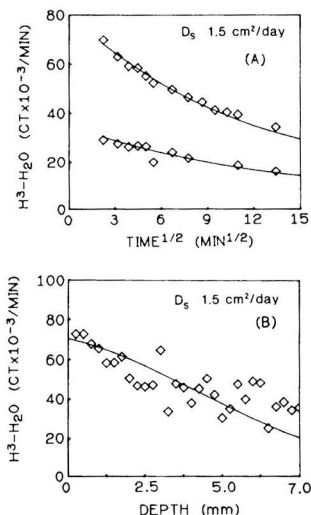


Figure 1. Tritiated water diffusion. Overlying water concentration vs. time (A). Total $^3\text{H}_2\text{O}$ concentration vs. depth after $t = 2.5$ h (B).

tween the molecular diffusion coefficient, D , and the apparent sediment diffusion coefficient, D_s , is (1)

$$D_s = D/\theta^2 \quad (15)$$

where θ is the tortuosity: the ratio of the length of the actual diffusion path to the linear length of the sediment. It has been found empirically (1) that

$$\theta^2 = \phi F \quad (16)$$

where F is the formation factor: $F = R/R_0$, the ratio of the electrical resistivity of the bulk sediment to the pore fluid. Analyses of actual sediments yield the relationship (10)

$$F = \phi^{-n} \quad (17)$$

where $n = 2.8$. If $n = 2$, this relationship is known as Archie's law. Thus

$$D_s = D\phi^{1.8} \quad (18)$$

For the syringe experiments, $\phi = 0.75$ and $D_{^3\text{H}_2\text{O}} = 1.81$ cm^2/day (11) so that the expected value is $D_{s,^3\text{H}_2\text{O}} = 1.08$ cm^2/day which can be compared to $D_{s,^3\text{H}_2\text{O}} = 1.5$ cm^2/day found experimentally.

Analysis of HCBP Diffusion

The distribution of an adsorbing chemical in a sediment is determined by the diffusive migration in the interstitial water and its adsorption-desorption behavior. If reversible adsorption-desorption is assumed, with a linear isotherm applicable to both adsorption and desorption, and if adsorption-desorption equilibrium is attained on a time scale that is short relative to the diffusive time constant, then it has been shown (1) that the governing equation is

$$\frac{\partial(\phi C_T)}{\partial t} - \frac{\partial}{\partial z} \left(\phi D_s^* \frac{\partial C_T}{\partial z} \right) = 0 \quad (19)$$

For the syringe experiments, the initial condition is

$$C_T(z,0) = C_{T0} \quad z > 0 \quad (20)$$

$$C_T(z,0) = 0 \quad z < 0 \quad (21)$$

where $z = 0$ is the interface boundary. If the syringe boundaries are far enough from the interface so that an

infinite spatial domain is a reasonable approximation, the solution is known to be (12)

$$C_{T1}(z,t) = \frac{C_{T0}}{2} \operatorname{erfc} \left(\frac{-z}{2\sqrt{D_s^*t}} \right) \quad z < 0 \quad (22)$$

$$C_{T2}(z,t) = \frac{C_{T0}}{2} \left[1 + \operatorname{erf} \left(\frac{z}{2\sqrt{D_s^*t}} \right) \right] \quad z > 0 \quad (23)$$

where

$$D_s^* = \frac{D_{s,\text{HCBP}}}{1 + m\pi/\phi} \quad (24)$$

$m = \rho_s(1 - \phi)$, the solids concentration, π is the partition coefficient, and $D_{s,\text{HCBP}}$ is the diffusion coefficient of HCBP in the sediment interstitial water in the absence of sorption.

The experimental measurements do not produce the continuous profiles that actually exist but rather the slice average concentrations. The theoretical slice average concentrations can be computed from eq 22-23 by spatially averaging the solutions

$$\bar{C}_T(z,t) = \frac{1}{d} \int_z^{z+d} C_T(z,t) dt \quad (25)$$

to yield

$$\bar{C}_{T1}(z,t) = \frac{C_{T0}}{2} \frac{\sqrt{4D_s^*t}}{d} \left[\operatorname{ierfc} \left(\frac{-z-d}{2\sqrt{D_s^*t}} \right) - \operatorname{ierfc} \left(\frac{-z}{2\sqrt{D_s^*t}} \right) \right] \quad (26)$$

$$\bar{C}_{T2}(z,t) = \frac{C_{T0}}{2} \left\{ 2 - \frac{\sqrt{4D_s^*t}}{d} \left[\operatorname{ierfc} \left(\frac{z}{2\sqrt{D_s^*t}} \right) - \operatorname{ierfc} \left(\frac{z+d}{2\sqrt{D_s^*t}} \right) \right] \right\} \quad (27)$$

where

$$\operatorname{ierfc}(z) = \frac{1}{\sqrt{\pi}} e^{-z^2} - z \operatorname{erfc}(z) \quad (28)$$

is the integral of the complimentary error function and d is the slice thickness.

In order to estimate the partition coefficient via eq 24, the molecular diffusion coefficient of HCBP, D_{HCBP} , is required. This is estimated by using the Wilke-Chang correlation to molal volume (13). The latter is computed from the Le Bas additive volume increments of the molecular constituents (C, H, Cl, corrected for the two six-membered rings). The accuracy of these methods is quite acceptable (13): average error $\sim 4\%$ (Le Bas) and $\sim 11\%$ (Wilke-Chang). The result is $D_{\text{HCBP}} = 0.461$ cm^2/day (20 $^\circ\text{C}$). By use of the known molecular diffusion coefficient (11) of water, $D_{\text{H}_2\text{O}} = 1.81$ cm^2/day (20 $^\circ\text{C}$), and the measured tritiated water diffusion coefficient in the syringe, $D_{s,^3\text{H}_2\text{O}} = 1.5$ cm^2/day it follows that the molecular diffusivity of HCBP in the syringe in the absence of sorption is $D_{s,\text{HCBP}} = (D_{s,^3\text{H}_2\text{O}}/D_{\text{H}_2\text{O}})D_{\text{HCBP}} = 0.382$ cm^2/day . This value is used in eq 24 which gives the apparent diffusion coefficient of HCBP in the syringe.

A correction is required for the tilted interface, since slicing through it produces a profile that indicates an apparent diffusive motion. The method adopted is to fit

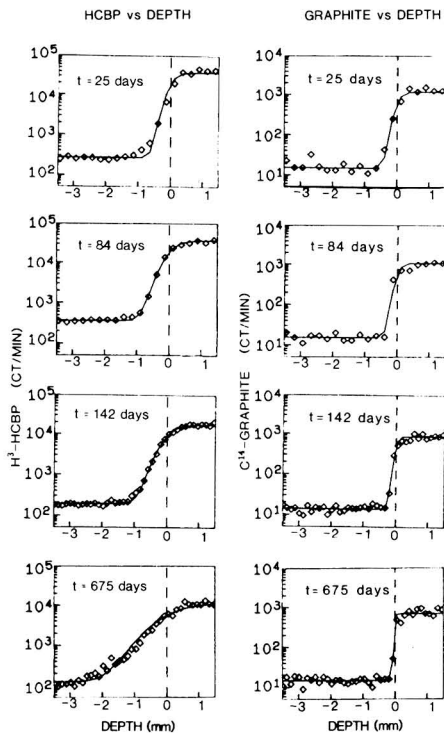


Figure 2. HCBP and graphite concentration vs. depth at various elapsed times. Curves are computed by using parameters in Table III.

simultaneously the $[^{14}\text{C}]$ graphite and $[^3\text{H}]$ HCBP data profiles to the solutions (eq 26 and 27 with $C_{T0} = 1$) normalized as

$$N_{\text{C}}(z) = N_{\text{CO}} + (N_{\text{C1}} - N_{\text{CO}})\bar{C}_{\text{T}}(z, t_g, D_{\text{s,HCBP}}^*) \quad (29)$$

$$N_{\text{H}}(z, t) = N_{\text{HO}} + (N_{\text{H1}} - N_{\text{HO}})\bar{C}_{\text{T}}(z, t_g + t', D_{\text{s,HCBP}}^*) \quad (30)$$

where t' is actual elapsed time from $t' = 0$, the start of the experiment, and N_{CO} , N_{HO} and N_{C1} , N_{H1} are the measured background (untagged region) and the tagged region counting rates for ^{14}C and ^3H , respectively, far from the interface. The location of the interface, $z = 0$, is chosen by examining the ^{14}C profiles. The idea is that at $t' = 0$ both the graphite and HCBP profiles are identical (this is the initial condition at $t = t_g$) and as t' increases HCBP diffuses relative to the graphite. This stratagem eliminates the need to solve eq 19 for an arbitrary initial condition. Rather a convenient initial condition, $\bar{C}_{\text{T}}(z, t_g, D_{\text{s,HCBP}}^*)$, is used which is itself a solution of eq 19 with t_g chosen to fit the graphite profile. As time, t' , increases, the HCBP profile, eq 30, evolves from that initial condition.

For the experimental data, the logs of the ^3H and ^{14}C counting rates are fit to eq 29 and 30 by using a nonlinear least-squares method (14) to estimate the two unknown parameters: π and t_g . Figure 2 illustrates the fits obtained for various elapsed times. Slice average concentrations are connected with a smooth curve for ease of presentation. The diffusive motion of HCBP relative to the graphite particle profile is evident. The observed HCBP profiles are remarkably regular and agree with the theoretical calculations over 2 orders of magnitude of HCBP concentration. Initially the slice thickness used was 0.254 mm. However, it was found that a more refined profile could

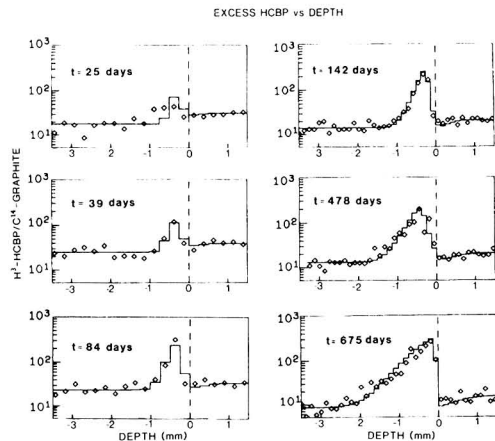


Figure 3. Excess HCBP (ratio of HCBP to graphite concentration) vs. depth at various elapsed times. Staircase curves are slice average ratios, computed by using parameters in Table III.

Table III. Estimates of Diffusion and Partition Coefficients

elapsed time, t , days	initial condition, t_g , days	$D_{\text{s,HCBP}}^*$, $\text{cm}^2/\text{day} \times 10^{-6}$	$\log \pi$, L/kg
25	23.3	4.82	4.95
39	28.3	4.43	4.99
69	37.3	3.66	5.07
71	12.4	4.56	4.98
83	0.21	2.26	5.28
84	16.1	5.70	4.88
140	28.4	2.60	5.22
142	9.7	4.44	4.99
478	45.1	2.66	5.21
675	0.35	4.43	4.99
		3.95 ± 1.12	5.06 ± 0.13

be obtained by using a slice thickness of 0.127 mm. This was the procedure used for the syringes with $t > 140$ days.

The initial apparent diffusive motion of HCBP at $t = 25$ day is actually due to a tilted interface. This can more clearly be seen in Figure 3 which presents the $[^3\text{H}]$ -HCBP/ $[^{14}\text{C}]$ graphite count ratio. This is the most sensitive measure of the extent of HCBP diffusion. Excess $^3\text{H}/^{14}\text{C}$ counting rate over the background ratio to the left of the interface can only be the result of diffusive migration of the $[^3\text{H}]$ HCBP in the interstitial water since the graphite particles are immobile. Depletion of HCBP to the right of the interface is also detectable at longer elapsed times. The computed slice average $^3\text{H}/^{14}\text{C}$ concentration ratios, $N_{\text{H}}(z, t)/N_{\text{C}}(z)$, are displayed as a staircase function over the slice thickness so that a more detailed comparison can be made to the data.

The lack of significant excess HCBP for $t = 25$ days indicates that no substantial interfacial mixing occurred during the preparation of the syringe or during the slicing procedure. The extent of migration increases regularly as elapsed time increases. However, even at the termination of the experiment (almost 2 years) the extent of migration is no more than 2-3 mm. It is this fact that necessitates the dual-tag experimental design. Table III tabulates the parameter estimates.

Discussion and Conclusions

As illustrated in Figures 2 and 3 the diffusion-linear reversible equilibrium model of chemical transport in

Table IV. PCB Sediment-Interstitial Water Partition Coefficients

chemical	sediment	organic carbon fraction, f_{oc} , %	$\log K_{oc} = \pi/f_{oc} \pm \log SD$, L/kg of organic carbon	reference
Aroclor 1242	Lake Michigan	0.7-3.8	4.17 ± 0.38	Eadie et al. (15)
Aroclor 1254	Lake Michigan	0.7-3.8	5.44 ± 0.55	Eadie et al. (15)
Aroclor 1254	pond	2.0	6.0	Halter and Johnson (16)
2,4,5,2',4',5'-HCBP	Saginaw Bay	2.8	6.61 ± 0.13	this study

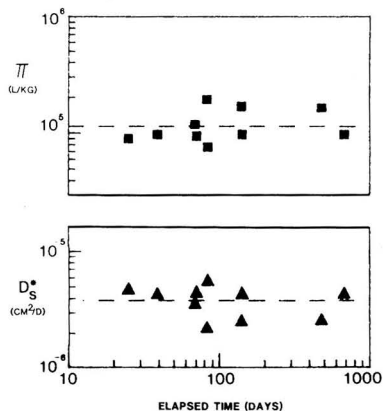


Figure 4. HCBP partition coefficient (upper and left axis) and apparent sediment diffusion coefficient (lower and right axis) vs. elapsed time for all syringes analyzed.

sediments satisfactorily reproduces the individual syringe observations. The estimates of apparent sediment diffusion and partition coefficients vs. elapsed time are shown in Figure 4. No temporal trends are evident so that the assumption of constant linear partition coefficient, $\pi = 10^{5.06 \pm 0.13}$, and therefore apparent sediment diffusivity, $D_{s,HCBP}^* = (3.95 \pm 1.12) \times 10^{-6} \text{ cm}^2/\text{day}$, is reasonable.

The partition coefficient for HCBP obtained from these experiments is compared in Figure 5 and Table IV to predictions from empirical hydrophobic partitioning equations based on the organic carbon fraction of the sediment, f_{oc} , and the octanol-water partition coefficient, K_{ow} , and with the few available direct (15) and indirect (16) observations of PCB partitioning in sediments. The octanol-water partition coefficients are somewhat uncertain for PCBs. Table V summarizes the available values. The value for HCBP is in reasonable accord with the predictions of the Karickhoff (17) correlations whereas the Lake Michigan results are somewhat lower although they are in reasonable accord with the Schwarzenback and Westall correlation (18).

Diffusion Coefficient. The situation with respect to inferred apparent diffusion coefficients for PCBs is less satisfactory. The results of leaching experiments using contaminated sediments have been reported in two cases (16, 19). An analysis based upon observed fluxes measured by recirculating the overlying water through a foam plug (19) indicated a sediment diffusion coefficient of $D_s^* = (0.0012-0.85) \times 10^{-6} \text{ cm}^2/\text{day}$ for four PCB isomers. An analysis of the reported overlying water PCB concentration vs. time in a static quiescent leaching experiment (16) which parallels the analysis used for the tritium penetration experiment yields $D_s^* = 0.05 \times 10^{-6} \text{ cm}^2/\text{day}$. These values are 1-3 orders to magnitude lower than the syringe results, $D_{s,HCBP}^* = 3.95 \times 10^{-6} \text{ cm}^2/\text{day}$.

For both these leaching experiments the organic carbon fraction of the sediments was similar to the syringe sediment so that these apparent diffusion coefficients would

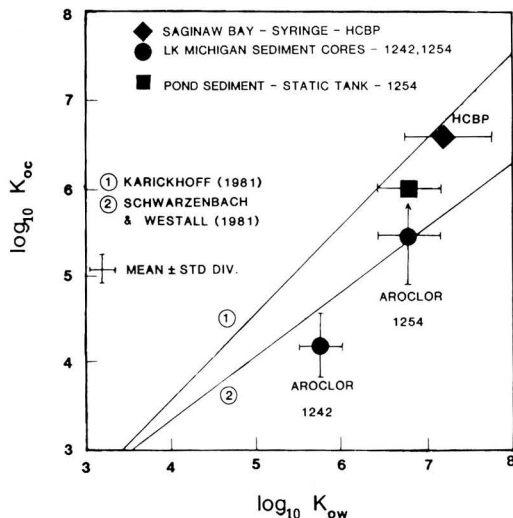


Figure 5. Sediment organic carbon partition coefficient (K_{oc}) vs. octanol-water partition coefficient (K_{ow}) for HCBP and PCB Aroclors.

Table V. log PCB Octanol-Water Partition Coefficient, K_{ow}

Aroclor 1242	Aroclor 1254	HCBP (2,2',4,4',5,5')	reference
5.58	6.72		Veith and Morris (25)
	6.47		Veith et al. (26)
		6.72	Chiou et al. (27)
5.90 ^a	7.17 ^a	7.75	Rapaport and Eisenreich (22)
		7.44	Bruggeman et al. (28)
		6.90	Woodburn et al. (29)
5.74 ± 0.23	6.79 ± 0.35	7.2 ± 0.48	mean \pm SD

^a Computed as $\sum f_i K_{owi} / \sum f_i$ for each fraction, f_i , of isomer with octanol-water partition coefficient K_{owi} in the mixture.

suggest PCB partition coefficient on an organic carbon basis, $K_{oc} = \pi/f_{oc}$ (L/kg of organic carbon), of $\log K_{oc} \sim 7.5-10.5$ by comparison to $\log K_{oc} = 6.6$ found for the syringe experiments (Table I and III). Such large partition coefficients appear unrealistic.

It may be that a large fraction, 90-99.9%, of the total PCB in the sediments used in the leaching experiments are nonreversibly bound. Since the framework used to estimate $D_{s,PCB}^*$ from these experiments assumes completely reversible behavior, the inferred partition coefficient would be artificially large in order to account for the large nonreversible fraction bound to the particles.

It should be pointed out that although the syringe experiments appeared to exhibit fully reversible behavior, this may not apply to native PCBs in sediment. For the Saginaw Bay sediment employed, 23 ng of [³H]HCBP/g were added to sieved Saginaw Bay Station 50 sediment.

Table VI. Partition Coefficients of HCBP for Saginaw Bay Station 50

		Syringe		
particle concn, m/ϕ , mg/L		$\log \pi/f_{oc}$, (L/kg of organic carbon)		ref
883000		6.61 ± 0.13		this work
		Suspensions		
particle concn, m/ϕ , mg/L	$\log \pi/f_{oc}$, L/kg of organic carbon			ref
	adsorption	reversible component		
10	6.30	6.18		30
25	6.05	5.9.		30
55	5.79	5.63		2
220	5.64	5.04		2
1100	5.40	4.21		4

Nonsieved Saginaw Bay sediments from similar locations have native Aroclor 1254 concentrations of ~400 ng/g (20, 21). Since 2,4,5,2',4',5'-HCBP is 3.67% of Aroclor 1254 (22), it is likely that >15 ng of HCBP/g of native chemical already was present in the sieved experimental sediment. In terms of the reversible-resistant model of PCB sorption (2), the additional radiolabeled chemical may not have sorbed to any available resistant sites (which would happen only if the tagged concentration were in excess of the native concentration) but, instead, only isotopically exchanged with the native reversible component already present. Since only the reversible component was radiolabeled, and since only very small concentrations migrated into the untagged (but HCBP containing) sediment, it is likely that the syringe experiment actually measured the reversible component partition coefficient, π_r . Whether native PCBs are fully reversible at these time scales remains to be determined.

It is also possible that unlike quiescent diffusion within a sediment the transport of PCBs between the sediment and overlying water in a leaching experiment is not well modeled when diffusion equation formulations are used. Very thin layers (<1 mm) at the sediment-water interface are involved in short-term leaching experiments, and the mass transport mechanisms may not be entirely diffusive in character. A 1-3 order of magnitude discrepancy invites a more careful experimental investigation of the mechanisms controlling static leaching fluxes.

Bioturbation of sediments by organisms also gives rise to apparent diffusive movement of sorbed chemical. Reported biodiffusion coefficients range from 10^{-1} - 10^{-2} cm²/day for near shore sediments to 10^{-3} - 10^{-4} cm²/day in pelagic sediments, to 10^{-5} - 10^{-6} cm²/day in deep sea sediments (1). Thus, in almost all cases transport by biological mixing will dominate the motion of highly sorbed chemicals in the bulk of the sediment. The mechanism controlling leaching of sorbed chemical to the overlying water, and the proper diffusion coefficient to be used in this case, with and without bioturbation, is still uncertain at present.

Particle Concentration Effects. It has been noted that the adsorption partition coefficient derived from dilute suspensions is a decreasing function of particle concentration (23). The syringe result is compared to the HCBP partition coefficients measured at various particle concentrations for the same sediment in Table VI. Note that whereas the suspension measurements decrease regularly with increasing particle concentration, the syringe result does not correspond to the extrapolation of this trend to the high particle concentrations characteristic of sediments but rather corresponds to the low particle con-

centration limit. A recently proposed model of reversible component sorption (24) attempts to rationalize this result. However, whatever the reason for this behavior is, it appears that the partition coefficient that applies to interstitial water-sediment sorption is the low particle concentration limit obtained in suspended sediment experiments. The result is in reasonable agreement with empirical correlations based upon less hydrophobic chemicals. The syringe methodology may be the most direct route for measuring partition coefficients of highly sorbed chemicals since no ambiguity results from particle concentration effects.

Acknowledgments

We are pleased to acknowledge the assistance and continuing support of our colleagues: the members of the EPA Large Lakes Research Station, William Richardson and Nelson Thomas (ERL-Duluth), and our group at Manhattan College, Donald O'Connor, Robert Thomann, and Lewis Horzempa (Envirosphere Corp.).

Registry No. HCBP, 26601-64-9; C, 7440-44-0.

Literature Cited

- Berner, R. A. "Early Diagenesis"; Princeton University Press: Princeton, NJ, 1980.
- Di Toro, D. M.; Horzempa, L. M. *Environ. Sci. Technol.* **1982**, *16*, 594-602.
- van Genuchten, M. Th.; Wierenga, P. J.; O'Connor, G. A. *Soil Sci. Soc. Am. J.* **1977**, *47*, 278-284.
- Di Toro, D. M.; Horzempa, L. M.; Casey, M. M.; Richardson, W. J. *Great Lakes Res.* **1982**, *8*, 336-349.
- Duursma, E. K. *Disposal Radioact. Wastes Seas, Oceans, Surf. Waters, Proc. Symp.* **1966**, 355-371.
- Walker, A.; Crawford, D. V. *Weed Res.* **1970**, *10*, 126-132.
- Hesslein, R. H. *Can. J. Fish. Aquat. Sci.* **1980**, *37*, 545-551.
- Officer, C. B. *Estuarine, Coastal Shelf Sci.* **1982**, *14*, 459-464.
- Carlsaw, H. S.; Jaeger, J. C. "Conduction of Heat in Solids", 2nd ed.; Oxford University Press: London, 1959; p 129.
- Manheim, F. T. *Earth Planet. Sci. Lett.* **1970**, *9*, 307-309.
- Wang, J. H.; Robinson, C. V.; Edelman, J. S. *J. Am. Chem. Soc.* **1953**, *75*, 466-470.
- Crank, J. "The Mathematics of Diffusion", 2nd ed.; Oxford University Press: London, 1975; p 39.
- Reid, R. C.; Prausnitz, J. M.; Sherwood, T. K. "The Properties of Gases and Liquids"; McGraw-Hill: New York, 1977; p 567.
- Marquardt, D. W. *J. Soc. Ind. Appl. Math.* **1963**, *11*, 431-441.
- Eadie, B. J.; Rice, C. P.; Frez, W. A. In "Physical Behavior of PCBs in the Great Lakes"; Mackay, D.; Paterson, S.; Eisenreich, S. J.; Simmons, M. S., Eds.; Ann Arbor Science: Ann Arbor, MI, 1983; pp 213-228.
- Halter, M. T.; Johnson, H. E. In "Aquatic Toxicology and Hazard Evaluation"; Mayer, F. L.; Hamelink, J. L.; Eds.; American Society for Testing and Materials: Philadelphia, 1977; ASTM STP 634, pp 178-195.
- Karickhoff, S. W. *Chemosphere* **1981**, *10*, 833.
- Schwarzenbach, R. P.; Westall, J. *Environ. Sci. Technol.* **1981**, *15*, 1360.
- Fisher, J. B.; Petty, R. L.; Lick, W. *Environ. Pollut., Ser. B* **1983**, *5*, 121-132.
- Richardson, W. L.; Smith, V. E.; Wethington, R. In "Physical Behavior of PCBs in the Great Lakes"; Ed. Mackay, D.; Paterson, S.; Eisenreich, S. J.; Simmons, M. S., Eds.; Ann Arbor Science: Ann Arbor, MI, 1983; pp 329-366.
- Thomann, R. V.; Mueller, J. A. In "Physical Behavior of PCBs in the Great Lakes"; Mackay, D.; Paterson, S.; Eisenreich, S. J.; M. S. Simmons, M. S., Eds.; Ann Arbor Science: Ann Arbor, MI, 1983; pp 283-310.
- Rapaport, R. A.; Eisenreich, S. J. *Environ. Sci. Technol.* **1984**, *18*, 163-170.

- (23) O'Connor, D. J.; Connolly, J. P. *Water. Res.* 1980, 14, 1517.
 (24) Di Toro, D. M. *Chemosphere*, in press.
 (25) Veith, G. D.; Morris, R. T. "A Rapid Method for Estimating Log P for Organic Chemicals". 1978, ERL-Duluth, EPA-600/3-78-049.
 (26) Veith, G. D.; De Foe, D. L.; Bergstedt, B. V. *J. Fish. Res. Board Can.* 1979, 36, 1040-1048.
 (27) Chiou, C. T.; Freed, V. H.; Schmedding, D. W.; Kohnert, R. L. *Environ. Sci. Technol.* 1977, 11, 475-478.
 (28) Bruggeman, W. A.; Van der Stenen, Jr.; Hutzinger, O. J. *Chromatography* 1982, 238, 335.
 (29) Woodburn, K. B.; Doucette, W. J.; Andren, A. W. *Environ. Sci. Technol.* 1984, 18, 457.
 (30) Di Toro, D. M.; Horzempa, L. M.; Casey, M. C. "Adsorption and Desorption of Hexachlorobiphenyl". Environmental Research Laboratory, Duluth, MN, 1983, Final Report to USEPA, EPA-600/53-83-088.

Received for review June 6, 1984. Revised manuscript received February 15, 1985. Accepted June 7, 1985. The research described in this paper was supported by U.S. EPA Grant R805229 and Cooperative Agreement CR807853.

Gas and Aerosol Wall Losses in Teflon Film Smog Chambers[†]

Peter H. McMurry*

Particle Technology Laboratory, Department of Mechanical Engineering, University of Minnesota, Minneapolis, Minnesota 55455

Daniel Grosjean

Daniel Grosjean and Associates, Inc., Suite 645, 350 North Lantana Street, Camarillo, California 93010

■ Large smog chambers (~60 m³) constructed of FEP Teflon film are frequently used to study photochemistry and aerosol formation in model chemical systems. In a previous paper (6) a theory for aerosol wall loss rates in Teflon film smog chambers was developed; predicted particle loss rates were in good agreement with measured rates. In the present paper, measurements of wall deposition rates and the effects of wall losses on measurements of gas-to-particle conversion in smog chambers are discussed. Calculations indicate that a large fraction (up to 83%; typical values of 33-70%) of the aerosol formed in several smog chamber experiments was on the chamber walls at the end of the experiment. Estimated values for particulate organic carbon yield for several precursor hydrocarbons increased by factors of 1.3-6.0 when wall deposition was taken into account. The theory is also extended to loss rates of gaseous species. Such loss rates are either limited by diffusion through a concentration boundary layer near the surface or by uptake at the surface. It is shown that for a typical 60-m³ Teflon film smog chamber, gas loss rates are limited by surface reaction rates if mass accommodation coefficients are less than 6×10^{-6} . It follows that previously reported loss rates of several gases in a chamber of this type (12) were limited by surface reactions.

Introduction

Smog chambers constructed of FEP Teflon (typically 0.005 cm in thickness) have been used by numerous investigators in studies of photochemistry and aerosol formation in model chemical systems (1-4). Teflon film smog chambers are inexpensive to build and are chemically inert. Also, Teflon film is transparent to sunlight for wavelengths greater than 300 nm and so can be used outside with natural radiation.

It is important to know aerosol-deposition rates when interpreting data from smog chamber experiments. Aerosol deposition affects mass balances of reacting compounds, net rates of aerosol formation, and size distributions. Understanding the effects of aerosol losses on size distributions is especially important when smog chamber

data are analyzed with the "growth law" technique. With this approach to data interpretation, changes in aerosol size distributions during an experiment are used to make inferences about chemical mechanisms of aerosol formation (2, 5). If wall deposition is sufficiently fast to affect the size distributions, it must be accounted for in the analysis.

Wall deposition of gas-phase species may also affect experimental results. The chemical systems that are studied in smog chambers are typically complex, involving many gas-phase species. The time dependence of any given species depends on its rates of formation and consumption by other species. Wall-deposition rates probably vary from species-to-species and thus introduce another removal rate in the differential equations that must be solved to determine the time history of the species. If wall-deposition rates are comparable or large compared to rates at which a species is consumed by chemical reactions, then wall deposition may affect the time history of this and other species.

In a recent paper, McMurry and Rader (6) reported on a theory for calculating particle wall-deposition rates in electrically charged vessels. The theory accounted for aerosol transport by natural convection, Brownian diffusion, electrostatic forces, and gravitational sedimentation. Theoretical predictions were compared with data for loss rates in 220-L Teflon film bags. Experiments were done with particles of known size and charge. It was shown that, for particles smaller than about 0.5 μm , charge has a major effect on deposition rates. For example, at 0.1 μm , loss rates of singly charged particles were a factor of 100 greater than loss rates of neutral particles. Theory and data were in good agreement.

The theory for particle wall-deposition rates in electrically charged chambers was also used to calculate particle wall-deposition rates in Teflon film smog chambers (6). It was shown that in a typical, well-stirred, 60-m³ chamber, wall-deposition rates for particles smaller than 0.05 μm are dominated by Brownian diffusion, while electrostatic deposition dominates for particles in the 0.05-1.0- μm diameter range. Gravitational sedimentation is the dominant loss mechanism for particles larger than 1.0 μm .

In this paper, data for aerosol wall-deposition rates in Teflon film smog chambers are presented, and the effects

[†]Particle Technology Laboratory Publication No. 508.

of aerosol wall losses on measurements of gas-to-particle conversion in smog chambers are discussed. In addition, the theory is extended to calculate wall-deposition rates for molecular species. Molecular species do not always stick to a surface on impact, and the extended theory accounts for nonaccommodation. It is shown that the rate-limiting process for gas losses can be either diffusion through a concentration boundary layer near the surface or uptake at the surface, depending on the mass accommodation coefficient for gas-surface collisions. The value of the mass accommodation coefficient that separates loss rates into diffusion-controlled and surface-controlled regimes depends upon turbulent mixing intensity within the chamber and on the mean thermal speed and diffusion coefficient of the gas.

Experimental Section

The data reported in this section were acquired at the smog chamber facility owned by Environmental Research Technology and located at the Camarillo, CA, airport. Data for particle- and gas-removal rates in large ($\sim 60 \text{ m}^3$) and small ($\sim 4 \text{ m}^3$) chambers are reported. Each of these pillow-shaped chambers was constructed from panels of 2-mil FEP Teflon film that were heat sealed together. A detailed description of the chamber facility can be found elsewhere (7).

Aerosol wall-deposition rates were determined by measuring rates at which the aerosol concentrations in several size ranges decreased with time. In each experiment, care was taken to ensure that changes in the aerosol size distribution were due primarily to wall deposition and not to other processes such as coagulation or gas-to-particle conversion. Coagulation effects were kept small by working at low concentrations ($< 25,000 \text{ cm}^{-3}$), and gas-to-particle conversion was minimized by working with systems that were not reacting chemically. Experiments were done with ambient aerosols (six runs) or with aerosols that were generated by photochemical reactions involving organics (six runs).

Data were obtained by measuring time-dependent aerosol size distributions with a TSI, Inc., Model 3030 electrical aerosol analyzer ($0.01 < \text{particle diameter} < 0.56 \mu\text{m}$) and with a Climet single-particle optical counter ($0.56 < \text{particle diameter} < 3.5 \mu\text{m}$). The electrical aerosol analyzer data were corrected for cross-sensitivity with the technique developed by Kapadia (8).

For each data set, the effects of coagulation were investigated. The AEROSOL code (9) with the transition regime collision frequency function of Fuchs (10) was used in these calculations. It was typically found that, for particles larger than $0.05 \mu\text{m}$, coagulation should have had no effect on decay rates. However, for particles smaller than this, coagulation was not always negligible. Typically, for particles of $0.013 \mu\text{m}$, coagulation accounted for about 25% of the observed loss rate.

For each experiment, particle loss rates for a range of particle sizes were determined by using the method of least squares to determine the best-fit first-order decay rate. Results were considered to be useful only when the decay rate could be determined to within a 95% confidence interval. Calculated loss rates were corrected for coagulation where necessary. Because the coagulation corrections were relatively small, the coupling of coagulation and wall deposition was neglected in making these corrections. Results of these wall loss measurements are shown in Figure 1.

McMurry and Rader (6) compared measured particle wall-deposition rates in the 60-m^3 chamber with theoretical predictions. Results of this comparison are presented in

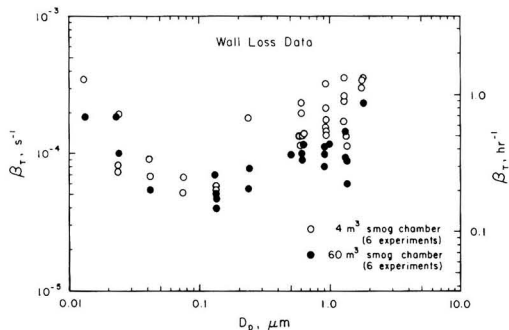


Figure 1. Measured aerosol wall-deposition rates as a function of particle size in small ($\sim 4 \text{ m}^3$) and large ($\sim 60 \text{ m}^3$) Teflon film smog chambers. Note that rates reach a minimum for particles of about $0.1\text{-}\mu\text{m}$ diameter.

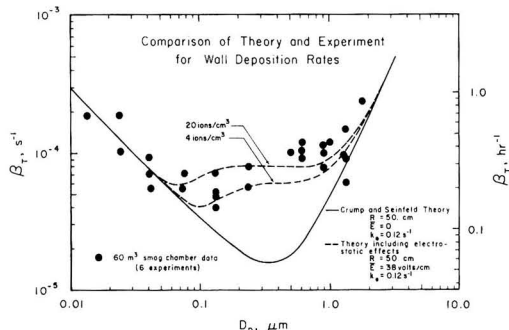


Figure 2. Comparison of measured and calculated aerosol wall-deposition rates in a 60-m^3 Teflon film smog chamber. Note that electrostatic effects must be included to explain observed particle loss rates.

Figure 2. Three theoretical curves are shown. The solid line applies to theoretical predictions for loss rates in a well-stirred chamber if Brownian diffusion and gravitational sedimentation are the only mechanisms of particle transport to the walls. The two dashed lines result when electrostatic deposition is also considered. (These curves apply for ion concentrations of 4 and 20 ions cm^{-3} , respectively. Ion concentration is important because particles acquire charge by collisions with ions. Deposition rates of charged particles can be several orders of magnitude faster than rates for neutral particles.) Note that electrostatic transport significantly affects deposition rates for particles in the $0.05\text{--}1.0\text{-}\mu\text{m}$ diameter range. Loss rates of smaller particles are dominated by Brownian diffusion; larger particles are lost primarily by sedimentation.

In one instance, the aerosol loss data obtained from size distribution measurements were complemented with a determination of aerosol loss based on chemical analysis of filter samples. The species thus determined, benzoic acid, was quantitated by ion chromatography with ultraviolet detection (11) following collection on Teflon filters. Benzoic acid was produced in situ by reaction of styrene ($\sim 1 \text{ ppm}$) and ozone ($\sim 0.5 \text{ ppm}$) in the dark by using a small ($\sim 4 \text{ m}^3$) FEP Teflon chamber as the reaction vessel. The chemical system was selected on the basis of chemical considerations (i.e., benzoic acid is the major, if not only, reaction product expected to be found in the condensed phase) as well as analytical constraints (the sensitive IC-UV method employed is suitable for short-term off-line measurements). Once the reaction was completed, as

Table I. Gaseous Species in FEP Teflon Film Chambers^a

compound	loss rate, $\times 10^{-6} \text{ s}^{-1}$		accommodation coefficients
	dark	sunlight	
O ₃	2.2 ^b 5.6 ^c	8.5 ^b 11 ^c	0.9×10^{-8} 1.75×10^{-8c}
NO	0.7 ^d	0.8	0.16×10^{-8}
NO ₂	-2.7 ^{d,e}	6.5	$<1.0 \times 10^{-8}$
NO _x	1.2 ^d	4.3	
SO ₂	2.2 ^d		0.73×10^{-8}
NH ₃	6.7-28 ^f		$(1.2-4.8) \times 10^{-8}$
HONO ₂	2.5		8.3×10^{-8}
n-butane	$<3.3^{d,g}$	<3.3	$<1.0 \times 10^{-8}$
n-pentane	$<3.3^{g}$	<3.3	$<1.2 \times 10^{-8}$
toluene	$<4.2^{d,g}$	<4.2	$<1.7 \times 10^{-8}$
styrene	$<4.0^{g}$		$<1.7 \times 10^{-8}$
β -methylstyrene	$<4.8^{g}$		$<2.2 \times 10^{-8}$
o-cresol	$<5.7^{g}$	<3.3	$<2.5 \times 10^{-8}$
benzaldehyde	5.7	NA ^h	$<2.4 \times 10^{-8}$
benzoic acid	18.		8.3×10^{-8}
biacetyl	$<4.2^{g}$	NA ^h	$<1.6 \times 10^{-8}$
pyruvic acid	$<4.2^{g}$	NA ^h	$<1.5 \times 10^{-8}$
CH ₃ ONO ₂	$<1.3^{g}$		$<0.5 \times 10^{-8}$
PAN	$<7.2^{d,g}$	6.5	$<1.5 \times 10^{-8}$

^a See Grosjean (12) for additional details about these measurements. ^b In large (60 m³) chamber. ^c In small (4 m³) chamber. ^d Measurements were carried out in both large and small chambers; results were not statistically different. ^e Loss in dark, if any, was offset by thermal oxidation of NO to NO₂. ^f Includes runs with humidified matrix air. ^g No measurable loss; upper limit calculated from experimental precision. ^h NA = not applicable; compound photolyzes in sunlight.

determined by monitoring ozone (complete disappearance) and styrene (constant concentration of unreacted hydrocarbon), filter samples were collected at 30-min intervals over a period of 3 h. The corresponding overall loss rate for benzoic acid aerosol to the chamber walls was determined to be $8 \times 10^{-5} \text{ s}^{-1}$, which falls within the range of $(3-20) \times 10^{-5} \text{ s}^{-1}$ for size-dependent aerosol losses determined by physical measurements for a variety of reactive systems in similar Teflon chambers.

Removal rates were also measured for a number of gaseous pollutants including inorganics (O₃, NO_x, and SO₂), hydrocarbons, oxygenates, and nitrogenous compounds. Experimental protocols and measurement methods are described in detail elsewhere (12). Loss rates were measured in the dark and, for compounds that are not photolabile, in sunlight. The results are summarized in Table I.

Results and Discussion

One important practical application of this work involves the computation of aerosol wall losses in smog chamber studies of chemically reactive systems and the correction of observed aerosol formation rates. While aerosol wall loss has often been cited in past studies as a possible cause for the poor carbon (or sulfur or nitrogen) mass balances obtained in smog chamber experiments, not even crude, order-of-magnitude estimates of the extent of such losses have been presented so far.

Accordingly, we have carried out aerosol wall loss calculations for three reactive systems involving 1-heptene, o-cresol, and methyl sulfide as aerosol precursors. Initial concentrations, experimental conditions, reaction products (including aerosol), and chemical mechanisms have been described in detail elsewhere (7, 14-17).

Size-dependent loss rates used in these calculations were averages of the measured rates. Figure 3 summarizes an example of aerosol wall loss as a function of reaction time

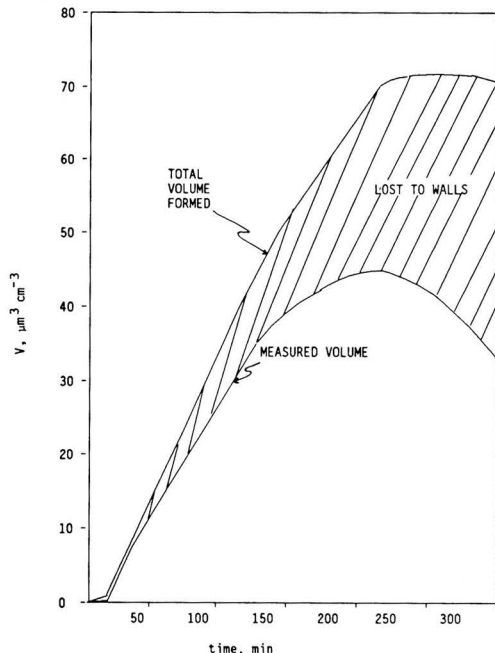


Figure 3. Measured aerosol volume concentrations and calculated losses to the walls. Note that after about 300 min, the amount of aerosol that had been lost to the walls was equal to the amount left in the chamber.

for an experiment involving sunlight irradiation of methyl sulfide and NO_x in purified, filtered air. The amount of aerosol lost to the walls was calculated by integrating time-dependent rates with respect to time. Time-dependent rates were determined by integrating size-dependent rates over measured particle size distributions. The total volume formed was assumed equal to the sum of the measured volume concentration and wall losses. Note that the total volume formed achieved a constant value after about 200 min, when aerosol formation had stopped. Note also that by the end of the experiment ($t = 300 \text{ min}$) only half of the aerosol formed during the experiment remained in the reactor.

Correction factors derived as indicated above were calculated for 33 experiments and are listed in Table II. These correction factors were in the range 1.2-3.4 for methyl sulfide (average = 2.0, 10 runs), 1.4-6.0 for 1-heptene (average = 2.6, 11 runs), and 1.1-2.5 for o-cresol (average = 1.5, 12 runs). These values clearly indicate that loss of aerosol to the walls must be taken into account as a major factor in smog chamber studies of aerosol formation.

Having established the extent of aerosol wall loss, we can now correct particulate organic aerosol formation rates and particulate organic carbon (POC) yields in the corresponding experiments. These results are listed in Table III for each chemically reactive system investigated. After corrections for aerosol loss to the chamber walls, POC formation rates are in the range 6-50 $\mu\text{g m}^{-3} \text{ h}^{-1}$ for 1-heptene, 0.2-27 $\mu\text{g m}^{-3} \text{ h}^{-1}$ for methyl sulfide, and 30-150 $\mu\text{g m}^{-3} \text{ h}^{-1}$ for o-cresol. The corresponding aerosol yields are 4-23%, 0.2-26%, and 4-20% for 1-heptene, methyl sulfide, and o-cresol, respectively.

It is of interest to compare the results in Table III to those obtained in previous studies. Despite the importance of establishing quantitative relationships between hydro-

Table II. Summary of Aerosol Wall Loss Data for Selected Reactive Systems in FEP Teflon Chambers

precursor organic	run ^a	irradiation time, min	aerosol volume concn, $\mu\text{m}^3 \text{cm}^{-3}$			correction factor ^b
			in chamber	lost to walls	total produced	
methyl sulfide ^c	65	347	110	260	370	3.36
	66	189	46	50	96	2.07
	67	169	33	31	64	1.91
	68	164	109	78	187	1.72
	69	141	67	32	99	1.48
	74	97	8.4	1.7	10	1.20
	75	287	35	35	70	2.00
	76	306	1.2	1.6	2.8	2.33
	77	336	42	82	124	2.96
	77F	72	27	7	34	1.25
	80	262	243	220	463	1.90
	80F	112	54	29	83	1.53
	81	149	256	84	340	1.32
	82	196	51	106	157	3.09
1-heptene ^d	82F	122	20	7	27	1.36
	87	140	4	20	24	5.97
	90A	222	14	24	39	2.69
	90B	202	17	21	38	2.23
	92A	351	0.7	3.4	4.1	5.86
	92B	323	3.7	2.3	6.0	1.62
	95	150	80	34	114	1.42
	117	190	62	52	114	1.84
	118	93	163	20	183	1.12
	196	138	18	6	24	1.34
	196F	36	0.2	0	0.2	
	197	143	36	12	48	1.34
	197F	117	29	8	37	1.27
	201	112	28	7.6	36	1.28
201F	214	27	22	49	1.81	
202	258	2.8	4.2	7.0	2.50	
203	99	50	9	59	1.18	
203F	231	31	32	63	1.97	
204	114	25.5	7.5	33	1.29	
nitrocresol ^f	186	255	51	150	201	3.92

^a See Grosjean et al. (7, 17–20) for experimental conditions, initial concentrations, and chemical mechanisms. Run numbers listed here are the same as in those references. ^b Correction factor = total aerosol produced/chamber aerosol concentration. ^c All runs are $\text{CH}_3\text{SCH}_3\text{-NO}_x$ irradiations. ^d Includes four types of experiments: 1-heptene–ozone in the dark (runs 87 and 90B), 1-heptene–ozone–ammonia in the dark (run 90A), 1-heptene– NO_x irradiation (run 92A), and 1-heptene– NO_x –ammonia irradiations (all other runs). ^e *o*-Cresol–ozone– NO_x in the dark (run 202) and *o*-cresol– NO_x irradiations (all other runs). ^f Nitrocresol– NO_x irradiation.

carbon emissions and organic aerosol formation in urban atmospheres (18, 19), experimental results concerning organic aerosol formation rates are only available for a few hydrocarbons. These results are summarized in Table IV and include the three precursors investigated in this work, three hydrocarbons we studied in an earlier phase of this project (7), four olefins including cyclic olefins (20), and toluene (21). For comparison, summertime POC levels in Los Angeles air (18) are in the range 7–47 (2-h average) or 4–28 $\mu\text{g m}^{-3}$ (24-h average), while POC formation rates in the Los Angeles area have been estimated to be in the range $\sim 1\text{--}5 \mu\text{g m}^{-3} \text{h}^{-1}$ (19).

Gas Loss Rates

Previous theoretical work for particle losses in well-stirred chambers (6, 13, 16) can be extended to calculate wall-deposition rates of molecular species. In this case diffusion is the only significant mechanism of transport to the chamber walls, and the steady-state concentration profile in the boundary layer near the surface is governed by

$$\nabla(D + D_e)\nabla C = 0 \quad (1)$$

where C = gas-phase concentration, D = diffusion coefficient, and D_e = eddy diffusion coefficient. The eddy diffusion coefficient, D_e , is determined by the turbulent mixing intensity within the bag and does not depend on

transport properties of the gases or particles. The expression used for D_e is

$$D_e = k_e x^2 \quad (2)$$

where k_e is referred to as the coefficient of eddy diffusion and x is the distance from the chamber wall.

For particle deposition by Brownian diffusion, eq 1 is subject to the boundary condition that particle concentrations approach zero at the chamber surface (6, 13, 16). This boundary condition applies only if species always stick to the surface upon impact (i.e., if accommodation coefficients equal 1.0) and if release from the surface to the gas phase after uptake does not occur. Accommodation coefficients for gases are likely to be less than unity. Steady-state concentrations will then be nonzero at the chamber surface. The solution to (1) is then (see, e.g., ref 13)

$$C(\xi) = C_1 - \frac{2}{\pi}(C_1 - C_0) \left\{ \frac{\pi}{2} - \tan^{-1} \xi \right\} \quad (3)$$

where C_1 = concentration of the gas in the well-mixed portion of the chamber (i.e., the measured concentration), C_0 = concentration at the surface, ξ = dimensionless distance from the chamber wall = $(k_e/D)^{1/2}x$, and x = actual (dimensional) distance from the chamber wall. The value of C_0 is related to the mass accommodation coefficient, α , for gas collisions at the chamber surface. For values of α

Table III. Wall Loss Corrected Particulate Organic Carbon (POC) Formation Rates and POC Yields

system	run	POC, $\mu\text{g m}^{-3}$	average POC formation rate, $\mu\text{g m}^{-3} \text{h}^{-1}$ ^a		POC yield, % ^b		
			measured	corrected for wall losses ^c	measured	corrected for wall losses ^c	
1-heptene-ozone (dark)	30	20	4.4		0.6		
	90B	13	2.6	5.8	1.9	4.2	
1-heptene-ozone-ammonia (dark)	90A	19	3.8	10.2	2.8	7.5	
1-heptene-NO _x (sunlight)	29	167	37.1		9.7		
	41-2	90	18.0		2.4		
	42-2	90	18.0		2.0		
	43-1	37	7.4		1.1		
	45-1	77	15.4		1.7		
	45-2	78	15.6		1.7		
	41-1	152	30.4		4.0		
	42-1	105	21.0		2.3		
1-heptene-NO _x -ammonia (sunlight)	43-2	128	25.6		3.7		
	80	157	26.2	49.8	4.5	8.5	
	81	96	16.0	21.1	3.4	4.5	
	82	64	11.6	35.8	3.7	11.4	
	83	124	22.5		1.8		
	92B	93	14.3	23.2	14.2	23.0	
	95	91	20.2	28.7	3.5	5.0	
	methyl sulfide-NO _x (sunlight)	39	68	17		6.9	
		47	60	15		4.1	
		65	28	4	13.4	4.8	16.1
66		6.5	1.6	3.3	0.26	0.54	
67		2.4	0.6	1.2	0.10	0.19	
68		49	16	27.5	6.9	11.9	
69		2.2	0.7	1.0	0.32	0.47	
74		0.8	0.4	0.5	0.35	0.42	
75		0.6	0.12	0.24	0.45	0.90	
76		2.0	0.4	0.9	1.6	3.7	
77		27	4.5	13.3	8.8	26.0	
113		18	3.0	3.7	2.7	3.4	
ethyl sulfide-NO _x (sunlight)		114	3.5	0.7		0.5	
	116	20	4.0		2.2		
	21	96	31		5.6		
<i>o</i> -cresol-NO _x (sunlight)	38	460	83		19.1		
	48	156	35		4.6		
	117	330	82	151	8.7	16.0	
	118	120	30	34	3.5	4.0	

^a POC measured at end of run divided by length of the run. ^b Percent of initial hydrocarbon (HC)₀, with (HC)₀ and POC in units of μg of carbon m^{-3} . ^c Using correction factors from Table II.

Table IV. Summary of Smog Chamber Studies of Organic Aerosol Formation

precursor hydrocarbon	POC formation rate, $\mu\text{g m}^{-3} \text{h}^{-1}$		POC yield, %	
	measured	corrected for wall losses	measured	corrected for wall losses
paraffins				
<i>n</i> -heptane ^a	<1		<0.06	
cyclohexane ^a	<1		<0.17	
olefins				
2,3-dimethyl-2-butene ^b	0		0	
1-hexene ^a	1.3-2.2		0.24-0.34	
1-heptene ^c	2.6-37	6-50	0.6-14	4-23
cyclopentene ^b	546-2460		33-39	
cyclohexene ^b	960		5-17	
1,7-octadiene ^b	90-258		7-13	
aromatics				
toluene ^d	5		1-2	
<i>o</i> -cresol ^c	30-80	35-150	3-9	4-16
organosulfur compounds				
methyl sulfide ^c	0.4-17	0.5-27	0.3-9	0.5-26
ethyl sulfide ^c	0.7-4		0.5-2.2	

^a Reference 7. ^b Reference 19. ^c Reference 17. ^d Reference 21.

less than 1.0, the net flux of gas molecules to the surface is

$$J = D \left. \frac{\partial C}{\partial x} \right|_{x=0} = \frac{\alpha C_0 \bar{v}}{4} \quad (4)$$

where \bar{v} = mean thermal speed of the gas molecules and α = mass accommodation coefficient. The right side of eq 4 derives from the kinetic theory of gases. It follows that the fractional loss rate of gas molecules to the surface, β_g , is

$$-\frac{1}{C_1} \frac{dC_1}{dt} = \beta_g = \left(\frac{A}{V}\right) \frac{\alpha \bar{v} / 4}{1.0 + (\pi/2)[\alpha \bar{v} / [4(k_e D)^{1/2}]]} \quad (5)$$

where A/V is the surface to volume ratio of the chamber. Note that no assumptions about chamber geometry were made in deriving this result.

Equation 5 shows that loss rates can be limited either by diffusion through the concentration boundary layer near the chamber walls or by rates of uptake at the surface. For sufficiently small values of α we have

$$\frac{\pi}{2} \frac{\alpha \bar{v}}{4(k_e D)^{1/2}} \ll 1.0 \quad (6)$$

It follows from (5) that in this limit of small α

$$\beta_g = \frac{A}{V} \frac{\alpha \bar{v}}{4} \quad (7)$$

This result applies when surface reactions limit removal rates. This is identical with loss rates that would be predicted from kinetic theory in the absence of a concentration boundary layer near the surface. On the other hand, if α is sufficiently large, than the removal rate is given by

$$\beta_g = \left(\frac{A}{V}\right) \frac{2}{\pi} (k_e D)^{1/2} \quad (8)$$

Note that this result is identical with the diffusion-limited result (see, for example, eq 19 in ref 6). We conclude that the value of α that separates loss rates into diffusion-limited and surface-reaction-limited uptake is

$$\alpha = \frac{8}{\pi} \frac{(k_e D)^{1/2}}{\bar{v}} \quad (9)$$

Grosjean (12) reported on loss rates of gaseous species in the 4- and 60-m³ Teflon film chambers used for measurements of particle wall loss rates in the present study (Figures 1 and 2). The value of k_e in the 60-m³ chamber was previously estimated to be 0.12 s⁻¹ (6). Using a similar methodology, we estimate a k_e value of 0.02 s⁻¹ for the small chamber. Characteristic values for gas diffusivity and mean thermal speed are 0.1 cm² s⁻¹ and 4.6 × 10⁴ cm s⁻¹. Using these values, we conclude that surface reactions will be dominant if measured accommodation coefficients are less than 6.1 × 10⁻⁶ and 2.5 × 10⁻⁶ for the large and small chambers, respectively.

Accommodation coefficients reported by Grosjean (12) are shown in Table I. Note that in all cases accommodation coefficients are small in comparison with the values calculated above. It follows that wall removal rates of these species are limited by reaction rates with the chamber surface.

In the above discussion, chemical removal processes are neglected. Conversely, the loss rates listed in Table I could be rationalized only in terms of removal by gas-phase reactions. Chemical removal is discussed in detail elsewhere (12) and will only be summarized here. Kinetic data for HC-ozone, HC-hydroxyl radical, and HC-nitrate radical, together with measured levels of ozone (< ppb) and NO_x impurities (6–12 ppb) in the matrix air, suggest that, at least for the most reactive hydrocarbons, chemical removal may have been important. For example, the loss rate for styrene by reaction with 1 ppb of ozone in the dark would be 8 × 10⁻⁷ s⁻¹ as compared to the measured value of ≤ 4 × 10⁻⁶ s⁻¹. In the same way, only 10⁻⁵ ppb (~2.5 × 10⁵ radicals cm⁻³) of the nitrate radical would be required to remove *o*-cresol at the rate given in Table I, and the measured loss rate of toluene in sunlight could be achieved

by reaction with 7 × 10⁴ OH radicals cm⁻³. Thus, both gas-phase removal and wall loss processes may contribute to the measured pollutant loss rates listed in Table I. If chemical reactions contributed to removal, then the actual accommodation coefficients would be smaller than values shown in Table I.

Conclusions

The effects of aerosol particle wall deposition on measurements of gas-to-particle conversion in Teflon film smog chambers were investigated. For the data that were examined, the influence of wall deposition tended to be relatively unimportant early in the experiments. However, calculations indicate that a large fraction (up to 83% typical values 33–70%) of the aerosol formed during an experiment was on the smog chamber walls at the end of a typical 3–4-h run. These calculations also indicate that actual particulate organic carbon yields (the fraction of the precursor hydrocarbon that is in the aerosol phase following chemical reactions) exceed values that have been reported previously. This is because previous data for POC yields did not account for aerosol deposition on the walls.

The theory can be extended to calculate wall-deposition rates for molecular species. In this case it is likely that not all collisions between gas molecules and the surface will result in uptake, and this is taken into account theoretically. It is shown that net wall loss rates of gaseous species can be limited either by rates of diffusion or by reactions with the surface. For a typical 60-m³ Teflon film chamber, rates will be limited by surface reactions provided that mass accommodation coefficients are less than 6 × 10⁻⁶. It follows that all gas loss rates reported by Grosjean (12) are limited by surface reaction rates.

Registry No. PAN, 2278-22-0; O₃, 10028-15-6; NO, 10102-43-9; NO₂, 10102-44-0; NO_x, 11104-93-1; SO₂, 7446-09-5; NH₃, 7664-41-7; HONO₂, 7697-37-2; CH₃ONO₂, 624-91-9; CH₃SCH₃, 75-18-3; *n*-butane, 106-97-8; *n*-pentane, 109-66-0; toluene, 108-88-3; styrene, 100-42-5; β -methylstyrene, 637-50-3; *o*-cresol, 95-48-7; benzaldehyde, 100-52-7; benzoic acid, 65-85-0; biacetyl, 431-03-8; pyruvic acid, 127-17-3; 1-heptene, 592-76-7; FEP Teflon, 25067-11-2.

Literature Cited

- Clark, W. E.; Whitby, K. T. *J. Colloid Interface Sci.* **1975**, *51*, 477–490.
- Heisler, S. L.; Friedlander, S. K. *Atmos. Environ.* **1977**, *11*, 158–168.
- Grosjean, D.; van Cauwenberghe, K.; Fitz, D. R.; Pitts, J. N., Jr. *Prepr. Pap.—Am. Chem. Soc. Div. Environ. Chem.* **1978**, *18*, 354.
- Kamens, R. M.; Jeffries, H. E.; Sexton, K. G.; Wiener, R. W. *Atmos. Environ.* **1982**, *16*, 1027–1034.
- McMurry, P. H.; Wilson, J. C. *J. Geophys. Res. C.: Oceans Atmos.* **1983**, *88*, 5101–5108.
- McMurry, P. H.; Rader, D. J. *Aerosol Sci. Technol.*, in press.
- Grosjean, D.; McMurry, P. H. National Technical Information Service, Springfield, VA, 1982, Report PB-82-262262.
- Kapadia, A. Ph.D. Thesis, University of Minnesota, Minneapolis, MN, 1980.
- Gelbard, F.; Seinfeld, J. H. *J. Comput. Phys.* **1978**, *28*, 357–375.
- Fuchs, N. A. "The Mechanics of Aerosols"; Pergamon Press: Oxford, 1964.
- Fung, K.; Grosjean, D. *Anal. Lett.* **1984**, *17*, 475–482.
- Grosjean, D. *Environ. Sci. Technol.*, in press.
- Crump, J. G.; Seinfeld, J. H. *J. Aerosol Sci.* **1981**, *12*, 405–415.
- Grosjean, D. *Sci. Total Environ.* **1984**, *37*, 195–211.
- Grosjean, D. *Atmos. Environ.* **1984**, *18*, 1641–1652.
- Grosjean, D. *Environ. Sci. Technol.* **1984**, *18*, 460–467.
- Grosjean, D.; McMurry, P. H. "Secondary Organic Aerosol Formation: Homogeneous and Heterogeneous Chemical

- Pathways", 219 Perimeter Center Parkway, Atlanta, GA, 1984, Phase 3 Final Report to Coordinating Research Council.
- (18) Grosjean, D. *Sci. Total Environ.* 1984, 32, 133-145.
- (19) Grosjean, D.; Smith, J. P.; Mischke, T. M.; Pitts, J. N., Jr. In "Atmospheric Pollution"; Benarie, M. M., Ed.; Elsevier: Amsterdam, 1976; pp 549-563.
- (20) Grosjean, D.; Friedlander, S. K. In "The Character and Origins of Smog Aerosols"; Hidy, G. M.; et al., Ed.; Wiley: New York, NY, 1979; pp 435-473.
- (21) Leone, J. A.; Flagan, R. C.; Grosjean, D.; Seinfeld, J. H. *Int. J. Chem. Kinet.* 1985, 17, 177-216.
- (22) Okuyama, K.; Kousaka, Y.; Hosokawa, T. In "Aerosols"; Liu, B. Y. H.; Pui, D. Y. H.; Fissan, H., Eds.; Elsevier: New York, 1984; pp 857-860.

Received for review December 17, 1984. Accepted June 3, 1985. This research was sponsored by the Coordinating Research Council, CAPA-20-80 project group.

Lead Cycling in an Acidic Adirondack Lake

Jeffrey R. White*

School of Public and Environmental Affairs, Indiana University, Bloomington, Indiana 47405

Charles T. Driscoll

Department of Civil Engineering, Syracuse University, Syracuse, New York 13210

Temporal and spatial variations in the concentration and transport of Pb were observed in acidic Darts Lake (Adirondack State Park, NY). Vertical deposition of Pb through the water column was most pronounced during stratification periods (winter and summer), while during high flow (spring and autumn) Pb was more conservative within the lake. Deposition of particulate Pb was strongly correlated with Al and organic carbon deposition. Increases in metal (Pb and Al) deposition occurred during periods of increasing pH. It appears that in-lake formation of particulate Al enhances the vertical transport of Pb in Darts Lake.

Introduction

A major consequence of depressed pH observed in dilute surface waters is elevated concentrations of Al (1, 2) and other trace metals (3-5). In addition, low concentrations of complexing ligands result in low trace metal buffering capacity (complexation of aquo metal) in these waters. Since the aquo form of trace metals is often toxic to aquatic organisms (6-8), an evaluation of trace metal chemistry and cycling in acidic lake systems is highly relevant. In particular, nearly all of the experimental data available on Pb toxicity (both in vitro and in vivo) show that the metabolic effects of Pb at concentrations as low as 10^{-6} M are of the inhibitory or adverse type (7). The U.S. Environmental Protection Agency recently proposed water quality criteria for Pb designed to protect freshwater aquatic life and its uses (9), where Pb concentrations (in each 30 consecutive days) must not exceed 7.2 nmol L^{-1} with an average concentration below 0.3 nmol L^{-1} (hardness = $120 \text{ } \mu\text{equiv L}^{-1}$). These criteria suggest that trace quantities of Pb in dilute acidic waters may be potentially deleterious to aquatic biota.

Acidic lake systems undergo temporal changes in the concentration of Al that appear to be associated with pH fluctuations (10). During the snowmelt period, waters that are high in H^+ , Al, and NO_3^- concentrations are introduced to acidic Adirondack New York lakes. During summer stratification biological processes of NO_3^- retentions (assimilatory and dissimilatory NO_3^- reduction) result in the generation of acid-neutralizing capacity and the neutralization of H^+ and Al acidity (11).

These seasonal variations in pH and soluble Al concentration may in turn be significant to the cycling of trace metals. In acidic lakes, slight increases in pH may result

in a decrease in aluminum solubility and conversion of aqueous aluminum to a particulate form. It is well established that oxides of aluminum and other metals (Fe, Si, and Mn) can regulate trace metal chemistry through surface adsorption processes (12-15). Therefore, in-lake formation of particulate aluminum may modify the cycling of trace metals through sorption (e.g., adsorption and coprecipitation) reactions.

Since Pb is known to have a high affinity for aluminum oxides even at pH levels between 4.5 and 5.5 (13), we hypothesize that oxide surfaces may play a significant role in regulating the transport of Pb within acidic lake systems with elevated concentrations of aluminum.

Experimental Section

Site and Sampling Description. A water column and sediment trap monitoring program was used to investigate important mechanisms regulating the chemistry and cycling of Pb in dilute acidic Darts Lake. Located in the drainage basin that forms the North Branch of the Moose River, Darts Lake is situated in the southwestern Adirondack region of New York State ($43^\circ 48' \text{ N}$, $74^\circ 52' \text{ W}$). Darts Lake is downstream from Big Moose Lake and is predominantly a drainage system with one major inlet stream and outlet (Figure 1).

Water samples were collected at the inlet, outlet, and a single pelagic sampling station (at 0.3-, 2-, 4-, 6-, 9-, 12-, and 14-m depths), approximately every 3 weeks from Sept 1981 to Nov 1982. Sediment traps (set in triplicate at 6- and 14-m depths) were used to assess the flux of particulate material settling through the water column in the pelagic region. The sediment trap design was consistent with the criteria established by Bloesh and Burns (16), including an aspect ratio (height/diameter) of 9 for each collector.

Analytical Methods. Stream height was measured on sampling dates by using flow-calibrated staff gauges at the inlet and outlet to monitor discharge. To provide an estimate of water flux through Darts Lake, correlations were made between on-site measurements of instantaneous discharge and continuous discharge recorded at the nearby Independence River site (Donnatsberg, NY) and a site on the Hudson River (Newcomb, NY). Correlations of flow per watershed area for Darts Lake were similar to either one or both continuous discharge sites throughout the study period. Thus, the estimated continuous flow for Darts Lake is believed to be representative of actual flow conditions. Our discharge data suggest that 95% of the

Darts Lake
 74° 52' W, 43° 48' N
 Surface Area 58 ha
 Volume 4.13×10^9 l

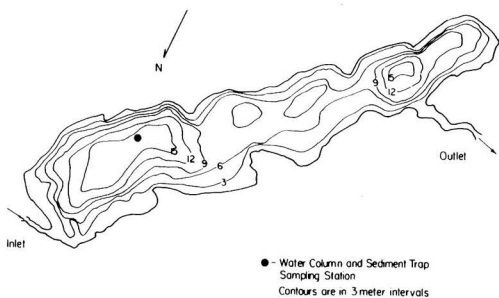


Figure 1. Darts Lake bathymetry and sampling sites.

outlet flow enters the lake at the major inlet (11).

Field measurements included dissolved oxygen (17), water column temperature, and daily on-site climatological data. The stream and water column chemical parameters monitored included dissolved organic carbon (18), monomeric Al forms (19, 20), and Pb. Al samples were extracted in the field, and pH was measured within 6 h of collection in the laboratory. To determine "dissolved Pb", centrifugation (5720 g for 30 min) was used to separate particulate metal from solution (21) and the supernatant acidified (0.5% v/v Ultrex HNO₃). Sediment trap samples were analyzed for trace metals (Al, Fe, Mn, and Pb), particulate carbon (18) and total and fixed solids (17). To determine the trace metal content, two 40-mL aliquots were decanted from homogenized sediment trap samples. One aliquot was centrifuged, and the supernatant was acidified (0.5% v/v Ultrex HNO₃) and analyzed as "dissolved metal". The second aliquot was first acidified to pH 1.0, digested for 1 h at 25 °C, and centrifuged to remove undissolved particulates; the supernatant was analyzed as "total metal". The difference between total metal and dissolved metal content yielded the acid-labile metals associated with deposited materials, including amorphous oxides (22). The flux of this acid-labile fraction (gross-deposition rate, D_g) is of interest in this study since deposition of "freshly formed" Al may occur in this form. Trace metal analysis of sediment trap and water column samples was conducted by atomic absorption spectrophotometry with graphite furnace. The total error (sampling and analytical) associated with soluble Pb and total monomeric Al analyses was 2.7 ± 0.6 nmol of Pb L⁻¹ (95% C.I. = 1.8–3.6 nmol of Pb L⁻¹) and 19.5 ± 0.2 μmol of Al L⁻¹ (95% C.I. = 19.2–19.8 μmol of Al L⁻¹), respectively. The fractional uncertainties for sediment trap collection and analysis are presented in Table I.

The electrophoretic mobility (EM) of the sediment trap particles was determined by using a microelectrophoresis unit (Rank Brothers Mark II, Cambridge, England). Immediately after a 2-min period on the magnetic stirrer, a 10-mL volume of the suspension was withdrawn from the sample and pipetted into a flat cell. The time required to travel 52 μm was measured for each of 20 particles, 10 at the front stationary point and 10 at the back stationary point. The polarity of the electrodes was reversed before each particle was tracked. The average and standard deviations of the 20 measured velocities were calculated and divided by the electric field strength within the cell, which was usually 10 V cm⁻¹, to obtain the mean and standard deviation of the electrophoretic mobility values in μm cm s⁻¹ V⁻¹.

Table I. Fractional Uncertainty^a in Sediment Trap Collection, Digestion, and Analysis

element	mean ^b	SD ^c	95% C.I.
Al	6.7	10.8	2.6–10.8
Pb	9.9	8.4	6.7–13.1
Mn	2.4	1.5	1.8–3.0
Fe	19.0	21.0	10.1–27.9
organic C	11.0	7.0	7.9–14.1

^a Error associated with collection, digestion, and analysis of triplicate sediment trap samples; expressed as coefficient of variation: C.V. = (SD/ \bar{x}) × 100. ^b Mean value (\bar{x}) of C.V. from triplicate sediment trap samples. ^c Standard deviation (SD) based on $n - 1$ degrees of freedom ($n = 24$).

A detailed description of the water chemistry of Darts Lake is beyond the scope of this paper. However, information on the water chemistry for the study year 1981–1982, with emphasis on the transformations of Al, is available elsewhere (11, 23).

Results

The flux of Pb into and out of Darts Lake was related to stream hydrology, pH, and Pb concentration (Figure 2). Stream flow during the study year was highly variable, with high flow occurring in the fall and in the spring snowmelt period; low flow was observed in summer and winter (Figure 2a). Stream pH was also variable (Figure 2b). Winter pH levels were consistently 5.1 until spring snowmelt, when pH values declined to an April/May minimum of 4.8. Increases in pH occurred throughout the summer, reaching a maximum in August (pH 5.4). A major rain storm in June did, however, briefly interrupt the increase in inlet pH (Figure 2b). Dissolved Pb concentrations in the inlet and outlet streams were reduced during low discharge in winter and summer. However, high flow periods in fall and spring were marked by increases in the concentration of dissolved Pb in the inlet and outlet streams (Figure 2c). Lead flux to and from Darts Lake was greatest during spring and fall periods of high Pb concentrations and elevated water discharge, also noted to be low pH periods. In contrast, low flow rates and reduced soluble Pb concentrations in the inlet and outlet during winter and summer resulted in significantly lower influx and efflux of Pb (Figure 2d). It is important to note that particulate Pb comprised typically less than 5% of the total concentration of Pb in these waters, and concentrations of total suspended solids in the inlet waters were less than 1 mg L⁻¹.

Chemical transformations in the water column appeared to play a significant role in Pb cycling. Darts Lake is dimictic and exhibited complete turnover (isothermal conditions) during November and April. During the turnover periods Pb concentrations and pH values exhibited an orthograde distribution (Figure 3a,b). During winter stratification, hypolimnetic concentrations of lead declined 5-fold to approximately 1 nmol L⁻¹, while pH levels were 5.4–5.6 (one-fourth the H⁺ activity at fall turnover). Elevated concentrations of Pb (11–13 nmol L⁻¹) were also observed during spring snowmelt when pH values in the system were lowest (4.8–5.0). The low pH and relatively high concentrations of Pb at the lake surface during the spring period may be attributed to inputs of acidic meltwater which are less dense than the bulk of the lake water (temperature ≈ 0 °C). Because of the thermal structure of the lake, acidic solutions containing relatively high concentrations of Pb were transported through the system along the lake-ice interface. Elevated concentrations of Pb were also observed in the hypolimnion during

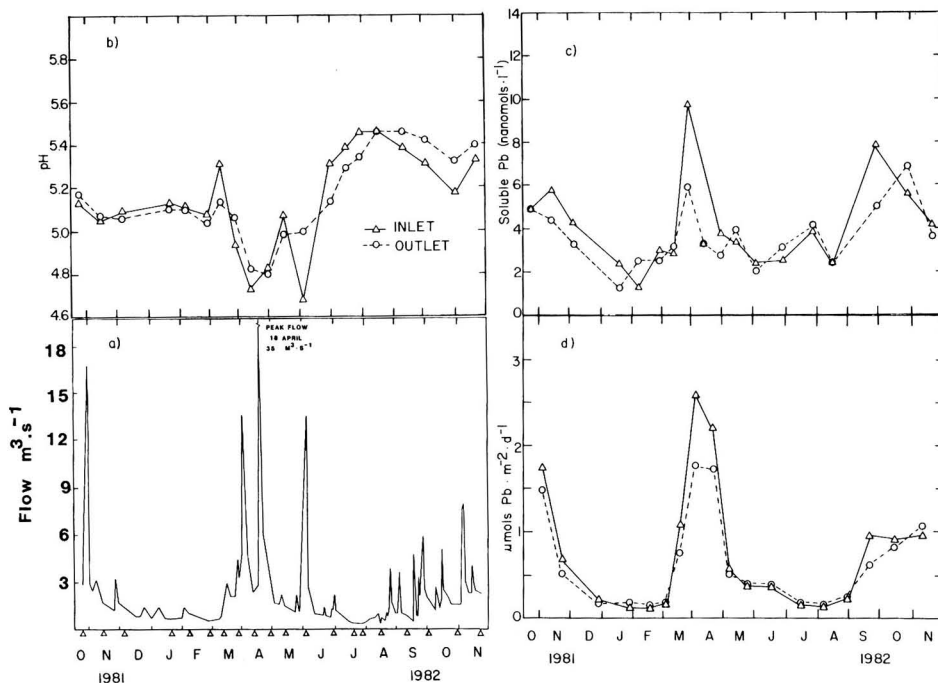


Figure 2. Temporal variations in (a) discharge, (b) inlet and outlet pH, (c) inlet and outlet concentrations of soluble Pb, and (d) Pb flux rates and from Darts Lake. Triangles represent sample collection dates.

the late summer, 1982. In contrast to spring snowmelt, an increase in pH values accompanied the appearance of Pb. From July through October the water column exhibited a heterograde pH profile, corresponding to epilimnetic depletions of Pb and a hypolimnetic enrichment of Pb. During this period oxygen reduction (minimum value = $50 \mu\text{mol L}^{-1}$ at 14 m on Oct 1, 1982) was evident in the lower waters. Elevated concentrations of dissolved organic carbon (DOC), Fe, Mn, and Al in the vernal hypolimnion (24) suggest that Pb remobilization may be linked to sediment processes. Mineralization of organic matter coupled with Fe and Mn reduction undoubtedly disrupted the sediment matrix and contributed to the reintroduction of Pb to the water column. Note that elevated concentrations of Pb were only observed during the summer of 1982. During the winter of 1981/1982 oxygen depletion was less pronounced (minimum value of $103 \mu\text{mol L}^{-1}$ at 14 m on March 27, 1982), and elevated concentrations of Pb were not observed in the hypolimnion.

Transformations in water chemistry appear to be very important in the cycling of Pb within Darts Lake. Increases in water column pH (Figure 3a) corresponded with increases in the vertical deposition of particulate Pb, as quantified by sediment traps (Figure 4). In addition, depletions in soluble Pb were observed in the water column (Figure 3b) during periods of high Pb deposition in winter and summer (Figure 4). Note that in the fall the concentration of soluble Pb increased in the hypolimnion prior to turnover (Figure 3). However, the highest rates of Pb deposition were observed in the 14-m trap during early August when water column concentrations of Pb were lowest.

Discussion

Seasonal variations in the concentration and transport of Pb in Darts Lake may be attributed to changes in

discharge as well as in-lake processes. Although a complex array of mechanisms may influence Pb transport, variations closely coincided with the chemistry and transport of Al. To illustrate this concept we present a saturation index (SI; eq 1) isopleth, with respect to the solubility of microcrystalline gibbsite (25), developed by Driscoll and Schafran (23) for Darts Lake (Figure 5). Briefly, these calculations were made by computing the distribution of aqueous Al (26) with the chemical equilibrium model MINEQL (27). Thermochemical calculations were corrected for variations in temperature and ionic strength.

$$\text{SI} = \log Q_p/K_p \quad (1)$$

Q_p is the ion activity product of the solution, and K_p is the theoretical solubility of microcrystalline gibbsite ($\log K_p = 9.35$ at 25°C (25)). An SI value greater than zero suggests oversaturation with respect to the solubility of microcrystalline gibbsite, while SI values that are near zero and negative suggest that solutions are in equilibrium and undersaturated with respect to the solubility of this mineral, respectively. Microcrystalline gibbsite was selected as a reference mineral for these calculations because it is a readily forming solid phase of Al.

During the snowmelt period, waters containing elevated concentrations of H^+ ($12\text{--}19 \mu\text{mol L}^{-1}$), Al ($17\text{--}31 \mu\text{mol L}^{-1}$), NO_3^- , and Pb were introduced to Darts Lake. Although these concentrations of Al were relatively high, solutions were significantly undersaturated with respect to the solubility of microcrystalline gibbsite (negative SI values; Figure 5). Mass balance calculations (Table II) and sediment trap observations (Figure 4b) were generally consistent with thermochemical calculations and suggest that during the snowmelt period Al was conservative within Darts Lake. (Note that the gross deposition of metals during the spring turnover period should be interpreted with caution because of turbulence and resuspension that

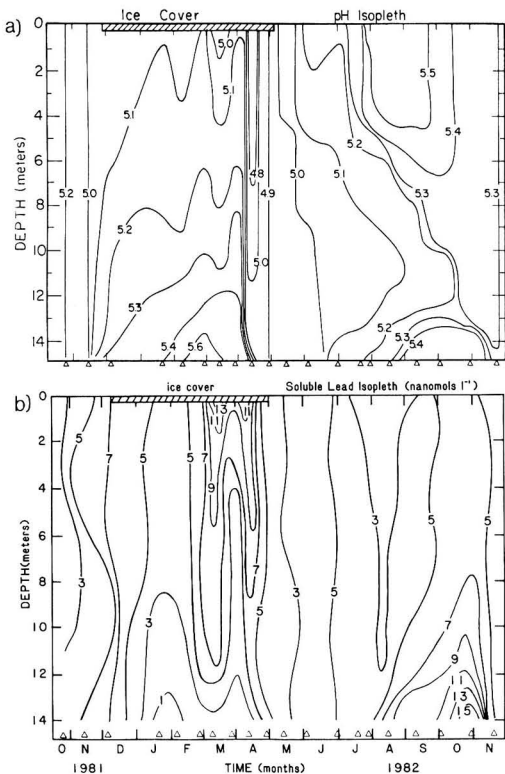


Figure 3. Temporal and spatial variations in (a) pH and (b) soluble Pb. Triangles represent sample collection dates. Isopleth lines were determined by linear interpolation between observations in data matrix.

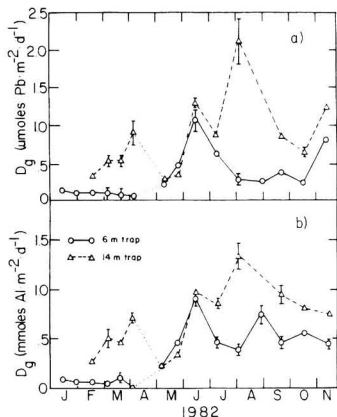


Figure 4. Temporal changes in gross deposition of (a) Pb and (b) Al in Darts Lake. Error bars represent the standard deviation of triplicate sediment traps. Note that metal deposition during spring turnover is not reported due to resuspension and turbulence within the lake.

Table II. Flux of Al in, out of, and Retained in the Sediments of Darts Lake (in $\text{mmol m}^{-2} \text{day}^{-1}$ (26))

period	influx	efflux	retention
annual average (10/1981-10/1982)	2.5	2.4	0.3
spring high flow (3/28-6/28/1982)	5.2	5.2	-0.1
summer base flow (7/28-10/29/1982)	1.2	0.9	0.4

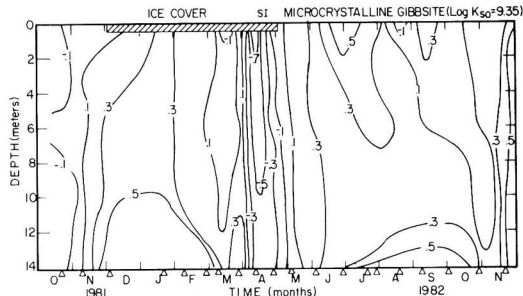


Figure 5. Temporal and spatial variation in saturation index (S.I.) with respect to microcrystalline gibbsite ($\log K_{sp} = 9.35$ at 25°C (25)). Triangles represent sample collection dates. Isopleth lines were determined by linear interpolation between observations in data matrix.

Table III. Ratios of Elemental Components to Suspended Solids in Sediment Material from Darts Lake^a

component	6-m depth		14-m depth	
	\bar{x}	C.V.	\bar{x}	C.V.
Al	4.8	106	3.0	53
Fe	2.2	177	4.3	91
Mn	0.05	113	0.03	85
organic C	59.3	110	78.3	54

^a Mean values (\bar{x}) are expressed as micromoles per milligram of suspended solids with coefficient of variation (C.V.). C.V. = $(SD/\bar{x}) \times 100$.

is characteristic of periods of high discharge and water column instability.)

After winter turnover, relatively high concentrations of H^+ ($15 \mu\text{mol L}^{-1}$), Al ($19 \mu\text{mol L}^{-1}$), NO_3^- ($40 \mu\text{mol L}^{-1}$), and Pb were observed throughout the water column. Immediately following ice-out, water column concentrations of NO_3^- were depleted, which caused the neutralization of H^+ and Al acidity (11). This process resulted in solutions that were oversaturated with respect to the solubility of microcrystalline gibbsite (positive SI values; Figure 5). Additional evidence confirming in-lake formation and retention of particulate Al during summer stratification is available through observations of high rates of Al deposition (Figure 4b) and mass balance calculations (Table II; 26).

A number of interrelated processes may account for the temporal and spatial variations in Pb chemistry and fluxes which have been observed in this study. On the basis of the results from water column and sediment trap analyses, Pb appears to have a significant affinity for particulate matter in Darts Lake. The nature of this solid matrix undoubtedly varied in composition and mass as a function of solution pH. Particles that might serve as adsorbing surfaces include algal cells, diatom frustules, clay particles, and other suspended mineral particulate, as well as other forms of detritus. These surfaces may act as nucleation sites for adsorption/precipitation of Al, Fe, Mn, and organic matter upon which Pb adsorption/coprecipitation may occur (12-15). Colloidal organics may also incorporate Al, Fe, and Mn through complexation and coagulation reactions, and hydrous oxides may adsorb/precipitate organic matter (28-31).

We hypothesize that in-lake formation of particulate Al facilitates the vertical deposition of Pb, particularly in the upper waters. During summer stratification, epilimnetic depletion of Pb coincided with a depletion of Al. Moreover, Al was a major constituent of solids deposited to 6-m

Table IV. Multiple Linear Regression of Deposition of Pb in Darts Lake Sediment Traps as a Function of Particulate Constituents

constituent	6-m trap		14-m trap	
	$p <$	partial r	$p <$	partial r
organic C	0.023	0.65	0.892	0.01
Al	0.043	0.59	0.004	0.85
Mn	0.072	0.54	0.022	0.74
Fe	0.165	0.42	0.331	0.36
multiple	0.0001	0.95	0.0001	0.98

sediment traps (Table III) comprising $13 \pm 14\%$ of fixed solids on a mass basis. Particulate organic carbon was also abundant in sediment traps, and deposition was strongly correlated with Al (for 6-m trap, $r = 0.63$ and $P < 0.01$; for 14-m trap, $r = 0.90$ and $P < 0.0001$). Undoubtedly water column Al enhances the deposition of particulate carbon through coagulation reactions. Multiple linear regression supports the notion that Pb deposition is linked to particulate organic carbon and Al deposition (Table IV).

In the lower waters Fe concentrations in sediment traps were more pronounced, probably due to Fe mobilization from the sediments (Table III). However, the deposition of Pb was strongly correlated with Al in the hypolimnetic waters rather than Fe (Pb deposition was correlated with Mn deposition, but the deposition rates of Mn were relatively low). While it is difficult to ascertain a single process responsible for Pb scavenging, Al deposition would appear to contribute.

Due to the presence of DOC, the existence of a fairly pure hydrous oxide surface was highly unlikely. A pure aluminum oxide particle at pH 5.0 would be expected to be positively charged (32) with an electrophoretic mobility (EM) of approximately $+5.5 \mu\text{m cm s}^{-1} \text{V}^{-1}$ (33). EM results from sediment trap analyses conducted in this study differ markedly from synthetic aluminum oxides. The mean EM value for sediment trap samples collected from Darts Lake was $-1.75 \pm 0.16 \mu\text{m cm s}^{-1} \text{V}^{-1}$ ($n = 49$) and did not vary significantly with pH or depth of sample. Hunter and Liss (34) and Tipping et al. (35) have discussed the uniformity of electrokinetic charge on suspended particles and attributed this behavior to organic surface films. Davis and Gloor (30) demonstrated the shift in EM of a pure aluminum oxide ($\gamma\text{-Al}_2\text{O}_3$) from 2.7 to $-2.3 \mu\text{m cm s}^{-1} \text{V}^{-1}$ at pH 5, following the addition of filtered lake water ($\text{DOC} = 0.28 \text{ mmol of C L}^{-1}$). Tipping et al. (35) obtained similar results with iron oxide. Davis (31) observed extensive (60%) DOC removal by aluminum oxide between pH 4.0 and pH 6.0. Therefore, even in acidic lake water containing a varied collection of particle types (various clay minerals, aluminosilicates, quartz grains, living and dead organisms, and detritus), oxide and/or organic films may determine the surface properties of suspended particles. Consequently, the solid matrix present in the system was probably composed of inorganic hydrous oxides (coatings) and adsorbed/coprecipitated organic matter. The interaction of Pb with this matrix appears to be sensitive to variations in pH. Changes in pH may affect Pb partitioning between the solid and solution through a number of possible mechanisms: matrix formation/dissolution, sorption/desorption of organic complexes and inorganic complexes, and H^+ ion exchange reactions.

Our observations of hypolimnetic enrichment of Pb during summer stratification may be significant in several respects. This Pb may be distributed to the water column following fall turnover. Sediment release of Pb may con-

tribute to the elevated concentrations of water column Pb observed prior to ice cover.

The apparent vertical cycling of Pb has implications in the interpretation of Pb deposition to acidic lake sediments. A number of investigators have reported increased rates of Pb deposition to the sediments of acidic lakes in recent years (36-42). These investigators have generally attributed this trend to increased atmospheric deposition of Pb. While we do not dispute the fact that changes in the atmospheric deposition of Pb have occurred, acidification processes such as the mobilization of Al and in-lake processes such as the formation of particulates may have varied through time, resulting in temporal changes in Pb retention in low ionic strength lakes. An increase in the efficiency of Pb scavenging by particulates would probably enhance Pb transport to sediments. Therefore, the pattern of increased Pb deposition to sediments may not entirely be due to atmospheric processes.

Moreover, the dating of lake sediments by ^{210}Pb , often used to compute sedimentation rates, is based on the assumption that Pb is immobile within sediments. Clearly our observation of hypolimnetic enrichment of Pb challenges this assumption for Darts Lake. Whether or not these processes are applicable to other acidic lakes or significantly influence the interpretation of the sediment record remains to be evaluated. However, these processes probably warrant consideration in future studies of sediment stratigraphy in acidic lakes.

Conclusions

Substantial variations in water column concentrations of Pb were observed in acidic Darts Lake. These variations were attributed to changes in the discharge and concentration of Pb in inflowing water and in-lake formation of particulates during stratified periods. In addition, hypolimnetic enrichment of Pb during summer stratification coincided with increased concentrations of Fe and DOC. This observation suggests that upward transport of Pb may follow the sedimentation and decomposition of organic matter and/or dissolution of redox-sensitive hydrous oxides. The apparent upward flux of Pb may be a significant process increasing water column concentrations of Pb following fall turnover and have implications for the interpretation of patterns and rates of Pb deposition in acidic lakes.

Acknowledgments

We thank L. G. Barnum, N. Peters, and particularly G. C. Schafran for their assistance in this study.

Registry No. Pb, 7439-92-1; Al, 7429-90-5; Mn, 7439-96-5; Fe, 7439-89-6; C, 7440-44-0.

Literature Cited

- Dickson, W. *Verh.—Int. Ver. Theor. Angew. Limnol.* **1978**, *20*, 851.
- Johnson, N. M.; Driscoll, C. T.; Eaton, J. S.; Likens, G. E.; McDowell, W. H. *Geochim. Cosmochim. Acta* **1981**, *45*, 1421.
- Schofield, C. L. *USDA For. Serv. Gen. Tech. Rep. NE 1976*, NE-2.
- Henriksen, A.; Wright, R. F. *Water Res.* **1978**, *12*, 101.
- Dickson, W. In "Ecological Impact of Acid Precipitation"; Drabls, D.; Tolan, A., Eds.; Proceedings of the International Conference, SNSF Project: Oslo, 1980; p 75.
- Schofield, C. L. *Ambio* **1976**, *5*, 228.
- Wong, P. T. S.; Silverberg, B. A.; Chau, Y. K.; Hodson, P. V. In "The Biogeochemistry of Lead in the Environment"; Nriagu, J. O., Ed.; Elsevier: Amsterdam, 1978.

- (8) Stumm, W.; Morgan, J. J. "Aquatic Chemistry"; Wiley-Interscience: New York, 1981.
- (9) *Fed. Regist.* **1984**, *49*, 4551-4554.
- (10) Driscoll, C. T.; Baker, J. P.; Bisogni, J. J.; Schofield, C. L. "Acid Precipitation: Geological Aspects"; Bricker, O. R., Ed.; Butterworths: Stoneham, MA, 1984.
- (11) Driscoll, C. T.; Schafran, G. C. *Nature (London)* **1984**, *310*, 308-310.
- (12) James, R. O.; Healy, T. W. *J. Colloid Interface Sci.* **1972**, *40*, 65.
- (13) Hohl, H.; Stumm, W. *J. Colloid Interface Sci.* **1976**, *55*, 281.
- (14) Davis, J. A.; Leckie, J. O. *J. Colloid Interface Sci.* **1978**, *67*, 90.
- (15) Millward, G.; Moore, R. *Water Res.* **1982**, *16*, 981.
- (16) Bloesch, J.; Burns, N. M. *Schweiz. Arch. Hydrol.* **1980**, *42*, 15.
- (17) "Standard Methods for the Examination of Water and Wastewater", 14th ed.; American Public Health Association: New York, 1976.
- (18) Menzel, D. W.; Vaccaro, R. F. *Limnol. Oceanogr.* **1964**, *9*, 138.
- (19) Barnes, R. B. *Chem. Geol.* **1975**, *15*, 177.
- (20) Driscoll, C. T. *Int. J. Environ. Anal. Chem.* **1984**, *16*, 267-283.
- (21) Salim, R.; Cooksey, B. *Water Res.* **1981**, *15*, 835.
- (22) Hsu, P. H. In "Minerals in Soil Environments"; Dixon, J. B.; Weed, S. B., Eds.; Soil Science Society of America: Madison, WI, 1977.
- (23) Driscoll, C. T.; Schafran, G. C. 1984, final report for USEPA/NCSU Acid Precipitation Program Project APP 0094-1981.
- (24) White, J. R., Ph.D. Thesis, Syracuse University, Syracuse, NY, 1984.
- (25) Hem, J. D.; Roberson, C. "Form and Stability of Aluminum Hydroxide Complexes in Dilute Solution. U.S. Government Printing Office: Washington, DC, 1967; U.S. Geological Survey Water Supply Paper, 1827-A.
- (26) Driscoll, C. T. *Trace Subst. Environ. Health* **1984**, *18th*, 215-229.
- (27) Westfall, J. C.; Zachary, J. L.; Morel, F. M. M. "MINEQL, a Computer Program for the Calculation of Chemical Equilibrium Composition of Aqueous Systems". Massachusetts Institute of Technology, 1976, Technical Note 18.
- (28) Schwertmann, U. *Nature (London)* **1966**, *212*, 645.
- (29) Kodama, H.; Schnitzer, M. *Geoderma* **1977**, *19*, 279.
- (30) Davis, J. A.; Gloor, R. *Environ. Sci. Technol.* **1981**, *15*, 1223.
- (31) Davis, J. A. *Geochim. Cosmochim. Acta* **1982**, *46*, 2381.
- (32) Parks, G. A. In "Equilibrium Concepts in Natural Water Systems"; American Chemical Society: Washington, DC, 1967; Adv. Chem. Ser. No. 67.
- (33) Letterman, R. D.; Vanderbrook, S. G.; Sricharoenchaikit, P. J.—*Am. Water Works Assoc.* **1982**, *74*, 44.
- (34) Hunter, K. A.; Liss, P. S. *Nature (London)* **1979**, *282*, 823.
- (35) Tipping, E.; Woof, C.; Cooke, D. *Geochim. Cosmochim. Acta* **1981**, *45*, 1411.
- (36) Galloway, J.; Likens, G. *Limnol. Oceanogr.* **1979**, *24*, 427.
- (37) Fuhs, G.; Reddy, M. "Abstracts of Papers", Proceedings of the ACS Division of Environmental Chemistry National Meeting, San Francisco, CA, 1980; American Chemical Society: Washington, DC, Vol. 20, No. 2, p 361.
- (38) Norton, S. A.; Hess, T. In "Ecological Impact of Acid Precipitation"; Drablos, D.; Tollan, A., Eds.; Proceedings of the International Conference, SNSF Project: Oslo, 1980.
- (39) Heit, M.; Tan, Y.; Klusek, C.; Burke, J. *Water Air Soil Pollut.* **1981**, *15*, 441.
- (40) Dickman, M.; Fortescue, J.; Barlow, R.; Teresmae, J. "Downcore Profiles for Diatom Inferred pH and Heavy Metals in an Acidified Lake Near Wawa, Ontario"; University of Toronto, 1982; SLANT/TRESLA, Vol. 4.
- (41) Hanson, D.; Norton, S. A.; Williams, J. S. *Water Air Soil Pollut.* **1982**, *18*, 227.
- (42) Kahl, J. S.; Norton, S. A.; Williams, J. S. In "Acid Precipitation: Geological Aspects"; Bricker, O. R., Ed.; Butterworths: Stoneham, MA, 1984.

Received for review August 29, 1984. Revised manuscript received April 29, 1985. Accepted June 20, 1985. This research was funded in part by the National Science Foundation (CME-8006733) and the USEPA/NCSU Acid Deposition Program. This research has not been subject to the EPA's peer and policy review and therefore does not necessarily reflect the views of the agency, and no official endorsement should be inferred. Contribution No. 39 of the Upstate Freshwater Institute.

Rapid Consumption of Bromine Oxidants in River and Estuarine Waters

Donald A. Jaworski[†] and George R. Helz*

Department of Chemistry, University of Maryland, College Park, Maryland 20742

■ Fluvial and estuarine waters possess a substantial reductive capacity that rapidly destroys strong oxidants introduced from natural or anthropogenic sources. The rapid reduction of bromine oxidants, which in marine waters are intermediates in the decomposition of both chlorine and ozone, has been studied electrochemically in the field and the laboratory with a rotating ring disk electrode. Patuxent estuary water was found to contain about 10^{-5} M of substances that reacted extremely rapidly with bromine. Estimated second-order rate constants were on the order of 10^7 M⁻¹ s⁻¹ or higher. Bromine consumption did not correlate with salinity, nor was it altered by addition of 10^{-4} M ethylenediaminetetraacetic acid or by ultrafiltration. However, destruction of organic matter by UV photolysis eliminated bromine consumption on the 10^{-2} s time scale of the experiments. Likewise, the bromine-consuming components could be titrated away with HOBr, indicating that they are not catalysts. Commercially available humic acid behaved qualitatively in a similar fashion to the natural reductants.

Introduction

Chlorination or ozonation of coastal waters produces bromine and its hydrolysis products as daughter oxidants (1-5). Various bromo carbons are generated subsequently (6-8). When typical doses on the order of 10^{-5} M are applied and when mixing is rapid, a significant fraction of the oxidant dose disappears from saline water too rapidly to be observed by conventional analytical techniques (8). This is also true when fulvic acid solutions are treated with chlorine in the laboratory (9).

Since it is important to understand the oxidant decay mechanisms that give rise to undesirable products, such as bromocarbons, we explored a rotating ring disk electrode method for studying extremely rapid reactions of bromine (10). With this method, Br₂ is generated electrochemically at a rotating platinum disk and detected electrochemically at an annular platinum ring. Any chemical reactions that consume bromine during its passage between the disk and ring are detected by a diminished signal at the ring.

This paper contains two parts. We will first present some shipboard rotating ring disk electrode (RRDE) measurements that characterize the fast bromine demand in the Patuxent Estuary, MD. Then we will describe some laboratory experiments that shed light on the nature of the components responsible for fast bromine demand.

Materials and Methods

The rotating ring disk electrode used in this work (Pine Instrument Co.) consists of a 2.55-mm platinum disk surrounded concentrically by a 0.48 mm wide platinum ring. The ring is separated from the disk by a 1.21 mm wide insulator gap. When the electrode is inserted into a beaker of solution and rotated at a constant rate, liquid is drawn vertically up toward the disk and then spun radially out across the ring surface (11-13).

Sample preparation for the rotating ring disk electrode (RRDE) experiments was minimal. All samples, were run at ambient pH (usually around 7.5), except where spe-

cifically mentioned to the contrary. Enough granular NaBr was added to the samples to bring the Br⁻ concentration to 0.1 M. All of the samples were run at ambient temperature (25 ± 4 °C), except where noted. In the shipboard experiments, the time between collection of a sample and initiation of a measurement was about 3 min.

The measurement procedure consisted of applying a potential to the disk electrode to generate Br₂ from the Br⁻ initially added to the sample. During the experiment, the disk potential was gradually shifted, under control of an Apple II computer, to steadily increase the anodic current and thus the rate of Br₂ production. At the ring electrode, a fixed potential (+0.4 V vs. colomel) was set to reduce back to Br⁻ all the oxidized bromine that had not been consumed by the sample in transit from disk to ring. Therefore, the cathodic current at the ring provided a measure of unreacted bromine. The transit time of solution from the disk to the ring was controlled by the rotational velocity of the electrode and could be varied in the range 10^{-2} to 1 s. The experiments reported in this paper were performed with a rotation rate of 3600 rpm, at which the transit time was about 35 ms. Scan time for an experiment was about 2 min. Details of the electrochemical instrumentation and software can be found elsewhere (10, 14).

Field measurements were made on the Patuxent Estuary, located 50-100 km SE of Washington, DC. Surface samples were collected in a polyethylene bucket, while near bottom waters were pumped onboard through polyethylene tubing. Temperature, salinity, pH, and dissolved oxygen (membrane probe) were also measured onboard. Ammonia [Solorzano method (15)] and dissolved organic carbon [Menzel and Vaccaro method (16); Oceanography International Analyzer] were determined later on filtered samples.

Results and Discussion

Field Data. Figure 1 shows some representative, titration-like data obtained on shipboard. Whereas the ring current always increased linearly with disk current in blanks (i.e., 0.1 M NaBr made with distilled water), there was initially no change in ring current with increasing disk current in natural waters. Only after a threshold was reached did ring current begin to rise. These results imply that the natural waters contain components which consume all the bromine generated at low disk currents. When the bromine generation rate (proportional to disk current) exceeded the delivery rate of reducing agents to the electrode (proportional to the rotational velocity of the disk), it became possible for the ring electrode to sense bromine.

From data such as shown in Figure 1, it is possible to calculate both the concentration of bromine-consuming components and the observed second-order rate constant for the reaction of bromine with these components (10, 11, 17). In Table I, values for the concentration of bromine-consuming components, designated C_b, are reported for the suite of Patuxent estuary samples. These values are means of triplicate determinations; individual measurements deviated from the mean by less than 5%. The surface and bottom water samples have been separated in this table. The bottom water samples all came from the southern part

[†]Present address: NASA Lewis Research Center, Cleveland, OH 44135.

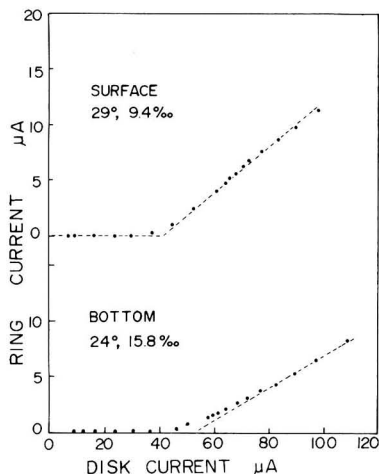


Figure 1. Ring current vs. disk current data for one site in the Patuxent estuary. The upper set of points is for surface water and the lower set for bottom water. Electrode rotation velocity 3600 rpm or 60 Hz. Samples were fortified with NaBr to 0.1 M.

Table I. Bromine Demand, C_b , and Water Composition in the Patuxent Estuary, July 21, 1983

C_b , ^a μ M	T , °C	salinity, g/kg	pH	NH_3 , μ M	DOC, ^b μ M
Surface Waters					
11.5	30.4	0.4	6.60	0.2	450
10.6	30.1	0.7	6.45	4.4	540
12.5	30.2	1.9	6.50	<0.1	430
14.2	34.7	7.3	6.68	1.5	390
11.3	30.7	6.9	7.20		
11.6	29.2	8.5	7.21	<0.1	360
13.5	29.9	8.9	7.71	0.5	380
12.0	29.1	8.9	7.04		
13.6	29.2	9.4	7.68	0.6	410
15.0	28.8	10.9	7.59		
13.4	29.0	12.5	8.18	<0.1	280
Bottom Waters ^c					
20.1	24.8	13.4	7.30		
23.3	24.4	15.8	6.65	9.9	260
23.6	24.9	16.5	7.25	8.7	250

^a Concentration of bromine needed to meet the fast demand; calculated from the RRDE experiments. Values given are averages of triplicate determinations. ^b Dissolved organic carbon expressed in micromolar units for comparison with C_b . ^c Samples had sulfide odor.

of the estuary, which was stratified, with anoxic conditions prevailing in the lower layer at the time of sampling. The higher C_b values in the bottom waters presumably reflect rapid reaction between bromine and sulfide.

The concentration of bromine demand, C_b , is plotted as a function of salinity in Figure 2 and shows no trend; nor does C_b vary appreciably with DOC, which decreases in a seaward direction. If one hypothesizes that organic carbon is responsible for the fast demand (see evidence below), then the ratio of C_b to DOC suggests that only 2-4% of the dissolved organic carbon atoms serve as sites for rapid oxidant demand. Qualls and Johnson (9), who studied the reaction of chlorine with fulvic acid, have similarly observed that 2% of the carbon sites in fulvic acid isolated from University Lake, NC, serve as sites for rapid oxidant demand.

Information on the rate of reaction is contained in the sharpness of the end point in data such as presented in

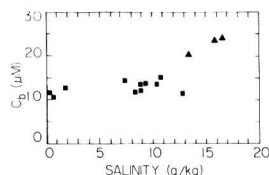


Figure 2. Concentration of fast bromine-consuming components vs. salinity in the Patuxent estuary. Squares denote surface waters, and triangles denote bottom waters, which were anoxic. All data were obtained at 0.1 M Br^- , ambient pH (see Table I), and 3600 rpm. Each point is an average of triplicate measurements.

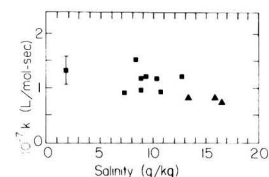


Figure 3. Observed second-order rate constant vs. salinity in the Patuxent estuary. The same conditions as in Figure 2 apply. Measurement uncertainty is depicted by the vertical bar.

Figure 1 (10, 11). Values of k , the apparent second-order rate constant, are shown in Figure 3. These also show no significant trend with salinity. The three sulfidic bottom-water samples appear to yield slightly lower values of k , suggesting that sulfide reacts slightly slower than the unknown components that contribute to fast bromine demand in the surface samples. The values in Figure 3 are also means of triplicate determinations. The precision of individual measurements was $\pm 15\%$. However, the measurements may be accurate only to the order of magnitude owing to their very large values, near the limit of determination by this electrochemical method.

Visual inspection of the electrode after three replicate scans of a sample sometimes revealed an "oxidized brass" colored film on the Pt disk, which was removed by washing in dilute HNO_3 . No film was detected on the adjacent ring. The intensity of the film was different at different stations but did not correlate with salinity. The coating did not seem to affect the C_b results markedly, although the triplicates did show a slight downward trend in C_b with time in those samples with the coating. The chemical nature of this coating has not been firmly established, although plasma emission and UV absorption spectrometric examination of HCl leachates suggested it may be ferric hydroxide. The coating was not formed when disk electrolysis was performed in samples to which no NaBr had been added. Thus, oxidized bromine appears to be essential for its formation.

Laboratory Experiments with Patuxent Water. A series of experiments were performed to provide more information about the nature of the components responsible for the fast consumption of bromine. Dilution of a sample collected at Solomons, MD (salinity 10 g/kg), yielded a linear dilution of the bromine-consuming components.

To determine if trace metals are important to the demand reaction, either in the role of a catalyst or in the role of a reactive substrate, ethylenediaminetetraacetic acid (EDTA) was added to the Patuxent sample at 10^{-5} and 10^{-4} M. The lower concentration of EDTA approximated the concentration of the unknown demand components. EDTA was also added to the blanks and showed no significant reaction with bromine during the transit time of the experiment. (A pseudo-first-order reaction between

Table II. Effect on Bromine Demand, C_b , of Modifying Patuxent Estuary Samples

modification	C_b , μM
Addition of Ethylenediaminetetraacetic Acid	
no EDTA	14.7
10^{-5} M EDTA	13.7
10^{-4} M EDTA	14.0
Ultrafiltration, Amicon UM2 Filter	
unfiltered	16.3
filtrate	17.6

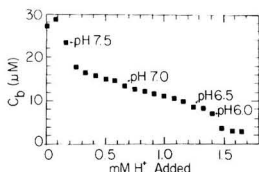


Figure 4. Decrease in the effective concentration of fast bromine-consuming components (C_b) in Patuxent water as pH is reduced by titration with HCl. Conditions: 0.1 M Br⁻; 3600 rpm; salinity approximately 11 g/kg.

EDTA and bromine became apparent at 10^{-3} M EDTA.) The results of the EDTA experiments are summarized in the top half of Table II. There was little difference between the samples with EDTA and those without, in terms of C_b .

Another Patuxent sample, collected from Solomons, MD, on April 25, 1983, was subjected to ultrafiltration through an Amicon UM-2 membrane (nominal cutoff 1000 daltons) and the filtrate examined by the RRDE method. The results, summarized in the bottom half of Table II, show that ultrafiltration has little effect on removing the components responsible for the oxidant demand. Rather, a small increase in C_b was observed as a result of ultrafiltration. This increase in C_b was probably due to a small amount of contamination from the filter.

It was found that the bromine demand components could be removed from Patuxent water by ultraviolet oxidation [using the method of Armstrong and Tibbitts (18)]. The fast bromine demand, C_b , was reduced from 15.4 μM to the level of a blank, after a 4-h irradiation with a 1200-W Hg lamp. After irradiation, the pH was adjusted to its preirradiation value before the decrease of C_b was measured.

Changes in pH affect the rapid oxidant demand. The pH and calculated bromine demand (C_b) were monitored while a Patuxent sample was titrated with 0.0128 M HCl from pH 7.6 to 4.5. Below pH 8.0, there was little change in a 0.1 M NaBr blank, indicating a stable base line for the experiment. The concentration, C_b , as a function of H^+ added is shown in Figure 4. The most striking feature of these results is the decrease in C_b with increasing H^+ . This could be caused by protonation reactions of the bromine-consuming components in solution, leading to less reactive materials. For example, it is known that bromine oxidation of alcohol and aldehyde functional groups proceeds by way of deprotonated anions (19, 20); consequently protonation reduces reactivity. Additionally, protonation can be expected to produce conformational changes in large dissolved organic molecules (21), due to increased hydrophobicity of the protonated forms. This may create steric barriers to reactions involving bromine.

The bromine demand components were also removed by manual titration of the sample with HOBr, as shown in Figure 5. This result indicates that the rapid demand

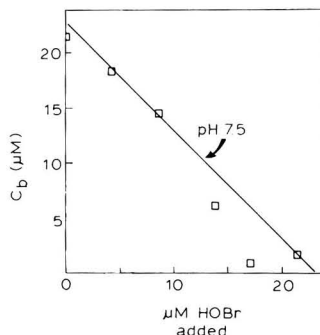


Figure 5. Decrease in the concentration of fast, bromine-consuming components (C_b) as HOBr is added. Sample from Solomons, MD (July 8, 1983), with an initial salinity near 11 g/kg. The pH was adjusted with HCl. Conditions: 0.1 M Br⁻; 3600 rpm.

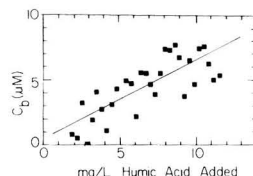


Figure 6. Increase in C_b as a function of increasing humic acid concentration. In this experiment a titrant containing 500 mg/L of sodium humate prepared from a commercial humic acid was added gradually to a 0.1 M NaBr solution. Conditions: 3600 rpm; pH \sim 6.5.

is caused by a reaction in which the demand is consumed. Thus, the demand does not involve catalytic decomposition of HOBr to O_2 and HBr (which are thermodynamically stable).

Experiments with Model Substances. Various model substances were added to demand-free NaBr solution in an attempt to obtain ring current vs. disk current titration curves similar to those observed in natural waters. On the basis of previous experiments with NH_3 and glycine (10, 14), these compounds do not react fast enough to exhibit the behavior observed in Figure 1. Hydrogen peroxide was tested and found to exert fast demand only when present in millimolar concentrations, about a thousandfold higher than concentrations of H_2O_2 measured in the Patuxent (22). Phenol was also tested, but it rapidly poisoned the disk electrode by forming a polymeric film. Attention was directed toward other substances, known for their fast demand, such as humic acid (9, 23) and a protein, bovine serum albumin (BSA).

A 500 mg/L stock solution of humic acid (Aldrich Chemical Co., lot no. H1675-2) was added dropwise to 0.1 M Br⁻ (at pH 6.5), and C_b was monitored at 3600 rpm. The ring current vs. disk current traces were similar to those in Figure 1. The C_b results are summarized in Figure 6. Although there was considerably more scatter in the data for this experiment than in the others, approximately 15 mg/L humic acid was required to yield a C_b signal comparable to that in the Patuxent (1×10^{-5} M). The calculated rate constants in this experiment were in the vicinity of $10^7 \text{ M}^{-1} \text{ s}^{-1}$. If the observed demand in the Patuxent were due solely to humic material, and if this material were 50% carbon, then a C_b signal of 1.0×10^{-5} M would correspond to 7 mg/L or 600 μM carbon. This is only slightly higher than the observed dissolved organic carbon. Marine humic materials are of low molecular weight (24, 25) and thus conceivably more reactive than the higher molecular weight, commercial humic acid tested here.

A similar experiment using bovine serum albumin (BSA) rather than humic acid was performed. Although this well-characterized protein also showed the typical second-order ring current vs. disk current titration curve, a concentration of 110 mg/L BSA was required to produce a C_b value of 1×10^{-5} M. The rate constants were again on the order of $10^7 \text{ M}^{-1} \text{ s}^{-1}$. This experiment suggests that proteins contain sufficiently reactive moieties but that unreasonably high concentrations of high molecular weight proteins such as BSA (M_r 70000) would be required to explain the fast demand for bromine displayed by Patuxent waters.

Sixteen of the 17 amino acids that constitute BSA were also subjected individually to RRDE analysis. Only four, cysteine, cystine, methionine, and histidine, reacted rapidly enough to yield titration curves such as those observed in the Patuxent. Unreactive on this time scale were valine, leucine, isoleucine, serine, threonine, proline, phenylalanine, tyrosine, aspartic acid, glutamic acid, lysine, arginine, and glycine.

Conclusion

The results presented in this paper indicate that the Patuxent estuary contains about 10^{-5} M substances that react rapidly with bromine, with rate constants on the order of $10^7 \text{ M}^{-1} \text{ s}^{-1}$ or higher. Rate constants of this magnitude are near the upper limit of measurement by RRDE methods. In waters of this type, trace concentrations of bromine oxidants will have a half-life of less than 7 ms. The extremely rapid nature of this process in natural waters has not been demonstrated in the previously published scientific literature.

The observed, relatively high concentration of bromine-consuming components in the Patuxent, the evidence that they are removed by UV photolysis, and the demonstration that they are not catalysts, but rather reactants consumed by Br_2 and HOBr, leave little doubt that the bromine-consuming materials are organic. The ultrafiltration results suggest that the bromine demand is provided by moderate- to small-sized molecules (M_r <1000), possibly akin to the marine fulvic acids (24, 25). Marine waters along the Georgia coast (26) have been shown to contain 50–300 μM dissolved organic carbon capable of passing through UM-2 ultrafilters.

Although four naturally occurring amino acids were found to simulate the characteristics of the natural bromine-consuming components, those compounds in the free form probably never reach concentrations of 10^{-5} M in natural surface waters. Limited, available information for the Patuxent (27) (A. C. Sigleo, personal communication) suggests that total dissolved free amino acids may reach 10^{-6} M; however, histidine and the three sulfur-containing amino acids would contribute less than 10% to this total. Nevertheless, the experiments with free amino acids help to delineate the types of organic functional groups that are required for fast bromine consumption.

The nondependence of bromine-consuming components on salinity suggests that the materials responsible for fast consumption of bromine are being generated within the Patuxent estuary, rather than being transported into the estuary from either the watershed or the ocean. Thus, byproducts of phytoplankton or salt marsh productivity are implicated as candidates for the rapid bromine-consuming components.

Registry No. Br_2 , 7726-95-6; C, 7440-44-0.

Literature Cited

- (1) Macalady, D. L.; Carpenter, J. H.; Moore, C. A. *Science (Washington, D.C.)* **1977**, *195*, 1335–1337.
- (2) Hall, L. W., Jr.; Helz, G. R.; Burton, D. T. "Power Plant Chlorination: A Biological and Chemical Assessment"; Ann Arbor Science: Ann Arbor, MI, 1981; pp 1–237.
- (3) Helz, G. R.; Hsu, R. V.; Block, R. M. In "Ozone/Chlorine Dioxide Oxidation Products of Organic Materials"; Rice, R. G.; Cotruvo, J. A.; Browning, M. E., Eds.; Ann Arbor Science: Ann Arbor, MI, 1978; pp 68–76.
- (4) Creclius, E. A. *J. Fish. Res. Board Can.* **1979**, *36*, 1006–1008.
- (5) Richardson, L. B.; Burton, D. T.; Helz, G. R.; Roderick, J. C. *Water Res.* **1981**, *15*, 1067–1074.
- (6) Helz, G. R.; Hsu, R. V. *Limnol. Oceanogr.* **1978**, *23*, 858–869.
- (7) Bean, R. M.; Mann, D. C.; Wilson, B. W.; Riley, R. G.; Lusty, E. W.; Thatcher, T. O. In "Water Chlorination, Environmental Impact and Health Effects"; Jolley, R. L.; Brungs, W. A.; Cumming, R. B.; Jacobs, V. A., Eds.; Ann Arbor Science: Ann Arbor, MI, 1980; Chapter 33.
- (8) Helz, G. R.; Sugam, R.; Sigleo, A. C. *Environ. Sci. Technol.* **1984**, *18*, 192–198.
- (9) Qualls, R. G.; Johnson, J. D. *Environ. Sci. Technol.* **1983**, *17*, 692–698.
- (10) Jaworske, D. A.; Helz, G. R. *Int. J. Environ. Anal. Chem.* **1985**, *19*, 189–202.
- (11) Alberry, W. J.; Hitchman, M. L. "Ring-Disc Electrodes"; Oxford University Press: London, 1971; pp 1–170.
- (12) Shuman, M. S.; Michael, L. C. *Int. Conf. Heavy Met. Environ., [Symp. Proc.]*, **1st 1975**, *1*, 227–248.
- (13) Levich, V. G. "Physico-Chemical Hydrodynamics"; Prentice-Hall: New York, 1962.
- (14) Jaworske, D. A. Ph.D. Dissertation, University of Maryland, College Park, MD, 1983.
- (15) Solorzano, L. *Limnol. Oceanogr.* **1969**, *14*, 799–801.
- (16) Menzel, D. W.; Vaccaro, R. F. *Limnol. Oceanogr.* **1964**, *9*, 138–142.
- (17) Riddiford, A. C. In "Advances in Electrochemistry and Electroanalytical Engineering"; Interscience Publishers: New York, 1966; Vol. IV, pp 47–116.
- (18) Armstrong, F. A. J.; Tibbitts, S. *J. Mar. Biol. Assoc. U.K.* **1968**, *48*, 143–152.
- (19) Perlmuter-Hayman, B.; Persky, A. *J. Am. Chem. Soc.* **1960**, *82*, 276–279.
- (20) Perlmuter-Hayman, B.; Weissman, V. *J. Am. Chem. Soc.* **1962**, *84*, 2323–2326.
- (21) Ghassemi, M.; Christman, R. F. *Limnol. Oceanogr.* **1968**, *13*, 583–597.
- (22) Helz, G. R.; Kieber, R. In "Water Chlorination: Chemistry Environmental Impact and Health Effects"; Jolley, R. L.; Bull, R. J.; Davis, W. P.; Katz, S.; Roberts, M. H.; Jacobs, V. A., Eds.; Lewis Publishers: Chelsea, MI, 1985; Vol. 5, in press.
- (23) Noack, M. G.; Doerr, R. L. In "Water Chlorination Environmental Impact and Health Effects"; Jolley, R. L., Eds.; Ann Arbor Science: Ann Arbor, MI, 1978; Vol. II, Chapter 4.
- (24) Harvey, G. R.; Boran, D. A.; Chesal, L. A.; Tokar, J. M. *Mar. Chem.* **1983**, *12*, 119–132.
- (25) Stuermer, D. H.; Harvey, G. R. *Nature (London)* **1974**, *250*, 480–481.
- (26) Wheeler, J. R. *Limnol. Oceanogr.* **1976**, *21*, 846–852.
- (27) Sigleo, A. C.; Hare, P. E.; Helz, G. R. *Estuarine Coastal Shelf Sci.* **1983**, *17*, 87–96.

Received for review March 7, 1984. Revised manuscript received May 28, 1985. Accepted July 12, 1985. This work was sponsored by the Maryland Power Plant Siting Program, the Electric Power Research Institute, and Public Service Electric and Gas of New Jersey.

Interference in the Bactericidal Properties of Inorganic Chloramines by Organic Nitrogen Compounds

Roy L. Wolfe, N. Robert Ward, and Betty H. Olson*

Environmental Analysis, Program in Social Ecology, University of California, Irvine, California 92717

■ The interference of nitrogenous organic compounds on the bactericidal activity of chloramines was examined. The amino acid glycine (0.1–0.5 mg/L as nitrogen) was supplemented into water samples obtained from a finished water reservoir to artificially increase the levels of organic nitrogen. Inactivation rates of total count bacteria were markedly slower with chloramines (1.6 mg/L; $\text{Cl}_2\text{-N}$, 3:1 w/w; pH 8) when preammoniation and concurrent application methods were compared to preformed chloramines. Levels of glycine as low as 0.1 mg (as nitrogen)/L reduced the bactericidal activity with the preammoniation procedure. No decrease in the bactericidal properties was observed when preformed chloramines were assayed in the presence of glycine. Significantly, the inorganic chloramine residuals (ammonia derived) and organic chloramine residuals (glycine derived) could not be distinguished by amperometric or ferrous ammonium sulfate–diethyl-*p*-phenylenediamine titration techniques. Hence, residual measurement by conventional analytical techniques may not indicate the true level of disinfection potential of chloramines.

The presence of nitrogenous organic compounds in water may significantly reduce the microbicidal activity of inorganic monochloramines by interfering with the formation and stability of this disinfectant. This interference results primarily from two sets of chemical reactions that lead to a progressive increase in the levels of organic *N*-chloro compounds and a corresponding decline in inorganic monochloramine. The initial distribution of organic and inorganic chloramines is determined by the concentrations and relative chlorination rates of organic nitrogenous compounds and ammonia (1). If the organic N compounds bind more rapidly with chlorine than ammonia, higher levels of organic chloramines will initially be formed. This kinetically determined distribution is followed by reaction toward equilibrium which frequently favors the formation of organic chloramines (2). As such, the expected level of inorganic chloramine residual may not be achieved during chloramine formation or the level of inorganic chloramine may decrease with extended residence time in the distribution system.

Significantly, many organic chloramine compounds, particularly the chlorinated amino acids, have little or no bactericidal activity (3, 4). Compounding this problem is the inability of current analytical techniques that measure combined chlorine residuals to distinguish between inorganic and many forms of organic chloramines (2, 5).

To our knowledge, there is no experimental evidence to date to verify that nitrogenous organic compounds reduce the disinfectant activity of inorganic chloramine as a direct result of preferential binding and exchange reactions. We report on a series of experiments designed to demonstrate interference in the bactericidal properties of inorganic chloramines by glycine when preammoniation and concurrent addition application techniques are used. This information is particularly pertinent for water treatment facilities using source water with elevated levels of interfering nitrogenous organic compounds because the amount of "active" inorganic chloramine in water cannot be quantified.

Unfortunately, knowledge of the types and concentrations of nitrogenous organic compounds in surface waters is limited (2, 6). However, the presence of amino acids and other primary amines such as peptides are thought to be among the most environmentally significant forms of organic nitrogen in water supplies due to their ubiquity and their interference with inorganic chloramine formation. In general, the concentrations of free amino acids in fresh water varies from a few to several hundred micrograms per liter (7). Gardner and Lee (8) found approximately 20 μg of several amino acids/L in moderately eutrophic lake water whereas Zygmuntowa (7) observed 50–200 μg of free amino acids/L in highly eutrophic pond water. Hutchinson (9) reported that free amino N, peptides, and non-amino N averaged 74, 171, and 194 $\mu\text{g}/\text{L}$, respectively, in 15 Wisconsin lakes. The concentrations of free amino N in these lakes ranged from 20 to 121 $\mu\text{g}/\text{L}$, whereas the levels of peptide N ranged from 70 to 300 $\mu\text{g}/\text{L}$. Although not stated, the nutrient status of the lakes most likely ranged from moderately oligotrophic to highly eutrophic. The degree of eutrophication in lake water is important because it will influence the amount of nitrogenous organic compounds present (10). By comparison, the concentration of free amino nitrogen in sewage effluents can be expected to be an order of magnitude greater than the levels found in oligotrophic fresh waters. Isaac and Morris (11) estimate that free amino nitrogen ranges from 200 to 750 $\mu\text{g}/\text{L}$ in domestic sewage effluent.

Our research findings during May and June 1982 in a finished water reservoir suggested that nitrogenous organic compounds interfered with disinfection when preammoniation and concurrent application techniques were utilized to form inorganic chloramine. In these studies, we noted that the total count bacteria were inactivated significantly ($p < 0.05$, $df = 16$, using linear regression analysis) more slowly at pH 8 when preammoniation and concurrent application techniques were used than when preformed inorganic chloramines were employed. Some of these data are presented in Table I. Organic amine containing compounds present in the San Joaquin Reservoir water were implicated as the interfering agents because the residual chloramine concentrations, determined by amperometric and ferrous ammonium sulfate–diethyl-*p*-phenylenediamine (FAS–DPD) titration procedures, were identical regardless of disinfection application techniques. To test indirectly that organic amine compounds were interfering with inorganic chloramine formation and disinfection, two experiments were conducted in which the amino acid glycine was supplemented into the San Joaquin Reservoir water to artificially increase the level of organic nitrogen.

These studies were conducted at 22 °C in sterile, 1-L beakers. Water samples were collected from the San Joaquin Reservoir between May and July 1982. The San Joaquin Reservoir (capacity 3000 acre-ft) is a finished water reservoir maintained by the Metropolitan Water District (MWD) of southern California and is utilized for short-term storage. Generally, the water received by the reservoir is a blend of California State Project Water and Colorado River water, treated at the Robert B. Diemer treatment plant. This water has received full treatment

Table I. Evidence of Interference in the Inactivation of Total Bacterial Populations from the San Joaquin Reservoir Using Different Chloramine Application Techniques

sample date	treatment ^a	\bar{X}_0^b	\bar{X}_{15}^b	\bar{X}_{25}^b	\bar{X}_{35}^b	residual concn, mg/L ^f
5/6/82	preform	4.02 ± 0.03 (100) ^c	2.62 ^e (4.0)	1.45 ± 0.17 (10.27)	0 (<0.19)	1.55
	preamm	4.02 ± 0.03 (100)	3.55 ± 0.13 (34.0)	3.44 ± 0.21 (24.3)	3.06 ± 0.11 (11.0)	1.60
	conc	4.02 ± 0.03 (100)	3.42 ± 0.19 (25.1)	3.28 ± 0.34 (18.3)	3.00 ± 0.08 (9.4)	1.60
5/17/82 ^d	preform	3.66 ± 0.06 (100)	2.48 ^e (6.0)	0 (<0.44)	0 (<0.44)	1.58
	preamm	3.66 ± 0.06 (100)	2.73 ± 0.19 (11.7)	2.52 ± 0.62 (7.2)	2.35 ± 0.87 (4.9)	1.60
	conc	3.66 ± 0.06 (100)	2.83 ± 0.20 (14.7)	2.70 ± 0.17 (11.0)	2.18 ± 0.14 (3.3)	1.62
5/20/82	preform	3.98 ± 0.03 (100)	2.55 ± 0.31 (3.7)	2.19 ± 0.31 (11.6)	1.80 ± 0.29 (0.67)	1.64
	preamm	3.98 ± 0.03 (100)	3.19 ± 0.15 (15.9)	2.76 ± 0.25 (5.9)	2.72 ± 0.18 (5.5)	1.60
	conc	3.98 ± 0.03 (100)	3.09 ± 0.09 (12.9)	2.74 ± 0.25 (5.7)	2.61 ± 0.24 (4.2)	1.60

^a Preform = preformed chloramines; preamm = preammoniation technique; conc = concurrent application technique. ^b Mean colony-forming units (log cfu/mL) and standard deviations after contact times of 0 (control), 15, 25, and 35 min. Each mean represents four observations. ^c Numbers in parentheses represent mean percent survival. ^d Contact times at 0, 11, 21, and 31 min. ^e Mean represents duplicate analysis. ^f Determined by ferrous ammonium sulfate-diethyl-*p*-phenylenediamine (FAS-DP) titrimetric procedure. Concentration measured immediately following assay.

Table II. Interference in the Bactericidal Activity of Preammoniation and Concurrent Application Techniques by Glycine^a

contact time, min	log mean cfu/mL bacteria surviving exposure ^b ± SD ^f					
	no glycine added			0.55 mg/L glycine added ^c		
	preform	preamm	conc	preform	preamm	conc
0	3.94 ± 0.043 (100) ^d	3.94 ± 0.043 (100)	3.94 ± 0.043 (100)	3.94 ± 0.043 (100)	3.94 ± 0.043 (100)	3.94 ± 0.043 (100)
15	2.29 ± 0.23 (2.24)	2.21 ± 0.13 (1.86)	2.16 ± 0.09 (1.66)	2.17 ± 0.30 (1.70)	3.74 ^e (63.0)	3.81 ^e (74.1)
30	1.87 ± 0.11 (0.85)	1.79 ± 0.18 (0.71)	1.87 ± 0.20 (0.85)	2.0 ± 0.24 (1.15)	3.58 ± 0.06 (43.7)	3.60 ± 0.05 (45.7)
60	1.14 ± 0.16 (0.16)	1.14 ± 0.14 (0.16)	1.11 ± 0.17 (0.15)	1.23 ± 0.14 (0.19)	2.98 ^e (11.0)	3.42 ^e (30.2)

^a Inactivation of total count bacteria from the San Joaquin Reservoir (7/2/82 sample date) using preformed, preammoniation, and concurrent addition techniques at 1.60 mg/L final chloramine concentration. Experiments were performed at pH 8 and 23 °C. ^b Represents geometric mean of four observation after contact times of 0 (control), 15, 30, and 60 min. ^c Represents 0.55 mg/L nitrogen (as glycine) added prior to experiment initiation. ^d Numbers in parentheses represent mean percents survived. ^e Means represent duplicate analysis. ^f SD = standard deviation.

consisting of coagulation, sedimentation, filtration, and chlorination. The water in the reservoir consistently ranges between pH 7.9 and pH 8.2 and carries no disinfectant residual.

Before analysis, the samples were allowed to equilibrate at room temperature (22 °C) and mixed to disperse any aggregated bacteria and/or particulate material. Five hundred milliliters of the pooled sample was added into each sterile beaker. The amino acid glycine was then supplemented and completely mixed into the 500-mL samples. The final concentrations of glycine in the beakers ranged from 0.1 to 0.55 mg/L (nitrogen). Glycine was selected as the organic nitrogen source because it is the simplest amino acid and does not possess disinfectant interfering side chains other than the amine group. Moreover, glycine is one of the most frequently occurring amino acids isolated from aquatic environments (12, 13). This amino acid has been purported to bind to chlorine approximately 13 times more rapidly than ammonia (14).

For the preammoniation studies, ammonium chloride (1.10 mg/L, nitrogen) was added and mixed 1 min prior to the addition of 500 mL of a double-strength chlorine solution (3.0–3.2 mg/L). Concurrent application studies were initiated by the simultaneous addition of ammonia and chlorine. For the preformed studies, water samples containing glycine were dosed with 500 mL of a double-strength chloramine solution (3.0–3.2 mg/L; Cl₂-N, 3:1 w/w). The solutions containing the disinfectant and samples were mixed at 100 rpm with a Phipps and Bird paddle stirrer for the duration of the assay. Disinfectant concentrations were measured before and after each inactivation experiment by using the amperometric and ferrous ammonium sulfate-diethyl-*p*-phenylenediamine

(FAS-DPD) titrimetric procedures (15).

At preselected contact times, aliquots were removed and added into 10 mL of 20 mM sodium thiosulfate (Baker) and 0.1% Bacto-Peptone (Difco). Appropriate portions of the neutralized samples were then filtered through 0.45 μM cellulose acetate membranes (Gelman GN-6) and washed with at least 50 mL of sterile rinse water containing 10 mM phosphate buffer and 0.1% Bacto-Peptone at pH 7.0. Membranes were placed on membrane Standard Plate Count Agar (16) and enumerated after a 7-day incubation at 24 °C. Data were statistically analyzed by linear regression and two-way analysis of variance (ANOVA) using packaged statistical programs (SPSS) contained on the Honeywell CP-6 at the University of California, Irvine.

In the first experiment, glycine was supplemented into water, collected on June 25, 1982, to a level of 1.10 mg/L as nitrogen. The concurrent, preammoniation, and preformed application methods were then employed. In each case, the concentration of ammonia nitrogen (3:1 w/w) was equivalent to the concentration of organic nitrogen. For comparative purposes, inactivation curves were also determined without supplementation of glycine by using the three application methods. These data revealed that the bactericidal activity of chloramines was significantly ($p < 0.05$, $df = 16$) reduced by glycine when preammoniation and concurrent addition techniques were utilized (Table II). No inhibition of the bactericidal activity, however, was noted in the presence of glycine when the preformed chloramines were tested. On this particular sampling date the rates of inactivation of the total count bacteria without glycine using preformed application were not significantly different ($p < 0.05$, $df = 16$) from preammoniation and concurrent addition techniques without glycine, suggesting

Table III. Combined Chlorine Determinations Using the Amperometric and FAS-DPD Procedures for San Joaquin Reservoir Samples Supplemented with Glycine

application technique	glycine, mg/L N	ammonia, mg/L N	NH ₂ Cl measured ^a		theoretical NH ₂ Cl concn ^b
			amperometric	FAS-DPD	
performed	0	0.55	1.54	1.63	1.60
preammoniation	0.1	0.55	1.50	1.60	1.39
preammoniation	0.25	0.55	1.50	1.63	0.79
preammoniation	0.55	0.55	1.52	1.63	0.32

^a Residual monochloramine concentration (inorganic + organic chloramine). ^b Theoretical distribution of NH₂Cl and *N*-chloroglycine on the basis (i) that nitrogen species bind a maximum of 5 × the weight of chlorine (5:1 Cl₂-N w/w) and (ii) that [NH₂Cl] = k_1 [NH₃][HOCl] and [NcGly] = k_2 [Gly⁻][HOCl] where [NH₃] = concentration of un-ionized ammonia at pH 8, [Gly⁻] = concentration of glycine anion at pH 8, [HOCl] = concentration of unionized free chlorine, k_1 = fundamental rate constant for reaction of NH₃ and HOCl at 20 °C = 3.85×10^6 (14), and k_2 = fundamental rate constant for reaction of Gly⁻ and HOCl at 20 °C = 4.94×10^7 (14).

that the levels of naturally occurring nitrogenous organic compounds in the water were low and did not interfere with chloramine formation and subsequent disinfection.

In the second experiment, die-off rates using the preammoniation technique were determined with the San Joaquin Reservoir samples collected on July 16, 1982, supplemented with glycine to final concentrations of 0.1, 0.25, and 0.55 mg/L as nitrogen. For comparative purposes, inactivation rates were also determined by using preammoniation and preformed application without addition of glycine. The final concentration of ammonia added to each solution was 0.55 mg/L as nitrogen. These data indicated that the bactericidal activity with preammoniation was significantly reduced ($p < 0.05$, $df = 16$) when a concentration of 0.1 mg/L organic nitrogen as glycine was tested (Figure 1). After 60 min, the counts in the preformed and preammoniation solutions that did not receive glycine supplementation were reduced from 7000 cfu/mL to 50 and 70 cfu/mL, respectively, and were not significantly different at $p < 0.05$. This suggested that interfering nitrogenous organic compounds in the reservoir were low on this sample date also, and hence, limited disinfection impairment of chloramines was observed. In contrast, bacterial levels in the glycine-supplemented solutions exposed to preammoniation for 60 min were 500 (0.1 mg/L as nitrogen), 2000 (0.25 mg/L as nitrogen), and 4000 cfu/mL (0.55 mg/L as nitrogen). Regression analyses of the inactivation rates in this experiment indicated that the rates for preammoniation with glycine supplementation (at 0.1, 0.25, and 0.55 mg/L) were statistically different at $p < 0.05$ ($df = 16$) from both preformed and preammoniated solutions without glycine. Moreover, the amperometric and FAS-DPD titrimetric procedures were unable to distinguish between organic and inorganic chloramines (Table III). The impact of relatively small concentrations of amino acids on inorganic chloramine formation is shown by the theoretically calculated concentrations of inorganic chloramine (Table III). For example, the presence of 0.1, 0.25, and 0.55 mg/L glycine (as nitrogen) reduces the active inorganic chloramine by 13%, 51%, and 80%, respectively.

Although the types and concentrations of organic N compounds in the San Joaquin Reservoir have not been quantified, determinations of the total Kjeldahl nitrogen and ammonia levels were determined from four locations within the Metropolitan Water District of southern California (MWD) system. The levels of total Kjeldahl nitrogen ranged from 0.19 to 0.32 mg/L. Ammonia concentrations were on the order of 0.1 mg/L, indicating that the levels of total organic nitrogen were approximately 0.1–0.2 mg/L. The concentration of total organic nitrogen for these locations appear low compared to values reported by others (6), but it is likely that these levels fluctuate

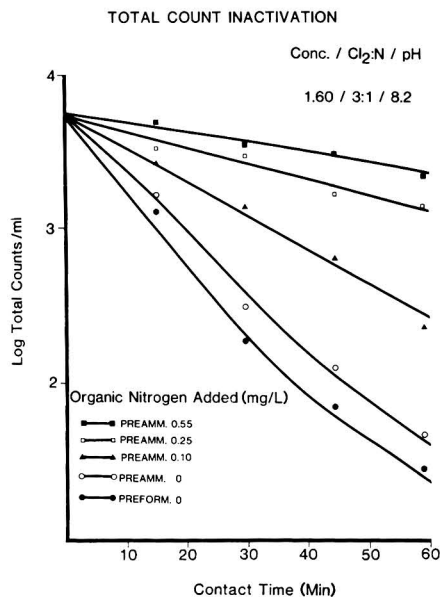


Figure 1. Inactivation of total count bacteria from the San Joaquin Reservoir using preammoniation and preformed application techniques (7/16/82 sample date). Glycine was supplemented into samples at levels of 0.1, 0.25, and 0.55 mg/L (final concentration as nitrogen) prior to preammoniation treatment. Experiments performed at pH 8.0 and 22 °C. Each datum represents the mean of two observations.

considerably during the year and are markedly influenced by the nutrient status of the reservoir and by seasonal events such as algal blooms. Morris et al. (6) observed that the concentration of total organic nitrogen in a New England municipal water supply increased from 2.2 to 21.7 mg/L during a summer algal bloom. Although not determined, the levels of amino acids and other primary amines in their samples most certainly increased in proportion to the concentration of total organic nitrogen. This suggests that interference by organic amine compounds is most likely to occur in systems that obtain source water from eutrophic lakes and rivers or during seasonal algal blooms.

Friend (17) and Morris (1) have studied the rate of reaction of chlorine with amino acids and other nitrogenous compounds. Some of Morris' revised data are presented in Table IV. It can be seen that the reaction of chlorine with certain nitrogenous compounds (alanine, glycine, methylamine, dimethylamine, and diethylamine) is more rapid than with others (ethyl aminoacetate, glycylglycylglycine). From these data the type of organic amine com-

Table IV. Chlorination Rates for Organic Nitrogen Compounds Relative to Ammonia

nitrogenous compound	relative reaction rate ($k_{\text{RNHCl}}/k_{\text{NH}_2\text{Cl}})^a$
amino acids	
glycine	13
alanine	16
leucine	14
serine	7.6
glutamic acid	13
peptides	
glycylglycine	1.9
glycylglycylglycine	1.7
others	
methylamine	77
dimethylamine	86
diethylamine	16
morpholine	9
diethanolamine	9
ethyl aminoacetate	2
chloramide	5.5×10^{-5}
N-chloromethylamine	1.8×10^{-4}

^a k_{RNHCl} = chlorination rate of organic nitrogen compound (1, 14); $k_{\text{NH}_2\text{Cl}}$ = chlorination rate of ammonia (14) = $3.85 \times 10^6 \text{ s}^{-1}$ at 20 °C.

pounds in the water will be more important in terms of their relative rates of N-chlorination and interference with inorganic chloramine formation than merely the amount of organic N present.

In addition, recent studies by Snyder and Margarum (18) and Isaac and Morris (2) have shown that chlorine (Cl^+) can be transferred from inorganic chloramines to amino acids and peptides via a direct-transfer mechanism. The rate and extent to which this reaction proceeds are largely dependent upon the type and concentration of the N substrate. Isaac and Morris (2) observed that with equimolar concentrations of NH_2Cl (pH 7, 25 °C) and several organic nitrogen compounds, including glycine (at 10^{-5} M), 50% of NH_2Cl was converted to organic chloramine in 1–2 days. With concentrations of individual nitrogenous compounds and 10^{-4} M, 50% conversion required only a few hours. The concentrations of nitrogenous compounds in their work were chosen to reflect the levels in oligotrophic freshwater and wastewater systems.

In summary, the preferential binding of amine-containing compounds such as amino acids and peptides with chlorine could greatly reduce the disinfection potential of inorganic chloramines. In addition, long retention times in distribution systems may result in conversion from inorganic chloramines to the less microbicidal organic chloramines. This problem is compounded by the inability of any currently employed analytical technique to specifically measure the levels of inorganic chloramine in drinking water. Current research efforts should be directed toward determining the types and concentrations of or-

ganic amine compounds in drinking water and their impact on disinfection with chloramines.

Acknowledgments

We thank Edward G. Means and Michael J. McGuire of the Metropolitan Water District of southern California (MWD) for their valuable comments on the manuscript.

Registry No. NH_2Cl , 10599-90-3; Gly, 56-40-6; N_2 , 7727-37-9.

Literature Cited

- (1) Morris, J. C. "Principles and Applications of Water Chemistry"; Faust, S. D.; Hunter, J. V., Eds.; Wiley: New York, 1967; Chapter 2.
- (2) Isaac, R. A.; Morris, J. C. *Environ. Sci. Technol.* **1983**, *17*, 738–742.
- (3) Feng, T. H. *J. Water Pollut. Control Fed.* **1966**, *38* (4), 614–628.
- (4) Krusé, C. W.; Hsu, Y.; Griffiths, A. C.; Stringer, R. "Halogen Action on Bacteria, Viruses and Protozoa". *Proc. Natl. Spec. Conf. Disinfect.*, **1970**, 113–136.
- (5) White, G. C. "Disinfection of Wastewater and Water for Reuse"; Van Nostrand Reinhold: New York, 1978; Chapter 2.
- (6) Morris, J. C.; Ram, N.; Baum, B.; Wajon, E. "Formation and Significance of N-chloro Compounds in Water Supplies". 1980, EPA-600/2-80-031.
- (7) Zygmontowa, J. *Acta Hydrobiol.* **1972**, *14*, 317–325.
- (8) Gardner, W. S.; Lee, G. F. *Environ. Sci. Technol.* **1973**, *7*, 719–724.
- (9) Hutchinson, G. E. "A Treatise on Limnology"; Wiley: New York, 1957; p 1015.
- (10) Gocke, K. *Arch. Hydrobiol.* **1970**, *67*, 285–367.
- (11) Isaac, R. A.; Morris, J. C. in "Water Chlorination: Environmental Impacts and Health Effects"; Jolley, R. L.; Brungs, W. A.; Cumming, R. B., Eds.; Ann Arbor Science: Ann Arbor, MI, 1980; Vol. 3, Chapter 17.
- (12) Litchfield, C. D.; Prescott, J. M. *Limnol. Oceanogr.* **1978**, *15*, 250–256.
- (13) Newell, I. L. *J. N. Engl. Water Works Assoc.* **1976**, *90*, 315–324.
- (14) Isaac, R. A.; Morris, J. C. "Water Chlorination: Environmental Impact and Health Effects"; Jolley, R. L.; Brungs, W. A.; Cotruvo, J. A.; Cumming, R. B.; Mattice, J. S.; Jacobs, V. A., Eds.; Ann Arbor Science: Ann Arbor, MI, 1983; Vol. 4, Chapter 3.
- (15) "Standard Methods for the Examination of Water and Wastewater", 14th ed.; American Public Health Association: Washington, DC, 1975.
- (16) Taylor, R. H.; Geldreich, E. E. *J.—Am. Water Works Assoc.* **1979**, *44*, 1110–1117.
- (17) Friend, A. G. Ph.D. Dissertation, Harvard University, Cambridge, MA, 1956.
- (18) Snyder, M. P.; Margarum, D. W. *Inorg. Chem.* **1982**, *71*, 2545–2550.

Received for review July 16, 1984. Revised manuscript received December 7, 1984. Accepted July 11, 1985. The research was supported by a grant (MWD 1373) from the Metropolitan Water District of Southern California.

Soil Sorption of Organic Vapors and Effects of Humidity on Sorptive Mechanism and Capacity

Cary T. Chiou*

U.S. Geological Survey, Denver Federal Center, Denver, Colorado 80225

Thomas D. Shoup

Department of Agricultural Chemistry, Oregon State University, Corvallis, Oregon 97331

■ Vapor sorption isotherms on dry Woodburn soil at 20–30 °C were determined for benzene, chlorobenzene, *p*-dichlorobenzene, *m*-dichlorobenzene, 1,2,4-trichlorobenzene, and water as single vapors and for benzene, *m*-dichlorobenzene, and 1,2,4-trichlorobenzene as functions of relative humidity (RH). Isotherms for all compounds on dry soil samples are distinctively nonlinear, with water showing the greatest capacity. Water vapor sharply reduced the sorption capacities of organic compounds with the dry soil; on water-saturated soil, the reduction was about 2 orders of magnitude. The markedly higher sorption of organic vapors at subsaturation humidities is attributed to adsorption on the mineral matter, which predominates over the simultaneous uptake by partition into the organic matter. At about 90% RH, the sorption capacities of organic compounds become comparable to those in aqueous systems. The effect of humidity is attributed to adsorptive displacement by water of organics adsorbed on the mineral matter. A small residual uptake is attributed to the partition into the soil-organic phase that has been postulated in aqueous systems. The results are essentially in keeping with the model that was previously proposed for sorption on the soil from water and from organic solvents.

Introduction

In earlier studies, we dealt with the soil sorption of nonionic organic compounds in water and in organic solvents (1–6). The sorption capacities of solutes on a given soil were linear with solute concentrations in water and were nonlinear and much higher in nonpolar organic solvents. These characteristics were interpreted by the assumption that the soil behaved as a dual sorbent, in which the mineral matter functioned as a conventional solid adsorbent and the organic matter as a partition medium. The linear isotherms in aqueous systems were attributed to partition in the organic matter, with concomitant suppression by water of adsorption on the mineral matter (1–5). The nonlinear isotherms from the organic solvents (which minimize partition in the organic matter) were attributed to adsorption on the mineral matter, on which the specific interactions of adsorbate polar groups reduced competition by the organic solvents (2, 5, 6).

We here consider the sorption behavior of organic vapors on one of the earlier studied soils, both as single vapor components and as functions of relative humidity. This study supplements earlier sorption studies in aqueous systems by enabling us to vary the chemical potential of water and thereby to study its adsorptive displacement effect in greater detail to simulate the sorption of organic compounds by natural soils under the wide variation in humidity that they may experience.

The studies have been carried out for some organic compounds on a soil sample (Woodburn soil) that was used in the earlier study on sorption from water solution. The vapor-phase sorption data determined here are compared with the corresponding data derived from aqueous systems.

Experimental Section

The soil uptake of selected organic compounds from the vapor phase at varying humidities was carried out by a dynamic-equilibrium sorption apparatus in a constant-temperature room (Figure 1). The test compound was blended with quartz sand and placed in a glass column (2.5 in. i.d. × 14 in.), which served as the chemical vapor generator when N₂ gas was passed from the bottom of the column. The column was connected to the vapor-mixing chamber at the top by a standard 71/60 taper joint. A separate glass column (1.5 in. i.d. × 16 in.), filled with water and cut pieces of Teflon tubing, served as a moisture generator, by passing dry N₂ gas from the bottom of the column. The top of this moisture generator column was connected to the vapor-mixing chamber by a standard 24/40 taper joint. Exit vapors from these two columns (controlled by valves V2 and V3) were combined and mixed with a third stream of makeup dry N₂ gas (controlled by valve V1) at the vapor-mixing chamber to produce a final stream of vapor mixture of test chemical and moisture in N₂ gas. This final vapor mixture was then brought in contact with the soil sample placed in a rotating flask to attain dynamic equilibria between vapors and soil.

Total gas-flow rates out of the mixing chamber were maintained in the range 100–250 mL/min in normal runs. By proper control of the flow rate of each column saturator and that of the makeup gas, steady vapor concentrations at a fixed relative humidity could be obtained. A heating tape was wrapped around the sand column, when needed, to increase the vapor concentration. Amounts of the organic vapor sorbed by soil at varying concentrations at a fixed humidity were determined by extraction of the soil. The resulting data were used to make an isotherm plot.

Vapor concentrations and relative humidities were measured prior to placing soil samples into the rotating flask. To do this, the total gas flow rate was first measured by a soap-bubble flow meter. Relative humidity (RH) was determined subsequently by inserting a glass tube containing 2–3 g of Dehydrite (magnesium perchlorate) at the end of the mixing chamber to trap the moisture. The concentration of water vapor was calculated on the basis of weight gain of magnesium perchlorate, total gas flow rate, and trapping time. Vapor concentrations of the test compound were determined by extracting the vapor at the outlet of the mixing chamber with a gas impinger (micro-bubbler, Ace Glass Co.) filled with hexane (20 mL) as the extracting solvent. To ensure steady flows of water and chemical vapor, these measurements were repeated as many times as needed.

When the vapor system reached a steady-state condition, the soil sample was placed in the (rotating) sample flask. After the sorption was measured for one combination of vapor concentration and RH, the vapor concentration was then varied by adjusting the flow rate through valve V2, while the RH was kept unchanged. This was done by adjusting the flow rate of the makeup gas to compensate for the variation of gas flow to the chemical-vapor gener-

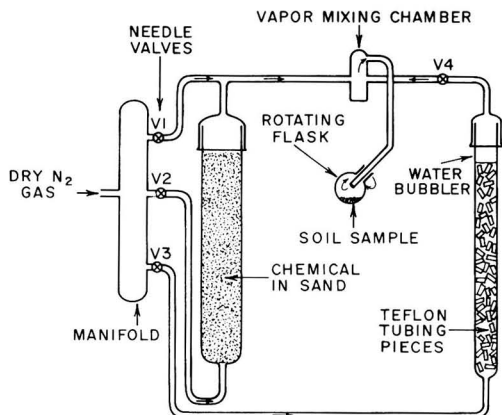


Figure 1. Schematic diagram of the dynamic vapor-sorption apparatus.

ator. This procedure reduced the time involved for conditioning the entire vapor system. With the control as described, the error in vapor concentration and RH is generally within $\pm 3\%$. However, some difficulty was experienced in maintaining constant RH above 85%, while the vapor concentration of the compound was varied; the resulting error was about $\pm 5\%$ for both organic and water vapors. To obtain 0% RH in the experiment, valves V3 and V4 were closed, and a column of Drierite (CaSO_4) was inserted to the end of the mixing chamber to remove residual moisture in the system.

To thoroughly mix the soil sample and to maximize the exposure of the soil to vapors, four indentations were made in the sides of the rotating sample flask. These indentations broke up the lumps of the soil, promoting exposure of the soil to vapors. Normally, an exposure time of about 4 h was sufficient for establishing the sorption equilibrium. The contact time was about 8 h in most runs.

The uptake of *m*-dichlorobenzene and water as single-component vapors by dry soil samples was also measured by using a static equilibrium-sorption apparatus described elsewhere (7) (this work was carried out by Professor P. J. Reucroft, Department of Materials Science, University of Kentucky, Lexington, KY). This method could only study the uptake of single vapors; the result was taken as a reference to check the precision of the isotherms of single vapors determined by the dynamic-sorption apparatus. Isotherms of *m*-dichlorobenzene on dry soil (0% RH) determined by both types of apparatus were within 5% in weight of soil uptake. The sorption isotherm of water in this report was based on results derived from the static-sorption apparatus, because steady and accurate humidities at RH < 20% by using the dynamic-sorption apparatus were difficult to maintain and because water uptake was very sensitive at low RH.

The Woodburn soil (60/80 mesh fraction) used in this study was from the same batch employed in the previous study on the uptake of organic compounds from water (4); the composition of the soil on a dry-weight basis was 1.9% organic matter, 9% sand, 68% silt, and 21% clay. X-ray diffraction indicated that kaolinite and mica were the predominant clay types. Soil samples were oven-dried at 140 °C for 48 h to remove moisture and then stored in a vacuum desiccator before being placed in the sample flask. Samples treated in this manner were considered to be "dry". Expectably, samples dried at this temperature would still retain a small amount of water that is tightly associated with soil minerals. This amount was not de-

termined, and we assumed that it was not significant. The air-dried Woodburn soil contained about 2.5% moisture.

The test organic compounds (benzene, chlorobenzene, *m*-dichlorobenzene, *p*-dichlorobenzene, and 1,2,4-trichlorobenzene) were all reagent-grade from Aldrich Chemical Co. and were used as received. Except for *p*-dichlorobenzene, the sorption isotherms of the other compounds from aqueous solution on Woodburn soil have been reported in the earlier study (4). Following the vapor-soil equilibrium, the soil was removed and extracted for the test compound by a mixture of acetone and hexane (1:1 volume ratio). The recovery of all compounds by this solvent mixture was greater than 97%. The extract was further diluted with hexane to appropriate concentrations for analysis. Chlorinated compounds were analyzed by a gas chromatograph equipped with a ^{63}Ni electron-capture detector, using a 2-mm i.d. \times 6 ft glass column packed with 6% SE 30 on Gas Chrom Q 60/80 mesh. Benzene was analyzed by a Cary 11 UV spectrophotometer.

Results and Discussion

Figures 2-6 show the equilibrium isotherms of vapor sorption on Woodburn soil. Isotherms are plotted as milligrams taken up per gram of whole soil (Q) vs. the relative vapor concentration of the compound (P/P^0), where P is the equilibrium partial pressure and P^0 is the saturation vapor pressure of the compound at the system temperature. The use of P/P^0 in the isotherm plot normalizes the activity (or chemical potential) of each compound with respect to its own pure state. This normalization permits a direct comparison between uptakes of different compounds from the vapor phase and also between uptakes of the same compounds from liquid and vapor phases; in aqueous systems, the isotherms are normalized by the relative concentration (C_e/C_s) (where C_e is the equilibrium concentration and C_s is the solubility of the compound). The P^0 values for the compounds studied are taken from the literature (8): benzene, 74.0 mmHg (20 °C); chlorobenzene, 10.7 mmHg (20 °C); *m*-dichlorobenzene, 1.67 (20 °C) and 3.00 mmHg (30 °C); 1,2,4-trichlorobenzene, 0.315 (20 °C) and 0.600 mmHg (30 °C); water, 22.1 mmHg (23.8 °C). The P^0 value of *p*-dichlorobenzene at 20 °C (0.65 mmHg) was determined experimentally by analyzing the concentration of the saturated vapor from the chemical-vapor generator. Figure 7 compares the vapor uptake of *m*-dichlorobenzene and 1,2,4-trichlorobenzene by Woodburn soil (in micrograms per gram of soil) at 90% RH with the corresponding uptake from water at 20 °C.

Figure 2 shows the isotherms on dry Woodburn soil at 20 °C for benzene, chlorobenzene, *m*-dichlorobenzene, *p*-dichlorobenzene, 1,2,4-trichlorobenzene, and water (23.8 °C). All isotherms show a steep rise at low P/P^0 , followed by a slower rise at intermediate P/P^0 , and then by another sharp rise as P/P^0 approaches 1. The shape of the isotherms corresponds to the Brunauer type-II adsorption, which is characteristic of vapor condensation to form multilayer adsorbates. Note that the isotherms with dry soil are highly nonlinear, in sharp contrast to the linearity of isotherms in aqueous systems, and with markedly greater capacities. For instance, the maximum capacity of *m*-dichlorobenzene with dry Woodburn soil is about 45 mg/g of soil, which is about 100 times the limiting uptake of the compound by the same soil from water (i.e., at $C_e/C_s = 1$). These differences indicate a powerful suppression by water of organic vapor adsorption on soil minerals, which is what one expects for adsorption on mineral adsorbents.

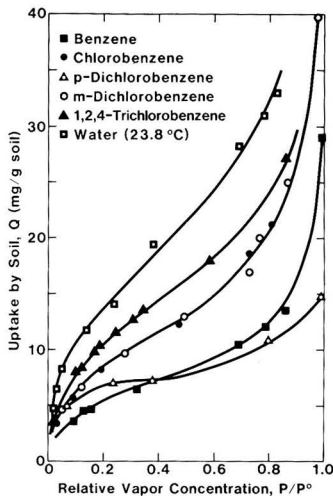


Figure 2. Uptake of organic vapors and moisture by dry Woodburn soil at 20 °C vs. relative vapor concentration.

The capacities of vapor uptake by dry Woodburn soil in Figure 2 are comparable to those of ethylene dibromide (EDB) vapor uptake by various soils and minerals as reported by Call (9) and Jurinak (10). In Call's study, the EDB uptake by dry soils at $P/P^0 \approx 0.50$ ranged from approximately 10 mg/g for Field Station soil (7.4% clay and 4.2% organic matter) to 55 mg/g for Boston Silt (46% clay and 4.6% OM), largely in proportion to clay content rather than organic matter content. Jurinak studied the vapor adsorption of EDB by different types of pure clays and the effect of cations associated with clays. At $P/P^0 = 0.90$, amounts of EDB adsorbed by calcium illite, calcium montmorillonite, and calcium kaolinite were approximately 180, 170, and 90 mg/g, respectively, and a significant variation of EDB adsorption was found among Na, Ca, and Mg-exchanged montmorillonites due to variations of BET surface areas. Although uptake capacities would obviously be different between soils because of differences in mineral types and compositions according to these analyses, the results from Figures 2 and 7 of the present study clearly reveal the dominant effect of mineral adsorption with dry Woodburn soil.

The high water uptake by dry Woodburn soil appears to be associated with strong polar interactions of water with polar minerals (2-4). Sorption capacities are significantly lower for organic compounds that are not strong wetting agents on polar mineral surfaces. The increasing uptake from benzene to the relatively more polar chlorobenzene, *m*-dichlorobenzene, and 1,2,4-trichlorobenzene also indicates the effect of polarity on mineral adsorption. Relative sorption capacities of organic vapors at low P/P^0 follow the order of 1,2,4-trichlorobenzene > *m*-dichlorobenzene \approx *p*-dichlorobenzene \approx chlorobenzene > benzene, roughly in proportion to the number of chlorines in the molecule. At high P/P^0 , *p*-dichlorobenzene shows markedly lower uptake than *m*-dichlorobenzene and other compounds. The difference in uptake between *m*-dichlorobenzene and *p*-dichlorobenzene at high P/P^0 occurs presumably because *p*-dichlorobenzene is a solid at room temperature (mp 54 °C), whereas *m*-dichlorobenzene and other compounds are liquids. The inability of a solid adsorbate to form a compact multilayer phase on mineral surfaces would thus lead to a lower capacity compared to those for liquids at high P/P^0 . For example, solid adsor-

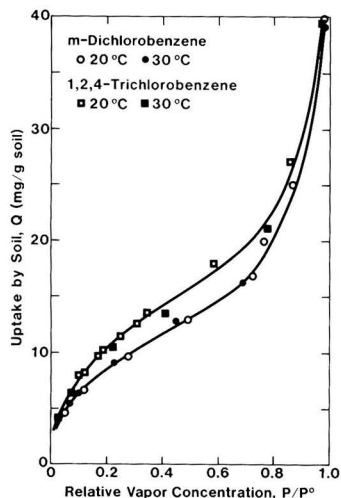


Figure 3. Vapor uptake of *m*-dichlorobenzene and 1,2,4-trichlorobenzene by dry Woodburn soil at 20 and 30 °C.

bates have been noted to show lower limiting capacities on activated carbon, presumably because of inefficient packing (11, 12).

The fact that adsorption on minerals is enhanced by adsorbate polarity makes water a powerful competitor to displace (nonionic) organic solutes from soil minerals in aqueous systems. The importance of polar interactions in mineral adsorption is also illustrated by the significantly higher uptake of the more-polar paraffin than the less-polar lindane from hexane on dry (Woodburn) soil (6). This feature is in sharp contrast to purely physical (London-force) adsorption, which is frequently exhibited by activated carbon, where the polarity effects are relatively unimportant; in this case, water is a weak adsorbate, allowing effective adsorption of organic solutes from water (11).

Figure 3 shows a comparison of the 20 and 30 °C isotherms of *m*-dichlorobenzene and 1,2,4-trichlorobenzene on dry Woodburn soil in a normalized plot. The coincidence of two isotherms at 20 and 30 °C at $P/P^0 > 0.05$ is evidence that the heats of (mineral) adsorption are essentially the same as the heats of vapor condensation. That is

$$\Delta \bar{H}_Q \approx -\Delta \bar{H}_v \quad (1)$$

where $\Delta \bar{H}_Q$ is the (molar) isosteric heat of adsorption at capacity Q and $\Delta \bar{H}_v$ is the heat of vaporization of the compound. The $\Delta \bar{H}_v$ value, calculated by the Clausius-Clapeyron equation using vapor pressure data (8), is 10.6 kcal/mol for *m*-dichlorobenzene and 11.7 kcal/mol for 1,2,4-trichlorobenzene. The proximity of $\Delta \bar{H}_Q$ to $-\Delta \bar{H}_v$ at $P/P^0 > 0.05$ is commonplace in adsorption, which is taken as a basic assumption in the BET adsorption theory with adsorbates approaching and exceeding the monolayer capacity (whereas the heat of adsorption below monolayer is considered to be greater than the heat of vapor condensation).

The monolayer adsorption capacity (Q_m) and the molar heat of adsorption ($\Delta \bar{H}_m$) at $Q \leq Q_m$ for each adsorbate on dry Woodburn soil can be determined according to the BET equation (13):

$$\frac{x}{Q(1-x)} = \frac{(C-1)x}{CQ_m} + \frac{1}{CQ_m} \quad (2)$$

Table I. BET Monolayer Adsorption Capacities (Q_m) and Associated Molar Adsorption Heats ($\Delta\bar{H}_m$) of Adsorbates on Dry Woodburn Soil at 20 °C

compound	Q_m , mg/g of soil	$\Delta\bar{H}_v^a$, kcal/mol	$-(\Delta\bar{H}_m + \Delta\bar{H}_v)$, kcal/mol
benzene	5.57	8.09	1.52
chlorobenzene	7.53	9.43	1.82
<i>m</i> -dichlorobenzene	7.42	10.6	1.86
<i>p</i> -dichlorobenzene (solid)	5.54	15.0	2.54
1,2,4-trichlorobenzene	9.53	11.7	1.93
water (23.8 °C)	11.7	10.3	2.14

^a Molar heats of vaporization determined from vapor pressure data (8).

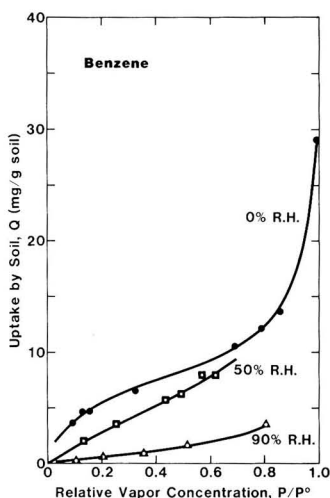


Figure 4. Vapor uptake of benzene by Woodburn soil at 20 °C as a function of relative humidity.

in which $x = P/P^0$, Q_m is the monolayer capacity of adsorbate on soil minerals (mg/g), and C is related to the net molar heat of adsorption at $Q \leq Q_m$ by

$$-\ln C \approx (\Delta\bar{H}_m + \Delta\bar{H}_v)/(RT) \quad (3)$$

where R is the gas constant and T is the system temperature. By eq 2, a plot of $x/[Q(1-x)]$ vs. x should yield a straight line, with a slope of $(C-1)/(CQ_m)$ and an intercept of $1/(CQ_m)$, from which Q_m and C can be determined. Data in Figure 2 give an excellent fit of eq 2 over the range $P/P^0 = 0.05-0.30$, as is typical in BET plots. Calculated values of Q_m and $-(\Delta\bar{H}_m + \Delta\bar{H}_v)$ for the adsorbates are presented in Table I. In calculating Q_m and $\Delta\bar{H}_m$, the weight of minerals was assumed to be the same as the dry soil, since the organic content is only 1.9%.

The BET monolayer adsorption capacities for all compounds with dry Woodburn soil were established at relatively low P/P^0 (≤ 0.18), except for benzene which occurred at $P/P^0 \approx 0.23$. Observed capacities at high P/P^0 greatly exceed the monolayer values. Since adsorption on mineral matter should depend on the types of minerals (particularly, clays) (9, 10), the calculated Q_m and $\Delta\bar{H}_m$ values represent weighted averages of all minerals in the soil. The $\Delta\bar{H}_m$ values (at $Q \leq Q_m$) are noticeably more exothermic than respective $-\Delta\bar{H}_v$ values by about 1.5–2.5 kcal/mol; these heat effects are consistent with the dominance of mineral adsorption with dry Woodburn soil.

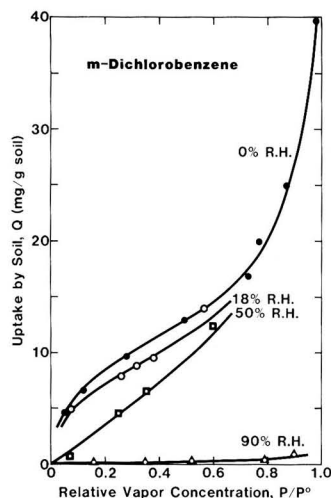


Figure 5. Vapor uptake of *m*-dichlorobenzene by Woodburn soil at 20 °C as a function of relative humidity.

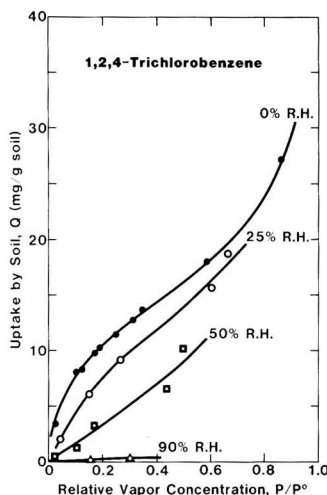


Figure 6. Vapor uptake of 1,2,4-trichlorobenzene by Woodburn soil at 20 °C as a function of relative humidity.

Consider now the effect of relative humidity on soil uptake of organic vapors. From the low uptake of solutes from water solution, one would expect the sorption of organic vapors to be strongly suppressed by water because of adsorptive competition on minerals. This effect should be most pronounced for low-organic-content mineral soils, since the amount sorbed through partition by soil-organic matter would be relatively insignificant. Figures 4–6 illustrate respectively the effect of humidity on the uptake of benzene, *m*-dichlorobenzene, and 1,2,4-trichlorobenzene by Woodburn soil. In spite of some uncertainty of the relative humidity (especially at 20% > RH > 85%), the progressive suppression of organic vapor uptake and resulting change in isotherm shape with an increase of RH are evident, as has been observed in the study of Call (9) on the uptake of ethylene dibromide by various soils.

In addition to the reduced capacities in the presence of water vapor, one notes that at RH $\geq 50\%$ isotherms for the organic vapors become practically linear at $P/P^0 \leq 0.5$; this may again be attributed to adsorptive displacement

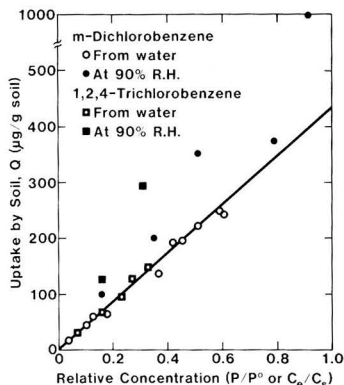


Figure 7. Comparison of the vapor uptake of *m*-dichlorobenzene and 1,2,4-trichlorobenzene by Woodburn soil at 90% RH (Q vs. P/P^0) at 20 °C with the corresponding uptake from water (Q vs. C_0/C_g) at 20 °C from ref. 4.

of organic adsorbates by water at highly active mineral surfaces (this displacement is foreseen in Figure 2, where water exhibits significantly greater uptake at $P/P^0 = 0.5$ than organic vapors at $P/P^0 \leq 0.5$). As adsorption by soil minerals is further reduced by increasing amounts of humidity, uptake by partition into the soil organic matter would become more a controlling factor, enhancing the linearity of isotherms. At about 90% RH, the resulting isotherms of *m*-dichlorobenzene and 1,2,4-trichlorobenzene fall into a range close to the corresponding isotherms obtained from aqueous solution (Q vs. C_0/C_g), as illustrated in Figure 7. The benzene isotherm at ~90% RH shows much greater deviations from the aqueous-phase isotherm (by more than a factor 5 in capacity), which may stem partly from the inaccuracy of high humidity values in our experiments. Overall, the observed isotherms at ~90% RH sufficiently demonstrate the dominance of solute partition with the soil-organic phase in sorption from water, in contrast to mineral adsorption as the dominant effect when the soil is dry or contains only subsaturation humidities. Finally, while one cannot exclude the possibility of a small amount of residual linear adsorption on the mineral matter in the presence of water, it may be recalled that the partition effect is distinguished from linear adsorption on mineral matter by the fact that it increases with increasing organic matter content (1, 4, 5).

We now relate the preceding results to earlier studies on the uptake of organic compounds by soils and minerals from organic solvents and under some other system conditions. As noted, high uptake of parathion from hexane by dehydrated soils and clays (6, 14, 15) and its suppression by water (6, 14) can be largely attributed to parathion adsorption on mineral matter and to subsequent competition of water for mineral adsorption. Our analysis is in keeping with Hance's finding (16) that a mineral-rich soil sorbs considerably more diuron from a (relatively nonpolar) petroleum solvent than from water, whereas the soil-organic matter shows the opposite effect. It also agrees with the finding by Spencer and co-workers (17, 18) that the partial pressures of dieldrin and lindane incorporated into an originally dehydrated soil increase greatly when the soil is hydrated. Moreover, it predicts the failure of the soil to take up (nonionic) organic solutes such as parathion (14) from polar organic solvents, which reduce

solute partition into organic matter by their good solvency and reduce adsorption on soil minerals because of their polarity. It explains the observation that nonpolar solvents (e.g., hexane) are less effective than polar solvents (e.g., acetone) for extracting organic pesticides from dry soils and that addition of water or polar solvents to hexane significantly improves the extraction efficiency (19).

In summary, the assumed roles of soil minerals and organic matter account both for the suppression of the soil uptake of organic vapors by water vapor and for the difference in sorption capacity from aqueous and organic solutions. Since the water content of surface soils can vary greatly with ambient humidity, the uptake of organic contaminants and pesticides by surface soils may be expected to be strongly influenced by ambient humidity.

Acknowledgments

Technical assistance from G. R. Wilson is gratefully acknowledged. We thank P. J. Reucroft of University of Kentucky (Lexington, KY) for providing isotherm data of water. We are grateful to Milton Manes (Kent State University, Kent, OH) and P. E. Porter (Modesto, CA) for valuable discussions.

Registry No. Water, 7732-18-5; chlorobenzene, 108-90-7; *p*-dichlorobenzene, 106-46-7; *m*-dichlorobenzene, 541-73-1; 1,2,4-trichlorobenzene, 120-82-1; benzene, 71-43-2.

Literature Cited

- Chiou, C. T.; Peters, L. J.; Freed, V. H. *Science (Washington, D.C.)* **1979**, *206*, 831.
- Chiou, C. T.; Peters, L. J.; Freed, V. H. *Science (Washington, D.C.)* **1981**, *213*, 684.
- Chiou, C. T. In "Hazard Assessment of Chemicals: Current Developments"; Saxena, J.; Fisher, F., Eds.; Academic Press: New York, 1981; Vol. 1, pp 117-153.
- Chiou, C. T.; Porter, P. E.; Schmedding, D. W. *Environ. Sci. Technol.* **1983**, *17*, 227.
- Chiou, C. T.; Porter, P. E.; Shoup, T. D. *Environ. Sci. Technol.* **1984**, *18*, 295.
- Chiou, C. T.; Shoup, T. D.; Porter, P. E. *Org. Geochem.* **1985**, *8*, 9.
- Chiou, C. T.; Reucroft, P. J. *Carbon* **1977**, *15*, 49.
- Weast, R. C. "Handbook of Chemistry and Physics", 53rd ed.; CRC Press: Cleveland, OH, 1972.
- Call, F. *J. Sci. Food Agric.* **1957**, *8*, 630.
- Jurinak, J. J. *Soil Sci. Soc. Am. Proc.* **1957**, *21*, 599.
- Manes, M.; Hofer, L. J. E. *J. Phys. Chem.* **1969**, *73*, 584.
- Chiou, C. T.; Manes, M. *J. Phys. Chem.* **1974**, *78*, 622.
- Adamson, A. W. "Physical Chemistry of Surfaces", 2nd ed.; Interscience Publishers: New York, NY, 1967; pp 584-594.
- Yaron, B.; Saltzman, S. *Soil Sci. Soc. Am. Proc.* **1972**, *36*, 583.
- Gerstl, Z.; Yaron, B. *J. Agric. Food Chem.* **1978**, *26*, 569.
- Hance, R. J. *Weed Res.* **1965**, *5*, 108.
- Spencer, W. F.; Cliath, M. M.; Farmer, W. J. *Soil Sci. Soc. Am. Proc.* **1969**, *33*, 509.
- Spencer, W. F.; Cliath, M. M. *Soil Sci. Soc. Am. Proc.* **1970**, *34*, 574.
- Filonow, A. B.; Shin, Y.-O.; Wolcott, A. R. In "Agrochemicals in Soils"; Banin, A.; Kafkafi, U., Eds.; Pergamon Press: Oxford, 1980; pp 83-89.

Received for review October 2, 1984. Revised manuscript received May 3, 1985. Accepted July 19, 1985. This work was supported in part by U.S. EPA Cooperative Research Grant CR-808046 from the EPA Environmental Research Laboratory at Corvallis, OR. Any use of trade names is for descriptive purposes only and does not constitute endorsement of the U.S. Geological Survey.

Estimation for Small Normal Data Sets with Detection Limits

Alan Gleit*

Versar, Inc., Springfield, Virginia 22151

■ Environmental data are characterized by the dual problems of small sample size and many values reported as "below detection limit". We propose several possible estimators and test them via simulation. We find a method that outperforms the usual arbitrary techniques (such as using the detection limit for the missing data).

Introduction

When environmental phenomena are measured, the measuring devices/procedures used are unable to detect low concentrations. Thus, concentrations below certain threshold levels are not measurable. Standard "detection limits" are set by various agencies for various phenomena for various types of measuring devices. Measured values below these limits are reported as "below detection limit" or as "trace" and are thus not available for statistical analysis. (Sometimes values below these limits are available, but their accuracy is greatly in doubt.) Consequently, the statistician often has a very basic problem facing him: how does he analyze data sets that contain a reasonable percentage of "below detection limit" entries?

Environmental data are characterized not only by detection limits but also by small sample size. Required measurements for compliance purposes often are performed annually, quarterly, or, at most, monthly due to the expense or disruption caused by the testing. Studies of pilot plants or demonstration plants are often of such short duration that 5-10 samples are all that are obtained. Thus, methods for estimating the parameters of environmental data using asymptotic or large sample size procedures are usually inapplicable.

In summary, environmental data usually have the following characteristics which make it difficult to analyze: (1) The data are cut off from below by detection limits. (2) The sample size is very small.

As an example, suppose we have taken eight samples of air near a chemical warehouse in order to see if there are leaks (fugitive emissions). Concentrations below 0.8 ppb, say, are below the reliability of the measurement procedure. Of the eight samples, suppose five are below the detection limit while the other three are measured to have concentrations of 1, 2, and 5 ppb. How do we find the average concentration? Surely the smallest value that the true average could be is

$$(0 + 0 + 0 + 0 + 0 + 1 + 2 + 5)/8 = 1 \text{ ppb}$$

while the largest is

$$(0.8 + 0.8 + 0.8 + 0.8 + 0.8 + 1 + 2 + 5)/8 = 1.5 \text{ ppb}$$

Hence, the true average lies somewhere between 1 and 1.5 ppb, but where? If this were a regulated pollutant with a standard set at 1.4 ppb, is the facility in violation? The U.S. Environmental Protection Agency often requires that the missing data be replaced by the detection limit; doing that, the facility appears to be in violation. Does that seem reasonable? Below we find a method (expected values)

that outperforms this somewhat arbitrary technique. Expected values give, in general, a more accurate estimate of the mean for each case in our simulation.

We study below the problem of below detection limit data coupled with small sample size via computer simulations. We suppose that we are given N data points, p of which are below detection limit L and $N - p$ of which have reported values larger than L . We suppose that the distribution for the underlying stochastic process is known to be either normal or log normal. We wish to estimate the mean and variance.

The problem we are addressing is one of censoring. In general, censoring means that observations at one or both extremes are not available. Our problem is one of left censoring; life testing usually involves right censoring (large values not available). Two types of life censoring have received much attention. Type I occurs when the test is terminated at a specified time; type II occurs when the test is terminated at a particular failure. In type I censoring the number of failures as well as the failure times are random variables. This, of course, makes type I censoring far more complicated. Consequently, type II methods have often been applied to type I data with the hope that the bias is not appreciable. Our problem is analogous to type I censoring since the number p of measurements below L is a random variable. As the normal distribution is symmetric, for that case we are considering type I censored, small sample size data.

The problem of estimating the parameters of censored normal data has been extensively studied. Maximum likelihood has been studied in ref 1-3. These procedures are inefficient and highly biased for small data sets and require numerical interpolation in extensive tables. Linear estimators have been studied in ref 2 and 4-6. These methods are based on type II censoring and so are badly biased for small type I data sets. A method using moments was suggested in ref 7 but was highly inefficient. Other methods involve the replacing of the missing data by the expected values of order statistics or by constants. We consider three possible constants: zero, half the detection limit, and (the most conservative estimator for the mean) the detection limit. Though this latter value is badly biased, it has often been suggested by the U.S. Environmental Protection Agency as their accepted procedure merely because of its conservatism.

Below we describe the results of a Monte Carlo simulation to investigate various techniques to estimate the mean and standard deviation for type I normally censored data. If our sample were log normal, we could apply the techniques to the logarithms of the data and then transform back. Thus, no separate analysis of log-normal data is required.

Maximum Likelihood Estimator

We assume $0 < p < N$ values of our N data points lie below the known limit L . We estimate the mean and standard deviation by those values that maximize the likelihood that the given data set would actually have been obtained. The procedure requires tables, found in ref 2, and at least two data points above the limit L , i.e., $p \leq N - 2$.

* Address correspondence to this author at Dowell Schlumberger, Inc., Tulsa, OK 74101.

Truncated Maximum Likelihood

Our next technique is easy to conceptualize: forget that data below L has been obtained, assume that the distribution of the remaining points are governed by the normal distribution truncated at L , and then use maximum likelihood estimators. This procedure again requires tables and at least two data points.

Fill-In with Constants

Various constants have been suggested as proxies for the data below L . The U.S. Environmental Protection Agency and various State Health Departments have a mandate to protect the environment and the human population from harmful pollutants. Thus, EPA often suggests that all censored values be replaced by the censoring value L to obtain the most conservative estimator for the mean pollutant levels. Clearly the most liberal policy is the one that substitutes zero for the censored data: If I cannot measure it, it is not there. Those suggesting some balance might use $L/2$.

Let us suppose that we use C as the proxy for the missing data. Then we "know" the N data points: the real values and p values of C . We then would be able to use the standard formulas for the mean and standard deviation.

Fill-In with Expected Values

The most appealing proxies for the missing data are their expected values, i.e., the expectation of the first p order statistics conditional on being less than the limit L . However, the expected value depends on the unknown mean and variance. So this procedure must be done iteratively on a computer. The algorithm can be easily described:

- (1) Select any initial convenient guesses for the mean and variance.
 - (2) On the basis of our tentative current values for the mean and variance, calculate the expected values for the first p order statistics conditional on being less than L .
 - (3) Now that the first p data points are "known", we can compute the mean and variance using the standard formulas (see Appendix). These are the updated estimates.
 - (4) If the current and updated versions are close, STOP. Otherwise, go back to step 2 using the updated versions as the current values.
- In practice, this algorithm converged rapidly when "close" was defined by 10^{-6} .

Linear Methods

We first order the $N - p$ data points that lie above the censoring value L . We then consider all linear estimators

$$G = \sum G_j X_j$$

and

$$H = \sum H_j X_j$$

with expected values μ and σ , respectively. From this collection, we may find those with minimal variance. Tables for the best coefficients can then be prepared (8).

Simulation

To evaluate the performance of our estimators, we performed a simulation. When the data are rescaled and translated, all the formulas depend on choosing two of the three parameters: the μ , σ , and L . We normalized the stimulated data to $L = 1$. Discussions with environmental engineers led us to believe that mean levels at the detection

Table I. $N = 5, p = 1, L = 1$, Mean Square Errors $\times 10^4$

	$\mu = 1.0$			$\mu = 1.33$		av
	$\sigma = 0.1$	$\sigma = 0.2$	$\sigma = 0.3$	$\sigma = 0.2$	$\sigma = 0.3$	
expected value	30	129	295	108	106	134
MLE	120	479	1078	255	574	501
fill-in with 0	192	77	53	683	530	307
fill-in with 0.5	19	31	135	280	213	136
fill-in with 1	46	185	416	78	96	164

Table II. $N = 5, p = 2, L = 1$, Mean Square Errors $\times 10^4$

	$\mu = 1.0$			$\mu = 1.33$	av
	$\sigma = 0.1$	$\sigma = 0.2$	$\sigma = 0.3$	$\sigma = 0.3$	
expected value	5	19	40	488	138
MLE	210	840	1889	1644	1146
fill-in with 0	1246	946	700	2470	1341
fill-in with 0.5	237	127	71	910	336
fill-in with 1	27	108	243	151	132

Table III. $N = 5, p = 3, L = 1$, Mean Square Errors $\times 10^4$

	$\mu = 0.67$		$\mu = 1.0$		av
	$\sigma = 0.3$	$\sigma = 0.1$	$\sigma = 0.2$	$\sigma = 0.3$	
expected value	362	8	68	204	161
MLE	4969	405	1620	3645	2660
fill-in with 0	438	3231	2885	2570	2281
fill-in with 0.5	102	722	570	444	460
fill-in with 1	1566	13	52	118	437

limit and one or two standard deviations above and below L were the cases to consider. Consequently, we selected the following seven combinations for μ and σ :

$$\mu = 0.67, \sigma = 0.2, 0.3$$

$$\mu = 1.00, \sigma = 0.1, 0.2, 0.3$$

$$\mu = 1.33, \sigma = 0.2, 0.3$$

We selected $N = 5, 10$, and 15 as representative small data set sizes.

Using a standard pseudo-random-number generator and the Box-Muller transformation, we generated one million standard normal random variates. Using these, we generated 50 000 data sets for each of the 21 combinations of N, μ , and σ . These data sets were then artificially censored at the cutoff $L = 1$ and passed to the several estimators to guess values for μ and σ . The data sets were then grouped by the value of p , the number of censored values, $p = 0, 1, \dots, N - 1$. We then computed the average bias and variance for each technique for each value of p which represented at least 5% of the total sample of 50 000 data sets (for $N = 5$ or 10) or 2.5% of the total sample (for $N = 15$).

The results are very consistent throughout for each value of p . The linear methods and truncated MLE were terribly biased and had huge variances. The MLE usually had large bias and had large variances. The fill-in with constants only did well when the mean and the proxy constant lined up: when $\mu = 1.33$, fill-in with 1.0 was acceptable; when $\mu = 0.67$, fill-in with 0.5 was acceptable. Fill in with expected values did a good job throughout the simulation.

Tables I-XXVII give the mean square error (square of bias plus variance of the estimator) for five techniques: fill-in with expected values, MLE, and fill-in with constants (0.0, 0.5, and 1.0). Each table reports the mean square

Table IV. $N = 5, p = 4, L = 1$, Mean Square Errors $\times 10^4$

	$\mu = 0.67$		$\mu = 1.0$			av
	$\sigma = 0.2$	$\sigma = 0.3$	$\sigma = 0.1$	$\sigma = 0.2$	$\sigma = 0.3$	
expected value	52	5	34	147	344	116
MLE	2055	1908	6149	5907	5672	4338
fill-in with 0	30	20	1477	1361	1254	828
fill-in with 1	1206	1331	4	16	36	519

Table V. $N = 10, p = 1, L = 1$, Mean Square Errors $\times 10^4$

	$\mu = 1.33$		av
	$\sigma = 0.2$	$\sigma = 0.3$	
expected value	36	55	46
MLE	83	238	161
fill-in with 0	165	100	133
fill-in with 0.5	73	57	65
fill-in with 1	32	64	48

Table VI. $N = 10, p = 2, L = 1$, Mean Square Errors $\times 10^4$

	$\mu = 1.33$		av
	$\sigma = 0.2$	$\sigma = 0.3$	
expected value	84	61	73
MLE	193	468	331
fill-in with 0	662	480	571
fill-in with 0.5	258	164	211
fill-in with 1	58	48	51

Table VII. $N = 10, p = 3, L = 1$, Mean Square Errors $\times 10^4$

	$\mu = 1.0$		$\mu = 1.33$		av
	$\sigma = 0.1$	$\sigma = 0.2$	$\sigma = 0.3$	$\sigma = 0.3$	
expected value	13	57	133	162	91
MLE	148	592	1333	838	728
fill-in with 0	601	369	202	1257	607
fill-in with 0.5	92	26	25	436	145
fill-in with 1	33	132	298	65	132

Table VIII. $N = 10, p = 4, L = 1$, Mean Square Errors $\times 10^4$

	$\mu = 1.0$			av
	$\sigma = 0.1$	$\sigma = 0.2$	$\sigma = 0.3$	
expected value	4	18	39	20
MLE	201	804	1808	938
fill-in with 0	1242	934	676	951
fill-in with 0.5	234	117	51	134
fill-in with 1	25	101	226	117

Table IX. $N = 10, p = 5, L = 1$, Mean Square Errors $\times 10^4$

	$\mu = 1.0$			av
	$\sigma = 0.1$	$\sigma = 0.2$	$\sigma = 0.3$	
expected value	1	3	5	3
MLE	272	1086	2444	1267
fill-in with 0	2119	1774	1464	1786
fill-in with 0.5	443	297	187	309
fill-in with 1	18	71	160	83

error for fixed values of p and N for all cases of (μ, σ) , which represent at least 5% of the 50000 data sets for $N = 5$ or 10 and 2.5% of the 50000 data sets for $N = 15$. We also computed the average mean square error for each

Table X. $N = 10, p = 6, L = 1$, Mean Square Errors $\times 10^4$

	$\mu = 1.0$			av
	$\sigma = 0.1$	$\sigma = 0.2$	$\sigma = 0.3$	
expected value	4	26	76	35
MLE	374	1497	3368	1746
fill-in with 0	3230	2883	2559	2891
fill-in with 0.5	721	565	432	573
fill-in with 1	12	46	104	54

Table XI. $N = 10, p = 7, L = 1$, Mean Square Errors $\times 10^4$

	$\mu = 0.67$		$\mu = 1.0$		av
	$\sigma = 0.3$	$\sigma = 0.1$	$\sigma = 0.2$	$\sigma = 0.3$	
expected value	136	20	149	442	187
MLE	6018	551	2203	4957	3432
fill-in with 0	1036	4572	4258	3957	3456
fill-in with 0.5	13	1064	917	784	695
fill-in with 1	1441	7	27	62	384

Table XII. $N = 10, p = 8, L = 1$, Mean Square Errors $\times 10^4$

	$\mu = 0.67$		av
	$\sigma = 0.2$	$\sigma = 0.3$	
expected value	71	72	72
MLE	4043	7943	5993
fill-in with 0	2025	1906	1966
fill-in with 0.5	26	17	22
fill-in with 1	1227	1326	1277

Table XIII. $N = 10, p = 9, L = 1$, Mean Square Errors $\times 10^4$

	$\mu = 0.67$		av
	$\sigma = 0.2$	$\sigma = 0.3$	
expected value	8	26	17
fill-in with 0	3117	3041	3079
fill-in with 0.5	118	105	112
fill-in with 1	1169	1218	1194

Table XIV. $N = 15, p = 1, L = 1$, Mean Square Errors $\times 10^4$

	$\mu = 1.33$		av
	$\sigma = 0.2$	$\sigma = 0.3$	
expected value	21	50	36
MLE	49	164	107
fill-in with 0	71	41	56
fill-in with 0.5	35	39	37
fill-in with 1	20	57	39

Table XV. $N = 15, p = 2, L = 1$, Mean Square Errors $\times 10^4$

	$\mu = 1.33$		av
	$\sigma = 0.2$	$\sigma = 0.3$	
expected value	37	33	35
MLE	95	273	184
fill-in with 0	282	166	224
fill-in with 0.5	110	57	84
fill-in with 1	27	38	33

value of p and N . This represents in some fashion the error that would result from the given techniques if each

Table XVI. $N = 15, p = 3, L = 1$, Mean Square Errors $\times 10^4$

	$\mu = 1.33$		av
	$\sigma = 0.2$	$\sigma = 0.3$	
expected value	75	47	61
MLE	174	430	302
fill-in with 0	653	466	560
fill-in with 0.5	249	149	199
fill-in with 1	45	32	39

Table XVII. $N = 15, p = 4, L = 1$, Mean Square Errors $\times 10^4$

	$\mu = 1.0$			$\mu = 1.33$	av
	$\sigma = 0.1$	$\sigma = 0.2$	$\sigma = 0.3$	$\sigma = 0.3$	
expected value	17	74	173	103	92
MLE	135	539	1213	643	633
fill-in with 0	436	233	101	947	429
fill-in with 0.5	58	10	34	317	105
fill-in with 1	36	143	322	42	136

Table XVIII. $N = 15, p = 5, L = 1$, Mean Square Errors $\times 10^4$

	$\mu = 1.0$			$\mu = 1.33$	av
	$\sigma = 0.1$	$\sigma = 0.2$	$\sigma = 0.3$	$\sigma = 0.3$	
expected value	8	39	93	217	89
MLE	161	645	1452	927	796
fill-in with 0	787	524	319	1611	810
fill-in with 0.5	131	43	15	562	188
fill-in with 1	30	119	267	68	121

Table XIX. $N = 15, p = 6, L = 1$, Mean Square Errors $\times 10^4$

	$\mu = 1.0$			av
	$\sigma = 0.1$	$\sigma = 0.2$	$\sigma = 0.3$	
expected value	4	16	37	19
MLE	198	791	1780	923
fill-in with 0	1241	931	669	947
fill-in with 0.5	29	114	44	62
fill-in with 1	25	98	220	114

Table XX. $N = 15, p = 7, L = 1$, Mean Square Errors $\times 10^4$

	$\mu = 1.0$			av
	$\sigma = 0.1$	$\sigma = 0.2$	$\sigma = 0.3$	
expected value	1	4	7	4
MLE	241	962	2166	1123
fill-in with 0	1800	1460	1160	1473
fill-in with 0.5	365	224	123	237
fill-in with 1	20	78	175	91

Table XXI. $N = 15, p = 8, L = 1$, Mean Square Errors $\times 10^4$

	$\mu = 1.0$			av
	$\sigma = 0.1$	$\sigma = 0.2$	$\sigma = 0.3$	
expected value	1	4	10	5
MLE	293	1172	2637	1367
fill-in with 0	2463	2112	1791	2122
fill-in with 0.5	528	375	251	385
fill-in with 1	15	59	134	69

value of μ and σ meeting our 5% or 2.5% criterion were equally likely. Of course, if the user had prior information

Table XXII. $N = 15, p = 9, L = 1$, Mean Square Errors $\times 10^4$

	$\mu = 1.0$			av
	$\sigma = 0.1$	$\sigma = 0.2$	$\sigma = 0.3$	
expected value	3	20	57	27
MLE	368	1475	3318	1720
fill-in with 0	3228	2879	2550	2886
fill-in with 0.5	720	561	425	569
fill-in with 1	11	45	101	52

Table XXIII. $N = 15, p = 10, L = 1$, Mean Square Errors $\times 10^4$

	$\mu = 0.67$		$\mu = 1.0$		av
	$\sigma = 0.3$	$\sigma = 0.1$	$\sigma = 0.2$	$\sigma = 0.3$	
expected value	262	8	68	192	133
MLE	5533	459	1836	4132	2990
fill-in with 0	804	4102	3775	3463	3036
fill-in with 0.5	29	944	792	655	605
fill-in with 1	1477	8	31	70	397

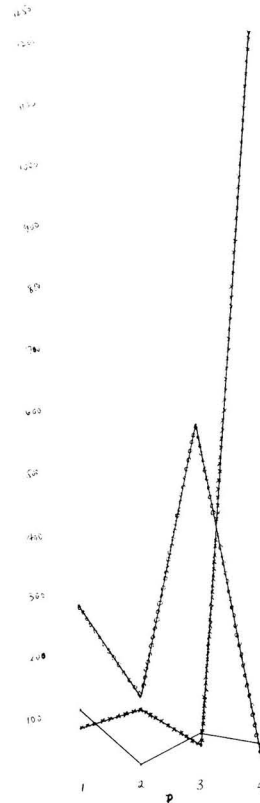


Figure 1. $N = 5, \sigma = 0.2$, mean square errors for three procedures. Circles is fill-in with 0.5. Crosses is fill-in with 1.0. Plain line is expected values.

about the mean and/or standard deviation, he would use the appropriate column(s).

Figures 1-3 present some of our results in terms of graphs. For each fixed sample size ($N = 5, 10$, and 15) and with σ fixed at 0.2, for each value of $p = 1, \dots, N - 1$, we selected the most likely of the three tested means. We

Table XXIV. $N = 15, p = 11, L = 1$, Mean Square Errors $\times 10^4$

	$\mu = 0.67$		$\mu = 1.0$		av
	$\sigma = 0.3$	$\sigma = 0.1$	$\sigma = 0.2$	$\sigma = 0.3$	
expected value	78	23	165	500	192
MLE	6457	628	2514	5657	3814
fill-in with 0	1296	5067	4767	4478	3902
fill-in with 0.5	4	1192	1050	918	791
fill-in with 1	1400	5	21	48	369

Table XXV. $N = 15, p = 12, L = 1$, Mean Square Errors $\times 10^4$

	$\mu = 0.67$		av
	$\sigma = 0.2$	$\sigma = 0.3$	
expected value	75	30	53
MLE	3995	7777	5886
fill-in with 0	2025	1906	1966
fill-in with 0.5	26	15	21
fill-in with 1	1226	1325	1276

Table XXVI. $N = 15, p = 13, L = 1$, Mean Square Errors $\times 10^4$

	$\mu = 0.67$		av
	$\sigma = 0.2$	$\sigma = 0.3$	
expected value	25	75	50
MLE	4894	10239	7567
fill-in with 0	2726	2632	2679
fill-in with 0.5	79	65	72
fill-in with 1	1188	1253	1221

Table XXVII. $N = 15, p = 14, L = 1$, Mean Square Errors $\times 10^4$

	$\mu = 0.67$		av
	$\sigma = 0.2$	$\sigma = 0.3$	
expected values	3	25	14
fill-in with 0	3534	3481	3508
fill-in with 0.5	164	152	158
fill-in with 1	1149	1180	1165

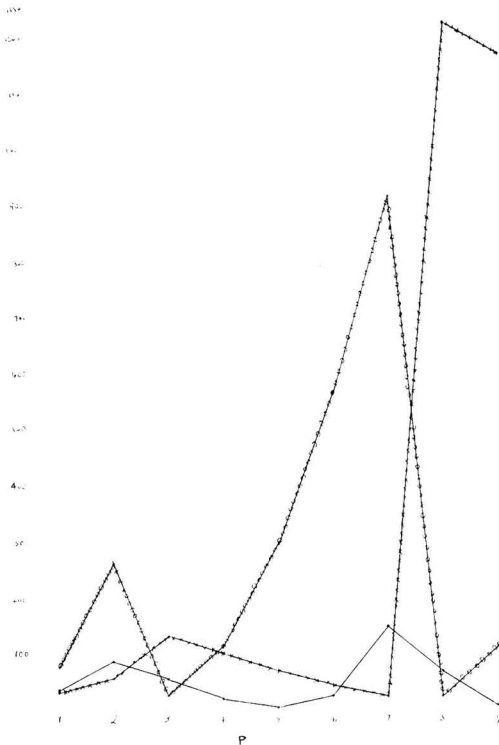


Figure 2. $N = 10, \sigma = 0.2$, mean square errors for three procedures. Circles is fill-in with 0.5. Crosses is fill-in with 1.0. Plain line is expected values.

display in the figures the mean square errors for three procedures (expected values, fill-in with 0.5, and fill-in with 1.0) for these selected means. The errors for the constants change radically with p as the true value for the mean is close or not to the filled-in value, while that of the expected value procedure is virtually always optimal.

Bias-Corrected Estimators

The estimators developed above are all biased. The problem is that they estimate the parameters conditioned

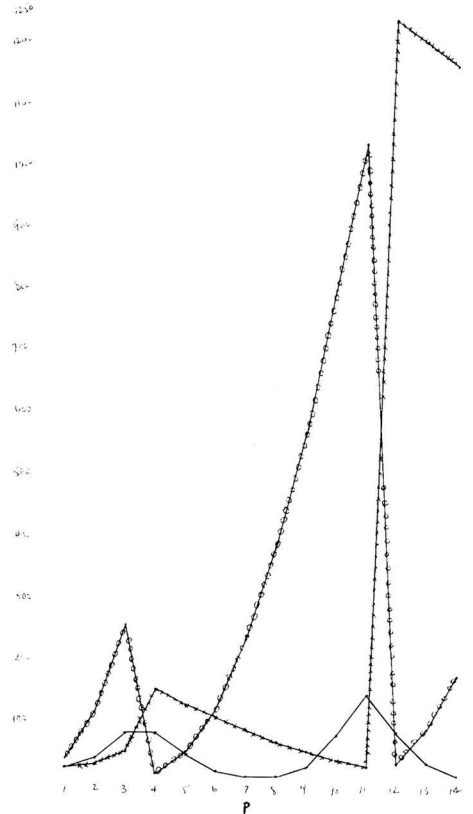


Figure 3. $N = 15, \sigma = 0.2$, mean square errors for three procedures. Circles is fill-in with 0.5. Crosses is fill-in with 1.0. Plain line is expected values.

on the knowledge of p , the number of missing values. It is possible to form other estimators that account somewhat for this bias. We tested both the original and bias-corrected versions of our estimators. These latter estimators so inflated the variance of the uncorrected estimators that they were (in general) worse, in the mean-square-error sense, than the versions reported above.

Conclusion

Fill-in with expected values is by far the best estimator. Fill-in with constants can be seen to be, in general, orders of magnitude worse.

Appendix

Let μ^* and σ^* be the estimators for fill-in with expected values. Let f and F be the probability density function and the cumulative distribution function for the standard normal distribution. Then

$$\mu^* = \frac{1}{N} \left[\sum x + p\mu^* - p\sigma^* \frac{f((L - \mu^*)/\sigma^*)}{F((L - \mu^*)/\sigma^*)} \right]$$

$$\sigma^{*2} = \frac{1}{N-1} \left[\sum x^2 + p\mu^{*2} + p\sigma^{*2} - (L + \mu^*)\sigma^*p \frac{f((L - \mu^*)/\sigma^*)}{F((L - \mu^*)/\sigma^*)} - N\mu^{*2} \right]$$

By use of these formulas and the tables for the MLE, the algorithm described above can be implemented.

Literature Cited

- (1) Cohen, A. C. *Ann. Math. Stat.* 1950, 21, 557-569.
- (2) Gupta, A. *Biometrika* 1952, 39, 260-273.
- (3) Harter, H.; Moore, A. H. *Biometrika* 1966, 53, 205-213.
- (4) Sarhan, A.; Greenberg, B. G. *Ann. Math. Stat.* 1956, 27, 427-451; *Ann. Math. Stat.* 1958, 29, 79-105.
- (5) Saw, J. *Biometrika* 1959, 46, 150-159.
- (6) Dixon, W. J. *Ann. Math. Stat.* 1960, 31, 385-391.
- (7) Ipsen, J. *Hum. Biol.* 1949, 21, 1-16.
- (8) Gleit, A. *Air Force Off. Sci. Res.*, [Tech. Rep.] AFOSR-TR (U.S.), in press.
- (9) Gleit, A. *Air Force Off. Sci. Res.*, [Tech. Rep.] AFOSR-TR (U.S.), in press.

Received for review July 12, 1984. Revised manuscript received March 21, 1985. Accepted July 22, 1985. This work was sponsored by the Air Force Office of Scientific Research under Contract F49620-82-C-0079.

Decomposition of Ozone in Water in the Presence of Organic Solutes Acting as Promoters and Inhibitors of Radical Chain Reactions[†]

Johannes Staehelin[‡] and Jürg Hoigné*

Swiss Federal Institute for Water Resources and Water Pollution Control, EAWAG, 8600 Dübendorf, Switzerland

■ The decomposition of aqueous ozone is generally due to a chain reaction involving ·OH radicals. Many organic solutes (impurities) can react with ·OH to yield ·O₂⁻ upon addition of O₂. ·O₂⁻ transfers its electron to a further ozone molecule in a rather selective reaction. The ozonide anion (·O₃⁻) formed immediately decomposes into a further ·OH radical. Compounds that convert ·OH radicals into ozone-selective ·O₂⁻, therefore, act as promoters of the chain reaction. The efficiencies of different ·OH to ·O₂⁻ converters (e.g., formic acid, primary and secondary alcohols (including sugars), glyoxylic acid, and humic acids) are tested in the presence of other ·OH radical scavengers that do not primarily produce ·O₂⁻ (carbonate, aliphatic alkyl compounds, and *tert*-butyl alcohol). The derived reaction kinetics allows one to qualitatively interpret the variation of the lifetime of O₃ found in model solutions and even in natural waters and during drinking water treatment.

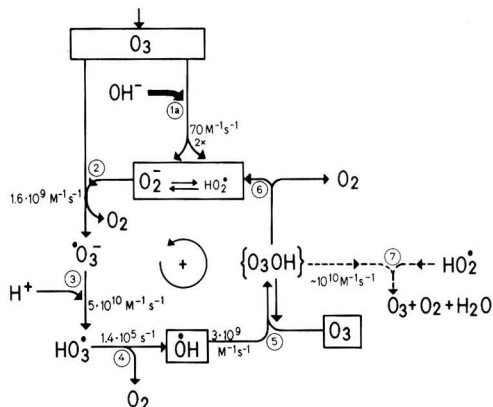
Introduction

The decomposition kinetics of aqueous ozone are of interest because of the wide application of ozone for water-treatment processes (see, e.g., ref 3) and because of their importance for the understanding of the chemistry of atmospheric water droplets and of other environmental systems (4).

[†]This publication is dedicated to Prof. Dr. Werner Stumm on the occasion of his 60th birthday (date of submission). It recognizes Stumm's early contribution to this field (1, 2) and his stimulating interest. Thirty years elapsed since Stumm observed and reviewed, in his first EAWAG project, that organic solutes present in lake waters, and even compounds such as sugars, can accelerate the catalytic decomposition of aqueous ozone. We hope that this study now presents him a rationalized answer to his early suggestions.

[‡]Present address: Swiss Federal Research Station for Fruit Growing, Viticulture and Horticulture, CH-8820 Wädenswil, Switzerland.

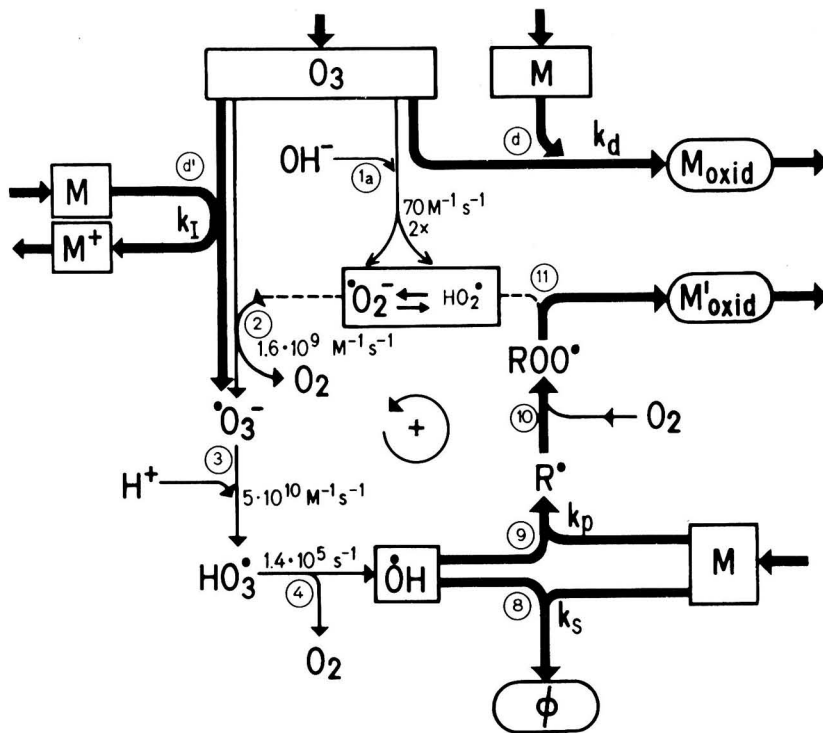
Scheme I. Reactions of Aqueous Ozone in "Pure Water"



In water, ozone may react directly with dissolved substances, or it may decompose to form secondary oxidants such as ·OH radicals, which then themselves immediately react with solutes. These different pathways of reactions lead to different oxidation products, and they are controlled by different types of kinetics (5). Therefore, their relative importance must be known when the oxidation effects of ozone and the rate of ozone consumption are to be predicted or generalized.

Early observations of the lifetime of aqueous ozone indicated that the decomposition of the ozone becomes accelerated by increasing the pH (for literature reviews see, e.g., ref 6 and 7). In addition, it became evident that, as suggested by Weiss (8, 9), the decomposition of ozone at a given pH is often accelerated by a radical-type chain reaction which in nonpure solutions can be initiated, promoted, or inhibited by various solutes (2, 10-12). Because of the interaction of multiple pathways, the empirical

Scheme II. Reactions of Aqueous Ozone in the Presence of Solutes M which React with O_3 or which Interact with $\cdot OH$ Radicals by Scavenging and/or Converting $\cdot OH$ into $HO_2\cdot$.



kinetic laws describing the rate of ozone depletion deduced by different authors disagree even with respect to the kinetic orders of the reactions (1, 2, 6, 7). We therefore started a research program to separate the kinetics of the successive individual reaction steps and to investigate their interdependency. In a preliminary study we analyzed the decomposition of ozone in pure water and in aqueous solutions in which radical-type chain reactions were inhibited by $\cdot OH$ radical scavengers such as bicarbonate (13). Because $\cdot OH$ and $\cdot O_2^-$ were the assumed intermediates, we then studied the reactions of these species with ozone by producing them independently using pulse radiolyses (14, 15). The interpretation of the results for "pure water" are summarized in Scheme I. When comparing our earlier experimental observations (10, 11, 16-18) with results published by radiation chemists (19-24), we then noticed that those organic solutes which are known to convert $\cdot OH$ radicals into $\cdot O_2^-$ always accelerate the decomposition of ozone unless an ample amount of other radical scavengers is present. The aim of the present publication is therefore to formulate an appropriate reaction model describing the decomposition of aqueous ozone in the presence of promoters and inhibitors and to test its applicability for interpreting the kinetic behavior of ozone in natural waters and wastewaters.

Reaction Model

Scheme II represents the reactions that we assume describe the decomposition kinetics of aqueous ozone in the presence of solutes which interact with the radical chain reactions. It is based on the following assumptions:

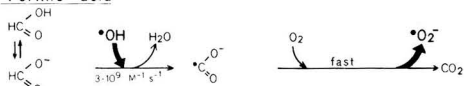
Initiation Step. The reaction between OH^- ions and ozone (step 1) leads to the formation of one superoxide anion ($\cdot O_2^-$) and one hydroperoxyl radical ($HO_2\cdot$) which are

in an acid-base equilibrium ($pK_a = 4.8$). For this initiation we determined a rate constant for free radical formation of $2 \times 70 M^{-1} s^{-1}$ whereby the factor 2 is due to the fact that two radicals are produced per reaction (13, 25). A comparable rate constant was found by Forni et al. (26) when measurements were made in the high pH range. In addition, solutes M may react with ozone and thereby either consume the ozone by a direct reaction (d) or produce an ozonide ion radical by an electron transfer (d').

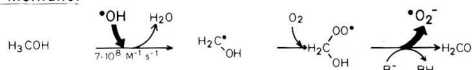
Propagation Step. Upon protonation $\cdot O_3^-$ decomposes into $\cdot OH$ radicals (steps 3 and 4) (14). These now react with solutes M. Typical rate constants for reactions of $\cdot OH$ with organic solutes are in the range 10^8 - $10^{10} M^{-1} s^{-1}$ (29). $\cdot OH$ even reacts with HCO_3^- and CO_3^{2-} with a rate constant of $2 \times 10^7 M^{-1} s^{-1}$ and $4 \times 10^8 M^{-1} s^{-1}$, respectively. Some functional groups present in organic molecules M are known to react with $\cdot OH$ to form an organic radical which adds O_2 and then eliminates $HO_2\cdot/\cdot O_2^-$ in a base-catalyzed reaction (see Figure 1, examples A and B; for literature review, see ref 23). The rate constant with which the $\cdot O_2^-$ formed reacts with additional ozone is very high when compared with that of its (slow) reactions with other solutes possibly present in ozonated water (for rate constants, see ref 29). Therefore, the conversions of the less ozone-selective $\cdot OH$ radical into the highly selective $\cdot O_2^-$ may promote the chain reaction.

Termination Step. Many other organic and inorganic substrates react with $\cdot OH$ radicals to form such secondary radicals which do not predominantly produce $HO_2\cdot/\cdot O_2^-$ (see Figure 1, examples C-F). These scavengers generally terminate the chain reaction (10). Even $\cdot OOCCH_2COO^-$ and $\cdot CO_3^-$ radicals formed when acetic acid or carbonate are used as $\cdot OH$ scavengers do not interact with further ozone (27, 28).

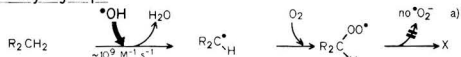
A. Formic acid



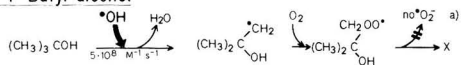
B. Methanol



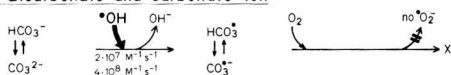
C. Alkyl groups



D. t-Butyl alcohol



E. Bicarbonate and carbonate ion



F. Phosphate ion

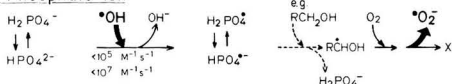


Figure 1. Schemes of reactions of typical $\cdot\text{OH}$ to $\cdot\text{O}_2^-$ radical converters acting as promoters P (cases A, B, and F) and $\cdot\text{OH}$ radical scavengers S (cases C–F). (Footnote a) Second-order processes can lead to the formation of the tetraoxide which may decompose and also form some $\cdot\text{O}_2^-$ or H_2O_2 (34).

Kinetic Formulations for Promoted and Inhibited Chain Reactions

An extended set of expressions for describing the kinetics of the decomposition of aqueous ozone by different chain reactions has been presented previously (8). We therefore can restrict our attention here to the type of system described by Scheme II. This is a hypothesis describing the cases of ozonation of drinking water or wastewater containing a mixture of different dissolved substrates M, which act as initiators, promoters, and inhibitors of the radical chain reaction. Even in such types of waters the highly selective $\cdot\text{O}_2^-$ species will predominantly react with ozone. The $\cdot\text{OH}$ radicals (or the corresponding $\{\text{O}_3\text{OH}\}$ adducts) react with a solute M before they encounter another radical. For instance, even if 10^{-5} mol/L ozone was to decompose per second to $\cdot\text{OH}$ radicals in the presence of 10^{-4} M of solutes consuming $\cdot\text{OH}$ or $\{\text{O}_3\text{OH}\}$ with a typical rate constant of $\geq 10^8 \text{ M}^{-1} \text{ s}^{-1}$, then the steady-state concentration of $\cdot\text{OH}$ would remain $\leq 10^{-9}$ M. This low concentration of radicals makes a radical-radical reaction much less probable than a reaction of the $\cdot\text{OH}$ with a solute M. Also the steady-state concentration of $\cdot\text{O}_2^-$ is estimated to be $\leq 10^{-9}$ M assuming that its rate of formation is $\leq 10^{-5}$ mol/L s and that an ozone concentration of 10^{-5} M controls its consumption rate. (This situation is different from that encountered in very pure waters or in atmospheric water droplets into which additional $\text{HO}_2\cdot$ radicals impinge from the atmosphere or in waters where extremely high concentrations of additional radicals are produced, e.g., by intensive pulse radiolyses.)

Reactions with Solutes. The kinetics of all reactions considered in Scheme II are first order with respect to the concentration of M and the oxidant (16–18, 29). The overall rate can therefore be expressed as a sum of the rates with which different types *i* of solutes M react. The following notations will be used:

rate of direct reaction, d, of ozone with solutes
(the sum comprises all solute species M_i)

$$r_d = \sum (k_{d,i}[M_i][\text{O}_3]) \quad (1)$$

rate of initiation of chain reaction by M and OH^-

$$r_i = \sum (k_{i,i}[M_i][\text{O}_3]) + 2k_1[\text{OH}^-][\text{O}_3] \quad (2)$$

For simplification only initiation reactions by M which directly lead to $\cdot\text{O}_3^-$ are considered here (for example, $\text{Fe}^{2+} + \text{O}_3 \rightarrow \text{Fe}_3^{3+} + \cdot\text{O}_3^-$). Initiation reactions that primarily produce $\cdot\text{O}_2^-$ or H_2O_2 are not included. (Their occurrence would not alter the conclusions except that the yield factor for radical initiation would become 2 instead of 1 and the first sum in eq 2 would have to be multiplied by 2.)

rate of $\cdot\text{OH}$ radical conversion to $\cdot\text{O}_2^-$
(promoting reaction, p)

$$r_p = \sum (k_{p,i}[M_i][\cdot\text{OH}]) \quad (3)$$

rate of $\cdot\text{OH}$ radical scavenging by M

(scavenging reaction, s)

$$r_s = \sum (k_{s,i}[M_i][\cdot\text{OH}]) \quad (4)$$

Those individual solutes M that predominantly act by one single pathway will be designated by I (initiator), P (promoter), or S (scavenger).

Chain Reaction. For the reactions indicated in Scheme II the rate of consumption of ozone due to the reactions within the chain cycle (subscript cc), excluding losses due to the initiation step or other direct reactions of ozone with substrate molecules, is given by

$$-(d[\text{O}_3]/dt)_{cc} = k_2[\cdot\text{O}_2^-][\text{O}_3] \quad (5)$$

In the steady state (subscript ss) the rate of $\cdot\text{O}_2^-$ depletion corresponds to the rate of its formation:

$$k_2[\cdot\text{O}_2^-]_{ss}[\text{O}_3] = 2k_1[\text{OH}^-][\text{O}_3] + k_p[\text{M}][\cdot\text{OH}]_{ss} \quad (6)$$

Substituting eq 6 into 5 we find

$$-(d[\text{O}_3]/dt)_{cc} = 2k_1[\text{OH}^-][\text{O}_3] + k_p[\text{M}][\cdot\text{OH}]_{ss} \quad (7)$$

An expression for $[\cdot\text{OH}]_{ss}$ may be derived by assuming that all proliferated $\cdot\text{O}_3^-$ eventually decomposes into $\cdot\text{OH}$. The rate of depletion of $\cdot\text{OH}$ then equals its rate of formation when

$$(k_s + k_p)[\text{M}][\cdot\text{OH}]_{ss} = k_1[\text{M}][\text{O}_3] + k_2[\cdot\text{O}_2^-]_{ss}[\text{O}_3] \quad (8)$$

Rearrangement and combination with eq 6 give

$$[\cdot\text{OH}]_{ss} = \frac{2k_1[\text{OH}^-] + k_1[\text{M}]}{k_s[\text{M}]} [\text{O}_3] \quad (9)$$

Substituting this expression for $[\cdot\text{OH}]_{ss}$ into eq 7 yields the rate of ozone depletion within the chain cycle:

$$\left(\frac{d[\text{O}_3]}{dt} \frac{1}{[\text{O}_3]} \right)_{cc} = 2k_1[\text{OH}^-] \left(1 + \frac{k_p}{k_s} \right) + k_1[\text{M}] \frac{k_p}{k_s} \quad (10)$$

or, if we consider the whole chain reaction (subscript c) including the loss of ozone by the initiation step (eq 2) and write the equation explicitly for the case that different types *i* of solutes M_i are present:

$$-\left(\frac{d[O_3]}{dt} \frac{1}{[O_3]}\right)_c = k_1[OH^-] + \{2k_1[OH^-] + \sum(k_{1,i}[M_i])\} \left(1 + \frac{\sum(k_{p,i}[M_i])}{\sum(k_{s,i}[M_i])}\right) = k_c' \quad (11a)$$

This shows that the rate of ozone depletion is first order in ozone concentration even if the entire chain reaction is considered. It can therefore be characterized by a pseudo-first-order rate constant, k_c' .

For expressing the total ozone consumption, eq 11a must be extended to account for the direct reactions of ozone which do not lead to free radicals:

$$-\left(\frac{d[O_3]}{dt} \frac{1}{[O_3]}\right)_{tot} = k_c' + \sum_i(k_{d,i}[M_i]) = k'_{tot} \quad (12)$$

Special Cases. In most types of waters of practical interest

$$k_1[M] \gg 2k_1[OH^-] \quad (13)$$

and if the scavenging of $\cdot OH$ radicals in these cases is due to special radical scavengers S which can be distinguished from M, eq 11a becomes

$$k_c' = k_1[M] \left(1 + \frac{k_p[M]}{k_s[S]}\right) \quad (11b)$$

Kinetic Chain Length. The number n of chain cycles occurring per initiation can be calculated by dividing eq 11a by the initiation term:

$$n = \frac{k_c' - k_1[OH^-] - \sum(k_{1,i}[M_i])}{2k_1[OH^-] + \sum(k_{1,i}[M_i])} \quad (14)$$

or, as a trivial conclusion from Scheme II:

$$n = \frac{\sum(k_{p,i}[M_i])}{\sum(k_{s,i}[M_i])} \quad (15)$$

This means n only depends on the relative rate with which the $\cdot OH$ radicals become converted to $\cdot O_2^-$, relative to the rate by which they are scavenged.

Selection of Model Substrates

Formic acid is the promoter substance of choice: Radiation chemists demonstrated that formate ions efficiently convert $\cdot OH$ into $\cdot O_2^-$ by reactions described in Figure 1A. In O_2 -equilibrated solutions (atmospheric pressure) the intermediate $\cdot CO_2^-$ radical reacts with O_2 within about 1 μs , prior to the occurrence of radical-radical reactions and thus leading to a nearly 100% conversion to $\cdot O_2^-$ (30, 31). Some formate, however, may also react with ozone in a direct reaction: $k_d \sim 100 \text{ M}^{-1} \text{ s}^{-1}$ (17). *Methanol, glycol, glucose, and other carbohydrates* are also well-studied converters of $\cdot OH$ to $\cdot O_2^-$ (Figure 1B) (19-22). Their direct reactions with ozone are rather slow (16). *Glyoxalic acid* ($pK_a = 3.2$), in the pH region of practical interest, is present as the anion that is known to accelerate the decomposition of ozone with an outstanding efficiency (17). This could be due to the fact that it not only reacts as a promoter but also as a chain initiator (8). *From higher alkyl alcohols*, $\cdot OH$ can also abstract an H atom that is not in the position α to the alcoholic ($-OH$) group (Figure 1C). Since such reactions are not followed by $\cdot O_2^-$ formation, they act as scavenging reactions. The relative importance of scavenging to promotion increases with the length of the alkyl chain, relative to the amount of H atoms in

position α to the $-OH$ groups. (For appropriate relative rate constants see ref 32). For *tert-butyl alcohol*, a direct elimination of $\cdot O_2^-$ from the secondarily formed peroxy group does not occur (see Figure 1D) and only at high radical concentrations can a bimolecular radical-radical addition lead to a tetraoxide that produces $\cdot O_2^-$ and H_2O_2 (24). With ozone it reacts very slowly. It is therefore a suitable $\cdot OH$ scavenger (16). *Bicarbonate and carbonate ions* do not react with ozone (18), but they scavenge $\cdot OH$ radicals (see Figure 1E) (11, 33, 34). Their reaction products do not react further with ozone (27). Our experimental experience, however, is that, it sometimes does not lead to a full inhibition of chain reactions. *Phosphate ions* do not react with ozone (18); however, they can slowly react with $\cdot OH$ radicals. The secondary radical formed is expected to abstract an H atom from some types of organic compounds (see Figure 1F) (35-37). Via this reaction they could at times interfere with the radical-type chain reaction and even act as a secondary promoter.

The literature does not give information on which of those compounds could act as initiators by their direct reaction with ozone, although some organic substances are well-known to produce radicals when reacting with O_3 (38).

Experimental Section

Reagents. Most reagents were commercial AR grade from Merck or Fluka and were used without further purification. The preparation of the ozone stock solutions and buffers is described by Hoigné and Bader (10) and Staehelin (8). The solutions of humic acid were prepared by dissolving 0.2 g/L Fluka humic acid in distilled water in which the pH was raised to 10-11 with NaOH. The nonsoluble residues were filtered off (0.45- μm pore size) after 80 min. The solution was diluted and immediately acidified with $HClO_4$ to pH 4 and preozonated by adding 0.75 mg/L ozone per mg/L humic acid. All aqueous solutions were prepared with deionized, redistilled water.

Instrumentation. Absorption measurements were performed on a Beckman DK 2A or a Uvikon 810 UV-vis spectrophotometer using thermostated 1-10-cm cells.

Methods. In general, the rate of ozone consumption was followed directly in 1-10-cm UV cells by recording the change of UV absorption at 258 nm as a function of time. The reactions were usually initiated by injecting the stock solution of aqueous ozone ($[O_3] \sim 30 \text{ mg/L}$) into the already mounted cell which contained the solution of the reactants. About 5 s elapsed between injection of the ozone and the start of the absorption measurement. In other cases in which the absorption at 258 nm was interfered by solutes other than ozone, the reactions were performed in stirred 10-mL flasks and stopped after a preset time interval by adding the Indigo Reagent which quenched the residual ozone and indicated its amount by the amount of discoloration determined at 600 nm (16, 39, 40). In still other cases where reactions were slow, the reaction was performed in an Erlenmeyer flask from which samples were withdrawn intermittently for determinations of the residual ozone by the indigo method (16). The pH was generally controlled by using phosphate buffers or, for measurements at pH ≤ 4 , by perchloric acid. All measurements were performed at $20 \pm 1^\circ C$ (8).

Results and Discussions

The previously formulated hypotheses were tested by experiments on model solutions in which the concentrations of typical promoters and inhibitors were varied.

According to eq 11 and 12 the rate of ozone depletion in solutions containing promoters and inhibitors and/or

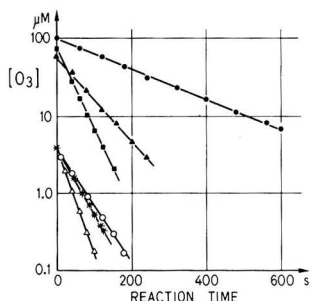


Figure 2. Exemplification of linearity of $\log [O_3]$ vs. time curves for solutions containing different promoters and scavengers S. (●) 3 mM glycol; [S] 300 μ M *tert*-butyl alcohol, pH 8.2. (▲) 3 mM glycol; [S] 60 μ M *tert*-butyl alcohol, pH 8.2. (■) 3 mM glycol; [S] 24 μ M *tert*-butyl alcohol, pH 8.2. (○) 2 mg/L humic acid, pH 3.5. (Δ) 2 mg/L humic acid, pH 4.5. (*) 0.2 mM formic acid; [S] 50 μ M *tert*-butyl alcohol, pH 4.

Table I. Effect of 0.2 mM Formic Acid and \bullet OH Scavengers (S) on Observed Overall Rate Constant of Ozone Depletion (k'_{tot}) and on Rate Constant of Chain Reaction (k'_c) at pH 4.0^a

[S]	$k'_{tot} \times 100, s^{-1}$	$k'_c \times 100, s^{-1d}$
0 ^a	15 ± 2	14 ± 2
50 mM phosphate	7.2 ± 0.6	5.9 ± 0.6
7 μ M <i>tert</i> -butyl alcohol	5.5 ± 0.4	4.2 ± 0.4
50 μ M <i>tert</i> -butyl alcohol	2.0 ± 0.2	0.7 ± 0.4
∞ <i>tert</i> -butyl alcohol	1.3 ± 0.2^b	0.0 ± 0.2
50 mM phosphate, blank without HCOOH	0.003^c	

^a pH adjustment with HClO₄. ^b x-axes intercept from k'_{tot} vs. $1/[S]$ plot. ^c From ref 13. ^d Corrected for rate of direct reaction of ozone with formate ions, calculated from values given in ref 17.

substrates that react directly with ozone should become first order with respect to the residual ozone concentration whenever the concentration of the reacting solutes remains constant. These types of kinetics could be verified in solutions containing typical promoters and inhibitors by testing the $\log [O_3]$ vs. time plots for linearity over the first three half-lives of ozone. Figure 2 gives examples of such plots; the linearity observed is typical of all systems investigated. Occasional deviations could generally be attributed to too low initial substrate concentrations. From the slope of the first-order plots the rate constants k'_{tot} for ozone depletion were determined (compare eq 12).

According to eq 11b the rate of ozone depletion due to the chain reaction increases with the rate of the promoting reaction, $k_p[M]$, but decreases with the rate of the inhibition, $k_i[S]$. A few examples of experimental tests of this subset of the general hypothesis are presented below.

Formic Acid as Promoter. Table I summarizes the pseudo-first-order rate constants for ozone depletion measured in aqueous solutions containing 0.2 mM formic acid. When compared with a blank containing only phosphate buffer (last line), formic acid gives a tremendous acceleration of the rate although its direct reaction with ozone is relatively slow. Already phosphate, which is known to react only slowly with \bullet OH radicals, acted in this case as an efficient inhibitor when applied in concentrations typically used in buffer solutions (see second line in Table I). Addition of a classical \bullet OH scavenger, *tert*-butyl alcohol, reduced the ozone consumption rate by a factor of 7 even when it was present in only one-fourth of the

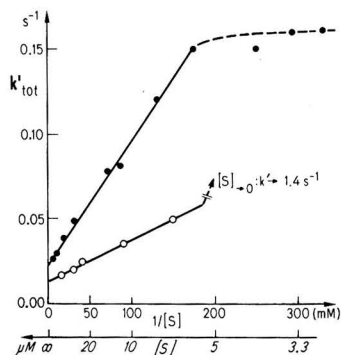


Figure 3. Rate constant for depletion of ozone in the presence of formic acid acting as promoter as a function of dilution of \bullet OH radical scavengers, $1/[S]$. (●) 0.24 mM formic acid, pH 6; 30 mM phosphate buffer. (○) 0.24 mM formic acid, pH 4; without phosphate buffer, [S] *tert*-butyl alcohol.

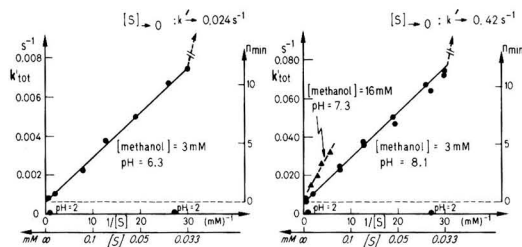


Figure 4. Rate constant for depletion of ozone in the presence of methanol (=promoter) vs. dilution of *tert*-butyl alcohol (=scavenger) ($1/[S]$); 6 mM phosphate buffer. Right scale: calculated kinetic chain length n .

concentration of the formic acid.

In Figure 3 the rate of ozone depletion is plotted vs. the dilution of the scavenger *tert*-butyl alcohol, i.e., vs. $1/[S]$. The linearity achieved for low $1/[S]$ values is in agreement with eq 11b. The intercept on the coordinate for infinite scavenger concentrations is as expected for the rate by which the ozone is consumed by its direct reaction with formic acid. The plateauing at high $1/[S]$ values can be explained by a residual scavenging effect exhibited by the phosphate buffer. In no cases did the experimentally determined slope of the linear part correspond with a value calculated from eq 11b when known \bullet OH reaction rate constants and initiation reactions were considered. We think that this discrepancy is due to further nondefined initiation rates. As experienced before, such reactions can only be avoided by using very special scavenging systems (13).

The rate constant for the ozone depletion increased more than linearly with the concentration of formic acid (8). This is expected for cases where also some reactions of ozone with the substrate produce free radicals ($k_i[M_i] \neq 0$). (For exemplification see case of glyoxylic acid.)

Primary Alcohols as Promoters. Figure 4 shows the increase of the rate of consumption of ozone in aqueous methanol vs. the dilution of *tert*-butyl alcohol which acts as inhibitor. Figure 5 shows the increase of the rate constant vs. the concentration of primary or secondary alcohols. Both cases give linear relationships over the entire range of concentrations applied in these experiments. This is again in good agreement with the behavior expected from eq 11a. Glycerine and glucose behaved similarly to methanol (also entry in Figure 5b).

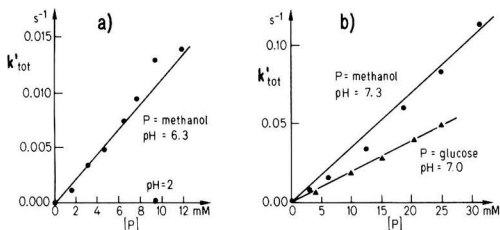


Figure 5. Rate constant for depletion of ozone vs. promoter concentration ($P =$ methanol and glucose) in the presence of an $\cdot\text{OH}$ radical scavenger ($S = 0.13$ mM *tert*-butyl alcohol); 6 mM phosphate buffer.

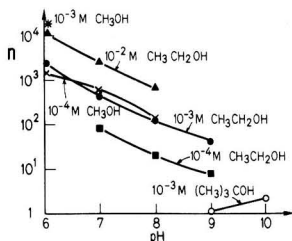


Figure 6. Mean kinetic chain length n for decomposition of ozone, calculated from measurements of k'_{tot} by using eq 14. Assumption: OH^- is the only chain initiator to be accounted for.

The upper limit for the kinetic chain length n can be estimated from experimental k'_c ($=k'_{\text{tot}}$) values using eq 14. Because of uncertainties considering the rate of additional initiation reactions, these n values must, however, be regarded as apparent. Figure 6 shows that they vary with pH. As expected, they decrease when the alkyl chains become longer and therefore become a better scavenger for $\cdot\text{OH}$ radicals.

In the presence of 1 mM ethanol an increase in the phosphate concentration from 0.5 to 50 mM resulted in the elevation of the rate constant k'_{tot} for the ozone depletion from 3×10^{-3} to $15 \times 10^{-3} \text{ s}^{-1}$. This enhancement may be due to the fact that the product of the reaction of an $\cdot\text{OH}$ radical with phosphate is a phosphate radical that selectively abstracts an H atom standing α to the alcoholic ($-\text{OH}$) group (see Figure 1, scheme F, and literature mentioned above). In this case, phosphate acts as a secondary chain carrier.

Glyoxylic Acid as Initiator and Promoter. The direct reaction of ozone with this substrate, determined at high scavenger concentrations (17), is significant but still relatively slow. Figure 7 shows that the acceleration of the decomposition of ozone increased approximately with the square of the concentration of the glyoxylic acid. This is formally expected from eq 11b for the case where the square term $k_i[\text{M}] \times k_p[\text{M}]$ cannot be neglected.

Benzene as a Promoter. The decomposition of ozone in an aqueous solution of benzene is highly reduced by adding $\cdot\text{OH}$ radical scavengers (8, 10, 11). It, however, increases with pH with an unusually high slope. On the basis of available literature, the possibility remains that aromatic hydrocarbons convert $\cdot\text{OH}$ into other reactive intermediates such as H_2O_2 . H_2O_2 also would act as a secondary chain carrier (13).

Humic Acid as a Promoter. In Figure 8, the results from systems containing preozonated humic acids are described. Preozonation was performed to eliminate the sites that exhibit a spontaneous ozone consumption. (In practice, this would correspond to the initial ozone consumption phase observed in a water-treatment plant.) In

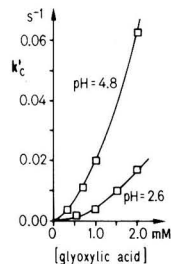


Figure 7. Rate constant for depletion of ozone vs. concentration of glyoxylic acid. k' values are corrected for direct reaction of glyoxylic acid with ozone.

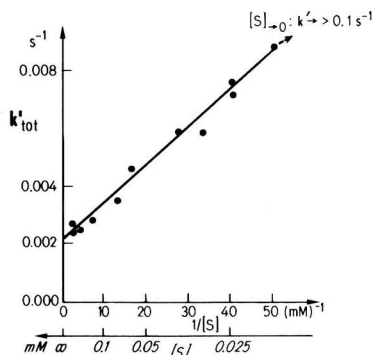


Figure 8. Rate constant for depletion of ozone in the presence of preozonated humic acid (2 mg/L) vs. dilution of *tert*-butyl alcohol ($=1/[\text{S}]$) (pH 8).

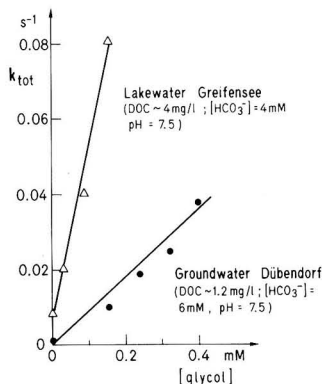


Figure 9. Rate constant for depletion of ozone in natural waters vs. additional concentrations of glycol acting as promoter.

this system also, addition of an efficient $\cdot\text{OH}$ radical scavenger inhibits the decomposition of ozone significantly. This effect decreases proportionally to the dilution of this scavenger. It depends strongly on pH (see also entries in Figure 2).

Constituents of Natural Waters as Promoters and Inhibitors. On the other hand, we have shown before (11) that *tert*-butyl alcohol spiked to natural waters or additional bicarbonate both act as efficient inhibitors for the decomposition of ozone. In addition, decarbonation (with later pH adjustment) before ozonation resulted in a faster ozone depletion (11). These effects were interpreted by assuming radical chain reactions which occur in not fully inhibited waters and which become further inhibited by

Table II. Typical Initiators, Promoters, and Inhibitors for Decomposition of Ozone by Radical-Type Chain Reaction, Encountered in Natural Waters and Wastewaters

initiator	promoter	inhibitor ^c
OH ⁻		
H ₂ O ₂ /HO ₂ ⁻	aryl-(R)	alkyl-(R)
Fe ²⁺ / ^a		HCO ₃ ⁻ /CO ₃ ²⁻
formate	formate	(humics)
humics	(humics)	(TOC)
(TOC)	O ₃	etc.
etc.	etc.	

^a Electron-transfer reaction (J. Hoigné and H. Bader, unpublished results). ^b Including polyalcohols and sugars. ^c Inhibitor corresponds with ·OH radical scavenger S.

the addition of scavengers. But the addition of glycol, which here acted as a model type chain promoter, accelerates the decomposition of ozone (see Figure 9). The intercepts on the k'_{tot} axis are rather high. From these four observations we conclude that the natural waters already contain constituents that can initiate, promote, and inhibit the chain reactions.

With the help of the reaction model now formulated it becomes easier to rationalize the phenomena of the varied lifetimes of ozone observed in different types of surface waters and groundwaters such as presented in Figure 2 of ref 2 or such as compiled in Figure 9 of ref 34. Also the effect of carbonate can now be better rationalized (compare Table II in ref 11).

Hydrogen Peroxide, a Further Chain Carrier. Ozonation of waters, which, e.g., contain aromatic hydrocarbons, produces H₂O₂, a fraction of which is dissociated into HO₂⁻ ($pK_a(\text{H}_2\text{O}_2) = 11.6$). This reacts with further ozone by producing ·O₂⁻ or ·O₃⁻ radicals, and it therefore acts as a further chain carrier. The analysis of such systems will be part of a forthcoming study in which H₂O₂ is also produced by combining UV irradiation with O₃.

Ozone as a Chain Promoter in Pure Water. In the case of very pure water ·OH radicals react with ozone before they become scavenged by other solutes (see Scheme I). Therefore, the ozone itself becomes the promoter acting as an ·OH to ·O₂⁻ "shuttle" (14, 15). Kinetic formulations show for this case that the decomposition rate of ozone will increase with the square of the ozone concentration (8).

In still other cases in which the radical formation becomes fast (e.g., pulse radiolysis or highly elevated pH values) the radical-radical reactions could control the termination step. In such cases the steady-state concentration of the free radicals and the decomposition rate of ozone can only increase with the square root of the initiation rate. These effects combined result in ozone decomposition rate laws varying between half, first, or even second order in ozone, depending on the purity of the water and the initiation rate, as has been so often observed in empirical studies.

Conclusions

The rate of decomposition of aqueous ozone in the presence of organic and inorganic solutes is generally controlled by a radical-type chain reaction. This becomes promoted by solutes that convert the nonselective ·OH radicals into ·O₂⁻ which is a more efficient chain carrier. Many types of substrates, even those present in drinking waters and wastewaters, contain such types of promoting functionalities. Such promoters counteract the inhibiting

effects of ·OH radical scavengers. Table II summarizes solutes that can be classified as typical initiators or promoters or inhibitors for the decomposition of aqueous ozone by the chain reaction.

In the case of impure waters, the overall kinetics due to radical-type chain reactions may still be first order in ozone concentration when the substrate concentrations stay constant. However, as a result of these chain reactions and the interaction of various solutes with the free radicals in solution, the solute concentration effects on the ozone decomposition rate are not additive.

The chemical and reaction kinetic information available for the individual reaction steps allows one to predict the trend of the kinetics of the chain reaction in cases where the concentrations of well-defined solutes are varied. In general, however, not all relevant data on the water composition are available. In addition, the kinetics of the radical-initiation reactions are too complex to be predictable at the present time. We therefore recommend that experiments for quantifying the rate of the ozone decomposition shall be performed on the water of interest. However, the planning of such measurements and the interpretation of the results must be based on the kinetic characteristics of the chain reactions involved, and it must account for the effects of changes of water composition.

Whenever conclusions on the product formations of ozonation reactions are to be generalized, it is absolutely necessary that the extent of possible direct reactions of ozone with dissolved compounds be compared with the extent of the indirect reactions proceeding by the primary formation of ·OH radicals. For this, the decomposition rate of ozone and its acceleration by different types of solutes must be known.

Acknowledgments

We thank Heinz Bader for much advice and for providing experimental techniques applied for these studies and Frank Scully, Werner Haag, and Susanne Masten for discussions and reviewing the manuscript.

Registry No. O₃, 10028-15-6; ·OH, 3352-57-6; ·O₂⁻, 11062-77-4; ·O₃⁻, 12596-80-4; CH₂CH₂OH, 64-17-5; *tert*-butyl alcohol, 75-65-0; glyoxylic acid, 298-12-4; ethylene glycol, 107-21-1; methanol, 67-56-1; D-glucose, 50-99-7; formic acid, 64-18-6.

Literature Cited

- (1) Stumm, W. *Helv. Chim. Acta* **1954**, *37*, 773-778.
- (2) Stumm, W. *Schweiz. Z. Hydrobiol.* **1956**, *18*, 201-207.
- (3) (a) Masschelein, W. J. "Ozonization Manual for Water and Wastewater Treatment"; Wiley: New York, 1982; (b) "L'ozonisation des eaux. Manuel pratique; Technique et Documentation"; Paris, 1980.
- (4) (a) Chameides, W. L.; Davis, D. D. *J. Geophys. Res.* **1982**, *87*, 4863-4877; (b) Hoigné, J. In "Gas-Liquid Chemistry of Natural Waters". Brookhaven National Laboratory: Upton, NY, 1984; BNL Report 51757, pp 13-1-14.
- (5) Hoigné, J. In "Ozone Technique and its Practical Applications"; Rice, R. G.; Netzer, A., Eds.; Ann Arbor Science: Ann Arbor, MI, 1984; Vol. I, pp 341-377.
- (6) Peleg, M. *Water Res.* **1976**, *10*, 361-365.
- (7) Gurol, M. D.; Singer, Ph. C. *Environ. Sci. Technol.* **1982**, *16*, 377-383.
- (8) Staehelin, J. Thesis, Swiss Federal Institute of Technology, Zürich, 1983, No. 7342.
- (9) Weiss, J. *Trans. Faraday Soc.* **1935**, *31*, 668-681.
- (10) Hoigné, J.; Bader, H. *Water Res.* **1976**, *10*, 377-386.
- (11) Hoigné, J.; Bader, H. *Vom Wasser* **1977**, *48*, 283-304.
- (12) Staehelin, J.; Hoigné, J. *Vom Wasser* **1983**, *61*, 337-348.
- (13) Staehelin, J.; Hoigné, J. *Environ. Sci. Technol.* **1982**, *16*, 676-682.
- (14) Bühler, R. E.; Staehelin, J.; Hoigné, J. *J. Phys. Chem.* **1984**, *88*, 2560-2564.

- (15) Staehelin, J.; Bühler, R. E.; Hoigné, J. *J. Phys. Chem.* **1984**, *88*, 5999-6004.
- (16) Hoigné, J.; Bader, H. *Water Res.* **1983**, *17*, 173-184.
- (17) Hoigné, J.; Bader, H. *Water Res.* **1983**, *17*, 185-194.
- (18) Hoigné, J.; Bader, H.; Haag, W. R.; Staehelin, J. *Water Res.* **1985**, *19*, 993-1004.
- (19) Rabani, J.; Klug-Roth, D.; Henglein, A. *J. Phys. Chem.* **1974**, *78*, 2089-2093.
- (20) Ilan, Y.; Rabani, J.; Henglein, A. *J. Phys. Chem.* **1976**, *80*, 1558-1562.
- (21) Schuchmann, M. N.; von Sonntag, C. *Z. Naturforsch. B: Anorg. Chem., Org. Chem.* **1978**, *33B*, 329-331.
- (22) Bothe, E.; Schulte-Frohlinde, D.; von Sonntag, C. *J. Chem. Soc.* **1978**, 416-420.
- (23) Bothe, E.; Schuchmann, M. N.; Schulte-Frohlinde, D.; von Sonntag, C. *Photochem. Photobiol.* **1978**, *28*, 639-644.
- (24) Schuchmann, M. N.; von Sonntag, C. *J. Phys. Chem.* **1979**, *83*, 780-784.
- (25) Staehelin, J.; Hoigné, J. *Ozone World Congr., 5th, Wasser Berlin, Colloq. Verlag Otto H. Hess* **1981**, 623.
- (26) Forni, L.; Bahnemann, D.; Hart, E. J. *J. Phys. Chem.* **1982**, *86*, 255-259.
- (27) Sehested, K.; Holcman, J.; Hart, E. J. *J. Phys. Chem.* **1983**, *87*, 1951-1954.
- (28) Sehested, K.; Holcman, J.; Bjergbakke, E.; Hart, E. J. *J. Phys. Chem.* **1984**, *88*, 4144-4147.
- (29) Farhatziz; Ross, A. B. "Selected Specific Rates of Reactions of Transients from Water in Aqueous Solution"; National Bureau of Standards: Washington, DC, 1977; NSRDS-NBS59.
- (30) Baxendale, J. H.; Khan, A. A. *Int. J. Radiat. Phys. Chem.* **1969**, *1*, 11-24.
- (31) Ilan, Y.; Rabani, J. *Int. J. Radiat. Phys. Chem.* **1976**, *8*, 609-611.
- (32) Anbar, M.; Meyerstein, D.; Neta, P. *J. Chem. Soc. B* **1966**, 742-747.
- (33) Weeks, J. L.; Rabani, J. *J. Phys. Chem.* **1966**, *70*, 2100.
- (34) Hoigné, J.; Bader, H. *Ozone: Sci. Eng.* **1979**, *1*, 357-372.
- (35) Black, E. D.; Hayon, E. *J. Phys. Chem.* **1970**, *74*, 3199-3203.
- (36) Nakashima, N.; Hayon, E. *J. Phys. Chem.* **1970**, *74*, 3290-3291.
- (37) Nakashima, N.; Hayon, E. *J. Phys. Chem.* **1979**, *83*, 780-782.
- (38) Pryor, A. W.; Gu, J.; Church, D. F. *J. Org. Chem.* **1985**, *50*, 185-189.
- (39) Bader, H.; Hoigné, J. *Ozone: Sci. Eng.* **1982**, *4*, 169-176.
- (40) Bader, H.; Hoigné, J. *Water Res.* **1981**, *15*, 499-454.

Received for review October 8, 1984. Revised manuscript received June 3, 1985. Accepted July 11, 1985. Parts of this paper were presented by J. Hoigné at the 6th Ozone World Congress of the International Ozone Association in Washington (May 1983) and by J. Staehelin at the Meeting on Aquatic Chemistry of the Gesellschaft Deutscher Chemiker, Norderney, FRG (May 1983).

Surface Charge and Adsorption Properties of Chrysotile Asbestos in Natural Waters

Roger C. Bales* and James J. Morgan

Department of Environmental Engineering Science, California Institute of Technology, Pasadena, California 91125

■ Changes in surface-charge adsorption properties of chrysotile asbestos aging in water were studied in a series of constant-pH laboratory experiments. Chrysotile freshly suspended in an inorganic electrolyte has a positive surface charge below pH 8.9. Charge reversal occurs within about 2 weeks due to more rapid dissolution of chrysotile's outer magnesium hydroxide surface relative to the underlying silica component of the mineral. The inorganic anions NO_3^- , Cl^- , HCO_3^- , and SO_4^{2-} did not adsorb. A constant-capacitance model can be used to relate surface charge to adsorption of protons over the pH range 7-9. At natural organic matter (NOM) concentrations at or below those encountered in natural waters, the particles can adsorb sufficient organic matter within 1 day to acquire a negative charge. Adsorption of NOM reached a maximum of 30×10^{-6} mg of C cm^{-2} after 21 h; catechol continued to adsorb over 5 days.

Introduction

Chrysotile asbestos is found in drinking water as a result of natural weathering of rocks and soil and due to corrosion of asbestos-cement pipe. Chrysotile fiber concentrations in the range of 10^8 fibers L^{-1} have been consistently found in drinking waters along the west coast of the U.S. (1, 2), in Quebec (3), and in Newfoundland (4). In California, fiber concentrations below major reservoirs range from 10^8 to 10^{11} L^{-1} (5). Fiber removal in reservoirs and in water-treatment plants is largely due to coagulation with larger

particles that subsequently settle out. The rate of removal depends on the number and surface charge of larger particles present and on the surface charge of the fibers.

The purpose of the research work described in this paper is to develop a better understanding of the chemical behavior and the influence of surface chemistry on the physical behavior of chrysotile asbestos particles in natural waters and in water-treatment processes. The relation between dissolution, adsorption, and surface-charge development is studied experimentally; surface charge is interpreted in terms of a coordination chemical model of the mixed magnesium hydroxide and silica surface.

Background

Chrysotile, a magnesium silicate serpentine mineral, forms crystals by repeated alternate stacking of its infinite magnesium hydroxide and silica sheets. The chemical formula for serpentine is $\text{Mg}_3\text{Si}_2\text{O}_5(\text{OH})_4$. Each chrysotile fiber is a single crystal, comprised of about 40 layers of spiral or concentric tubes, with the external surface of an ideal crystal being magnesium hydroxide. Removal of the outermost magnesium and hydroxide ions (e.g., by dissolution) would leave a silica surface. Outer oxides or hydroxides coordinated to magnesium (>Mg-OH) or silicon (>Si-OH) are possible adsorption sites for protons, other cations, or anions. It is assumed that ions adsorb to both >Mg-OH and >Si-OH sites as inner-sphere complexes. One valid thermodynamic description of surface adsorption is the constant-capacitance model, which provides a simple, mathematical statement of the relation between proton adsorption and surface charge. Although choice of surface species and values of parameters are model dependent, the constant-capacitance model can provide a self-consistent

* Address correspondence to this author at the Department of Hydrology and Water Resources, University of Arizona, Tucson, AZ 85721.

fit to potentiometric titration data (6). In the model employed, the following intrinsic equilibrium constants describe proton coordination at the chrysotile surface:

$$K_{a1(int)}^s = \frac{\{>Mg-OH\}[H^+]}{\{>Mg-OH_2^+\}} e^{-e\psi/(kT)} \quad (1)$$

$$K_{a2(int)}^s = \frac{\{>Mg-O\}[H^+]}{\{>Mg-OH\}} e^{-e\psi/(kT)} \quad (2)$$

$$K_{as(int)}^s = \frac{\{>Si-O\}[H^+]}{\{>Si-OH\}} e^{-e\psi/(kT)} \quad (3)$$

Concentrations of surface species, in braces, are in mol cm⁻² and solution species, in brackets, are in mol L⁻¹. ψ is surface potential (volts), e is the charge on an electron, k is Boltzmann's constant, and T is temperature. Surface charge arises due to ion adsorption and is defined by

$$\sigma = F(\{>Mg-OH_2^+\} - \{>Mg-O\} - \{>Si-O\}) \quad (4)$$

where σ has units of C cm⁻², and F is the Faraday constant. Surface charge can be calculated from a proton balance (mathematically equivalent to the electroneutrality expression) in the suspension. For chrysotile in the pH range 7–9, the electroneutrality expression is

$$\{>Mg-OH_2^+\} - \{>MgO\} - \{>Si-O\} = (1/sA)(C_A - C_B - 2[Mg^{2+}] - [Mg-OH^+] + [H_3SiO_4^-] + 2[H_2SiO_4^{2-}] + [OH^-]) \quad (5)$$

C_A and C_B are the concentrations of acid and base added to hold pH constant, s is the particle concentration (g L⁻¹), and A is particle surface area (cm² g⁻¹). The relation between charge and potential is given by

$$C = \sigma/\psi \quad (6)$$

where C is capacitance, a constant in this model.

The mole balance for the surface is

$$S_T = \{>Mg-OH_2^+\} + \{>Mg-OH\} + \{>Mg-O\} + \{>Si-OH\} + \{>Si-O\} \quad (7)$$

S_T is the total concentration of surface sites, a constant, and is calculated from unit cell dimensions to be 12 ion nm⁻² (2×10^{-9} mol cm⁻²). Although the relative concentration of magnesium sites (S_m) and silica sites (S_s) may vary depending on the ratio of magnesium to silica released from the surface via dissolution, the sum of the two is a constant, S_T . At time t after the start of dissolution, S_m and S_s can be expressed as functions of S_T , their values at $t = 0$, and the amount of magnesium and silica released into solution:

$$S_m(t) = S_m(0) - [Mg^{2+}] - [MgOH^+] + \frac{3}{2}[H_4SiO_4] + \frac{3}{2}[H_3SiO_4^-] \quad (8)$$

$$S_s(t) = S_s(0) + [Mg^{2+}] + [MgOH^+] - \frac{3}{2}[H_4SiO_4] - \frac{3}{2}[H_3SiO_4^-] \quad (9)$$

The $\frac{3}{2}$ term on silica reflects the stoichiometric ratio in the solid.

Materials and Methods

Experimental Setup. Dissolution and surface-charge behavior were monitored in constant-pH, constant-temperature suspensions of 2 g of chrysotile/200 mL of 0.01–0.1 M electrolyte (KNO₃, NaNO₃, NaCl, or Na₂SO₄). Some experiments were done with either catechol (1,2-dihydroxybenzoic acid) or oxalic acid present. Duration

was from 3 to 5 days, chosen as sufficient to establish a linear dissolution rate after the initial 1-day nonlinear dissolution startup period. A constant-pressure nitrogen or nitrogen-carbon dioxide (350 ppm) atmosphere was maintained by bubbling gas through the suspensions. Further details of the experimental apparatus and analytical procedures are described elsewhere (7).

Electrophoretic mobility was measured on 5–10 mg L⁻¹ chrysotile suspensions, again at constant pH. Conditions were chosen to parallel those of the potentiometric experiments, but with solids concentration approximately 1000-fold lower. Electrolyte concentrations were generally 0.01 M. In a typical experiment, the mobility of the particles at constant pH in 0.01 M NaCl was monitored for 24–48 h, a known concentration of organic acid was added, and mobility was monitored for 24–48 h longer. In many cases, more than one experiment was performed under the same conditions to determine the reproducibility of results. Electrophoretic mobility measurements were made by using a Rank Brothers (Cambridge, England) particle microelectrophoresis apparatus, Mark II, equipped with a cylindrical cell and 3-mW He/Ne laser illuminator. From 20 to 40 particles were time in each sample, half at each stationary level. Voltage gradients ranged from 4 to 12 V cm⁻¹. Mobility did not depend on field strength for the cylindrical chrysotile particles.

Adsorption of catechol, oxalate, and NOM was measured in parallel with electrophoretic experiments. Conditions were like those of the potentiometric experiments. As with the electrophoretic experiments, electrolyte concentrations were generally 0.01 M. Organic concentrations were higher in the adsorption experiments, to maintain the same solid-to-organic ratio as in the mobility experiments. Batch adsorption experiments lasting up to 36 h were also carried out. These were at room temperature ($\sim 25^\circ\text{C}$) and open to the atmosphere; pH was held constant.

Chrysotile Particles. The starting material was raw chrysotile ore from near Coalinga, CA. Impurities were removed by aqueous decanting and stirring, with the resulting material having physical characteristics much like the fibers found in natural waters (7). Surface area, measured by single-point BET nitrogen adsorption, was 48.5 m² g⁻¹.

Natural Organic Matter. Dissolved natural organic matter was concentrated from a 190-L surface-water sample taken in Dec 1983 from Castaic reservoir in southern California. Castaic has a capacity of 0.4 km³, an area of 9.0 km², and a maximum depth of 100 m. California aqueduct water enters Castaic from Pyramid reservoir, which is about half of the size of Castaic. The combined detention time for the two reservoirs is 3 years.

Water was collected in 20-L plastic carboys that had been rinsed successively with 0.1 M NaOH, 0.1 M HCl, and double-distilled water. Samples were acidified to pH 2 with HCl within 2 h of sampling and stored at 4 °C. Extraction onto 500 cm³ of XAD-8 resin in a 5.4 cm i.d. and 50 cm long column was begun the same day and was completed within 48 h. The XAD-8 had been previously extracted in a Soxhlet apparatus and stored in methanol; cleanup after packing followed that used by Dempsey (8). All 190 L of lake water were pumped through the column in a downflow mode at the rate of 6 L h⁻¹. The column was eluted by first lowering the liquid level to just above the resin and then recirculating (upflow mode) 1 L of a pH 10 sodium hydroxide solution at 5.4 L h⁻¹ until obvious color was removed from the resin. Double-distilled water was used to displace the final volume of eluent. The 1.5 L of 90 mg L⁻¹ TOC eluent recovered was filtered through

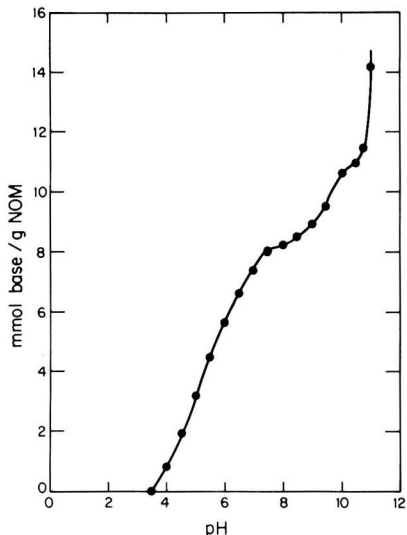


Figure 1. Titration curve of dissolved NOM from Castaic reservoir. Points were determined from the amount of 0.1 M NaOH needed to titrate a 90 mg of C/L of NOM solution less that needed to titrate 0.1 M NaCl.

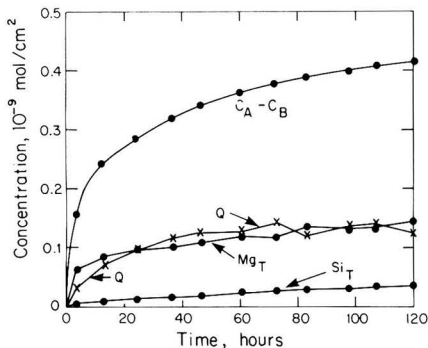


Figure 2. Results of typical constant-pH dissolution experiment: pH 8, 10 g L⁻¹ chrysotile, 0.1 M NaCl, N₂ atm, 25 °C. *Q* is the surface charge in mol cm⁻² (σ/F); the sum of dissolved magnesium species (Mg_T), sum of dissolved silica species (Si_T), and acid or base added ($C_A - C_B$) are expressed per unit surface area.

a 0.45- μ m Millipore filter and stored in a brown glass bottle in the dark at 4 °C until used.

A titration curve for the stock NOM solution is shown in Figure 1. Titration of carboxyl groups appears to be complete at about pH 7.5. A second, smaller inflection appears at pH 10.5.

Results and Discussion

Experiments yielded information on adsorption and surface charge, as well as on dissolution rates for chrysotile; dissolution behavior is described elsewhere (9). Results of a typical experiment are shown in Figure 2, in which magnesium release, silica release, and surface charge were determined from samples taken at about 12-h intervals. Chrysotile was dissolving throughout the experiments and did not reach solubility or adsorption equilibrium over the times studied. Adsorption data for organics are therefore interpreted as quasi-equilibrium values in terms of a simple Langmuir-type equation and are not incorporated into the general surface model (eq 1-7) that is used to relate extent

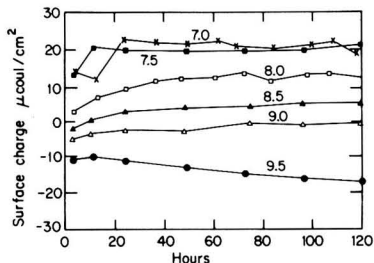


Figure 3. Surface charge in constant-pH, dissolution experiments: 10 g L⁻¹ chrysotile, N₂ atm, 25 °C, 0.1 M NaCl; pH values from 7 to 9.5.

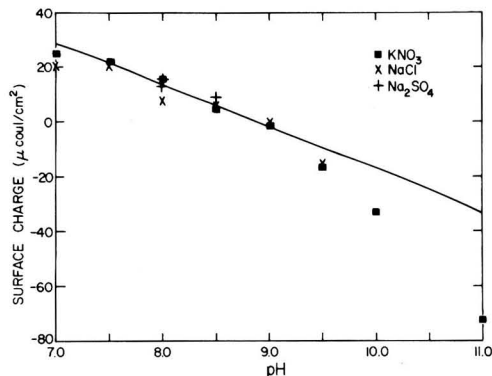


Figure 4. Surface charge at longer times (72–120 h) in constant-pH, dissolution experiments as a function of pH. Line is calculated by using the best-fit model parameters: $S_T = 2.0 \times 10^{-9}$ mol cm⁻², $S_m = 0.9S_T$, $S_s = 0.1S_T$, $pK_{a1}^* = 8$, $pK_{a2}^* = 10$, $pK_{as}^* = 6.7$, and $C = 3.6$ C V⁻¹ cm⁻².

of proton adsorption to surface charge. The quasi-equilibrium interpretations that follow enable making relative comparisons between extents of adsorption and magnitudes of surface charge for different organics and at different pHs and organic-to-surface ratios.

Titration-Derived Surface Charge. Surface-charge development for six representative experiments done at different pHs in 0.1 M NaCl are shown in Figure 3. The initial 24–48-h rise is probably due to slow breakup of fiber bundles into individual fibers. Slow achievement of steady-state proton adsorption is also a possible explanation. Although chrysotile was crushed to break up the solid cake that formed during sample preparation, many clumps of particles were visible during the first day of each experiment. Electron micrographs of samples taken at the end of the 5-day experiments showed that particles were well dispersed into individual fibers. Breakup of larger particles to expose more surface area would result in a greater total proton uptake, giving an increase in surface charge (eq 5). The decrease at longer times is likely due to removal of positively charged $>Mg-OH_2^+$ sites in the outer brucite sheet (by dissolution) and accompanying exposure of underlying $>SiO^-$ sites on the surface.

The average surface charge at longer times (72–120 h), shown in Figure 4, is zero at pH 8.9; this is the same value estimated by Parks for serpentine minerals (10). Reported values for pH_{iep} for freshly suspended chrysotile fibers are in the range 10–11.8 (11, 12). A pH_{zpc} of 10 is reported for freshly suspended fibers (13). The estimated pH_{zpc} of magnesium hydroxide is ≤ 12.5 (10), suggesting that $>Mg-OH_2^+$ should be the predominant surfaces species in the pH range of interest, 7.5–8.5. The reported pH_{zpc} 's

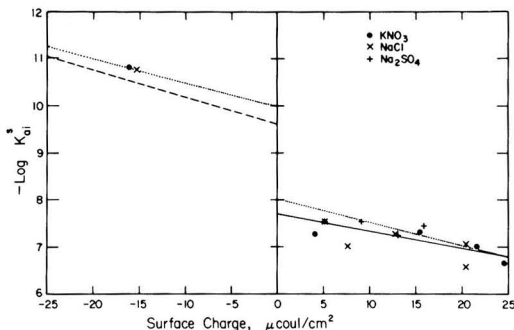


Figure 5. Determination of surface equilibrium constants. Points are from experimental data, assuming $S_m = S_T$ at the outset of the experiment: (—) best fit to points, (---) best overall model fit assuming $S_m = 0.9S_T$ at outset, and (- - -) best fit to brucite data.

for silica are variable, but average about 2 (14).

Differences in the observed surface charge in KNO_3 , NaCl , and Na_2SO_4 media are small. There was also no significant difference in surface charge for a 0.01 M vs. 0.1 M SO_4^{2-} solution, suggesting that inorganic anion-surface interactions are weak. Sulfate and chloride show some evidence of complexation with Mg^{2+} in solution, with $\text{p}K_1$ values of -2.28 and -0.91 , respectively (15). At 0.1 M ligand, the respective $[\text{MgL}^{(2-z)+}][\text{Mg}^{2+}]^{-1}$ ratios would thus be 0.1 and 0.01. The $\text{p}K$ value for Mg^{2+} and H_3SiO_4^- complexation is -1.24 (15); at 0.1 M total silica, the $[\text{MgL}^{(2-z)+}][\text{Mg}^{2+}]^{-1}$ ratio would be only 0.0001. Further, it has been observed that silica concentrations below those needed to precipitate silica from solution ($10^{-3.5}$ M) have little effect on chrysotile electrophoretic mobility (13).

A second possible explanation for the small difference in charge is that the ions studied interact similarly with the surface, but the equilibrium constant for MgSO_4 is 20 times that for MgCl^+ , and there is no evidence of a MgNO_3^+ complex. In the absence of adsorption of ions other than H^+ and OH^- , the species contributing to surface charge are given by (eq 4), and the pH_{iep} is equivalent to the pH_{zpc} .

Estimation of Surface Equilibrium Constants.

From a least-squares fit to the titration data below the pH_{zpc} and for the initial surface assumed to be entirely magnesium hydroxide, $\text{p}K_{\text{a1}}^s$ is estimated to be near 7.7, with no systematic differences apparent between the three electrolytes NaCl , Na_2SO_4 , and KNO_3 (Figure 5). The corresponding constant capacitance from this fit is $4.8 \text{ C V}^{-1} \text{ m}^{-2}$. Considering the surface speciation and charge relationships (eq 1-4) together, taking the initial surface to be 10% silica (90% magnesium hydroxide), and given a pH_{zpc} of 8.9 (average value for longer times, 72-120 h), a best fit to the data is obtained by using $\text{p}K_{\text{a1}}^s = 8.0$, $\text{p}K_{\text{a2}}^s = 10.0$, $\text{p}K_{\text{as}}^s = 6.7$, and $C = 3.6 \text{ C V}^{-1} \text{ m}^{-2}$. Lines with the same slope as these best-fit lines for $\text{p}K_{\text{a1}}^s$ and $\text{p}K_{\text{a2}}^s$ are also plotted in Figure 5. The relation derived in preliminary experiments on brucite, which suggests a capacitance of $3.1 \text{ C V}^{-1} \text{ m}^{-2}$ and a lower $\text{p}K_{\text{a2}}^s$ (9.6), is also shown (7). S_T is assumed to be equal to the surface hydroxide density, calculated from unit cell dimensions to be 12 ion nm^{-2} ($2 \times 10^{-9} \text{ mol cm}^{-2}$). The calculated relation of pH vs. σ , based on the above constants, is shown in Figure 4. The model describes observations best near the pH_{zpc} and deviates most at high pH . The fit could be made better by using different capacitances above and below the pH_{zpc} , which would add one more fitting parameter to the model. As is apparent from those results and from the data of others, the charge-potential relations on metal oxide am-

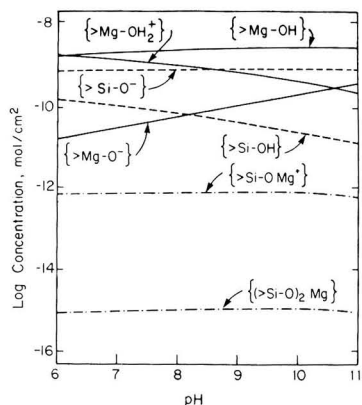


Figure 6. Predicted magnesium silicate surface speciation. See Figure 4 for model parameters.

photeric surfaces may be quite different above and below the pH_{zpc} (16, 17).

It has been noted that magnesium binds to a silica surface, with equilibria given (constant-capacitance model) by

$$*K_{\text{Mg}}^s = \frac{[\text{>Si-OMg}^+][\text{H}^+]}{[\text{>SiOH}][\text{Mg}^{2+}]} e^{-e\psi/(kT)} \quad (10)$$

$$*\beta_{\text{Mg}}^s = \frac{\{(\text{>Si-O})_2\text{Mg}\}[\text{H}^+]^2}{[\text{>Si-OH}]^2[\text{Mg}^{2+}]} \quad (11)$$

Recently reported values for these constants are $\text{p}^*K_{\text{Mg}}^s = 7.3$ and $\text{p}^*\beta_{\text{Mg}}^s = 14.7$ (18). The predicted behavior for a magnesium hydroxide surface is shown in Figure 6 by using these reported constants and the above-noted values for $\text{p}K_{\text{a1}}^s$, $\text{p}K_{\text{a2}}^s$, $\text{p}K_{\text{as}}^s$, and C . Of the silica sites, the species >Si-O^- and >Si-OH predominate. Adsorption of Mg^{2+} is thus considered unimportant.

Adsorption of Organics. The amount of catechol adsorbed to chrysotile was observed to increase during the first 15-36 h of constant-pH adsorption and dissolution experiments (Figure 7). A quasi-equilibrium comparison of the results at different pHs is made by fitting the observed relations at 21 h to a Langmuir-type equation of the form:

$$\Gamma = \frac{C_s K \Gamma_m}{1 + C_s K} \quad (12)$$

giving the results shown in Figure 8 for adsorption of catechol on chrysotile. Γ is the adsorption density and is expressed in mass (mg cm^{-2}) and molar (mol cm^{-2}) units in Figures 7 and 8, respectively; Γ_m is the maximum adsorption density, expressed in the same units. C_s is the total solution concentration of the adsorbing solute, expressed in the corresponding mass (mg L^{-1}) or molar (mol L^{-1}) units; K is the adsorption constant, or affinity for adsorption, and has units of reciprocal concentration. Γ_m is $0.73 \times 10^{-9} \text{ mol cm}^{-2}$, which corresponds to 4.4 ion nm^{-2} , or about one-third that of S_T .

The increase in affinity for catechol at higher pH is consistent with a predicted increase in magnesium-catechol complexation in solution at high pHs. The greater catechol adsorption in going from $\text{pH} 7.5$ to 8.5 could also be due to adsorption on >Si-OH as well as >Mg-OH surface sites. Catechol does slightly enhance silica dissolution at neutral to slightly alkaline pHs (7, 14).

At longer times, the UV absorbance peak for catechol in the presence of chrysotile was observed to broaden as

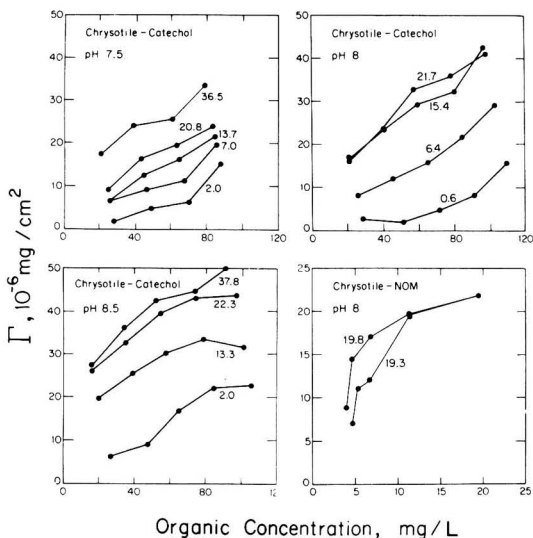


Figure 7. Batch adsorption experimental results for catechol and NOM: 0.01 M NaCl, room temperature open to atmosphere; chrysothile 1.02 g L⁻¹; times from 0.6 to 37.8 h.

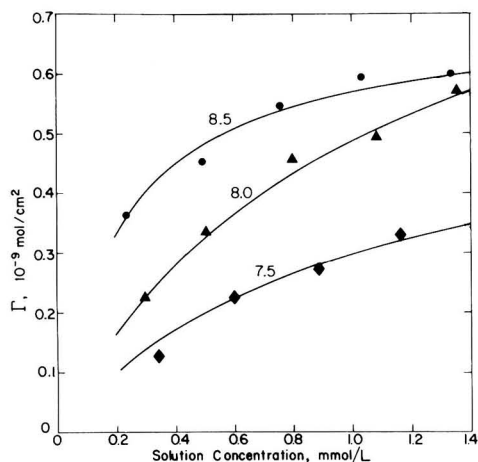
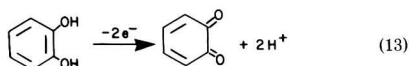


Figure 8. Adsorption isotherms for catechol on chrysothile after a 21-h equilibration at constant pH. Data from Figure 7 ($0.1 \times 10^{-9} \text{ mol cm}^{-2} = 0.6 \text{ ion nm}^{-2} = 7.2 \times 10^{-6} \text{ mg cm}^{-2}$).

well as become smaller in magnitude. This was accompanied by a darkening in color of the suspensions and a need to add base to hold pH constant, suggesting that oxidative polymerization of catechol was occurring. Either trace amounts of oxygen from the nitrogen-carbon dioxide gas mixture used in the experiments or Fe(III) impurities in the chrysothile could participate in a reaction of the form (19):



The *o*-quinone products may then react further to form complex humic acid type polymers as the main products (20), a process that has previously been observed to be enhanced in the presence of manganese oxide surfaces (21). Alternately, adsorption of catechol at >Si-OH or >Si-O⁻

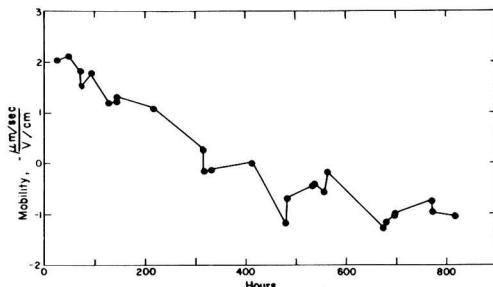


Figure 9. Mobility of stock chrysothile suspension: solids concentration 10.0 mg L⁻¹, 25 °C, 0.01 M NaCl, and 350 ppm of CO₂ in N₂ atm, pH 8.0.

sites, with the accompanying higher local OH⁻ concentration, could enhance the oxidation by either iron or molecular oxygen.

Oxalate adsorption also exhibited a gradual increase with time in the dissolution experiments. The adsorption densities, up to approximately $0.6 \times 10^{-9} \text{ mol cm}^{-2}$, are slightly less than those for catechol. No significant change in adsorption over the pH range 7.5–8.5 was observed. Oxalate appears to adsorb more strongly onto chrysothile than onto either goethite (near zero at pH 8 to $\sim 0.1 \times 10^{-9} \text{ mol cm}^{-2}$ at pH 4.2 (22)) or gibbsite (near zero above pH 7 to $\sim 0.05 \times 10^{-9} \text{ mol cm}^{-2}$ at pH 5 (23)).

The amount of natural organic matter adsorbed to chrysothile at pH 8 reached a steady value after about 20 h. At most $\sim 60\%$ of the NOM was removed from solution in the chrysothile-NOM experiments. The apparent amount adsorbed corresponds to approximately $8 \times 10^{-6} \text{ mg of C cm}^{-2}$.

Electrophoretic Mobilities. The positive to negative shift in mobility of chrysothile particles aging in a non-binding electrolyte at constant pH is illustrated in Figure 9. This shift occurs as the surface becomes more silica-like and less brucite-like due to preferential release of magnesium during dissolution. Qualitatively similar behavior was observed for chrysothile suspended in pH 4 and pH 6.8 acetic acid solution (24).

Acetic acid forms only weak complexes with magnesium, so the charge reversal was apparently due to dissolution rather than adsorption. Freshly suspended, natural-chrysothile samples from different sources may exhibit widely varying mobilities, reflecting differing ratios of outer brucite to outer silica area (25).

The addition of organic anions makes the surface charge and mobility of chrysothile negative in two ways: by adsorption of negatively charged species to the surface and by a short-term enhancement of release of magnesium from the surface. Results of a 10-day mobility and adsorption experiment are shown in Figure 10. The effect of adsorbed catechol in giving chrysothile a negative mobility is apparent during the first 24 h after adding the organic. During that time, catechol is adsorbed to an extent equal to about 40% of Γ_m .

The apparent oxidative polymerization and adsorption of catechol noted above were accompanied by a decrease in the magnitude of the negative mobility, which is consistent with oxidation of adsorbed organics to form uncharged, polymeric species. That the decrease in absorbance at $\lambda = 256 \text{ nm}$ is associated with catechol removal from solution was confirmed by the TOC analyses shown in Figure 10.

A series of subsequent experiments examined the short-term charge reversal apparent on Figure 10 over a

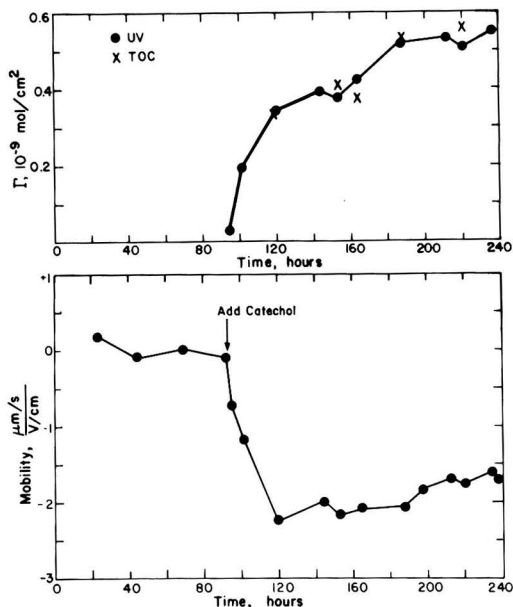


Figure 10. Chrysotile surface charge and mobility resulting from catechol adsorption: pH 8, 0.01 M NaCl, 25 °C, N₂-CO₂ (350 ppm) atm, solids 10.9 mg L⁻¹ (mobility) and 1.02 g L⁻¹ (adsorption); 1.9 × 10⁻⁹ mol cm⁻² catechol added.

shorter period of time, from 1 day prior to organic addition to several days after organic addition. Aliquots were withdrawn from the stock suspension whose mobility is shown in Figure 9, catechol, oxalic acid, or NOM was added, and the effect was noted. All mobility curves showed qualitatively the same behavior, as did those for preliminary experiments done with phthalic acid (7). Within 24 h after addition of the organic, a new, lower steady-state mobility value was reached. Figure 11 summarizes these steady-state values for the range of conditions studied. If charge reversal was due only to anion adsorption at the maximum densities suggested by Figures 7 and 8, there should be little charge enhancement beyond an organic to surface molar ratio of one (e.g., >10⁻³ mg of C/cm²). The presence of an enhancement at higher ratios suggests either multilayer adsorption, increased magnesium removal, or both.

Oxalate has less of an effect on chrysotile mobility than does catechol, consistent with the above-noted slightly lower adsorption of oxalate on the surface. The mobility data provide additional evidence that catechol adsorbs to both >Si-OH and >Mg-OH surface sites.

Adsorption of NOM in the range 10⁻⁵-10⁻³ mg of C cm⁻² caused greater charge reversal on chrysotile than did either oxalic acid or catechol. Charge reversal at low organic concentrations is consistent with the findings of Tipping and Cooke (26), who observed reversal of mobility with adsorption of as little aquatic humus as 10 mg/g (~60 × 10⁻⁶ mg cm⁻²) onto goethite at pH 7.

Particles in samples taken from the Feather river in May 1983 all showed mobilities of -1.1 ± 0.5 μm s⁻¹ V cm⁻¹. The chrysotile fiber concentration in these samples was on the order of 10⁸ L⁻¹, and the concentration of larger (2-100 μm) particles was about 10⁷ L⁻¹ (7). This suggests that even far upstream in natural waters, chrysotile fibers, as well as other particles present, have a negative charge. The magnitude of that charge is equal to or lower than that

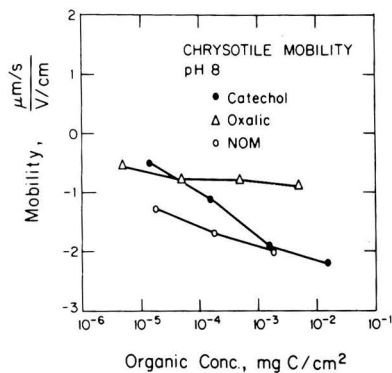


Figure 11. Mobility of chrysotile in the presence of increasing organic concentrations (amount of organic added).

observed in the laboratory, with little variation in individual mobilities despite the wide range of particle sizes and presumably particle identities in the river water samples. This is consistent with observations by others (27).

Conclusions

An ideal, unweathered chrysotile fiber has a magnesium hydroxide outer surface, and fibers freshly suspended in water of pH below 8.9 have a positive surface charge. Chrysotile particles aging in natural waters acquire a negative surface charge by rapid (within 1 day) adsorption of natural organic matter. In inorganic electrolytes, the positive-to-negative shift occurs within about 2 weeks and is due to the faster dissolution of the positively charged brucite sheet relative to the negatively charged silica sheet in chrysotile's outer layer. After 4 weeks, further changes in surface charge (electrophoretic mobility) are slow, possibly reflecting a new steady state in fiber dissolution.

The amount of catechol that is lost from solution (adsorbs) in the presence of chrysotile in the pH range 7.5-8.5 does not reach equilibrium but increases over 5 days. After 1 day the maximum adsorption density on chrysotile, estimated by using a Langmuir adsorption equation, is 0.7 × 10⁻⁹ mol cm⁻² (50 × 10⁻⁶ mg of C cm⁻²). This is approximately one-third of the estimated number of surface sites available for proton exchange. Adsorption densities for oxalate, a stronger acid, are about 15% lower. The corresponding maximum density for adsorption of natural organic matter was near 30 × 10⁻⁶ mg of C cm⁻². These densities suggest that, in most surface waters, chrysotile fibers should be essentially completely covered with NOM. Further, changes in suspended particle concentration over at least 2 orders of magnitude will have little effect on the amount of NOM in a water.

The steady increase in amount adsorbed with time in catechol experiments is apparently due to further adsorption of oxidized polymers of catechol. Oxidation and polymerization of catechol are enhanced in the presence of a chrysotile surface. The oxidant in these experiments is thought to be molecular oxygen, present in trace amounts in the N₂ gas used to exclude CO₂ from the reactor. Oxidation by Fe(III), present as an impurity in the chrysotile, is also possible.

Chrysotile's surface charge was the same in the presence of the different inorganic anions NO₃⁻, Cl⁻, HCO₃⁻, and SO₄²⁻, suggesting that adsorption of these anions is weak.

A constant-capacitance model can be used to relate surface charge to adsorption and desorption of protons over a limited, 1.5-2 pH unit, range. The best-fit model pa-

rameters are $pK_{a1}^s = 8.0$, $pK_{a2}^s = 10.0$ for $>Mg-OH$ and $pK_{as}^s = 6.7$ for $>Si-OH$, and a capacitance of $3.6 \text{ C V}^{-1} \text{ m}^{-2}$.

Acknowledgments

We have benefited from discussions with M. Hoffmann and A. Stone.

Registry No. MgOH, 12141-11-6; chrysotile, 12001-29-5; catechol, 120-80-9; oxalic acid, 144-62-7.

Literature Cited

(1) Polissar, L.; Severson, R. K.; Boatman, E. S.; Thomas, D. B. *J. Epidemiol.* **1982**, *116*, 314-328.
 (2) Hayward, S. B. *J.—Am. Water Works Assoc.* **1984**, *76*, 66-73.
 (3) Lawrence, J.; Zimmermann, H. W. *Water Res.* **1976**, *10*, 195-198.
 (4) Toft, F.; Wigle, D.; Meranger, J. C.; Mao, Y. *Sci. Total Environ.* **1981**, *18*, 77-89.
 (5) Bales, R. C.; Newkirk, D. D.; Hayward, S. B. *J. Am. Water Works Assoc.* **1984**, *76*, 66-74.
 (6) Morel, F. M. M.; Westall, J. C.; Yeasted, J. G. In "Adsorption of Inorganics at Solid-Liquid Interfaces"; Anderson, M. A.; Rubin, A. J., Eds.; Ann Arbor Science: Ann Arbor, MI, 1981; pp 263-294.
 (7) Bales, R. C. Ph.D. Thesis, California Institute of Technology, Pasadena, CA, 1985.
 (8) Dempsey, B. A. Ph.D. Thesis, University of North Carolina, Chapel Hill, NC, 1981.
 (9) Bales, R. C.; Morgan, J. J. *Geochim. Cosmochim. Acta*, in press.
 (10) Parks, G. A. In "Equilibrium Concepts in Natural Water Systems"; Gould, R. F., Ed.; American Chemical Society: Washington, DC, 1967; pp 121-160.
 (11) Pundsack, F. L. *J. Phys. Chem.* **1955**, *59*, 892-895.
 (12) Martinez, E.; Zucker, G. L. *J. Phys. Chem.* **1960**, *64*, 924-926.

(13) Ahmed, S. M. In "Adsorption from Aqueous Solutions"; Tewari, P. H., Ed.; Plenum, Press: New York, 1981; pp 213-226.
 (14) Iler, R. K. "The Chemistry of Silica"; Wiley: New York, 1979.
 (15) Martel, A. E.; Smith, R. M. "Critical Stability Constants: Other Organic Ligands"; Plenum Press: New York, 1976; Vol. 3.
 (16) Hohl, H.; Stumm, W. *J. Colloid Interface Sci.* **1976**, *55*, 281-288.
 (17) Sigg, L.; Stumm, W. *Colloids Surf.* **1981**, *2*, 101-117.
 (18) Schindler, P. W. In "Adsorption of Inorganics at Solid-Liquid Interfaces"; Anderson, M. A.; Rubin, A. J., Eds.; Ann Arbor Science: Ann Arbor, MI, 1981; pp 1-48.
 (19) Mihailovic, M. L.; Cekovic, Z. In "The Chemistry of the Hydroxyl Group"; Pati, S., Ed.; Interscience: London, 1971; Part 1, pp 505-592.
 (20) Musso, H. In "Oxidative Coupling of Phenols"; Taylor, W. I.; Battersby, A. R., Eds.; Marcel Dekker: New York, 1967; pp 1-94.
 (21) Stone, A. T. Ph.D. Thesis, California Institute of Technology, Pasadena, CA, 1983.
 (22) Parfitt, R. L.; Farmer, V. C.; Russell, J. D. *J. Soil Sci.* **1977**, *28*, 29-39.
 (23) Parfitt, R. L.; Fraser, A. R.; Russell, J. D.; Farmer, V. C. *J. Soil Sci.* **1977**, *28*, 40-47.
 (24) Chowdhury, S.; Kitchener, J. A. *Int. J. of Miner. Process.* **1975**, *2*, 277-285.
 (25) Erkova, L. N.; Skvortsova, T. A.; Lazarea, S. Y.; Grachev, O. I. *Zh. Prikl. Khim. (Leningrad)* **1981**, *59*, 1986-1990.
 (26) Tipping, E.; Cooke, D. *Geochim. Cosmochim. Acta* **1982**, *46*, 75-80.
 (27) Hunter, K. A. *Limnol. Oceanogr.* **1980**, *25*, 807-822.

Received for review November 21, 1984. Accepted June 24, 1985. This research was supported by a grant from the Andrew W. Mellon Foundation to the California Institute of Technology's Environmental Quality Laboratory and by a grant from the Metropolitan Water District of Southern California.

Studies on Microbial and Chemical Conversions of Chlorolignins

Karl-Erik Eriksson,* Marie-Claude Kolar, Pierre O. Ljungquist, and Knut P. Kringstad

Swedish Forest Products Research Laboratory, S-114 86 Stockholm, Sweden

■ High relative molecular mass material (chlorolignins) in spent liquors from the chlorination and alkali extraction stages of the bleaching of softwood kraft pulp were found to be chemically unstable under conditions that may prevail in receiving water systems. The material very slowly decomposed to products that included various chlorinated catechols and guaiacols. A number of bacteria consortia, as well as a white-rot fungus, degraded the catechols and guaiacols, although a proportion were first methylated to the corresponding and more persistent veratrole compounds. Methylation was observed only in cases where a complete mixture of bacteria, or the white-rot fungus alone, was used and appears to be common in nature.

Introduction

In the conventional bleaching of chemical pulp, between 45 and 90 kg of organic material/ton of pulp is dissolved in the bleaching liquors. The dissolved material is chlorinated and, in the case of softwood kraft pulp, contains 4-5 kg of organically bound chlorine/ton of pulp (1). A major part of the material is of high relative molecular mass. A better understanding of the chemical and microbiological transformations of such material (chloro-

lignins), and of the nature and properties of the metabolites formed, is desirable, since considerable quantities of spent bleach liquors are continuously released into rivers, lakes, and oceans (1). Recently, Neilson et al. (2) found that incubation of spent bleach liquor material with monocultures of various bacteria isolated from areas subject to discharge of spent bleach liquors led to the production of metabolites that were seemingly resistant to further transformation. These metabolites, consisting of various chlorinated veratroles, were formed from chlorinated guaiacols as well as from the high relative molecular mass fraction of the material present in spent chlorination (C-stage) and alkali extraction (E-stage) liquors.

In the present investigation, the microbial conversion of chlorolignins was studied by using mixed bacterial cultures obtained from different aerated lagoons receiving wastewaters from forest industries. The investigation was carried out primarily to gain information on the stability of chlorolignins and to determine if toxic, low molecular mass compounds were produced under conditions similar to those prevailing in receiving waters.

Materials and Methods

Spent Bleach Liquors. Spent chlorination (C-stage) liquor was sampled from a pulp mill producing bleached

softwood kraft pulp using a conventional bleaching sequence. At the time of sampling the bleach plant parameters were the following: kappa number of the unbleached pulp 36, charge of chlorine 63 kg of Cl_2 /ton of pulp, pH of spent liquor 2.1, and total effluent volume 78.2 m^3 /ton of pulp. Spent alkali extraction (E-stage) liquor was sampled on another occasion at the same mill. The bleach plant parameters were the following: kappa number of the unbleached pulp 37 (charge of chlorine in C stage 50 kg/ton of pulp), charge of alkali 26 kg of NaOH /ton of pulp, pH of spent liquor 11.2, and total effluent volume 8.3 m^3 /ton of pulp.

Isolation of Material with High Relative Molecular Mass from the Chlorination Liquor (HM-C) and Alkali Extraction (HM-E) Liquors. The spent chlorination liquor (150 L) was adjusted to pH 5 with 2 M NaOH . The liquor was ultrafiltered (Department of Food Technology, University of Lund, Sweden) on a 2.5- m^2 Romocon PM2 membrane with a relative molecular mass cutoff of 2000 daltons, a filtration pressure of 2 bars, and a circulation flow of 6 m^3 /h. After being washed twice with 30 L of distilled water, the concentrated filtrate was readjusted to pH 1.9 with 1 M H_2SO_4 and frozen in 2-L portions until used.

The spent alkali extraction liquor (50 L) was adjusted to pH 7 with 1 M H_2SO_4 and ultrafiltered as described above. After being washed 5 times with 15 L of distilled water, the concentrated filtrate was readjusted to pH 11 with 2 M NaOH and frozen in 2-L portions until used.

Ether Extraction of HM-C and HM-E Solutions. To remove any remaining low relative molecular mass compounds, the concentrated filtrate samples were extracted with ether at 20 °C for 48 h. For the C-stage filtrate, the extraction was carried out directly on the samples obtained from the workup procedure described above. For the E-stage filtrate, the pH was first adjusted to 2 with 1 M H_2SO_4 . The sample was then diluted to the original volume with distilled water and then extracted with ether.

After extraction, both filtrate types (water fractions) were adjusted to pH 6 with 2 M NaOH and residual quantities of ether removed by evaporation at 26 °C. The filtrates were then supplemented with mineral salts (see Media) and filter-sterilized. Although the HM-E fraction had been restored to the original concentration, the HM-C fraction was now concentrated 10-fold. However, the data given in the figures for both HM-C and HM-E are presented in terms of original concentrations.

Organisms. Mixed cultures of bacteria were obtained from aerated lagoons from three different paper mills in Sweden (FR, KM, F2).

From the mixed bacterial culture FR, five different bacterial types were isolated and identified by the National Bacteriological Laboratory, Solna, Sweden, as follows: FR 1, *Pseudomonas putida*; FR 2, group II L-1 (similar to *Pseudomonas*); FR 3, *Enterobacter* species; FR 4, group II K-1 (similar to *Pseudomonas*); FR 5, *Pseudomonas stutzeri*.

The white-rot fungus *Sporotrichum pulverulentum* Nov. (ATCC 32629) (SP) was also used in the microbial degradation experiments.

Media

Bacteria. To 1 L of the respective filtrates (HM-C and HM-E) the following salts were added: 7 g of K_2HPO_4 , 2 g of KH_2PO_4 , 0.5 g of sodium citrate trihydrate, 0.1 g of $\text{MgSO}_4 \cdot 7\text{H}_2\text{O}$, 1 g of $(\text{NH}_4)_2\text{SO}_4$, and 1 mg of FeCl_3 .

***Sporotrichum pulverulentum*.** KA-78 medium (3) was used. Bacto-Penassay Broth (Difco Manual) was used for plate counts.

Cultivation Techniques. (1) **Bacteria.** A total of 150 mL of the respective media was distributed separately into 250-mL Erlenmeyer flasks and inoculated with the bacterial cultures to give an initial concentration of approximately 10^6 cells/mL. The bacterial treatment was carried out in darkness at 28 °C on a rotary shaker (150 rpm, rotation diameter 40 mm). Sterile media kept under the same conditions as the inoculated media served as controls.

The numbers of surviving bacteria were determined by the plate count method. Spread plates (four replicates) were incubated for 5 days at 25 °C.

(2) ***S. pulverulentum*.** A total of 50 mL of the E-stage medium was distributed in 250-mL Erlenmeyer flasks, inoculated with 2×10^6 fungal spores/mL of culture solution, and incubated without agitation at 28 °C. The culture solution was readjusted to pH 4.2 after 2 days. To avoid contamination in the uninoculated control flasks, HgCl_2 was added at a concentration of 250 ppm.

Storage under Sterile Conditions. Samples of sterile media (pH 7.2) were maintained at 5, 12, 20, and 28 °C, and the sterility was controlled at various periods of time.

Chemical Analysis. (1) **Chlorinated Phenols, Guaiacols, and Catechols** (4). A total of 5 mL of culture suspension was adjusted to pH 6 and mixed with 5 mL of 0.1 M K_2CO_3 and 0.1 mL of ethanol containing 2,6-dibromophenol (internal standard) in a 15-mL test tube fitted with a Teflon-coated screwcap. Acetic anhydride (0.2 mL) was added and the mixture shaken thoroughly for 2 min. After 1.5 mL of distilled *n*-hexane was added, the mixture was shaken for an additional 1 min. To improve the phase separation, test tubes were centrifuged at 5000 rpm for 10 min. The hexane phase was washed with 10 mL of 0.1 M K_2CO_3 , centrifuged for 5 min, transferred to 2-mL well-sealed vials, and immediately analyzed by GC.

(2) **Chlorinated Veratroles.** To 5 mL of the culture suspension, adjusted to pH 6, was added 5 mL of 0.1 M K_2CO_3 and 1.5 mL of *n*-hexane. After the suspension was thoroughly shaken, the hexane phase was transferred to 2-mL vials and analyzed immediately by GC.

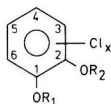
(3) **Gas Chromatography.** A Carlo Erba Fractovap 4100 gas chromatograph equipped with an electron capture detector (^{63}Ni) coupled to a Hewlett-Packard 3390 integrator was used for sample analysis. A DB-1 fused silica column (20 mm \times 30 m) from J&W Scientific, Inc., was used with He as carrier gas (1 mL/min) and with a split ratio of 1:50. The column temperature was maintained at 180 °C, the injector at 250 °C, and the detector at 320 °C. Detected chlorinated compounds were quantified by using response factors obtained from reference substances and related to 2,6-dibromophenol as internal standard. Response factors, which were controlled repeatedly throughout the complete program of experiments, and retention times are presented in Table I. Values were subject to a standard deviation of 3% and a detection limit for the original liquors of 10 ng/L.

(4) **GC-MS.** Chlorinated compounds were identified by using a Carlo Erba (Fractovap MOD 2900) gas chromatograph-Finnigan mass spectrometer (3200F) with an on-line computer system (6000). Mass spectra were run in electron ionization (EI) mode with 70 eV electrons. The injector temperature was 300 °C, transfer-line temperature 320 °C, and the ion source temperature 80 °C. Identification was based on matching spectra with authentic compounds.

(5) **^{13}C NMR.** A varian (CFT-20) 20 MHz was used to verify the structure of 4,5,6-trichloroguaiacol. Chemical shifts (in ppm) relative to trimethylsilane were the fol-

Table I. Gas Chromatographic Retention and Response Factors of Chlorinated Phenols, Guaiacols, Catechols, and Veratroles

compounds	relative retention time	response factor
2,4-dichlorophenol acetate	0.76	12.2
4-monochloroveratrole	0.80	29.2
2,4,6-trichlorophenol acetate	0.90	3.7
2,6-dibromphenol acetate (i.s.)	1.00	1.0
4,5-dichloroveratrole (VII)	1.00	16.7
4,5-dichloroguaiacol acetate (III)	1.21	14.1
3,4,5-trichloroveratrole (VIII)	1.37	1.8
tetrachlorophenol acetate	1.38	2.5
3,4,5-trichloroguaiacol acetate (IV)	1.68	2.2
tetrachloroveratrole (IX)	1.71	0.9
4,5,6-trichloroguaiacol acetate (V)	1.80	2.9
3,4,5-trichlorocatechol acetate (I)	2.23	2.7
pentachlorophenol acetate	2.27	1.2
tetrachloroguaiacol acetate (VI)	2.43	1.4
tetrachlorocatechol acetate (II)	3.22	1.8



- I $R_1 = R_2 = H$, $x = 3$ (3,4,5 pos.)
- II $R_1 = R_2 = H$, $x = 4$
- III $R_1 = H$, $R_2 = CH_3$, $x = 2$ (4,5 pos.)
- IV $R_1 = H$, $R_2 = CH_3$, $x = 3$ (3,4,5 pos.)
- V $R_1 = H$, $R_2 = CH_3$, $x = 3$ (4,5,6 pos.)
- VI $R_1 = H$, $R_2 = CH_3$, $x = 4$
- VII $R_1 = CH_3$, $R_2 = CH_3$, $x = 2$ (4,5 pos.)
- VIII $R_1 = CH_3$, $R_2 = CH_3$, $x = 3$ (3,4,5 pos.)
- IX $R_1 = CH_3$, $R_2 = CH_3$, $x = 4$

Figure 1. Chlorinated catechols, guaiacols, and veratroles studied.

lowing: ^{13}C NMR ($CDCl_3$) 20.2 (CH_3 in acetate), 56.6 (OCH_3), 112.2 (C2), 123.6 (C5), 128.6 (C6), 134.8 (C1), 151.0 (C3), and 167.4 (C= in acetate).

(6) **Reference Compounds.** Reference compounds not available commercially were kindly provided by Alasdair Neilson, The Swedish Environmental Research Institute, and by Krister Lindström and Lars M. Strömberg, The Swedish Forest Products Research Laboratory.

Results and Discussion

Chemical Transformations in the High Relative Molecular Mass Materials (HM). To determine the chemical stabilities of the materials, sterile solutions of HM-C and HM-E (pH 7.2) were stored at four different temperatures. Aliquots were aseptically withdrawn at intervals and analyzed for the chlorinated guaiacols and catechols most commonly occurring in spent bleach liquors as listed in Figure 1. Results for HM-E are shown in Figure 2. (Almost identical results were obtained for HM-C.)

It is clear that neither HM-C nor HM-E is stable under the conditions described. In both systems there is a continuous formation of various chlorinated guaiacols at measurable rates even at 5 °C. 3,4,5-Trichloroguaiacol (IV) was the dominating guaiacol formed in HM-C samples. In HM-E solutions, 4,5-dichloroguaiacol (III) was most evident although high concentrations of 3,4,5- and 4,5,6-trichloroguaiacols (IV and V) were also detected. In the case of chlorinated catechols both 3,4,5-trichloro- and tetrachlorocatechol (I and II) were present in both starting

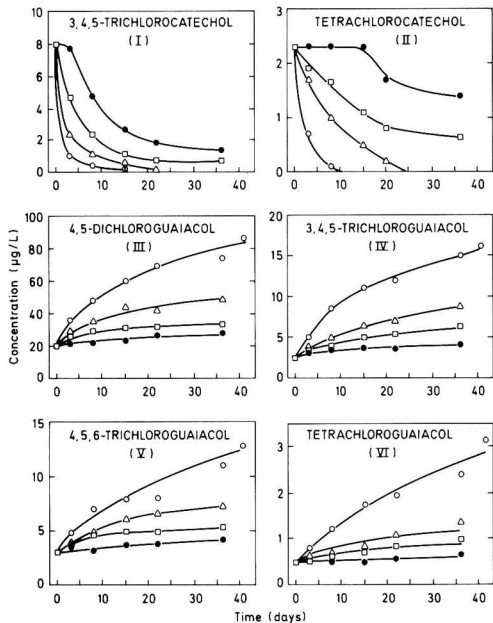


Figure 2. Formation and elimination of various chlorinated guaiacols and catechols during storage, under sterile conditions, of a solution of high relative molecular mass material from spent alkali extraction liquor (HM-E) from bleaching of softwood kraft pulp. pH 7.2. Temperature: 28 (O), 20 (Δ), 12 (□), and 5 °C (●).

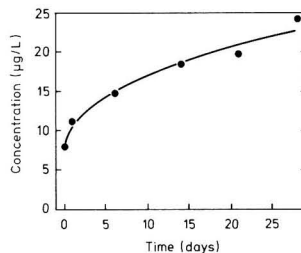


Figure 3. Formation of 3,4,5-trichlorocatechol (I) during storage, under sterile conditions, of a solution of high relative molecular mass material from spent alkali extraction liquor (HM-E) from the bleaching of softwood kraft pulp. pH 4.2. Temperature 28 °C.

solutions, possibly due to incomplete separation during ultrafiltration and ether extraction of the spent liquors. However, upon storage, the concentrations of these catechols decreased rapidly in both solutions to low levels particularly at the higher storage temperatures. This may have resulted from secondary reactions in which any chlorinated catechols formed rapidly underwent further transformations, e.g., oxidation to quinonoid and/or other products, thus escaping detection. This view is supported by a much reduced rate of oxidation of catechols observed in solutions of HM-E maintained at pH 4.2. As shown in Figure 3, the amount of 3,4,5-trichlorocatechol (I) in the solution increased continuously during storage under these conditions. Taken together, these results show that the HM material in spent chlorination and alkali-extraction liquors from the bleaching of softwood kraft pulp is chemically unstable. The material may, under conditions similar to those prevailing in receiving waters, transform to yield decomposition products that include chlorinated guaiacols and catechols. At present, the mechanisms un-

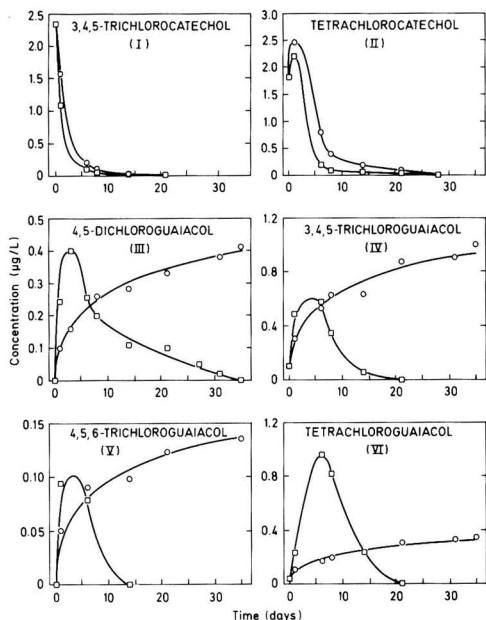


Figure 4. Formation and elimination of various chlorinated guaiacols and catechols in a solution of high relative molecular mass material from chlorination liquor (HM-C) from the bleaching of softwood kraft pulp during storage under sterile conditions (O) or in the presence of a mixed bacterial culture isolated from a paper mill aerated lagoon (□). pH 7.2. Temperature 28 °C. Shaking conditions.

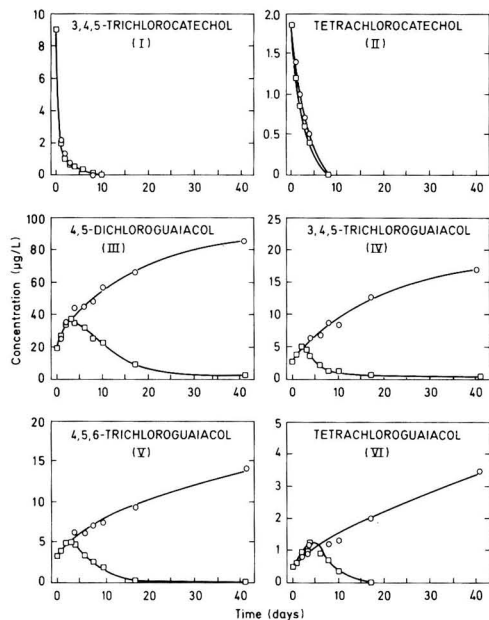


Figure 5. Formation and elimination of various chlorinated guaiacols and catechols in a solution of high relative molecular mass material from spent alkali extraction liquor (HM-E), from the bleaching of softwood kraft pulp during storage under sterile conditions (O) or in the presence of a mixed bacterial culture isolated from a paper mill aerated lagoon (□). pH 7.2. Temperature 28 °C. Shaking conditions.

derlying the decomposition reactions are unknown.

Available data allow only a rough estimate of the yields of chlorinated guaiacols and catechols formed. The TOC contents of the HM-C and HM-E solutions at the start of the storage experiments were 40 and 700 mg/L, respectively. These levels correspond to starting concentrations of HM-C and HM-E in the order of 100 and 1500 mg/L, respectively (5, 6). According to these figures, the combined yields of the chlorinated guaiacols and catechols formed in both types of solutions amounted to only 0.01% or less of the total weight of starting material. Thus, the rate of decomposition is rather low. The shapes of the various curves in Figures 3 and 4 indicate that the formation of chlorinated guaiacols and catechols would have continued if the time of storage had been extended beyond the limits of the present investigation. However, recent studies have clearly demonstrated that both HM-C and HM-E are materials of extreme complexity (5-10), making it impossible to predict with any accuracy the extent of continued decomposition.

Bacterial Transformation of the HM Materials. Solutions of HM-C and HM-E were inoculated with a mixed bacteria culture (FR) and maintained under the conditions described above. The individual bacteria isolated from FR consortia of bacteria were identified as *Pseudomonas* and *Enterobacters*. At least the first types of bacteria are also common in lakes and marine environments (11, 12). Aliquots were aseptically withdrawn at regular intervals and analyzed for chlorinated guaiacols and catechols.

Results obtained are shown in Figures 4 and 5, respectively. For comparison, the results obtained after storage under sterile conditions are also included. Figure 4 shows that, in the case of HM-C, the levels of 4,5-dichloro-, 3,4,5-trichloro-, 4,5,6-trichloro-, and tetrachloroguaiacol

(III-VI) were markedly higher during the first 5 days of incubation when the bacterial consortium was present. In the case of tetrachloroguaiacol, the levels were very much higher. However, after approximately 5 days (VI), levels of chlorinated guaiacols began to decrease and reach very low levels after a few days of further incubation. The fate of the two chlorinated catechols followed a somewhat different pattern. Here, there was no intermediate increase in concentrations. Instead, the rate of disappearance of both compounds was enhanced.

No intermediate increase in the concentration of the chlorinated compounds studied was detected in HM-E samples incubated with the mixed bacterial culture (Figure 5). However, the rapid removal of the compounds in the presence of the bacterial consortium was similar to the response observed for the HM-C solution.

The effects of incubating the HM materials with the mixed bacterial culture raise questions of both environmental and biochemical interest. For example, to what degree is the removal of the chlorinated guaiacols and catechols the result of actual degradation by the bacteria or conversion to more persistent veratrole type compounds as observed recently by Neilson et al. (2). Is the mixed bacterial culture able to attack the polymeric chlorolignins and to degrade these to low molecular mass compounds, including chlorinated guaiacols and catechols, which are subsequently degraded and/or methylated? Previous investigations have shown that, in general, bacteria are unable to propagate efficiently on high relative molecular mass lignins (13-15) but will easily degrade a number of dimeric lignin model compounds (16).

Some evidence for the conversion of chlorinated guaiacols and catechols to the respective methylated products by the mixed bacterial culture is seen on closer scrutiny of Figure 4. Thus, the observed increase in the levels of

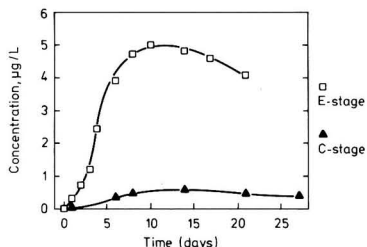


Figure 6. Formation and elimination of 3,4,5-trichloroveratrole in solutions of high relative molecular mass material from spent chlorination (HM-C) (▲) and alkali extraction liquor (HM-E) (□) from the bleaching of softwood kraft pulp during storage in the presence of a mixed bacterial culture isolated from a paper mill aerated lagoon. pH 7.2. Temperature 28 °C. Shaking conditions.

4,5-dichloro-, 3,4,5-trichloro-, 4,5,6-trichloro-, and tetrachloroguaiacol (III–VI) during the first days of incubation is very likely due to the methylation of one phenolic hydroxyl group in the corresponding chlorinated catechols. For example, the increase in the concentration of tetrachloroguaiacol (VI) (at the maximum level) is of the same order of magnitude as the observed decrease in the level of tetrachlorocatechol (II). A similar relationship exists between the increase in the combined concentrations of 3,4,5-trichloro- and 4,5,6-trichloroguaiacol (IV and V) and the disappearance of 3,4,5-trichlorocatechol (I). In support of this postulate, it was furthermore observed that when 3,4,5-trichlorocatechol was added to HM-E solution or treated as pure compound, a corresponding increase in the levels of 3,4,5-trichloroguaiacol (IV) and 4,5,6-trichloroguaiacol (V) was obtained.

As already stated, it was not possible to detect an intermediate increase in the concentrations of the various chlorinated guaiacols when the HM-E solution was incubated with the mixed bacterial culture. This may be due to the quite different relative distribution of chlorinated catechols and guaiacols in the HM-E solution as compared to the HM-C solution.

The importance of bacterial methylation was further supported by analyzing the inoculated liquors for chlorinated veratroles. When levels of 4,5-dichloro-, 3,4,5-trichloro-, and tetrachloroveratrole (VII–IX) were determined, the trisubstituted compound was found to be by far the most dominant (Figure 6). In both solutions, the veratrole was already detectable after about 1 day. Concentrations increased to reach maxima after about 8–10 days (corresponding to the logarithmic phase of bacterial growth) followed by a subsequent slow decrease. 3,4,5-Trichloroveratrole (VIII) may result from the methylation of 3,4,5- as well as of 4,5,6-trichloroguaiacol (IV and V), both of which are present in the solutions. To determine the relative contribution of each guaiacol compound, 3,4,5-trichloroguaiacol (IV) or 4,5,6-trichloroguaiacol (V) was added to a solution of HM-E inoculated with the mixed bacterial culture. It is clear from Figure 7 that the major part of the 3,4,5-trichloroveratrole (VIII) is formed by methylation of 4,5,6-trichloroguaiacol (V). This confirms the observations made by Neilson et al. (2) during an investigation involving two strains of bacteria provisionally assigned to the genus *Arthrobacter*.

As far as the extent of methylation is concerned, a comparison of Figures 4–6 shows that in the case of the HM-E solution the quantity of 3,4,5-trichloroveratrole (VIII) formed (at the maximum level) corresponds to about 30% of the sum of the quantities of 3,4,5-trichloro- and 4,5,6-trichloroguaiacols (IV and V) removed. An estimate

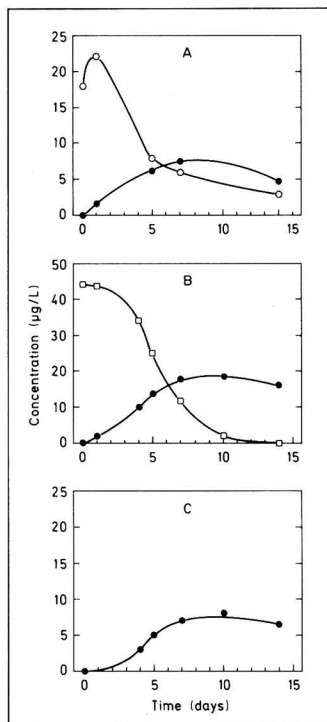


Figure 7. Formation of 3,4,5-trichloroveratrole (VIII) (O) in a solution of high relative molecular mass material from spent alkali extraction liquor (HM-E) from the bleaching of softwood kraft pulp during storage in the presence of a mixed bacterial culture isolated from a paper mill aerated lagoon. (A) With the addition of 17 µg/L 3,4,5-trichloroguaiacol (IV) (O). (B) With the addition of 42 µg/L 4,5,6-trichloroguaiacol (V) (□). (C) Without additions. pH 7.2. Temperature 28 °C. Shaking conditions.

based exclusively upon the removal of 4,5,6-trichloroguaiacol (V) results in a “methylation yield” of more than 80%. Parallel estimates involving the HM-C solution give similar results.

Taken together, these data therefore show that the mixed bacterial culture is able to remove chlorinated catechols and guaiacols from aqueous solutions, and to a large extent, this is a result of degradation of these chlorinated compounds. However, a proportion is transformed to more persistent, chlorinated veratrole-type compounds. It is not possible from these results to draw any definite conclusions relating to the ability of the bacterial culture to depolymerize HM-C and HM-E. However, the very similar levels of chlorinated catechols, guaiacols, and veratroles observed in the various solutions suggest that, under the conditions and time intervals used here, the culture does not cause depolymerization.

Effects of Individual Microorganisms. Five different strains were isolated and identified from the mixed bacterial culture (FR). Four strains were assigned to the genus *Pseudomonas* and one to the genus *Enterobacter*. These strains were used separately or in various combinations to inoculate the HM-E solution. In each case, the number of viable cells in the inoculum was equal to that in the mixed culture. Over a 20-day period under conditions identical with those used for the mixed culture, aliquots were taken and analyzed for chlorinated catechols, guaiacols, and 3,4,5-trichloroveratrole (VIII). None of the pure strains were found to remove chlorinated guaiacols

or produce 3,4,5-trichloroveratrole (VIII). The same was true for all combinations of the strains except for one comprising four strains (FR 2, 3, 4, and 5) which produced approximately one-fifth of the amount of 3,4,5-trichloroveratrole (VIII) produced by the original mixed culture. Recombination of all five strains was as effective as the original culture. Earlier Neilson et al. (2) found that individual strains of bacteria obtained from sediments in areas subject to discharge of spent bleach liquors were capable of methylation and removal of chlorinated guaiacols. The reason for the different behavior of the bacteria used in the present study is not known but metabolically complete systems are reported to exhibit complementary metabolism (17).

To test the general validity of our conclusions concerning the effects of the mixed bacterial culture FR, a solution of HM-E was treated with two additional mixed bacterial cultures obtained from other aerated lagoons receiving effluents from forest industries. A treatment using the white-rot fungus *Sporotrichum pulverulentum*, an efficient and well-characterized degrader of lignocellulosic material in general (18), was also included. However, the optimal conditions for lignin degradation by this fungus (pH 4.2-4.5) are such that the fungus is unlikely to be of any great importance in receiving water systems. Experiments show that the mixed bacterial cultures as well as the fungus (at pH 4.2) produced quite similar quantities of 3,4,5-trichloroveratrole (VIII) from the HM-E solution. This applied even though the composition of the different bacterial mixtures varied considerably in terms of individual strains. The rates at which the chlorinated guaiacols disappeared were also similar in all cases. Taken together with the results recently obtained by Neilson et al. (2), these data indicate that the observed microbial transformations (methylations) of the chlorinated phenolic compounds are common in nature and may very well occur in receiving water systems. Research to establish the extent of methylation in receiving water systems should, therefore, be given high priority.

Acknowledgments

The research presented in this paper is part of a joint Nordic Research Project on "Reduction of Environmental Impact of Bleach Plants Effluents". Thanks are due to

John Buswell, Paisley College of Technology, Scotland, for valuable suggestions for the improvement of the manuscript.

Registry No. I, 56961-20-7; II, 1198-55-6; III, 2460-49-3; IV, 57057-83-7; V, 2668-24-8; VI, 2539-17-5; VII, 2772-46-5; VIII, 16766-29-3; IX, 944-61-6; chlorolignin, 8068-02-8.

Literature Cited

- (1) Kringstad, K. P.; Lindström, K. *Environ. Sci. Technol.* **1984**, *18*, 236A.
- (2) Neilson, A. H.; Allard, A.-S.; Hynning, P.-Å.; Remberger, M.; Landner, L. *Appl. Environ. Microbiol.* **1983**, *45*, 774.
- (3) Ander, P.; Hatakka, A.; Eriksson, K.-E. *Arch. Microbiol.* **1980**, *125*, 189.
- (4) Voss, R. H.; Wearing, J. F.; Wong, A. In "Advances in the Identification and Analysis of Organic Pollutants in Water"; Keith, L. H., Ed.; Ann Arbor Science: Ann Arbor, MI, 1981; Vol. 2, p 1059.
- (5) Österberg, F.; Lindström, K. Swedish Forest Products Research Laboratory, personal communication.
- (6) Lindström, K.; Österberg, F. *Holzforchung* **1984**, *38*, 201.
- (7) Erickson, N.; Dence, C. W. *Sven. Papperstidn.* **1976**, *80*, 201.
- (8) Shimada, K. *Mokuzai Gakkaishi* **1977**, *23*, 243.
- (9) Hardell, H.-L.; de Sousa, F. *Sven. Papperstidn.* **1977**, *80*, 110.
- (10) Hardell, H.-L.; de Sousa, F. *Sven. Papperstidn.* **1977**, *80*, 201.
- (11) Baumann, L.; Baumann, P.; Mandel, M.; Allen, R. D. *J. Bacteriol.* **1972**, *11*, 402.
- (12) Lee, I. V.; Gibson, D. M.; Shewan, I. M. *J. Gen. Microbiol.* **1977**, *98*, 439.
- (13) Odier, E.; Janin, G. *Appl. Environ. Microbiol.* **1981**, *41*, 337.
- (14) Kirk, T. K. In "Trends in the Biology of Fermentation for Fuels and Chemicals"; Hollaender, A., Ed.; Plenum Press: New York, 1981; p 131.
- (15) Zeikus, J. G. *Adv. Microb. Ecol.* **1981**, *5*, 211.
- (16) Pellinen, J. G.; Väisänen, E.; Salkinoja-Salonen, M.; Brunow, G. *Ekman-Days 1983, Int. Symp. Wood Pulping Chem.* **1983**, *4*, 174.
- (17) de la Torre, M.; Campillo, G. G. *Appl. Microbiol. Biotechnol.* **1984**, *19*, 430.
- (18) Eriksson, K.-E. *Pure Appl. Chem.* **1981**, *53*, 33.

Received for review November 26, 1984. Revised manuscript received May 23, 1985. Accepted July 16, 1985. Financial support was provided by the Nordic Fund for Technology and Industrial Development.

Evaluation of the Perfluorocarbon Tracer Technique for Determining Infiltration Rates in Residences

Brian P. Leaderer*

The John B. Pierce Foundation Laboratory and Department of Epidemiology and Public Health, Yale University School of Medicine, New Haven, Connecticut 06519

Luc Schaap

Department of Architecture and Building Technology, Eindhoven University of Technology, Eindhoven, The Netherlands

Russell N. Dietz

Department of Applied Science, Brookhaven National Laboratory, Upton, New York 11973

■ A simple passive perfluorocarbon tracer (PFT) technique, for determining air infiltration rates into homes and buildings, was evaluated in a well-defined environmental chamber under experimental conditions of (1) constant temperature and ventilation rate, (2) constant temperature but variable ventilation rate, and (3) variable temperature but constant ventilation rate. Two PFT sources of known emission rate and temperature dependence produced chamber concentrations of 100–300 nL/m³ (parts per trillion). The average relative standard deviation for sampling and analysis of 16 paired samplers in experiment 1 was ±1.9 ± 1.0%, and there was negligible consequence of sampler orientation. For a 3-fold variation in ventilation rates (experiment 2), the passive samplers accurately measured the average chamber tracer concentration, but the PFT-determined ventilation rate had a 10% negative bias. Temperature cycling differences of as much as 8 °C were accommodated to provide essentially no bias in the PFT-determined ventilation rate. The PFT technique is applicable to the expected range of conditions in homes and buildings.

Introduction

Efforts to reduce energy consumption in residences have led to the construction of energy efficient homes and the undertaking of residential weatherization programs which, in turn, have raised concerns about the quality of indoor air. The reduction of air infiltration rates in residences is an effective way to conserve energy by reducing heating and air conditioning demands. Reductions in infiltration rates, however, could result in the occurrence of air contaminants indoors at concentrations that may result in human exposures in excess of health- and comfort-related standards. The determination of infiltration rates in residences is necessary in order to assess the effectiveness of weatherization programs and to develop and evaluate models for infiltration and assessment of indoor air contaminant levels. This paper presents an evaluation of a new tracer system for determining infiltration rates.

The only direct measure of air infiltration in residences under normal occupancy conditions is by the tracer gas technique, which is applied to assessing infiltration rates in two ways. The first method is generally referred to as the tracer gas decay method (1, 2) and the second is referred to as the steady-state tracer gas method (3–5).

Considering a residence as a well-mixed single chamber and letting C = concentration of tracer in chamber (nL/m³), V = volume of chamber (m³), S' = source strength of tracer (nL/h), $S = S'/V$ (nL/hm³), R_E = rate of air exfiltration or leakage (m³/h), and $n = R_E/V$ or number of air changes per hour (ach) (h⁻¹), a mass balance around the chamber gives

$$dc/dt = S - nC \quad (1)$$

Integrating from C_0 at $t = 0$ to C_t , the tracer concentration at time t , gives

$$C_t = \frac{S}{n} + \left(C_0 - \frac{S}{n} \right) e^{-nt} \quad (2)$$

For the tracer decay approach, in which a small amount of tracer is well-mixed into the chamber and the source is turned off ($S = 0$), eq 2 becomes

$$C_t = C_0 e^{-nt} \quad (3)$$

and hence

$$\ln C_t = \ln C_0 - nt \quad (4)$$

When the natural logarithm of the tracer concentration vs. time is plotted, the air changes per unit time, n , is obtained as the negative of the slope as shown by eq 4. In practice, the tracer gas concentration in the space is measured as a function of time via either continuous monitors or a series of grab samples transported to a laboratory for subsequent analysis. This method has employed a number of gases as tracers (SF₆, CH₄, N₂O, CO₂, CO, C₂H₆, He, etc.) which have been evaluated in a number of studies (6–8). The tracer gas decay method provides a short-term measurement of air exfiltration rates, usually on the order of a few hours.

The steady-state tracer gas method uses SF₆ or a perfluorocarbon tracer gas. The tracer gas is emitted into the space at a constant rate either via a mechanical or microprocessor system (3, 5, 9) or via a liquid permeation source (4). The tracer gas is allowed to come to steady-state conditions in the space and then is sampled in the space either continuously, periodically with a sequential sampling system into a collection media such as syringes or bags, or passively using adsorption tube samplers. The latter two collection methods require subsequent laboratory analysis. At steady state ($dC/dt = 0$), eq 1 becomes

$$n = \frac{S}{C} = \frac{S'}{VC} \quad (5)$$

The number of air changes per hour, n , is simply the known tracer source rate divided by the volume of the house and the measured steady-state average tracer concentration.

One steady-state tracer gas method for assessing air-exchange rates, developed at Brookhaven National Laboratory and called the Brookhaven National Laboratory Air Infiltration Measurement System (BNL/AIMS) (10), is being extensively employed in large field studies of indoor air quality and impact of weatherization (11–14). The BNL/AIMS method consists of miniature perfluorocarbon tracer (PFT) sources and miniature passive capillary ad-

sorption tube samplers (CATS). The sources and samplers are about the size of a cigarette. The PFT sources use one of four perfluorocarbon compounds: perfluorodimethylcyclohexane (PDCH); perfluoromethylcyclohexane (PMCH); perfluoromethylcyclopentane (PMCP); perfluorodimethylcyclobutane (PDCB). Vapors from the perfluorocarbon liquid in the PFT sources permeate through an elastomeric plug crimped into one end. The PFT sources emit the tracer gas at a constant rate for 2-7 years. The emission rate, however, does vary with temperature (15). The emission rates are determined gravimetrically.

The CATS device is a passive sampler utilizing about 50 mg of type XE-347 Ambersorb as the collection media. After sampling, the collected tracer gas is thermally desorbed into a gas chromatograph for determination of the PFT concentration. One type of PFT source can be used for a single-compartment model, while up to a four-compartment model (air-exchange rates between the space and outdoors as well as between compartments or rooms in the space) can be evaluated by using four different types of PFT sources, one type per compartment. This method is typically used to obtain integrated air-exchange rates over periods of 1 day to several weeks or months. Use of a programmable sampler with sampling pump will allow for multiple short-term (<1 h) sample collections for determinations of air exchange rates on a short-term basis. The small size of the sources and samplers, their passive nature (e.g., no pumps), wide range of sampling times (from hours to weeks or months), ease of analysis, and relative low cost have made the BNL/AIMS ideally suited to large-scale field studies of infiltration rates in residences and large buildings (16).

This paper presents the results of experiments conducted in an environmental chamber to evaluate the BNL/AIMS system for determining air-exchange rates. The accuracy of the BNL/AIMS system by comparison with CO₂ tracer decay, the impact of orientation of the CATS samplers with respect to flow direction, and the impact of variations in infiltration rate and temperature are evaluated under conditions of near ideal air mixing in the chamber.

Methods

Environmental Chamber. Figure 1 presents a schematic view of the environmental chamber with associated control equipment. The box on the right, actually a cross-sectional schematic of the 34-m³ chamber itself, displays within it the range of operating conditions. All ductwork and internal surfaces were constructed of aluminum. The floor, 11 m², consisted of uniformly perforated aluminum sheets overlaid with an aluminum grating. The perforated floor served as an air diffuser. Air entered the chamber via a plenum beneath the floor and flowed upward through the perforations to the ceiling. The design allowed a volume flow of up to 2000 cfm (1 m³/s) with low linear velocity and very rapid mixing. The volume flow (recirculation rate) could be varied from 400 to 2000 cfm (0.2-1.0 m³/s) which corresponded to 20-100 air changes per hour (ach) and a vertical velocity of 0.02-0.09 m/s. A variable percentage of the recirculated air could comprise fresh ventilation air. The fresh air brought into the chamber could be varied from 0 to 400 cfm (0-0.2 m³/s) which corresponded to 0-20 ach of fresh air. The chamber possessed excellent temperature and humidity control. Air cleaning could be accomplished by diverting the recirculated air through an electronic air cleaner or granular filter media. At no time during these experiments were the air cleaning capabilities of the chamber utilized.

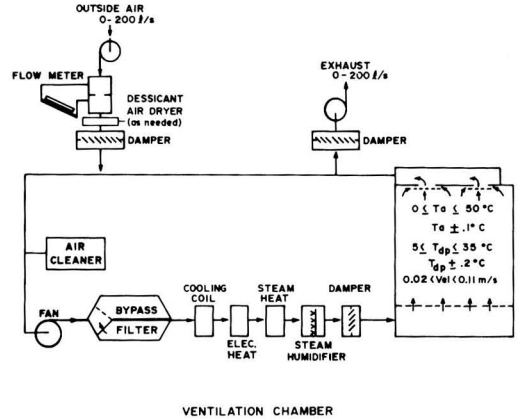


Figure 1. Schematic view of environmental chamber and control equipment. Arrows in box at right portray the flow of air from the plenum beneath the floor to the return ducts in the ceiling.

BNL/AIMS. The PFT sources and CATS were supplied by the Department of Applied Science, Brookhaven National Laboratory (BNL). Analysis of the passive samplers and emission rate determinations of the PFT sources were done by BNL. In this set of experiments, two perfluorodimethylcyclobutane (PDCB) PFT sources were used. The emission rates of these PFT sources were determined gravimetrically at a stabilized temperature of 25 °C. The PFT sources were shipped via mail to the chamber facility laboratory where they were stored at 23 °C for over 2 weeks prior to their use. The average PFT source strengths were adjusted to the 23 °C base temperature at which the experiments took place according to the following formula (15):

$$S'_t = S'_{25} e^{-4000(1/T-1/298)} \quad (6)$$

where S'_t = PFT source strength at the average base temperature (t , °C) in nL/h, S'_{25} = PFT source strength at 25 °C (determined gravimetrically as 5688 ± 120 nL/h), and T = average base temperature (t , °C) in kelvin at which the PFT source is used. For short-term (less than 48 h) temperature changes, the exponential constant was found to be half that for long-term (greater than 10 days) changes (15). Thus, when the temperature of the chamber was varied for short-term changes

$$S'_t = S'_{23} e^{-2000(1/T-1/296)} \quad (7)$$

where S'_t = PFT source strength at chamber temperatures in nL/h, S'_{23} = PFT source strength at 23 °C base temperature (from eq 6) in nL/h, and T = chamber temperature in K.

The CATS were delivered to this laboratory by hand and stored in a separate building prior to and after use in order to minimize contamination. Two unopened but deployed CATS were included as controls in this set of experiments. After use, the CATS were returned to BNL for analysis by gas chromatography. BNL was blind as to the placement of the passive samplers and chamber conditions for each experiment. A detailed description of the BNL/AIMS method can be found elsewhere (10, 15).

CO₂ Decays. Ventilation rates (n) throughout these experiments were determined by the tracer gas decay method using CO₂ as the tracer gas. At regular intervals during each experiment CO₂ was injected into the chamber until the concentration in the chamber reached 1%. The gas was then shut off and the decay of CO₂ recorded

Table I. Average Measured PCB Concentrations for Paired CATS vs. Sampler Orientation and Chamber Location
 [Experiment 1: $av\ ach_{CO_2} = 0.601 \pm 0.011\ h^{-1}$, $S = 152.8 \pm 4.3\ nL/(h \cdot m^3)$ at 23 °C]

passive sampler orientation to flow	average PCB concn of paired samplers \pm SD, ^a nL/m ³ (%), ^b at chamber location				CATS orientation average
	A	B	C	D	
1 (perpendicular)	246.3 \pm 3.4 (1.4)	243.3 \pm 3.0 (1.2)	237.7 \pm 3.0 (1.2)	244.1 \pm 8.3 (3.4)	242.9 \pm 5.0 (2.1)
2 (away)	231.3 \pm 1.4 (0.6)	240.0 \pm 2.2 (0.9)	235.3 \pm 1.4 (0.6)		235.5 \pm 4.1 (1.7)
3 (into)	244.9 \pm 3.0 (1.2)	237.9 \pm 5.3 (2.2)	234.6 \pm 9.9 (4.2)		241.5 \pm 4.6 (1.9) ^c
4 (shielded)	234.6 \pm 6.2 (2.7)	235.5 \pm 6.0 (2.5)	241.4 \pm 5.6 (2.3)		237.1 \pm 5.7 (2.4)
5 (perpendicular)	241.7 \pm 2.9 (1.2)	244.5 \pm 5.3 (2.2)	246.9 \pm 6.3 (2.6)		244.4 \pm 4.5 (1.9)
average	239.8 \pm 6.8 (2.8)	240.2 \pm 4.9 (2.0)	239.2 \pm 6.6 (2.7) ^c	244.1 \pm 8.3 (3.4)	240.4 \pm 5.7 (2.4) ^{c,d}

^aThe average of 16 paired standard deviations was $4.6 \pm 2.4\ nL/m^3$ ($1.9 \pm 1.0\%$) with a range of 1.4–9.9 (0.6–4.2%) and a median of 5.3 (2.2%). ^bQuantities in parentheses are the percent relative standard deviations. ^cOne concentration excluded from location C (orientation 3) in computation of the overall averages. ^dCalculated overall average PCB concentration was 254.2 ± 12.8 (5.0%).

continuously on a Beckman LB-2 infrared CO₂ analyzer. Background CO₂ levels were also recorded. The CO₂ analyzer was calibrated before and after each experiment with NBS traceable gases. For each decay, background levels were subtracted. The natural logarithms of 11 concentrations per decay (5-min intervals) were plotted vs. time, and a least-squares linear regression was used to obtain the slope and hence ventilation rate (eq 4).

Experiments. Three experiments were conducted to evaluate the BNL/AIMS infiltration measurement method under controlled conditions in the environmental chamber, as outlined in Figure 2. The two PFT sources used throughout all experiments were placed in the center of the chamber 1.9 m above the floor. This ensured that the PCB tracer gas was well mixed in the recirculation loop before exposure to the samplers. Although the PFT sources were stored at 23 °C before use, they were allowed to equilibrate at a temperature of 23 °C for 3 days in the chamber before the experiments began in order to ensure that a steady-state concentration of the PCB tracer gas was achieved in the chamber under the conditions of an air recirculation rate of 60 ach and a fresh air ventilation rate of about 0.6 ach.

(a) Experiment 1. The impact of CATS orientation during sample collection and accuracy of the BNL/AIMS method at a known and constant ventilation rate were evaluated in the first experiment. A constant temperature of 23 °C, an air recirculation rate of 60 ach, and a fresh air rate of about 0.6 ach were maintained throughout the experiment. The CATS samplers were placed on four chairs, equidistantly spaced in the chamber. The five positions of the CATS samplers placed on each chair are shown in Figure 2. The open end (only one end during sampling) was facing up in position 2, down in position 3, and off the back of the chair in position 5. All samples were taken in duplicate. One of the chairs (location D) had CATS in position 1 only, for a total of 32 CATS samples in the chamber. Hour-long CO₂ decays were obtained at six equally spaced times during the course of this 44-h experiment.

(b) Experiment 2. The accuracy of the BNL/AIMS method in measuring the average ventilation rate over a period of time where the ventilation rate was varied in discrete steps was evaluated in this experiment. A constant temperature of 23 °C was maintained throughout the run while the ventilation rate was varied in a series of 11 steps among three levels of about 0.60, 1.29, and 1.64 ach. The chamber was well-mixed (recirculation rate greater than 60 ach) and duplicate CATS samples only for position 1 were obtained on all four chairs (eight CATS samples). A total of twenty 1-h CO₂ decays (one after each new ventilation rate was set and, generally, a duplicate run later)

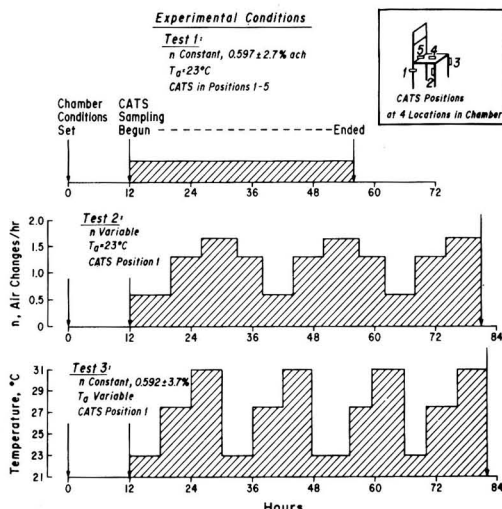


Figure 2. Experimental conditions in the environmental chamber for each of three tests for evaluating the BNL/AIMS method for determining ventilation rates. CO₂ decays performed throughout each of the three experiments served as the basis for comparison.

were obtained for this 69-h experiment.

(c) Experiment 3. The impact of varying temperature on the PFT source emission rate in determining ventilation rates was evaluated in this experiment. After the initial equilibration period at 23 °C, the temperature was cycled among three temperature settings (23, 27, and 31 °C) for a total of 12 steps as shown in Figure 2. The ventilation rate was constant at about 0.6 ach and the recirculation rate at 60 ach during this 72-h experiment. The standard temperature correction factor (eq 6) was applied to the PCB PFT sources in calculating the emission rate at 23 °C and the short-term correction (eq 7) for the 27 and 31 °C rates. Sixteen hour-long CO₂ decays were obtained, one after each temperature change and an occasional repeat. Duplicate CATS samples were obtained in position 1 for all four chairs (eight CATS samples).

Results

Experiment 1. The average measured concentrations, standard deviations, and relative standard deviations of the 16 paired samplers are shown in Table I, arranged according to sampler orientation and location within the chamber. The average of the 16 paired standard deviations was $4.6 \pm 2.4\ nL/m^3$ which, for an overall average concentration of $240.4 \pm 5.7\ nL/m^3$, corresponded to an av-

Table II. Comparison of BNL/AIMS Measured vs. Calculated PDCB Concentrations

experiment	conditions	no. of changes	average PDCB concn, nL/m ³		measd/calcd
			measured ^a	calculated ^b	
1	constant temp, constant ach	0	240.4 ± 5.7	254.2 ± 12.8	0.946 ± 0.074
2	constant temp, variable ach	11	139.3 ± 2.5	149.2 ± 7.7	0.934 ± 0.068
3	variable temp, constant ach	12	290.5 ± 8.0	280.9 ± 19.3	1.034 ± 0.107

^a Measured concentrations were determined with CATS. ^b Calculated concentrations were obtained either from eq 5 (experiment 1) or from eq 9 (experiments 2 and 3), time-weighted over each measurement period.

erage relative standard deviation of 1.9 ± 1.0% with a range of 0.6–4.2% and a median of 2.2%. Thus, the expected precision of duplicate samplers, ±2%, demonstrates that there is no need to perform duplicate sampling during actual field use, since the sampling rates, handling, and analytical procedures for the CATS are consistent and reproducible.

All 32 sampler analyses results are shown in Figure 3, where they are plotted vs. both sampler orientation and chamber location. Also included are the means (crosses) and standard deviations (bars) for all samplers in each orientation and location as well as the overall average and standard deviation for 31 samplers (one result at orientation 3 and location C, which had a value of 227.6 nL/m³, was statistically low and was excluded from all averaging).

Figure 3 clearly shows that the averages of the 10 samplers in each of the three chamber locations (A–C) were statistically identical. In fact, excluding location D because there were only two samplers, the maximum difference between the three averages was only 0.4%, indicating that the chamber concentration was uniformly identical at all locations.

Figure 3 does show that sampler orientation did affect the average sampling rate. Positions 1 and 5 both exposed the samplers at right angles to the chamber flow; their averages were identical within 0.7% and about 1.3% above the overall mean. Position 3, CATS facing into the direction of flow, had an average that was 0.5% above the overall average. The lowest mean concentrations were for positions 2 (facing away from the direction of flow) and 4 (shielded by the chair seat), probably because those positions prevent turbulence at the sampling end. Those means were 2.0 and 1.4% below the overall mean. As shown in the figure, only position 2 was statistically different (more than 1 standard deviation) from the overall average.

The average chamber ventilation rate, *n*, based on five of the six CO₂ decay measurements was 0.601 ± 0.011 h⁻¹. The tracer source strength, *S*, based on gravimetric measurements at 25 °C was 5688 ± 120 nL/h. Substituting into eq 6 gave *S*₂₃ = 5195 ± 145 nL/h, and dividing by the chamber volume (*V* = 34 m³) gave *S* = 152.8 ± 4.3 nL/(h·m³). The PDCB concentration can then be calculated from eq 5:

$$C = \frac{S}{n} = \frac{152.8 \pm 4.3}{0.601 \pm 0.011} = 254.2 \pm 12.8 \text{ nL/m}^3$$

which, as shown in Table II, is identical within the standard deviation of the average of the measured concentrations.

Experiment 2. Unlike experiment 1, which was conducted at steady-state conditions of constant temperature and ventilation rate, experiments 2 and 3 were performed over multiple periods in which the temperature and ventilation rate were constant during each period, but at least one of the two was changed from the previous period. The tracer concentration at any time, *t*, during the period is

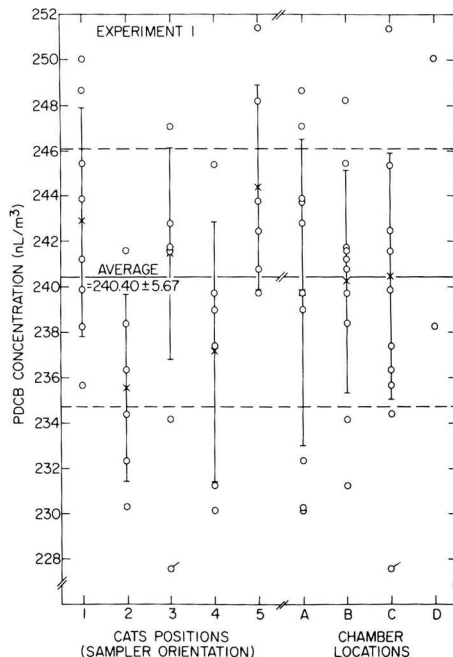


Figure 3. PDCB concentrations (O), averages (X), and standard deviations (—) for 16 paired CATS vs. sampler orientation (position 1, 90° from into the wind; position 2, 180°; position 3, 0°; position 4, shielded; position 5, 90°) and chamber location.

given by eq 2 where *C*₀ is the concentration at the end of the previous period.

The average concentration during each period is given by

$$\bar{C} = \frac{1}{\tau} \int_0^{\tau} C_t dt \tag{8}$$

Substituting eq 2 into eq 8 and integrating give

$$\bar{C} = \frac{S}{n} - \left(\frac{C_0 - S/n}{n\tau} \right) (e^{-n\tau} - 1) \tag{9}$$

where τ is the duration of each period (h).

The ach (*n*) and duration (τ) for each period of experiment 2 (constant temperature and variable ach) are given in Table III and were used in eq 2 and 9 to compute the concentration as a function of time and the average concentration for each period as shown in Figure 4 (top). The series of exponential curves, when integrated over each period, gave the average concentrations listed in Table III; the calculated overall average concentration for the 69-h period was 149.2 ± 7.7 nL/m³.

Table IV lists the measured concentrations obtained with the eight CATS. The relative standard deviation of

Table III. Conditions and Calculated Results for Variable Infiltration Rate Experiment [Experiment 2: $S = 152.8 \pm 4.3$ nL/(h•m³) at 23 °C]

period	average ach _{CO₂} ± SD, h ⁻¹ (%) ^a	time of period, h		calcd av PDCB ^b concn, nL/m ³
		duration	from-to	
1	0.608 ± 0.004 (0.7)	8	0-8	251.3 ± 8.8
2	1.306 ± 0.069 (5.3)	6	8-14	134.1 ± 10.8
3	1.627	7	14-21	95.9 ± 6.2
4	1.312 ± 0.062 (4.7)	5	21-26	113.0 ± 8.5
5	0.599 ± 0.014 (2.4)	6	26-32	217.6 ± 11.4
6	1.298 ± 0.046 (3.5)	6	32-38	134.9 ± 9.0
7	1.623 ± 0.021 (1.3)	7	38-45	96.2 ± 4.3
8	1.263 ± 0.014 (1.1)	5	45-50	116.7 ± 4.7
9	0.567	6	50-56	227.3 ± 8.6
10	1.273 ± 0.001 (0.1)	6	56-62	138.9 ± 4.6
11	1.624 ± 0.070 (4.3)	7	62-69	96.4 ± 6.8
av ^c	1.190 ± 0.033 (2.8)			149.2 ± 7.7(5.1%)

^a Average of two measurements per period with standard deviation and percent relative standard deviation in parentheses. ^b Calculated from eq 9 including the error in S and ach_{CO₂} (n). ^c Time-weighted average.

Table IV. Measured PDCB Concentrations for Variable Infiltration Rate Experiment (Experiment 2: Calculated Time-Weighted Average PDCB Concentration = 149.2 ± 7.7 nL/m³)

chamber location	CATS sampler	PDCB concn, nL/m ³	
		measured	average ± SD (%) ^a
A	5621	142.2	142.0 ± 0.3 (0.2)
	5391	141.8	
B	5366	139.2	139.1 ± 0.2 (0.1)
	5655	138.9	
C	5332	131.4	133.4 ± 2.8 (2.1)
	5627	135.4	
D	4682	140.4	138.8 ± 2.3 (1.7)
	5379	137.1	
av ^b		139.3 ± 2.5 (1.8)	

^a Average of two measurements with standard deviation and percent relative standard deviation in parentheses. ^b CATS 5332 not included in overall average.

the four sets of duplicate measurements ranged from 0.1 to 2.1%, similar to the experiment 1 paired results. The overall average PDCB concentration was 139.3 ± 2.5 nL/m³ which, as shown in Table II, agrees with the calculated concentration for experiment 2 within the standard deviation of each determination.

Table V. Conditions and Calculated Results for Variable Temperature Experiment [Experiment 3: $S = 152.8 \pm 4.3$ at 23 °C, 167.2 ± 5.8 at 27 °C, 182.5 ± 7.5 nL/(h•m³) at 31 °C]

period	chamber temp, °C	av ach _{CO₂} ± SD h ⁻¹ ^b	time of period, h		calcd av PDCB ^c concn, nL/m ³
			duration	from-to	
1	23.0	0.577 ± 0.009	6	0-6	264.8 ± 11.8
2	27.0	0.566	6	6-12	286.7 ± 18.3
3	31.0	0.611	6	12-18	297.5 ± 22.3
4	23.0	0.593 ± 0.018	6	18-24	268.8 ± 17.9
5	27.0	0.567	6.75	24-30.75	285.7 ± 19.6
6	31.0	0.621	5.5	30.75-36.25	293.9 ± 22.0
7	23.0	0.588 ± 0.018	7.5	36.25 ± 43.75	267.5 ± 17.5
8	27.0	0.585	4.25	43.75-48	276.4 ± 18.4
9	31.0	0.596	6.5	48-54.5	300.5 ± 22.5
10	23.0	0.626	4.5	54.5-59	264.7 ± 18.5
11	27.0	0.597	7	59-66	272.5 ± 18.6
12	31.0	0.621 ± 0.026	6	66-72	290.1 ± 23.7
av ^d	27.0	0.595 ± 0.022			280.9 ± 19.3

^a The time-weighted average S was 167.5 ± 5.9 nL/(h•m³). ^b A standard deviation of ±0.02 h⁻¹ was assumed for the single measurement periods. ^c Calculated from eq 9 including the error in S and ach_{CO₂} (n). ^d Time-weighted average.

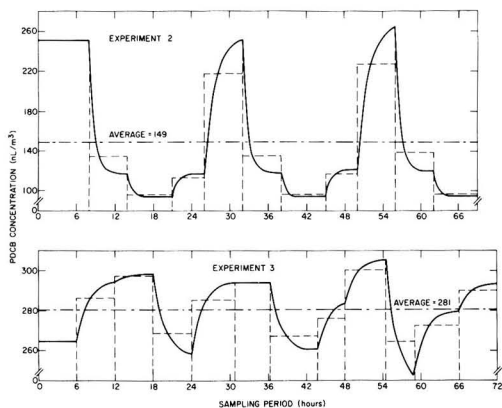


Figure 4. Calculated PDCB concentrations vs. sampling time: (top panel) effect of 11 step changes in ventilation rate; (bottom panel) effect of 12 temperature step changes (between 23 and 31 °C) and minor ventilation rate changes.

Experiment 3. The chamber temperature and its effect on the PDCB source strength term (S), the ach (n), and the duration (τ) for each period of this variable temperature experiment are given in Table V and were used in eq

Table VI. Measured PCB Concentrations for Variable Temperature Experiment (Experiment 3: Calculated Time-Weighted Average PCB Concentration = 280.9 ± 19.3 nL/m³)

chamber location	sampler	PCBC concn, nL/m ³	
		measured	av ± SD (%) ^a
A	5461	312.5	296.9 ± 22.1 (7.4)
	4678	281.3	
B	5251	292.4	298.6 ± 8.7 (2.9)
	5361	304.7	
C	5513	281.5	287.2 ± 8.1 (2.8)
	5641	293.0	
D	5476	292.4	290.3 ± 3.0 (1.0)
	5551	288.2	
controls	5656	0.33	
	5297	0.28	
average ^b		290.5 ± 8.0 (2.8)	

^a Average of two measurements with standard deviation and percent relative standard deviation in parentheses. ^b CATS 5461 (location A) and controls not included in average.

2 and 9 to compute the PCB concentration vs. time and the average for each of the 12 periods as shown in Figure 4 (bottom) and listed in Table V; the time-weighted overall calculated average concentration was 280.9 ± 19.3 nL/m³ for the 72-h experiment.

Table VI lists the measured concentrations obtained with the eight CATS plus the levels from the two controls which were never opened; the controls showed levels of about 0.1% of the sampled values. The relative standard deviations of three pairs (locations B–D) ranged from 1.0 to 2.9%, similar to that of experiment 1; location A had a high difference for the CATS pair (±7.4%). Excluding the high value from the overall average gave a measured concentration of 290.5 ± 8.0 nL/m³ which, as shown in Table II, agreed with the calculated average for experiment 3 and was well within the standard deviation of each determination.

Discussion

As summarized in Table II, for each of these experiments (constant temperature and ventilation rate, constant temperature but variable ventilation, and constant ventilation but variable temperature), the ratio of the PCB concentration measured by the CATS samplers divided by the calculated concentration determined from CO₂ decay measured ventilation rates and known PCB source strengths was equal to 1 within the standard deviation associated with some of the errors. Thus, the passive sampling method does give an accurate measure of the average concentration that existed during a measurement period.

The agreement was even more within the error bounds than indicated in Table II because certain errors in the

measurement technology were not included such as the error associated with the absolute sampling rate of the CATS (±2%) and the uncertainty in the gas calibration standards (±2%).

Experiment 1. The chamber recirculation rate in each experiment was 60 ach, equivalent to an upward air velocity of 0.052 m/s. Typical between-zone air-exchange rates can be as large as 200 m³/h (10). Assuming that CATS are sampling the air in a room near a doorway, that there are four doors per zone, and that the cross-sectional area for flow is about one-fourth the area of a doorway (i.e., about 0.4 m²), the maximum anticipated velocity in a home is of the order of 0.04 m/s, comparable to the chamber velocity. Some actual horizontal velocity measurements in a home showed levels from 0.05 to 0.2 m/s (17) in the more turbulent regime within 0.5 m of the ceiling.

The effect of wind speed and orientation into the wind was studied for a passive NO₂ sampler (18). From their data, the rate of sampling relative to still air for different orientations was correlated with wind speed and then used to calculate the effect at the chamber velocity of 0.052 m/s. As shown in Table VII, the agreement of the Palmes measurements with those from this study was very good and consistent, with the largest effect occurring at 90° to the wind, the next lowest effect at 0° (facing into the wind), and the least effect at 180° (facing away from the wind). It can be seen that the maximum bias in the sampling rate at velocities expected in homes and buildings is less than 2–3% and can be ignored. In fact, by placing the sampler on a flat surface within the room, any local wind effects can be blocked.

The ventilation rate computed by the BNL/AIMS technique using the computed source strength [$S = 152.8 \pm 4.3$ nL/(h·m³)] and CATS average measured concentration (240.4 ± 5.7 nL/m³) is given by eq 5 as

$$n = \frac{S}{C} = \frac{152.8 \pm 4.3}{240.4 \pm 5.7} = 0.636 \pm 0.034 \text{ h}^{-1}$$

in agreement with the CO₂-decay average value of 0.601 ± 0.011 h⁻¹. Thus, under constant ventilation rate and constant temperature conditions, there was no bias in the determination of the average ventilation rate with the BNL/AIMS approach.

Experiment 2. As shown in Figure 4 (top), the widely varying ventilation rate caused significant swings in the calculated PCB chamber concentration vs. time. But, as expected, the CATS measured concentration of 139.3 ± 2.5 nL/m³ was in agreement with the calculated average value of 149.2 ± 7.7 nL/m³.

Although the passive samplers are capable of determining the correct average tracer concentration over a measurement period, it has been shown that the reciprocal of an average concentration, \bar{C} , the quantity measured, is close to but not identical with the average of reciprocal concentrations. For example, for conditions of constant temperature (S is constant) but multiple equal-duration

Table VII. Effect of Air Velocity and Direction on Passive Samplers (Experiment 1)

CATS orientation	angle from into wind	av PCB concn, nL/m ³	PCBC concn relative to still air	
			from this study ^a	calcd from Palmes measurements ^b
1	90°	242.86 ± 5.04	1.024 ± 0.047	1.014 ± 0.038
2	180°	235.54 ± 4.09	0.993 ± 0.042	0.976 ± 0.010
3	0°	241.46 ± 4.65	1.018 ± 0.045	1.004 ± 0.027
4	shielded	237.14 ± 5.68		
5	90°	244.37 ± 4.53	1.030 ± 0.045	1.014 ± 0.038

^a The CATS shielded by the chair was assumed to be in still air. ^b Calculated from linear regression fit of data collected for wind velocity from 0.5 to 2.6 m/s (18) for the chamber velocity of 0.052 m/s.

periods (m) of different ventilation rates (i.e., different \bar{C}_k), eq 5 becomes

$$n = S \frac{1}{m} \sum_{k=1}^m \frac{1}{\bar{C}_k} \approx \frac{S}{\bar{C}} \quad (10)$$

Substituting the explicit values of S and \bar{C} from Table III gives

$$n \approx \frac{152.8 \pm 4.3}{149.2 \pm 7.7} \text{ or } 1.02 \pm 0.09 \text{ h}^{-1}$$

However, Table III shows that the actual time-weighted average ventilation rate was $1.19 \pm 0.03 \text{ h}^{-1}$. Thus, for a measurement period in which the ventilation rate varied about 2.7-fold on a cyclical basis, there was an explicit underestimate of the true average ventilation rate by about 14%.

Such periodic variation can occur in actual building measurements on a diurnal basis because the ventilation driving force, the inside-outside temperature difference, increases at night and decreases during the day; a 1.5-2-fold variation on a daily basis is not unreasonable. However, the cycle in experiment 2 as shown in Figure 4 (top) is biased somewhat by the constant rate in the first period (0-8 h). By looking at periods 2-9 inclusive in Table III, which includes exactly two complete up-down cycles, the average concentration would have been $141.2 \pm 7.9 \text{ nL/m}^3$ corresponding to an apparent ventilation rate of $1.08 \pm 0.10 \text{ h}^{-1}$, and the true average ventilation rate would have been $1.21 \pm 0.04 \text{ h}^{-1}$, for a rate underestimate of less than 11%. Thus, for measurement periods of several days or longer, it can be expected that the BNL/AIMS approach may underestimate the true ventilation rate by about 3-6%, a tolerable bias for this convenient technique.

Experiment 3. Figure 4 (bottom) showed that the 8°C swing in chamber temperatures from 23 to 31°C and down again caused less than a 1.2-fold variation in the concentration, and again, as shown in Table II, the CATS-measured concentration of $290.5 \pm 8.0 \text{ nL/m}^3$ was in agreement with the expected concentration of $280.9 \pm 19.3 \text{ nL/m}^3$.

Since both the source strength, S , and the PDCB concentration, C , are different for each period, for multiple equal-duration periods (m), eq 5 becomes

$$n = \frac{1}{k} \sum_{k=1}^m \frac{S_k}{\bar{C}_k} \approx \frac{1}{\bar{C}} \frac{1}{k} \sum_{k=1}^m S_k \approx \frac{\bar{S}}{\bar{C}} \quad (11)$$

The reciprocal concentration term can be more accurately factored out in the case of the temperature cycling because the magnitude of the concentration swings is much less and more accurately represented by an average value than was the case for experiment 2.

The time-weighted averages of source strength and concentration were $167.5 \pm 5.9 \text{ nL/(h}\cdot\text{m}^3)$ and $280.9 \pm 19.3 \text{ nL/m}^3$, respectively (cf. Table V). Substituting in eq 11 gives

$$n = \frac{167.5 \pm 5.9}{280.9 \pm 19.3} \text{ or } 0.596 \pm 0.067 \text{ h}^{-1}$$

which is essentially identical with the measured average ventilation rate of $0.595 \pm 0.022 \text{ h}^{-1}$. Thus, the BNL/AIMS technique is not biased to any significant extent if the appropriate temperature for the source is known.

For these chamber experiments, the base temperature was 23°C , the value at which the sources were conditioned before the experiment began. The source strengths for the two other temperatures, 27 and 31°C , were computed from eq 7 because these were short-term temperature adjustments; the total duration of the experiment was only 3 days.

If these measurements had been conducted over a 2-week or longer period, then the average source strength could have been estimated from the time-weighted average source temperature and used in eq 6; this would be the procedure for a ventilation rate determination in a home, where the time-weight average thermostat setting would be used as the average base temperature. Assuming long-term equilibration at the chamber base temperature of 27°C , eq 6 becomes

$$S'_{27} = \frac{5688 \pm 120}{34} e^{-4000(1/300-1/298)} = 182.9 \text{ nL/(h}\cdot\text{m}^3)$$

which, divided by the average concentration, gives

$$n = \frac{182.9}{280.9} = 0.651 \text{ h}^{-1}$$

This is about 9.4% higher than the true ventilation rate of 0.595 h^{-1} because the sources had not equilibrated at the experiment 3 base temperature of 27°C in the 3-day period.

One can reverse the procedure and use the measured ventilation rate and average PDCB concentration from Tables V and VI, respectively, to compute the source strength and hence the estimated average chamber temperature. From eq 5

$$S_i = nC = (0.595 \pm 0.022)(290.5 \pm 8.0) = 172.8 \pm 11.3 \text{ nL/(h}\cdot\text{m}^3)$$

Equation 6 becomes

$$172.8 \pm 11.3 = \frac{5688 \pm 120}{34} e^{-(4000+300)(1/T-1/298)}$$

or $T = 298.9 \pm 2.2 \text{ K}$ ($25.7 \pm 2.2^\circ\text{C}$). This average chamber temperature of 25.7°C is, as expected, above the preexperiment base temperature of 23°C and below the long-term time-weighted chamber temperature of 27°C , confirming the applicability of the BNL/AIMS approach in variable temperature scenarios.

Conclusions

The relative standard deviation of multiple paired passive samplers is $\pm 1.9 \pm 1.0\%$, indicating that the reproducibility in the manufacture, handling, and analysis of the CATS is sufficiently good to preclude the necessity of duplicate sampling in field experiments.

For the low air movement velocities in homes ($<0.2 \text{ m/s}$, away from any forced air vents), the effect of sampler orientation is not consequential on the sampling rate, having less than a 2-3% positive bias in the worst case.

Under conditions of widely varying concentrations, the passive sampler accurately measures the correct time-weighted average tracer concentration. However, because the determination of ventilation ratios requires the determination of the average reciprocal tracer concentration rather than the reciprocal of the average tracer concentration, which is the item measured by the passive sampler, there is an estimated negative bias in the ventilation rate determination of about 3-6%, a tolerable bias for this convenient technique.

By use of a time-weighted average temperature for determining the estimated source strength, room temperature fluctuations or intentional cycling differences of as much as 8°C (14°F) can be accounted for in order to produce essentially no bias in the determination of ventilation rates.

Acknowledgments

Appreciation is expressed to Bob Wieser for the manufacture and calibration of the PFT sources and passive

samplers, to Bob Goodrich and Ed Cote for the analytical determination, and to Ted D'Ottavio for suggestions with the modeling.

Literature Cited

- (1) Hunt, C. M. In "Building Air Change Rate and Infiltration Measurements"; Hunt, C. M.; King, J. C.; Treschel, H. R., Eds.; American Society for Testing and Materials: Philadelphia, PA, 1980; ASTM STP 719, pp 3-23.
- (2) "ASTM Standard E 741-80"; ASTM: Philadelphia, 1980.
- (3) Totzke, D.; Quackenboss, J.; Kaarakka, P.; Flukenger, J. In "Indoor Air: Buildings, Ventilation and Thermal Climate"; Berglund, B.; Lindvall, T.; Sandell, J., Eds.; Swedish Council for Building Research: Stockholm, 1984; Vol. 5, pp 459-464.
- (4) Dietz, R. N.; Cote, E. A. *Environ. Int.* 1982, 8, 419-433.
- (5) Condon, P. E.; Grimsrud, D. T.; Sherman, M. H.; Kameru, R. C. In "Building Air Change Rate and Infiltration Measurements"; Hunt, C. M.; King, J. C.; Treschel, H. R., Eds.; American Society for Testing and Materials: Philadelphia, PA, 1980; ASTM STP 719, pp 60-72.
- (6) Grimsrud, D. T.; Sherman, M. H.; Janssen, J. E., Jr.; Pearman, A. N.; Harrie, D. T., *ASHRAE Trans.* 1980, 86, 258-267.
- (7) Shaw, C. Y. *ASHRAE Trans.* 1984, 2816, 212-225.
- (8) Bassett, M. R.; Shaw, C. Y.; Evans, R. G. *ASHRAE Trans.* 1981, 87, 361-371.

- (9) Harrie, D. T.; Hunt, C. M.; Treado, S. J.; Malik, N. J. Center for Environmental Studies, Princeton University, Princeton NJ, Report 13.
- (10) Dietz, R. N.; Goodrich, R. W.; Cote, E. A.; Wieser, R. F. Brookhaven National Laboratory, 1983, Report BNL 33846.
- (11) Leaderer, B. P.; Zagananiski, R. T.; Berwick, M.; Stolwijk, J. A. J., *Am. J. Epidemiol.* in press.
- (12) Spengler, J., Harvard School of Public Health, personal communication, 1985.
- (13) Janssen, J., Honeywell Control Systems, personal communication, 1985.
- (14) Grimsrud, D., Lawrence Berkeley Laboratory, personal communication, 1985.
- (15) Dietz, R. N.; Goodrich, R. W.; Cote, E. A.; Wieser, R. F. Brookhaven National Laboratory, 1985, Report BNL 36327.
- (16) Dietz, R. N.; Goodrich, R. W.; Cote, E. A.; Wieser, R. F. Brookhaven National Laboratory, 1984, Report BNL 35249.
- (17) Harlos, D., Harvard School of Public Health, personal communication, 1984.
- (18) Palmes, E. D.; Gunnison, A. F.; DiMattio, J.; Tomczyk, C. *Am. Ind. Hyg. Assoc. J.* 1976, 37, 570-577.

Received for review March 25, 1985. Accepted June 27, 1985. This research was supported in part with funds from Grant ES-00354 from the National Institute of Environmental Health Sciences and the Office of Buildings and Community Systems of the U.S. Department of Energy.

Determination of Alkylethoxylated Sulfates in Wastewaters and Surface Waters

Thomas A. Neubecker*

Environmental Safety Department, The Procter & Gamble Company, Cincinnati, Ohio 45217

■ A novel method was developed for the determination of parts per billion levels of alkylethoxylated sulfates (AES) in wastewaters and surface waters. The analysis scheme involves concentration of the AES on an anion-exchange resin, elution off the resin with methanolic HCl, hydrolysis of the AES to alkylethoxylate (AE), extraction of the AE from the remaining ionic species, derivatization to the corresponding alkyl bromides, and analysis of the alkyl bromides by gas chromatography. Recovery of several AES homologues through this scheme ranged from 68 to 78% with an estimated sensitivity of ~1 ppb for each alkyl-chain homologue of AES. AES levels were measured in several wastewater and surface water samples by using this method and the nonspecific methylene blue active substance (MBAS) method. Results indicate that only about 10% of the total MBAS response arises from AES.

Introduction

Alkylethoxylated sulfates (AES) are a major class of anionic surfactants used in consumer cleaning products. They are components of light-duty dishwashing liquids, shampoos, and other household specialty products. In the United States, production of AES exceeds 128 million pounds/year (1).

The structure of AES consists of a long-chain alkyl group (normally C₁₂-C₁₈) bound to a variable length ethoxylate chain (normally E₁-E₁₂) and terminated by a sulfate group. Its general formula is represented by



Commercial materials are often supplied as either the NH₄⁺ or Na⁺ salts and are sold under trade names such as Alfonic (Conoco), Neodol (Shell), and Polystep (Stephan).

AES occurs in domestic wastewater and is extensively removed from sewage by wastewater treatment (85-100% removal; see ref 2). Thus, in wastewater effluents or surface waters, only parts per billion (ppb) levels are anticipated. To date, analysis of AES in wastewater or surface waters was conducted by nonspecific anionic surfactant analyses (3, 4), the most common method being the MBAS (methylene blue active substance) procedure (5). The MBAS method measures AES, other anionic surfactants such as LAS (linear alkylbenzenesulfonate) and alkyl sulfates, and some naturally occurring anionic materials. Thus, any value for AES obtained by this nonspecific method is exaggerated. The method presented here offers considerable improvement in terms of selectivity and sensitivity. It takes advantage of the selective cleavage of the sulfate functionality and the conversion of the anionic surfactant into a nonionic material. After this conversion, a specific analysis for the nonionic species is obtained by hydrolysis to an alkyl bromide followed by gas chromatographic measurement.

Experimental Section

Materials. The alkylethoxylated sulfate was prepared by Procter & Gamble via sulfonation of the corresponding alkylethoxylates. Shell Neodol 23-12 (a C₁₂₋₁₃E₁₂ alkylethoxylate) was the starting material. The C₁₂₋₁₃E₁₂S

*Address correspondence to this author at the Miami Valley Laboratories, Human Safety Department, The Procter & Gamble Co., Cincinnati, OH 45247.

produced had a 40/60 distribution of C₁₂/C₁₃ alkyl groups with an average ethoxylate length of 12. These distributions were determined by gas chromatography (GC) analysis of the HBr cleavage products (6).

Standards of the C₁₂-C₁₈ bromides were obtained from the following sources: C₁₂Br and C₁₄Br from J. T. Baker (Phillipsburg, NJ), C₁₃Br from Aldrich (Milwaukee, WI), C₁₅Br, C₁₆Br, and C₁₈Br from Eastman Organic Chemicals (Rochester, NY), and C₁₇Br from Fluka (Hauppauge, NY). Anion-exchange resin (AG1-X2) was obtained from Bio-Rad (Richmond, CA). For MBAS analysis, methylene blue reagent was obtained from MCB Chemicals (Gibbstown, NJ). All other materials were of reagent-grade quality unless otherwise noted.

Apparatus. Chromatographic analysis of the alkyl bromides was performed on a Hewlett-Packard Model 5840A gas chromatograph equipped with an integrator and flame ionization detector. The column was a 6-ft, stainless steel column packed with 10% OV-17 on Chromosorb W from Hewlett-Packard. The GC response was calibrated by injection of C₁₂-C₁₈ bromide standards using C₁₇Br as the internal standard.

MBAS colorimetric analyses were performed on a Beckman Model 25 recording spectrophotometer.

Sample Collection. Wastewater influent and effluent samples were collected from the Colerain Heights wastewater treatment plant in Cincinnati, OH. This is a small, extended-aeration plant that receives primarily domestic wastewater. The influent was collected after comminution and effluent samples before chlorination. The river water was collected from the Ohio River at Anderson Ferry and at Saylor Park, OH. These points are above and below Cincinnati's Muddy Creek wastewater treatment plant outflow, respectively.

All samples were preserved after collection by addition of formalin to a level of 1% to prevent biodegradation of the surfactants. Sample sizes used in the analysis depended on the anticipated levels of AES in the sample. For wastewater influent a 50-mL sample was sufficient, while for wastewater effluent a 200-mL sample or larger was desirable. For river waters, 1 L or more of sample was used for analysis. Recovery measurements with radiolabeled material showed particulate matter does not interfere, so in all cases the samples were used without filtration.

Analysis Procedure

Concentration and Hydrolysis. An appropriate volume of unfiltered sample was passed through an ion-exchange column containing ~6 g of AG1-X2 anion-exchange resin at a rate of ~1 drop/s. The column was next washed with 50 mL of methanol to elute hydrophobically adsorbed materials. This methanol was discarded. Next, four 25-mL aliquots of 10% HCl in methanol were passed through the column and collected. This quantitatively eluted the AES as well as other adsorbed anionic materials. This eluant was then evaporated on a steam bath to <10 mL to remove the methanol. (Note: If taken to dryness, loss of AES occurs.)

Extraction. The previous step hydrolyzed the AES to form the corresponding nonionic alkylethoxylate. Common arylsulfonates such as LAS do not hydrolyze under these conditions. The concentrated eluant was then diluted to 100 mL with water and transferred to an extraction funnel. Five grams of MgSO₄ was added to the funnel in order to salt out the alkylethoxylate, and the mixture was extracted with four 25-mL portions of chloroform. (Note: The original container was rinsed with chloroform and the chloroform transferred to the extraction funnel.) After extraction, the aqueous layer was discarded. The chloro-

form layer was evaporated to <10 mL on a steam bath and carefully transferred to a 15-mL test tube with a Teflon-lined screw cap. The funnel was washed with a small amount of chloroform, and the washings were also transferred to the test tube. This solution was then taken to dryness under N₂ gas with mild heat (~60 °C). Prolonged heating was avoided to prevent loss of the slightly volatile nonionic material.

Derivatization/Detection. Ten micrograms of C₁₇Br in hexane was added as an internal standard to the residue in the test tube. C₁₇Br was selected because none of the samples contained a natural background of C₁₇ materials. There is a natural background for many of the other alkyl bromides, however. Next, approximately 0.5 mL of HBr (30-32% in HOAc) was added to the test tube and the cap securely attached. The sample was then placed in a heating block at 90 °C overnight (~16 h). In this step, the alkylethoxylate fully hydrolyzed to form the corresponding alkyl bromide and an amount of 1,2-dibromoethane equivalent to the number of ethoxylates originally present in the molecule. Next, 4.0 mL of water and 1.00 mL of toluene were added to the sample. This mixture was stirred on a vortex mixer for 30 s and centrifuged to completely separate the layers. Ten microliters of the toluene layer (top layer) was injected for chromatographic analysis.

Temperature programming used in the analysis was 2 min at 100 °C followed by an 8 °C/min rise to 250 °C followed by 8 min at 250 °C. An injector temperature of 275 °C was used and a He flow rate of ~30 cm³/min. In all instances a 6-ft column (10% OV-17 on Chromosorb W) was used.

Data Handling. The response of the GC was calibrated by injection of a standard mixture of C₁₂-C₁₈ alkyl bromides in toluene. In this mix and the samples to be analyzed, C₁₇Br was selected as the internal standard. After normalization to the C₁₇Br response, the amount of alkyl bromide in the sample was calculated from the integrated areas. The amount of AES in the sample was calculated by multiplying the alkyl bromide concentration by the ratio of the molecular weights of the parent and brominated compounds. For example, for C₁₂Br generated from C₁₂E₁₂S, the expression would be

$$[C_{12}E_{12}S] = [C_{12}Br] \frac{\text{molecular weight of } C_{12}E_{12}S}{\text{molecular weight of } C_{12}Br}$$

This calculation is valid for spiked samples where the degree of ethoxylation of the spiked AES is known. For this study, concentrations and recoveries were based on the actual material spiked. However, for background AES, a degree of ethoxylation of 7 was assumed. Normal AES's range from 1 to 12 in ethoxylate length so an average of 7 is reasonable. The error in this assumption would be no more than 45% if the actual ethoxylate distribution averaged as low as 1 or as high as 12. A variation of this magnitude is not significant at environmental levels.

MBAS Analyses. For comparative purposes, MBAS analyses were made on the same samples of wastewater influent and effluent and river waters. The MBAS method was found in ref. 5. The only difference in the method was the generation of a standard curve based on the concentration of AES rather than the usual LAS. The response was linear over the range 0-150 µg of C₁₂₋₁₃E₁₂S.

Results and Discussion

Several recovery experiments were performed on pure AES samples or dilute samples prepared in filtered, deionized water. After recoveries were established, the

Table I. Removal of AES via Sewage Treatment (Concentrations in ppm)^a

sample	C ₁₂ E ₇ S	C ₁₃ E ₇ S	C ₁₄ E ₇ S	C ₁₅ E ₇ S	C ₁₆ E ₇ S ^b	C ₁₈ E ₇ S	total AES
influent	0.34 ± 0.02	0.12 ± 0.05	0.58 ± 0.02	0.22 ± 0	0.22 ± 0.02	0.40 ± 0.06	1.88
effluent	0.02 ± 0.01	ND	0.01 ± 0.01	ND	0.01 ± 0	0.02 ± 0	0.06
removal, %	94	100	98	100	95	95	97

^a All concentrations expressed as the E₇ homologue. ^b Estimated by peak height rather than by integration. ^c ND, not detectable.

Table II. Recovery of AES from Sewage Influent/Effluent Samples

sample	no. of replicates	ppm spiked		ppm recovered		% recovery	
		C ₁₂ E ₁₂ S	C ₁₃ E ₁₂ S	C ₁₂ E ₁₂ S	C ₁₃ E ₁₂ S	C ₁₂ E ₁₂ S	C ₁₃ E ₁₂ S
influent	3	0.80	1.20	0.52 ± 0.06	0.78 ± 0.06 ^a	65	65
influent	2	0	0	0.48 ± 0.04	0.17 ± 0.07		
effluent	3	0.050	0.075	0.028 ± 0.004 ^a	0.050 ± 0.005 ^a	55	67
effluent	2	0	0	0.029 ± 0.012	ND		
						60 ± 7 ^b	66 ± 1 ^b
direct hydrolysis of standard		40 ^c	40 ^c	37 ^c	46 ^c	93	77

^a Corrected for background levels of AES. ^b Average recovery from sewage. ^c Units: micrograms.

method was validated on several environmental samples including wastewater influent and effluent and river water.

Recovery. A 1-L water sample was prepared containing 100 µg (total) of C₁₂₋₁₃E₁₂S. On the basis of the homologue distribution, this corresponds to 40 µg of the C₁₂E₁₂S homologue and 60 µg of the C₁₃E₁₂S homologue. This sample was analyzed by using the method described. Figure 1 shows the resulting chromatogram along with the calibration chromatogram.

The amount of C₁₂Br and C₁₃Br found was 12 and 13 µg, respectively, which corresponds to a C₁₂E₁₂S level of 38 µg and C₁₃E₁₂S level of 41 µg, or 97% and 67% recoveries. Samples of the AES hydrolyzed directly with the HBr and not taken through the concentration/cleanup steps showed a similar difference in recovery (93% for the C₁₂ homologue and 77% for the C₁₃ homologue). The reason for this variation in conversion efficiency is not known.

Wastewater Influent/Effluents. Figure 2 and Table I show the results of an analysis performed on 50-mL samples of wastewater influent and 200-mL samples of wastewater effluent.

As seen in Figure 2A, materials generating C₁₂-C₁₈ alkyl bromides were present in influent wastewater. (A sample with no C₁₇Br internal standard was also analyzed, confirming the absence of natural C₁₇Br-generating material.) The concentrations of AES corresponding to these concentrations of alkyl bromide are listed in Table I. Less than 2 ppm of total AES was found in the wastewater influent, with the C₁₄ homologue being the largest contributor. These concentrations are only estimates of the actual level of AES because they assume an average ethoxylate length of 7. We feel this is a good assumption on the basis of AES materials produced by different manufacturers.

Figure 2C shows a similar chromatogram from wastewater effluent collected at the same time as the influent. Note that virtually all of the AES is removed by the extended aeration process with only very low levels of C₁₂, C₁₄, C₁₆, and C₁₈ remaining (see Table I). In this case, a much larger sample was taken (200 mL) in anticipation of the lowered levels. Thus, on the basis of these data, removals of AES greater than 97% are found.

In both the wastewater influent and wastewater effluent samples, the recovery of added AES was determined to

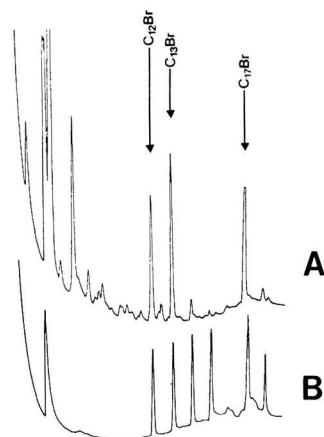


Figure 1. (A) Chromatogram of C₁₂₋₁₃E₁₂S spiked into high quality water at a 0.100 ppm level and converted to alkyl bromides. (B) Alkyl bromide calibration standards.

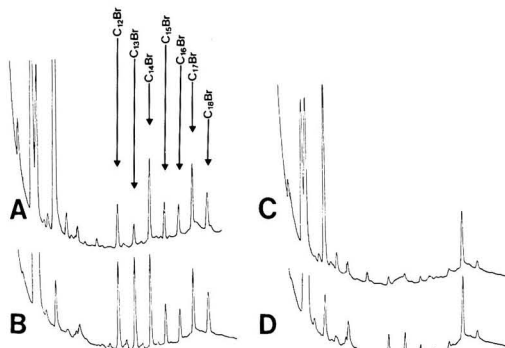


Figure 2. Chromatogram of (A) wastewater influent, (B) wastewater influent plus 2.0 ppm of C₁₂₋₁₃E₁₂S, (C) wastewater effluent, and (D) wastewater effluent plus 0.125 ppm of C₁₂₋₁₃E₁₂S.

ensure that the wastewater matrix did not adversely affect the analysis. Recovery was measured by adding 2 ppm

Table III. Recovery from Ohio River Water Samples

sample	ppm spiked		ppm recovered		% recovery	
	C ₁₂ E ₁₂ S	C ₁₃ E ₁₂ S	C ₁₂ E ₁₂ S	C ₁₃ E ₁₂ S	C ₁₂ E ₁₂ S	C ₁₃ E ₁₂ S
above STP	0.020	0.030	0.016 ± 0.002 ^a	0.021 ± 0.001 ^a	80	70
above STP	0.040	0.060	0.032 ± 0 ^a	0.042 ± 0.001 ^a	80	70
above STP	0	0	0.006	0.002		
below STP	0.020	0.030	0.019 ± 0.001 ^a	0.019 ± 0.001 ^a	95	63
below STP	0.040	0.060	0.038 ± 0.008 ^a	0.041 ± 0.006 ^a	95	68
below STP	0	0	0.004	0.004		
					88 ± 9 ^b	68 ± 3 ^b

^a Corrected for background levels of AES. ^b Average recovery from Ohio River water.

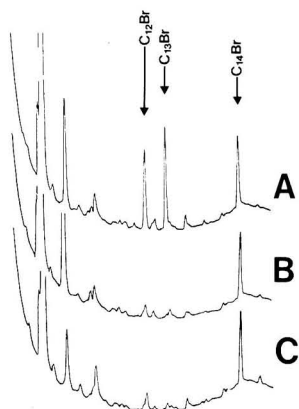


Figure 3. Chromatogram of (A) Ohio River water spiked with 0.050 ppm of C₁₂₋₁₃E₁₂S, (B) Ohio River water sampled above the wastewater treatment plant outflow, and (C) Ohio River water sampled below the wastewater treatment plant outflow.

(total) of C₁₂₋₁₃E₁₂S to the wastewater influent (background concentration was ~0.7 ppm) and 0.125 ppm (total) to the wastewater effluent (background concentration of ~0.03 ppm). Table II and Figure 2B,D show the results of these experiments. Recovery of added C₁₂E₁₂S averaged 60 ± 7% while a 66 ± 1% recovery was seen for added C₁₃E₁₂S. This was reasonable when compared with the 67–97% recovery seen for aqueous standards.

River Water Analyses. Measurable levels of AES might be found in some river waters that receive large wastewater loads and have low dilution factors. Therefore, we validated this method on several river water samples.

Samples of Ohio River water were taken both above (Sayler Park) and below (Anderson Ferry) the outflow of Cincinnati's Muddy Creek Municipal Sewage Treatment Plant (STP). Because very low levels were anticipated on the basis of wastewater effluent measurements, 1-L samples were analyzed. Figure 3 and Table III show the results of these analyses.

In general, no measurable difference was found in the AES level for river water from the two sampling locations. Less than 0.01 ppm of total C₁₂₋₁₃E₁₂S was measurable in either sample. In addition recovery was determined by spiking 0.05 and 0.10 ppm of C₁₂₋₁₃E₁₂S into both samples of river water. Recovery of spikes was good with 80–95% of the C₁₂ homologue and 63–70% of the C₁₃ homologue recovered.

Comparison with MBAS. As mentioned earlier, other methods for AES analysis are nonspecific and depend on a general analysis for anionic surfactants. The most commonly used method is the MBAS analysis. In order to compare the present method with the MBAS method,

Table IV. Comparison Analysis Obtained via MBAS and GC Methods

grab samples	no. of analyses	MBAS, ppm	GC, ppm	% of MBAS as AES ^a
sewage influent	2	31.6	1.9	6
sewage effluent	2	0.48	0.06	13
Ohio River water (above STP)	1	0.10	0.008	8
Ohio River water (below STP)	1	0.12	0.008	7

^a Includes C₁₂–C₁₈ AES calculated as containing seven ethoxylate groups.

MBAS analyses were made on several of the above samples. Table IV shows the results of those measurements.

In general, the contribution of AES to the MBAS response was only about 6–13% of the total and was independent of sample type. These results are not surprising because LAS (linear alkylbenzenesulfonate) is used at higher levels than AES and thus would be expected to be the larger anthropogenic source of MBAS response. In addition, many natural substances also contribute to the MBAS signal. Thus, MBAS measurements overestimate actual levels of AES in environmental samples by about a factor of 10.

Conclusions

The method presented here offers an improved analysis for AES for the following reasons: (1) The method is specific for AES and not anionic surfactants in general. (2) It allows the determination of specific alkyl chain length homologues of AES. (3) It has a sensitivity of ~1 µg per AES homologue, roughly 25× lower than the MBAS method. The method was tested on a number of environmental samples including wastewater influent/effluent and river water. In wastewater treatment, AES is extensively removed (>97%); thus, only very low levels are discharged to surface waters. These low levels were confirmed by measurements in river water receiving sewage outflow.

Acknowledgments

I thank J. P. Bray for his help in carrying out this work.

Registry No. Water, 7732-18-5.

Literature Cited

- U.S. International Trade Commission "Synthetic Organic Chemicals. U.S. Production and Sales of Surface-Active Agents"; U.S. Government Printing Office: Washington, DC, 1979.
- Arthur D. Little Co. "Human Safety and Environmental Aspects of Major Surfactants". Arthur D. Little Co., Cambridge, MA, Feb 20, 1981, Report to the Soap and

Detergent Association (Supplement).

- (3) Llenado, R. A.; Jamieson, R. A. *Anal. Chem.* **1981**, *53*, 174R-182R.
- (4) Llenado, R. A.; Neubecker, T. A. *Anal. Chem.* **1983**, *55*, 93R-102R.
- (5) American Public Health Association "Standard Methods for the Examination of Water and Wastewater", 14th ed.; APHA: New York, NY, 1975; pp 600-603.
- (6) Wee, V. T. In "Advances in the Identification and Analysis of Organic Pollutants in Water"; Keith, L. H., Ed.; Ann Arbor Science: Ann Arbor, MI, 1981; Vol. I.

Received for review January 23, 1985. Accepted June 28, 1985. This work was presented before the Division of Environmental Chemistry, American Chemical Society, Seattle, WA, March 1983.

AUTHOR INDEX TO VOLUME 19, 1985

- Aggett, J.**
—; O'Brien, G. A.
Detailed model for the mobility of arsenic in lacustrine sediments based on measurements in Lake Okakuri. 231
- Akimoto, H.** See Hatakeyama, S.
- Akita, K.** See Koda, S.
- Akland, G. G.**
—; Hartwell, T. D.; Johnson, T. R.; Whitmore, R. W.
Measuring human exposure to carbon monoxide in Washington, DC, and Denver, Colorado, during the winter of 1982-1983. 911
- Albritton, D. L.** See Roberts, J. M.
- Allen, E. R.** See Kerkhoff, M. J.
- Alsberg, T.**
—; Stenberg, U.; Westerholm, R.; Strandell, M.; Rannug, U.; Sundvall, A.; Rømer, L.; Bernson, V.; Pettersson, B.
Chemical and biological characterization of organic material from gasoline exhaust particles. 43
- Amaral, D. A. L.** See Morgan, M. G.
- Anderson, J. W.**
—; McQuerry, D. L.; Kiesser, S. L.
Laboratory evaluation of chemical dispersants for use on oil spills at sea. 454
- Anderson, M. A.** See Hansmann, D. D.
—; Tejedor-Tejedor, M. I.; Stanforth, R. R.
Influence of aggregation on the uptake kinetics of phosphate by goethite. 632
- Anderson, P. R.**
—; Benjamin, M. M.
Effect of silicon on the crystallization and adsorption properties of ferric oxides. 1048
- Andren, A. W.** See Bauer, C. F.; Burkhard, L. P.
- Ari, M.** See Crittenden, J. C.
- Armstrong, D. E.** See Burkhard, L. P.
- Aschmann, S. M.** See Atkinson, R.
- Ashbrook, P. C.**
—; Reinhardt, P. A.
Hazardous wastes in academia. Colleges and universities are trying to develop ways to manage hazardous wastes. 1150
- Atkinson, R.** See Biermann, H. W.; Pitts, J. N. Jr.; Tuazon, E. C.
—; Aschmann, S. M.
Rate constants for the gas-phase reaction of hydroxyl radicals with biphenyl and the monochlorobiphenyls at 295 ± 1 K. 462
—; Aschmann, S. M.; Winer, A. M.; Carter, W. P. L.
Rate constants for the gas-phase reactions of nitrate radicals with furan, thiophene, and pyrole at 295 ± 1 K and atmospheric pressure. 87
—; Aschmann, S. M.; Winer, A. M.; Pitts, J. N. Jr.
Kinetics and atmospheric implications of the gas-phase reactions of nitrate radicals with a series of monoterpenes and related organics at 294 ± 2 K. 159
- Badin, E. J.**
—; Frazier, G. C.
Sorbents for fluidized-bed combustion. 894
- Baker, J. E.**
—; Eisenreich, S. J.; Johnson, T. C.; Halfman, B. M.
Chlorinated hydrocarbon cycling in the benthic nepheloid layer of Lake Superior. 854
- Bales, R. C.**
—; Morgan, J. J.
Surface charge and adsorption properties of chrysotile asbestos in natural waters. 1213
- Bandow, H.** See Hatakeyama, S.
- Banerjee, S.**
Calculation of water solubility of organic compounds with UNIFAC-derived parameters. 369
- ; Howard, P. H.; Tullis, D. L.
Rebuttal: A general kinetic model for biodegradation and its application to chlorophenols and related compounds. 374
- Barisas, B. G.**
Acute toxicity screening of water pollutants using a bacterial electrode. Reply to comments. 871
- Barkley, R. M.** See Hawthorne, S. B.
- Barron, D. M.** See Coates, M.
- Bauer, C. F.**
—; Andren, A. W.
Emissions of vapor-phase fluorine and ammonia from the Columbia coal-fired power plant. 1099
- Becher, G.**
—; Carlberg, G. E.; Gjessing, E. T.; Hong, J. K.; Monarca, S.
High-performance size exclusion chromatography of chlorinated natural humic water and mutagenicity studies using the microscale fluctuation assay. 422
- Behmyer, T. D.**
—; Hites, R. A.
Photolysis of polycyclic aromatic hydrocarbons adsorbed on simulated atmospheric particulates. 1004
- Bell, D.** See Kamens, R.
- Beltrame, P.**
—; Beltrame, P. L.; Carniti, P.
Comment on "Development of a general kinetic model for biodegradation and its application to chlorophenols and related compounds". 374
- Beltrame, P. L.** See Beltrame, P.
- Benjamin, M. M.** See Anderson, P. R.
- Bernson, V.** See Alsberg, T.
- Berry, D. F.**
—; Boyd, S. A.
Decontamination of soil through enhanced formation of bound residues. 1132
- Biermann, H. W.**
—; MacLeod, H.; Atkinson, R.; Winer, A. M.; Pitts, J. N. Jr.
Kinetics of the gas-phase reactions of the hydroxyl radical with naphthalene, phenanthrene, and anthracene. 244
- Bishop, D. J.** See Harrison, F. L.
- Black, S. C.** See Schweitzer, G. E.
- Boyd, S. A.** See Berry, D. F.
- Breck, J. E.**
Comment on "Fish/sediment concentration ratios for organic compounds". 198
- Bremen, W. M.** See Guro, M. D.
- Brorstrom-Lunden, E.**
—; Lindskog, A.
Degradation of polycyclic aromatic hydrocarbons during simulated stack gas sampling. 313
- Brown, D. W.** See Varanasi, U.
- Brown, K. W.** See Davidson, C. I.
- Brown, M. P.**
—; Werner, M. B.; Sloan, R. J.; Simpson, K. W.
Polychlorinated biphenyls in the Hudson River. 656
- Brownawell, B.** See Murphy, T. J.
- Brumbaugh, W. G.**
—; Kane, D. A.
Variability of aluminum concentrations in organs and whole bodies of smallmouth bass (*Micropterus dolomieu*). 828
- Brunelle, D. J.**
—; Mendiratta, A. K.; Singleton, D. A.
Reaction removal of polychlorinated biphenyls from transformer oil: treatment of contaminated oil with poly(ethylene glycol)/potassium hydroxide. 740
- Buchanan, G. W.** See Ramaswamy, S.
- Burkhard, L. P.**
—; Andren, A. W.; Armstrong, D. E.
Estimation of vapor pressures for polychlorinated biphenyls: a comparison of eleven predictive methods. 500
—; Armstrong, D. E.; Andren, A. W.
Henry's law constants for the polychlorinated biphenyls. 590
- Buseck, P. R.** See Post, J.
- Butler, F. E.** See Cox, X. B. III.
- Byron, C.** See Schure, M. R.
- Caldwell, K. D.** See Schure, M. R.
- Campbell, J. R.**
—; Luthy, R. G.
Prediction of aromatic solute partition coefficients using the UNIFAC group contribution model. 980
- Capizzi, T.**
—; Oppenheimer, L.; Mehta, H.; Naimie, H.; Fair, J. L.
Statistical considerations in the evaluation of chronic aquatic toxicity studies. 35
- Carlberg, G. E.** See Becher, G.
- Carniti, P.** See Beltrame, P.
- Carter, W. P. L.** See Atkinson, R.; Tuazon, E. C.
- Chan, K. P.** See Schure, M. R.
- Cherry, J. A.** See Mackay, D. M.
- Chiu, C. T.**
Partition coefficients of organic compounds in liquid-water systems and correlations with fish bioconcentration factors. 57
—; Shoup, T. D.
Soil sorption of organic vapors and effects of humidity on sorptive mechanism and capacity. 1196
- Cholak, J.** See Saltzman, B. E.
- Ciarcia, D.** See Di Toro, D. M.
- Claxton, L.** See Kamens, R.
- Claxton, L. D.** See Kleindienst, T. E.; Shepson, P. B.
- Coates, M.**
—; Connell, D. W.; Barron, D. M.
Aqueous solubility and octan-1-ol to water partition coefficients of aliphatic hydrocarbons. 628
- Cofer, W. R. III.**
—; Collins, V. G.; Talbot, R. W.
Improved aqueous scrubber for collection of soluble atmospheric trace gases. 557
- Cohen, Y.**
—; Ryan, P. A.
Multimedia modeling of environmental transport: trichloroethylene test case. 412
- Colberg, P. J.** See Kuhn, E. P.
- Cole, J. A.**
—; Kramlich, J. C.; Seeker, W. R.; Heap, M. P.; Samuelson, G. S.
Activation and reactivity of calcareous sorbents toward sulfur dioxide. 1065
- Collins, V. G.** See Cofer, W. R. III.
- Connell, D. W.** See Coates, M.
- Conner, W. D.**
—; Knapp, K. T.
Comparison of an optical particle size monitor and a cascade impactor for in-stack source testing. 458
- Connor, M. S.**
Reply to comment on "Fish/sediment concentration ratios for organic compounds". 199
Rebuttal on: "Comparison of the carcinogenic risks from fish vs. groundwater contamination by organic compounds". 646
- Conrad, R.**
—; Seiler, W.
Characteristics of abiogenic carbon monoxide formation from soil organic matter, humic acids, and phenolic compounds. 1165
- Cosby, B. J.**
—; Hornberger, G. M.; Galloway, J. N.; Wright, R. F.
Time scales of catchment acidification. A quantitative model for estimating freshwater acidification. 1144
- Cox, X. B. III.**
—; Linton, R. W.; Butler, F. E.
Determination of chromium speciation in environmental particles. Multitechnique study of ferrochrome smelter dust. 345

- Craig, P. J.**
—; Rapsomanikis, S.
Methylation of tin and lead in the environment: oxidative methyl transfer as a model for environmental reactions. 726
- Cretney, J. R.**
—; Lee, H. K.; Wright, G. J.; Swallow, W. H.; Taylor, M. C.
Analysis of polycyclic aromatic hydrocarbons in air particulate matter from a lightly industrialized urban area. 397
- Crittenden, J. C.**
—; Hand, D. W.; Loper, S. W.; Ari, M.; Luft, P.
Prediction of multicomponent adsorption equilibria using ideal adsorbed solution theory. 1037
- Cupitt, L. T.** See Kleindienst, T. E.; Shepson, P. B.
- Dalrymple, R. J.** See Snodgrass, W. J.
- Damste, J. S. S.** See De Leer, E. W. B.
- Dasch, J. M.**
Direct measurement of dry deposition to a polyethylene bucket and various surrogate surfaces. 721
- Dasgupta, P. K.** See Hwang, H.
- Davani, B.** See Eiceman, G. A.
- Davidson, C. I.**
—; Wiersma, G. B.; Brown, K. W.; Goold, W. D.; Mathison, T. P.; Reilly, M. T.
Airborne trace elements in Great Smoky Mountains, Olympic, and Glacier National Parks. 27
- Davison, W.**
—; Hilton, J.; Lishman, J. P.; Tutin, W. P.
Contemporary lake transport processes determined from sedimentary records of copper mining activity. 356
- De Galan, L.** See De Leer, E. W. B.
- Dehl, T. G.** See Kleopfer, R. D.
- De Leer, E. W. B.**
—; Damste, J. S. S.; Erkelens, C.; De Galan, L.
Identification of intermediates leading to chloroform and C-4 diacids in the chlorination of humic acid. 512
- DeMarco, J.** See Loper, J. C.
- De Sousa, F.** See Kringstad, K. P.
- Dietrich, A.** See Kamens, R.
- Dietz, R. N.** See Leaderer, B. P.
- Di Toro, D. M.**
—; Jeris, J. S.; Ciarcia, D.
Diffusion and partitioning of hexachlorobiphenyl in sediments. 1169
- Dodson, J. A.** See Eiceman, G. A.
- Donard, O. F. Y.**
—; Weber, J. H.
Behavior of methyltin compounds under simulated estuarine conditions. 1104
- Driscoll, C. T.** See Effler, S. W.; White, J. R.
—; Newton, R. M.
Chemical characteristics of Adirondack lakes. Individual lakes respond differently to acid deposition. 1018
- Easley, D. M.** See Kleopfer, R. D.
- Eaton, H. G.** See Fraser, M. E.
- Edney, E. O.** See Kleindienst, T. E.; Shepson, P. B.
- Effler, S. W.**
—; Driscoll, C. T.
Calcium chemistry and deposition in ionically enriched Onondaga Lake, New York. 716
- Eganhouse, R. P.**
—; Kaplan, I. R.
 α -Tocopherol acetate as an indicator of municipal waste contamination in the environment. 282
- Eiceman, G. A.**
—; Davani, B.; Wilcox, M. E.; Gardea, J. L.; Dodson, J. A.
High molecular weight hydrocarbons including polycyclic aromatic hydrocarbons in natural gas from consumer distribution pipelines and in pipeline residue. 603
- Eisenreich, S. J.** See Baker, J. E.
- Elzerman, A. W.** See Talbot, R. W.
- Engleman, E. E.** See Jackson, L. L.
- Eriksson, K. E.**
—; Kolar, M. C.
Microbial degradation of chlorolignins. 1086
- ; Kolar, M. C.; Ljungquist, P.; Kringstad, K. P.
Studies on microbial and chemical conversions of chlorolignins. 1219
- Erkelens, C.** See De Leer, E. W. B.
- Eynon, B. P.** See Holcombe, L. J.
- Fair, J. L.** See Capizzi, T.
- Falk-Petersen, I. B.** See Sydnes, L. K.
- Farzanah, F. F.**
—; Kaplan, C. R.; Yu, P. Y.; Hong, J.; Gentry, J. W.
Condition numbers as criteria for evaluation of atmospheric aerosol measurement techniques. 121
- Fehsenfeld, F. C.** See Roberts, J. M.
- Femia, R.**
—; Scypinski, S.; Love, L. J. C.
Fluorescence characteristics of polychlorinated biphenyl isomers in cyclodextrin media. 155
- Filby, R.** See Markowski, G. R.
- Formanski, L. J.** See Murphy, T. J.
- Fox, J. B.**
Distribution of mercury during simulated in-situ oil shale retorting. 316
- Franks, B. J.** See Goerlitz, D. F.
- Fraser, M. E.**
—; Eaton, H. G.; Sheinson, R. S.
Initial decomposition mechanisms and products of dimethyl methylphosphonate in an alternating current discharge. 946
- Frazier, G. C.** See Badin, E. J.
- Fuwa, K.** See Shiraishi, H.
- Galloway, J. N.** See Cosby, B. J.
- Gamble, D. S.** See Underdown, A. W.
- Garbarini, D. R.**
—; Lion, L. W.
Evaluation of sorptive partitioning of nonionic pollutants in closed systems by headspace analysis. 1122
- Gardea, J. L.** See Eiceman, G. A.
- Gentry, J. W.** See Farzanah, F. F.
- Giddings, J. C.** See Schure, M. R.
- Giger, W.** See Schwarzenbach, R. P.
- Gjessing, E. T.** See Becher, G.
- Glavas, S.**
—; Schurath, U.
Peroxyacetyl nitrate forming potential of five prototype hydrocarbons. 950
- Gleit, A.**
Estimation for small normal data sets with detection limits. 1201
- Godsy, E. M.** See Goerlitz, D. F.
- Goerlitz, D. F.**
—; Troutman, D. E.; Godsy, E. M.; Franks, B. J.
Migration of wood-preserving chemicals in contaminated groundwater in a sand aquifer at Pensacola, Florida. 955
- Goldstein, S. D.**
—; Hopke, P. K.
Environmental neutralization of polonium-218. 146
- Goncalves, M. d. L. S.**
—; Sigg, L.; Stumm, W.
Voltammetric methods for distinguishing between dissolved and particulate metal ion concentrations in the presence of hydrous oxides. A case study on lead(II). 141
- Goodman, R.** See Kamens, R.
- Goold, W. D.** See Davidson, C. I.
- Gordon, G. E.** See Tuncel, S. G.
- Gorse, R. A. Jr.** See Salmeen, I. T.
- Grosjean, D.** See McMurry, P. H.
Reactions of α -cresol and nitroresol with nitrogen oxides (NO_x) in sunlight and with ozone-nitrogen dioxide mixtures in the dark. 968
- ; Wall loss of gaseous pollutants in outdoor Teflon chambers. 1059
- ; Harrison, J.
Peroxyacetyl nitrate: comparison of alkaline hydrolysis and chemiluminescence methods. 749
- ; Response of chemiluminescence NO_x analyzers and ultraviolet ozone analyzers to organic air pollutants. 862
- Grossman, R. F.**
—; Holloway, R. W.
Concentrations of krypton-85 near the Nevada Test Site. 1128
- Gschwend, P. M.**
—; Wu, S.
On the constancy of sediment-water partition coefficients of hydrophobic organic pollutants. 90
- Gu, C. L.**
—; Rynard, C. M.; Hendry, D. G.; Mill, T.
Hydroxyl radical oxidation of isoprene. 151
- Gunderson, C. A.** See Squier, S. A.
- Gurol, M. D.**
—; Bremen, W. M.
Kinetics and mechanism of ozonation of free cyanide species in water. 804
- Haas, B. B. Jr.** See Kleopfer, R. D.
- Haas, C. N.**
—; Kaplan, B. M.
Toluene-humic acid association equilibria: isopiestic measurements. 643
- Hahn, C. J.** See Roberts, J. M.
- Halfman, B. M.** See Baker, J. E.
- Halfon, E.**
—; Regression method in ecotoxicology: a better formulation using the geometric mean functional regression. 747
- Hand, D. W.** See Crittenden, J. C.
- Hansen, S. H.** See Sydnes, L. K.
- Hansmann, D. D.**
—; Anderson, M. A.
Using electrophoresis in modeling sulfate, selenite, and phosphate adsorption onto goethite. 544
- Hansson, H. C.**
—; Nyman, C.
Microcomputer-controlled two size-fractionating aerosol sampler for outdoor environments. 1110
- Harger, W. P.** See Pitts, J. N. Jr.
- Harrison, F. L.**
—; Bishop, D. J.; Mallon, B. J.
Comparison of organic combustion products in fly ash collected by a Venturi wet scrubber and an electrostatic precipitator at a coal-fired power station. 186
- Harrison, J.** See Grosjean, D.
- Hartwell, T. D.** See Akland, G. G.
- Hassett, J. P.**
—; Millicic, E.
Determination of equilibrium and rate constants for binding of a polychlorinated biphenyl congener by dissolved humic substances. 638
- Hatakeyama, S.**
—; Tanonaka, T.; Weng, J.; Bandow, H.; Takagi, H.; Akimoto, H.
Ozone-cyclohexene reaction in air: quantitative analysis of particulate products and the reaction mechanism. 935
- Havas, M.**
—; Hutchinson, T. C.; Likens, G. E.
Reply to comments on "Red herrings in acid rain research". 646
- Hawthorne, S. B.**
—; Sievers, R. E.; Barkley, R. M.
Organic emissions from shale oil wastewaters and their implications for air quality. 992
- Heap, M. P.** See Cole, J. A.
- Heinen de Carlo, E.**
—; Thomas, D. M.
Removal of arsenic from geothermal fluids by adsorptive bubble flotation with colloidal ferric hydroxide. 538
- Helz, G. R.** See Jaworske, D. A.
- Hemmingsen, T. H.** See Sydnes, L. K.
- Hendry, D. G.** See Gu, C. L.
- Henrion, M.** See Morgan, M. G.
- Hilton, J.** See Davison, W.
- Hites, R. A.** See Behymer, T. D.; Jaffe, R.
- Hoffmann, M. R.** See Jacob, D. J.
- Hojnig, J.** See Staehelin, J.
- Holcombe, L. J.**
—; Eynon, B. P.; Switzer, P.
Variability of elemental concentrations in power plant ash. 615
- Holloway, R. W.** See Grossman, R. F.
- Hong, J.** See Farzanah, F. F.
- Hongslo, J. K.** See Becher, G.
- Hopke, P. K.** See Goldstein, S. D.
- Hopkins, G. D.** See Roberts, P. V.
- Hornberger, G. M.** See Cosby, B. J.
- Hornshy, A. G.** See Nkedi-Kizza, P.
- Hoshi, A.** See Yoshizumi, K.
- Howard, P. H.** See Banerjee, S.
- Hoves, J. E. Jr.** See Lewis, R. G.
- Huang, G. L.** See Miller, M. M.
- Hutchinson, T. C.** See Havas, M.
- Hwang, H.**
—; Dasgupta, P. K.
Thermodynamics of the hydrogen peroxide-water system. 255
- Inman, G. W. Jr.**
—; Johnson, J. D.
Kinetics of monobromamine disporportionation dibromamine formation in aqueous ammonia solutions. 287
- Innes, W. B.**
—; Comment on "Red herrings in acid rain research". 646

- Isaac, R. A.**
—; Morris, J. C.
Transfer of active chlorine from chlora= mine to nitrogenous organic compounds. 2. Mechanism. 810
- Iyer, D. R.** See Letterman, R. D.
- Jackson, D. E.** See Kleopfer, R. D.
- Jackson, L. L.**
—; Engleman, E. E.; Peard, J. L.
Determination of total sulfur in lichens and plants by combustion-infrared analysis. 437
- Jacob, D. J.**
—; Waldman, J. M.; Munger, J. W.; Hoff= mann, M. R.
Chemical composition of fogwater collected along the California coast. 730
- Jaffe, R.**
—; Hites, R. A.
Identification of new, fluorinated biphe= nyls in the Niagara River-Lake Ontario area. 736
- Jafvert, C. T.** See Valentine, R. L.
- Jaworske, D. A.**
—; Helz, G. R.
Rapid consumption of bromine oxidants in river and estuarine waters. 1188
- Jeris, J. S.** See Di Toro, D. M.
- Jiang, Z. P.** See Yonge, D. R.
- Jimenez, B. D.** See McCarthy, J. F.
- Johnson, J. D.** See Inman, G. W. Jr.
- Johnson, T. C.** See Baker, J. E.
- Johnson, T. R.** See Aklund, G. G.
- Jorgensen, A. D.** See Stetter, J. R.
—; Stetter, J. R.; Stamoudis, V. C.
Interactions of aqueous metal ions with organic compounds found in coal gasifi= cation: model systems. 919
- Kamens, R.**
—; Bell, D.; Dietrich, A.; Perry, J.; Good= man, R.; Claxton, L.; Tejada, S.
Mutagenic transformations of dilute wood smoke systems in the presence of ozone and nitrogen dioxide. Analysis of select= ed high-pressure liquid chromatography fractions from wood smoke particle extracts. 63
- Kane, D. A.** See Brumbaugh, W. G.
- Kaplan, B. M.** See Haas, C. N.
- Kaplan, C. R.** See Farzanah, F. F.
- Kaplan, I. R.** See Eganhouse, R. P.; Ka= wamura, K.
- Karickhoff, S. W.**
—; Morris, K. R.
Impact of tubificid oligochaetes on pollu= tant transport in bottom sediments. 51
- Karttunen, J. O.** See Nelson, D. M.
- Kaufherr, N.**
—; Shenasa, M.; Lichtman, D.
X-ray photoelectron spectroscopy studies of coal fly ashes with emphasis on depth profiling of submicrometer particle size fractions. 609
- Kawamura, K.**
—; Ng, L. L.; Kaplan, I. R.
Determination of organic acids (C₁-C₁₀) in the atmosphere, motor exhausts, and engine oils. 1082
- Keinath, T. M.** See Yonge, D. R.
- Kelly, N. A.**
—; Olson, K. L.; Wong, C. A.
Tests for fluorocarbon and other organic vapor release by fluorocarbon film bags. 361
- Kerkhoff, M. J.**
—; Lee, T. M.; Allen, E. R.; Lundgren, D. A.; Winefordner, J. D.
Spectral fingerprinting of polycyclic aro= matic hydrocarbons in high-volume ambient air samples by constant energy synchronous luminescence spectroscopy. 695
- Kiessler, S. L.** See Anderson, J. W.
- King, C. J.** See Mohr, D. H.
- Kleindienst, T. E.** See Shepson, P. B.
—; Shepson, P. B.; Edney, E. O.; Cupitt, L. T.; Claxton, L. D.
Mutagenic activity of the products of propylene photooxidation. 620
- Kleopfer, R. D.**
—; Easley, D. M.; Haas, B. B. Jr.; Deihl, T. G.; Jackson, D. E.; Wurrey, C. J.
Anaerobic degradation of trichloroethylene in soil. 277
- Knapp, K. T.** See Conner, W. D.
- Koda, S.**
—; Yoshikawa, K.; Okada, J.; Akita, K.
Reaction kinetics of nitrogen dioxide with methanol in the gas phase. 262
- Kolar, M. C.** See Eriksson, K. E.
- Kramlich, J. C.** See Cole, J. A.
- Kringsstad, K. P.** See Eriksson, K. E.
—; De Sousa, F.; Stroemberg, L. M.
Studies on the chlorination of chlorolig= nins and humic acid. 427
- Kuhn, E. P.**
—; Colberg, P. J.; Schnoor, J. L.; Wanner, O.; Zehnder, A. J. B.; Schwarzenbach, R. P.
Microbial transformations of substituted benzenes during infiltration of river water to groundwater: laboratory column studies. 961
- Kuwabara, J. S.**
—; Phosphorus-zinc interactive effects on growth by *Selenastrum capricornutum* (Chlorophyta). 417
- Langer, S. H.** See Pate, K. T.
- Langford, C. H.** See Underdown, A. W.
- Larson, R. A.** See Voudrias, E. A.
- Leaders, B. P.**
—; Schapp, L.; Dietz, R. N.
Evaluation of the perfluorocarbon tracer technique for determining infiltration rates in residences. 1225
- Lee, H. K.** See Cretney, J. R.
- Lee, L. C.** See Suto, M.
- Lee, T. M.** See Kerkhoff, M. J.
- Lesht, B. M.** See Streets, D. G.
- Letterman, R. D.**
—; Iyer, D. R.
Modeling the effects of hydrolyzed alumi= num and solution chemistry on floccula= tion kinetics. 673
- Leuenberger, C.** See Westall, J. C.
—; Ligocki, M. P.; Pankow, J. F.
Trace organic compounds in rain. 4. Identities, concentrations, and scavenging mechanisms for phenols in urban air and rain. 1053
- Lewis, R. G.**
—; Martin, B. E.; Sgontz, D. L.; Howes, J. E. Jr.
Measurement of fugitive atmospheric emissions of polychlorinated biphenyls from hazardous waste landfills. 986
- Lichtman, D.** See Kaufherr, N.
—; Mroczkowski, S.
Scanning electron microscopy and ener= gy-dispersive x-ray spectroscopy analysis of submicrometer coal fly ash particles. 274
- Ligocki, M. P.** See Leuenberger, C.
- Likens, G. E.** See Havas, M.
- Lindberg, S. E.**
—; Lovett, G. M.
Field measurements of particle dry deposi= tion rates to foliage and inert surfaces in a forest canopy. 238
- Lindskog, A.** See Brorstrom=Lunden, E.
- Linton, R. W.** See Cox, X. B. III.
- Lion, L. W.** See Garbarini, P. D.
- Lipari, F.**
—; Swarin, S. J.
2,4-Dinitrophenylhydrazine-coated Flori= sial sampling cartridges for the determina= tion of formaldehyde in air. 70
- Lipfert, F. W.**
—; Mortality and air pollution: is there a meaningful connection? 764
- Lishman, J. P.** See Davison, W.
- Ljungquist, P.** See Eriksson, K. E.
- Lockwood, R. N.** See Riggan, P. J.
- Loenning, S.** See Sydes, L. K.
- Loper, J. C.**
—; Tabor, M. W.; Rosenblum, L.; DeMar= co, J.
Continuous removal of both mutagens and mutagen-forming potential by an experimental full-scale granular activated carbon treatment system. 333
- Loper, S. W.** See Crittenden, J. C.
- Lopez, E. N.** See Riggan, P. J.
- Louw, R.** See Manion, J. A.
- Love, L. J. C.** See Femia, R.
- Lovett, G. M.** See Lindberg, S. E.
- Ludke, J. L.** See Schmitt, C. J.
- Luft, P.** See Crittenden, J. C.
- Lundgren, D. A.** See Kerkhoff, M. J.
- Luthy, R. G.** See Campbell, J. R.; Walters, R. W.
- McCarthy, J. F.**
—; Jimenez, B. D.
Interactions between polycyclic aromatic hydrocarbons and dissolved humic mate= rial: binding and dissociation. 1072
- McDonald, M. E.**
—; Acid deposition and drinking water. 772
- Mackay, D.** See Miller, M. M.
- Mackay, D. M.**
—; Roberts, P. V.; Cherry, J. A.
Transport of organic contaminants in groundwater. 384
- MacLeod, H.** See Biermann, H. W.
- McMurry, P. H.**
—; Grosjean, D.
Gas and aerosol wall losses in Teflon film smog chambers. 1176
- McQuerry, D. L.** See Anderson, J. W.
- Mage, D. T.** See Spengler, J. D.
—; Comment on: "Predicting future pollution exceedances under emission controls". 866
- Malaiyandi, M.** See Ramaswamy, S.
- Mallon, B. J.** See Harrison, F. L.
- Manion, J. A.**
—; Mulder, P.; Louw, R.
Gas-phase hydrogenolysis of polychlorobi= phenyls. 280
- Manzanares, E. R.** See Suto, M.
- Markowski, G. R.**
—; Filby, R.
Trace element concentration as a function of particle size in fly ash from a pulver= ized coal utility boiler. 796
- Martin, B. E.** See Lewis, R. G.
- Mathison, T. P.** See Davidson, C. I.
- Mauney, T.** See Schure, M.
- Means, J. C.** See Uhler, A. D.
- Mehlhoff, P.** See Nelson, D. M.
- Mehta, H.** See Capizzi, T.
- Meiners, B. G.** See Saltzman, B. E.
- Mendiratta, A. K.** See Brunelle, D. J.
- Merrill, E. G.**
—; Wade, T. L.
Carbonized coal products as a source of aromatic hydrocarbons to sediments from a highly industrialized estuary. 597
- Meyer, J. A.** See Murphy, T. J.
- Milicic, E.** See Hasset, J. P.
- Mill, T.** See Gu, C. L.
- Miller, M. M.**
—; Wasik, S. P.; Huang, G. L.; Shiu, W. Y.; Mackay, D.
Relationships between octanol-water partition coefficient and aqueous solubil= ity. 522
- Mirabella, V. A.** See Seigneur, C.
- Mohr, D. H.**
—; King, C. J.
Identification of polar organic compounds in coal-gasification condensate water by gas chromatography-mass spectrometry analysis of high-performance liquid chromatography fractions. 929
- Molton, L. S.** See Ricci, P. F.
- Monarca, S.** See Becher, G.
- Morgan, J. J.** See Bales, R. C.
- Morgan, M. G.**
—; Henrion, M.; Morris, S. C.; Amaral, D. A. L.
Uncertainty in risk assessment. 662
- Morris, J. C.** See Isaac, R. A.
- Morris, K. R.** See Karickhoff, S. W.
- Morris, S. C.** See Morgan, M. G.
- Mroczkowski, S.** See Lichtman, D.
- Mulder, P.** See Manion, J. A.
- Munger, J. W.** See Jacob, D. J.
- Munz, G.** See Roberts, P. V.
- Murphy, T. J.**
—; Formanski, L. J.; Brownawell, B.; Mey= er, J. A.
Polychlorinated biphenyl emissions to the atmosphere in the Great Lakes region. Municipal landfills and incinerators. 942
- Myers, M. N.** See Schure, M. R.
- Naimie, H.** See Capizzi, T.
- Namie, G. R.** See Shepson, P. B.
- Natusch, D. P. S.** See Schure, M.
- Nelson, D. M.**
—; Penrose, W. R.; Karttunen, J. O.; Mehl= hoff, P.
Effects of dissolved organic carbon on the adsorption properties of plutonium in natural waters. 127
- Neubecker, T. A.**
—; Determination of alkylthoxylated sulfates in wastewaters and surface waters. 1232
- Newton, R. M.** See Driscoll, C. T.
- Ng, L. L.** See Kawamura, K.
- Niimi, A. J.** See Oliver, B. G.
- Niki, H.** See Wu, C. H.
- Nkedi-Kizza, P.**
—; Rao, P. S. C.; Hornsby, A. G.
Influence of organic cosolvents on sorption of hydrophobic organic chemicals by soils. 975

- Nyman, S.** See Hansson, H. C.
- O'Brien, G. A.** See Aggett, J.
- Oestgaard, K.** See Sydnæs, L. K.
- Okada, J.** See Koda, S.
- Oliver, B. G.**
—; Nimitz, A. J.
Bioconcentration factors of some halogenated organics for rainbow trout: limitations in their use for prediction of environmental residues. 842
- Oliver, R. M.**
Predicting future pollution exceedances under emission controls. 225
Rebuttal to: "Predicting future pollution exceedances under emission controls". 867
- Ollis, D. F.**
Contaminant degradation in water. 480
- Olmez, I.** See Tuncel, S. G.
- Olson, B. H.** See Wolfe, R. L.
- Olson, K. L.** See Kelly, N. A.
- Oppenheimer, L.** See Capizzi, T.
- Otsuki, A.** See Shiraishi, H.
- Otz, W. R.**
Total human exposure. 880
- Overcamp, T. J.**
A theory for critical flow through hypodermic needles. 1134
- Pankow, J. F.** See Leuenberger, C.
- Parrington, J. R.** See Tuncel, S. G.
- Parrish, R.**
Acute toxicity screening of water pollutants using a bacterial electrode. Comments. 871
- Pate, K. T.**
—; Langer, S. H.
Electrogenative reduction of nitric oxide for pollution abatement. 371
- Peard, J. L.** See Jackson, L. L.
- Penrose, W. R.** See Nelson, D. M.
- Perry, J.** See Kamens, R.
- Pettersson, B.** See Alsborg, T.
- Pierson, W. R.** See Salmeen, I. T.
- Pilkington, N. H.** See Shiraishi, H.
- Pittman, J. H.** See Shephson, P. B.
- Pitts, J. N. Jr.** See Atkinson, R.; Biermann, H. W.
—; Sweetman, J. A.; Zielinska, B.; Atkinson, R.; Winer, A. M.; Harger, W. P.
Formation of nitroarenes from the reaction of polycyclic aromatic hydrocarbons with dinitrogen pentoxide. 1115
- Porter, W. R.**
Comment on: "Equilibrium adsorption of polycyclic aromatic hydrocarbons from water onto activated carbon". 869
- Post, J.**
—; Buseck, P. R.
Quantitative energy dispersive analysis of lead halide particles from the Phoenix urban aerosol. 682
- Poznanska, K.** See Yonge, D. R.
- Ramaswamy, S.**
—; Malaiyandi, M.; Buchanan, G. W.
Phase-transfer-catalyzed methylation of hydroxyaromatic acids, hydroxyaromatic aldehydes, and aromatic polycarboxylic acids. 507
- Rannug, U.** See Alsborg, T.
- Rao, P. S. C.** See Nkedi-Kizza, P.
- Rapsomanikis, S.** See Craig, P. J.
- ; Weber, J. H.**
Environmental implications of methylation of tin(II) and methyltin(IV) ions in the presence of manganese dioxide. 352
- Reichert, W. L.** See Varanasi, U.
- Reilly, M. T.** See Davidson, C. I.
- Reinhardt, P. A.** See Ashbrook, P. C.
- Ricci, P. F.**
—; Molton, L. S.
Regulating cancer risks. 473
- Riggan, P. J.**
—; Lockwood, R. N.; Lopez, E. N.
Deposition and processing of airborne nitrogen pollutants in Mediterranean-type ecosystems of southern California. 781
- Riojas, A. H.** See Roberts, P. V.
- Roberts, J. M.**
—; Hahn, C. J.; Fehsenfeld, F. C.; Warneck, J. M.; Albritton, D. L.; Sievers, R. E.
Monoterpene hydrocarbons in the nighttime troposphere. 364
- Roberts, P. V.** See Mackay, D. M.
- ; Hopkins, G. D.; Munz, C.; Riojas, A. H.**
Evaluating two-resistance models for air stripping of volatile organic contaminants in a countercurrent, packed column. 164
- Romert, L.** See Alsborg, T.
- Rosenblum, L.** See Loper, J. C.
- Ryan, P. A.** See Cohen, Y.
- Rynard, C. M.** See Gu, C. L.
- Saksa, D. J.**
—; Smart, R. B.
Chemiluminescent analysis of chlorine dioxide with a membrane flow cell. 450
- Salmeen, I. T.**
—; Gorse, R. A. Jr.; Pierson, W. R.
Ames assay chromatograms of extracts of diesel exhaust particles from heavy-duty trucks on the road and from passenger cars on a dynamometer. 270
- Saltzman, B. E.**
—; Chohai, J.; Schafer, L. J.; Yeager, D. W.; Meiners, B. G.; Svetlik, J.
Concentrations of six metals in the air of eight cities. 328
- Samuelson, G. S.** See Cole, J. A.
- Sanborn, H. R.** See Varanasi, U.
- Saxena, P.** See Seigneur, C.
- Schaap, L.** See Leaderer, B. P.
- Schafer, L. J.** See Saltzman, B. E.
- Schaffner, C.** See Schwarzenbach, R. P.
- Schlotzauer, P. F.** See Zepp, R. G.
- Schmitt, C. J.**
—; Ludke, J. L.
Comment on "Comparison of the carcinogenic risks from fish vs. groundwater contamination by organic compounds". 645
- Schnoor, J. L.** See Kuhn, E. P.
- Schurath, U.** See Glavas, S.
- Schure, M.**
—; Soltys, P. A.; Natusch, D. F. S.; Mauney, T.
Surface area and porosity of coal fly ash. 82
- Schure, M. R.**
—; Myers, M. N.; Caldwell, K. D.; Byron, C.; Chan, K. P.; Giddings, J. C.
Separation of coal fly ash using continuous steric field-flow fractionation. 686
- Schwarzenbach, R. P.** See Kuhn, E. P.; Westall, J. C.
—; Giger, W.; Schaffner, C.; Wanner, O.
Groundwater contamination by volatile halogenated alkanes: abiotic formation of volatile sulfur compounds under anaerobic conditions. 322
- Schweitzer, G. E.**
—; Black, S. C.
Monitoring statistics. An important tool for groundwater and soil studies. 1026
- Scypinski, S.** See Femia, R.
- Seeker, W. R.** See Cole, J. A.
- Seigneur, C.**
—; Saxena, P.; Mirabella, V. A.
Diffusion and reaction of pollutants in stratus clouds: application to nocturnal acid formation in plumes. 821
- Seiler, W.** See Conrad, R.
- Selvidge, W. J.** See Squier, S. A.
- Sgontz, D. L.** See Lewis, R. G.
- Shannon, J. D.** See Streets, D. G.
- Sheinson, R. S.** See Fraser, M. E.
- Shenasa, M.** See Kaufherr, N.
- Shephson, P. B.** See Kleindienst, T. E.
—; Edney, E. O.; Kleindienst, T. E.; Pittman, J. H.; Namie, G. R.; Cupitt, L. T.
Production of organic nitrates from hydroxyl and nitrate radical reaction with propylene. 849
—; Kleindienst, T. E.; Edney, E. O.; Cupitt, L. T.; Claxton, L. D.
The mutagenic activity of the products of ozone reaction with propylene in the presence and absence of nitrogen dioxide. 1094
—; Kleindienst, T. E.; Edney, E. O.; Namie, G. R.; Pittman, J. H.; Cupitt, L. T.; Claxton, L. D.
Mutagenic activity of irradiated toluene nitrogen oxide (NO₂/air) mixtures. 249
- Shiraishi, H.**
—; Pilkington, N. H.; Otsuki, A.; Fuwa, K.
Occurrence of chlorinated polynuclear aromatic hydrocarbons in tap water. 585
- Shiu, W. Y.** See Miller, M. T.
- Shoup, T. D.** See Chiou, C. T.
- Sievers, R. E.** See Hawthorne, S. B.; Roberts, J. M.
- Sigg, L.** See Goncalves, M. d. L. S.
- Simpson, K. W.** See Brown, M. P.
- Singleton, D. A.** See Brunelle, D. J.
- Sink, R. M.** See Zepp, R. G.
- Skare, S.** See Sydnæs, L. K.
- Sloan, R. J.** See Brown, M. P.
- Smart, R. B.** See Saksa, D. J.
—; Stewart, E. E.
Differential pulse anodic stripping voltammetry of cadmium(II) at a membrane-covered electrode: measurement in the presence of model organic compounds. 137
- Snodgrass, W. J.**
Lake Ontario oxygen model. 2. Errors associated with estimating transport across the thermocline. 180
—; Dalrymple, R. J.
Lake Ontario oxygen model. 1. Model development and application. 173
- Snoeyink, V. L.** See Voudrias, E. A.
- Soczek, M. L.** See Spengler, J. D.
- Soltys, P. A.** See Schure, M.
—; Treitman, R. D.; Tosteson, T. D.; Mage, D. T.; Soczek, M. L.
Personal exposures to respirable particulates and implications for air pollution epidemiology. 700
- Squier, S. A.**
—; Taylor, G. E. Jr.; Selvidge, W. J.; Gunderson, C. A.
Effect of ethylene and related hydrocarbons on carbon assimilation and transpiration in herbaceous and woody species. 432
- Stachelin, J.**
—; Hoigne, J.
Decomposition of ozone in water in the presence of organic solutes acting as promoters and inhibitors of radical chain reactions. 1206
- Stamoudis, V. C.** See Jorgensen, A. D.; Stetter, J. R.
- Stanforth, R. R.** See Anderson, M. A.
- Stauffer, R. E.**
Use of solute tracers released by weathering to estimate groundwater inflow to seepage lakes. 405
- Stein, J. E.** See Varanasi, U.
- Stenberg, U.** See Alsborg, T.
- Stetter, J. R.** See Jorgensen, A. D.
—; Stamoudis, V. C.; Jorgensen, A. D.
Interactions of aqueous metal ions with organic compounds found in coal gasification: process condensates. 924
- Stevens, R. K.** See Tuncel, S. G.
- Stewart, E. E.** See Smart, R. B.
- Strandell, M.** See Alsborg, T.
- Streets, D. G.**
—; Lesht, B. M.; Shannon, J. D.; Veselka, T. D.
Climatological variability. 887
- Stroemberg, L. M.** See Kingstad, K. P.
- Stumm, W.** See Goncalves, M. d. L. S.
- Sundvall, A.** See Alsborg, T.
- Suto, M.**
—; Manzanares, E. R.; Lee, L. C.
Detection of sulfuric acid aerosols by ultraviolet scattering. 815
- Svetlik, J.** See Saltzman, B. E.
- Swallow, W. H.** See Cretney, J. R.
- Swarin, S. J.** See Lipari, F.
- Sweetman, J. A.** See Pitts, J. N. Jr.
- Switzer, P.** See Holcombe, L. J.
- Sydnæs, L. K.**
—; Hemmingsen, T. H.; Skare, S.; Hansen, S. H.; Falk-Petersen, I. B.; Loening, S.; Oestgaard, K.
Seasonal variations in weathering and toxicity of crude oil on seawater under Arctic conditions. 1076
- Tabor, M. W.** See Loper, J. C.
- Tagaki, H.** See Hatakeyama, S.
- Talbot, R. W.** See Cofer, W. R. III.
—; Elzerman, A. W.
Acidification of southern Appalachian lakes. 552
- Tanonaka, T.** See Hatakeyama, S.
- Tare, V.**
—; Venkobachar, C.
New conceptual formulation for predicting filter performance. 497
- Taylor, G. E. Jr.** See Squier, S. A.
- Taylor, M. C.** See Cretney, J. R.
- Tejada, S.** See Kamens, R.
- Tejedor-Tejedor, M. I.** See Anderson, M. A.
- Thomas, D. M.** See Heinen de Carlo, E.
- Tosteson, T. D.** See Spengler, J. D.
- Treitman, R. D.** See Spengler, J. D.

- Troutman, D. E.** See Goerlitz, D. F.
- Tuazon, E. C.**
—; Atkinson, R.; Carter, W. P. L.
Atmospheric chemistry of *cis*- and *trans*-3-hexene-2,5-dione. 265
- Tullis, D. L.** See Banerjee, S.
- Tuncel, S. G.**
—; Olmez, I.; Parrington, J. R.; Gordon, G. E.; Stevens, R. K.
Composition of fine particle regional sulfate component in Shenandoah Valley. 529
- Tutin, W. P.** See Davison, W.
- Uhler, A. D.**
—; Means, J. C.
Reaction of dissolved chlorine with surficial sediment: oxidant demand and production of trihalomethanes. 340
- Underdown, A. W.**
—; Langford, C. H.; Gamble, D. S.
Light scattering studies of the relationship between cation binding and aggregation of a fulvic acid. 132
- Valentine, R. L.**
—; Jafvert, C. T.
Comment on "Kinetics of monobromamine disproportionation-dibromamine formation in aqueous ammonia solutions". 286
- Van Cauwenberghe, K. A.** See Van Vaeck, L.
- Van Noort, P. C. M.**
—; Wondergem, E.
Scavenging of airborne polycyclic aromatic hydrocarbons by rain. 1044
- Van Vaeck, L.**
—; Van Cauwenberghe, K. A.
Characteristic parameters of particle size distributions of primary organic constituents of ambient aerosols. 707
- Varanasi, U.**
—; Reichert, W. L.; Stein, J. E.; Brown, D. W.; Sanborn, H. R.
Bioavailability and biotransformation of aromatic hydrocarbons in benthic organisms exposed to sediment from an urban estuary. 836
- Venkobachar, C.** See Tare, V.
- Veselka, T. D.** See Streets, D. G.
- Vo-Dinh, T.**
Development of a dosimeter for personnel exposure to vapors of polyaromatic pollutants. 997
- Voice, T. C.**
—; Weber, W. J. Jr.
Sorbent concentration effects in liquid/solid partitioning. 789
- Voudrias, E. A.**
—; Larson, R. A.; Snoeyink, V. L.
Effects of activated carbon on the reactions of free chlorine with phenols. 441
- Wade, T. L.** See Merrill, E. G.
- Waldman, J. M.** See Jacob, D. J.
- Walters, R. W.**
—; Luthy, R. G.
Rebuttal to: "Equilibrium adsorption of polycyclic aromatic hydrocarbons from water onto activated carbon". 870
- Wanner, O.** See Kuhn, E. P.; Schwarzenbach, R. P.
- Ward, N. R.** See Wolfe, R. L.
- Warnock, J. M.** See Roberts, J. M.
- Wasik, S. P.** See Miller, M. M.
- Weber, J. H.** See Donard, O. F. X.; Rapso-manikis, S.
- Weber, W. J. Jr.** See Voice, T. C.
- Weng, J.** See Hatakeyama, S.
- Werner, M. B.** See Brown, M. P.
- Westall, J. C.**
—; Leuenberger, C.; Schwarzenbach, R. P.
Influence of pH and ionic strength on the aqueous-nonaqueous distribution of chlorinated phenols. 193
- Westerholm, R.** See Alsberg, T.
- White, J. R.**
—; Driscoll, C. T.
Lead cycling in an acidic Adirondack lake. 1182
- Whitmore, R. W.** See Akland, G. G.
- Wiersma, G. B.** See Davidson, G. I.
- Wilcox, M. E.** See Eiceman, G. A.
- Winefordner, J. D.** See Kerkhoff, M. J.
- Winer, A. M.** See Atkinson, R.; Biermann, H. W.; Pitts, J. N. Jr.
- Witz, S.**
Effect of environmental factors on filter alkalinity and artifact formation. 831
- Wolfe, R. L.**
—; Ward, N. R.; Olson, B. H.
Interference in the bactericidal properties of inorganic chloramines by organic nitrogen compounds. 1192
- Wondergem, E.** See Van Noort, P. C. M.
- Wong, C. A.** See Kelly, N. A.
- Wright, G. J.** See Cretney, J. R.
- Wright, R. F.** See Cosby, B. J.
- Wu, C. H.**
—; Niki, H.
Fluorescence spectroscopic study of kinetics of gas-surface reactions between nitrogen dioxide and adsorbed pyrene. 1089
- Wu, S.** See Gschwend, P. M.
- Wurrey, C. J.** See Kleopfer, R. D.
- Yeager, D. W.** See Saltzman, B. E.
- Yonge, D. R.**
—; Keinath, T. M.; Poznanska, K.; Jiang, Z. P.
Single-solute irreversible adsorption on granular activated carbon. 690
- Yoshikawa, K.** See Koda, S.
- Yoshizumi, K.**
—; Hoshi, A.
Size distributions of ammonium nitrate and sodium nitrate in atmospheric aerosols. 258
- Yu, P. Y.** See Farzanah, F. F.
- Zehnder, A. J. B.** See Kuhn, E. P.
- Zepp, R. G.**
—; Schlotzhauer, P. F.; Sink, R. M.
Photosensitized transformations involving electronic energy transfer in natural waters: role of humic substances. 74
- Zielinska, B.** See Pitts, J. N. Jr.

KEYWORD INDEX TO VOLUME 19, 1985

- Ac discharge decompn methylphosphonate 946
 Academic institution hazardous waste management 1150
 Acid arom methylation 507
 Acid deposition drinking water review 772
 Acid deposition redn climat variability 887
 Acid fog compn California coast 730
 Acid lake lead cycle aluminum 1182
 Acid org detn atm exhaust 1082
 Acid rain lake Appalachians US 552
 Acid rain research polemic 646
 Acidification catchment time scale 1144
 Acidification lake atm acid deposition 1018
 Activated carbon mutagen removal water 333
 Activated carbon phenol reaction chlorine 441
 Adsorption aq arom carbon polemic 869 870
 Adsorption crystn ferrihydrate silicon effect 1048
 Adsorption equil multicomponent caln theory 1037
 Adsorption phenol active carbon 690
 Adsorption phosphate coagulation kinetics goethite 632
 Adsorption plutonium sediment org colloidal 127
 Aerosol atm ammonium sodium nitrate 258
 Aerosol atm dry deposition forest 238
 Aerosol atm org particle size 707
 Aerosol formation cyclohexene ozone reaction 935
 Aerosol lead halide Phoenix Arizona 682
 Aerosol sampler air analysis 1110
 Aerosol smog chamber wall loss 1176
 Aerosol sulfate pollution mortality assessment 682
 Aggregation fulvic acid cation binding 132
 Air analysis org acid 1082
 Air chlorobiphenyl emission sampling 986
 Air infiltration building perfluorodimethylcyclobutane tracer 1225
 Air nitrogen oxide ozone detn 862
 Air peroxyacetyl nitrate detn method 749
 Air pollutant loss smog chamber 1059
 Air pollutant phenol scavenging mechanism 1053
 Air pollution carbon monoxide exposure 911
 Air pollution coal firing 1065
 Air pollution control climat variability 887
 Air pollution cresol reaction 968
 Air pollution cyclohexene ozone reaction 935
 Air pollution effect mortality review 764
 Air pollution hydrocarbon mutagen formation 620
 Air pollution krypton 85 US 1128
 Air pollution nitro polyarom hydrocarbon 1115
 Air pollution PCB hazardous landfill 986
 Air pollution sampling fluoropolymer 361
 Air pollution spent shale cooling 992
 Air pollution sulfur detn lichen 437
 Air polyarom hydrocarbon sampling detn 695
 Air polyarom hydrocarbon scavenging rain 1044
 Air stripping volatile org model 164
 Air sulfate detn artifact formation 831
 Airborne particulate polyarom hydrocarbon photolysis 1004
 Airborne polyarom occupational exposure monitor 397
 Airborne trace element remote US 27
 Aldehyde arom methylation 507
 Aldehyde formation cyclohexene ozone reaction 935
 Aliph compd coal fly ash 186
 Aliph hydrocarbon atm aerosol particle size 707
 Aliph hydrocarbon octanol water partition 628
 Alkane coal fly ash 186
 Alkyl filter sulfate artifact formation 831
 Alkyl halide water pollutant transformation 322
 Alkyl sulfide formation groundwater pollution 322
 Alkylthioxylated sulfate detn water wastewater 1232
 Aluminum collector dry deposition atm 721
 Aluminum hydroxide flocculation kinetics 673
 Aluminum lead cycle acid lake 1182
 Aluminum Micropterus 828
 Ames assay chromatogram diesel exhaust 270
 Ammonia aq bromamine disproportionation kinetics polemic 286 287
 Ammonia fluorine pollution flue gas 1099
 Ammonium sodium nitrate atm aerosol 258
 Anaerobic biodegrdn trichloroethylene soil 277
 Aniline coal gasification tar 924
 Anthracene reaction hydroxyl radical kinetics 244
 Aq soly aliph hydrocarbon 628
 Aquatic environment methylation divalent tin 352
 Aquatic human chlorination mutagen formation 422
 Aquatic sediment hexachlorobiphenyl diffusion partitioning 1169
 Aquatic toxicity statistical evaluation 35
 Aquifer biodegrdn dichlorobenzene dimethylbenzene 961
 Aquifer org pollutant transport review 384
 Arene reaction hydroxyl radical kinetics 244
 Arom aq adsorption carbon polemic 869 870
 Arom compd coal fly ash 186
 Arom hydrocarbon metab benthic organism 836
 Arom hydrocarbon polycyclic humic substance 1072
 Arom hydrocarbon polycyclic luminescence spectrometry 695
 Arom hydrocarbon polycyclic sampling artifact 313
 Arom hydrocarbon reaction dinitrogen pentoxide 1115
 Arom hydroxy aldehyde methylation 507
 Arom partition UNIFAC group contribution 980
 Arom polycyclic hydrocarbon natural gas 603
 Arom polycyclic hydrocarbon scavenging rain 1044
 Arom polycyclic photolysis airborne particle 1004
 Arsenic cycling lake New Zealand 231
 Arsenic removal geothermal power wastewater 538
 Artifact polycyclic arom hydrocarbon sampling 313
 Artifact sulfate formation filter alky 831
 Aryl hydrocarbon hydroxylase exhaust particulate 43
 Ash coal compn power plant 615
 Ash fly size fractionation method 686
 Atm acid deposition lake acidification 1018
 Atm aerosol ammonium nitrate sodium 258
 Atm aerosol dry deposition forest 238
 Atm aerosol org particle size 707
 Atm dry deposition measurement surface 721
 Atm nitrogen deposition water pollution 781
 Atm particulate photolysis polyarom hydrocarbon 1004
 Bacterial electrode water pollutant polemic 871
 Bactericidal activity chloramine interference organonitrogen 1192
 Bag fluoropolymer fluorocarbon release 361
 Bass organ aluminum 828
 Below detection limit data estn 1201
 Benthic organism arom hydrocarbon metab 836
 Benzene vapor sorption soil Woodburn 1196
 Biacetyl photolysis kinetics 968
 Bioavailability chromium ferrochrome smelter dust 345
 Bioconcn haloorg rainbow trout 842
 Bioconcn org partition lipid water 57
 Biodegrdn anaerobic trichloroethylene soil 277
 Biodegrdn chlorophenol modeling 374
 Biodegrdn dichlorobenzene dimethylbenzene aquifer 961
 Biphenyl chlorinated vapor pressure method 500
 Biphenyl chloro identification cyclodextrin fluorometry 155
 Biphenyl fluoromethylated chlorinated water pollution 736
 Biphenyl polychlorinated emission hazardous landfill 986
 Biphenyl polychlorinated gas phase hydrolysis 289
 Biphenyl polychlorinated Henrys law 590
 Biphenyl polychlorinated removal transformer oil 740
 Biphenyl reaction hydroxyl gas phase 462
 Bleaching pulp chlorination pollution chlorination 427
 Bleaching pulp wastewater microbial degrdn 1086
 Boiler firing line sorbent 1065
 Bromamine disproportionation kinetics ammonia polemic 286 287
 Bromine reaction org matter estuary 1188
 Bromoalkane pollutant sulfide formation groundwater 322
 Building perfluorodimethylcyclobutane tracer air 1225
 By promoter inhibitor aq ozone decompn 1206
 Cadmium detn water surfactant presence 137
 Calcination sorbent sulfur dioxide 1065
 Calcite formation lake New York 716
 Calcium chem lake New York 716
 Calcium dry deposition forest canopy 238
 Calcium pollution lake sediment transport 356
 Cancer risk regulation std review 473
 Carbon activated mutagen removal water 333
 Carbon activated phenol reaction chlorine 441
 Carbon active phenol adsorption 690
 Carbon adsorption aq arom polemic 869 870
 Carbon metab ethylene plant photosynthesis 432
 Carbon monoxide formation soil org matter 1165
 Carbon monoxide human exposure measurement 911
 Carboxylation phenol chlorine activated carbon 441
 Carboxylic acid atm aerosol particle size 707
 Carboxylic acid detn atm exhaust 1082
 Carboxylic acid formation cyclohexene ozone reaction 935
 Carcinogen containment soil humus formation 1132
 Carcinogen fish water pollution polemic 645 646
 Catchment acidification time scale 1144
 Cation binding fulvic acid aggregation 132
 Chem characterization Adirondack lake 1018
 Chem microbial transformation chlorolignin 1219
 Chemiluminescence chlorine dioxide detn water 450
 Chemiluminescence peroxyacetyl nitrate detn 749
 Chloramine bactericidal activity interference organonitrogen 1192
 Chlorinated biphenyl vapor pressure method 500

- Chlorinated fluoromethylated biphenyl water pollution 736
 Chlorinated polyarom tap water Japan 585
 Chlorination aquatic human mutagen formation 422
 Chlorination chlorolignin reaction product 427
 Chlorination humic acid chlorinated product 512
 Chlorination organonitrogen compd chloroa= mine mechanism 810
 Chlorination phenol chlorine activated carbon 441
 Chlorine dioxide detn water chemiluminescence 450
 Chlorine reaction org adsorbed sediment 340
 Chlorine reaction phenol activated carbon 441
 Chloro hydrocarbon nepheloid layer lake 854
 Chloroalkane pollutant sulfide formation groundwater 322
 Chloroamine chlorination organonitrogen compd mechanism 810
 Chlorobenzene vapor sorption soil Woodburn 1196
 Chlorobiphenyl decompn potassium hydroxide polyoxyethylene 740
 Chlorobiphenyl Hudson River US review 656
 Chlorobiphenyl partitioning water sediment 90
 Chlorobiphenyl reaction hydroxyl kinetics 462
 Chlorobiphenyl waste hydrogenolysis 280
 Chloroform formation humic acid chlorination 512
 Chlorohydroxybiphenyl formation phenol chlorine carbon 441
 Chlorolignin chem microbial transformation 1219
 Chlorolignin chlorination reaction product 427
 Chlorolignin wastewater degrdn sporotrichum pulverulentum 1086
 Chlorophenol biodegrdn modeling 374
 Chlorophenol formation chlorolignin chlorination 427
 Chlorophenol partition pH ionic strength 193
 Chromatog gas mass spectroscopy acid 1082
 Chromatog natural gas residue 603
 Chromium air pollution urban US 328
 Chromium cadmium air pollution urban US 328
 Chromium speciation ferrochrome smelter dust 345
 Chrysole water surface charge adsorption 1213
 Climatol variability acid deposition redn 887
 Cloud flue gas pollutant transformation 821
 Coagulation kinetics goethite phosphate adsorption 632
 Coal ash compn power plant 615
 Coal combustion fine particulate Virginia 529
 Coal combustion gas sorbent review 894
 Coal firing lime sorbent 1065
 Coal fly ash compn depth 609
 Coal fly ash compn morphol 274
 Coal fly ash fume compn 796
 Coal fly ash org constituent 186
 Coal gasification tar water partition 919
 Coal gasification tar water partitioning 924
 Coal gasification wastewater org identification 929
 Coal power plant air pollution 1099
 Coal product polyarom sediment Virginia 597
 Colloidal silica lead voltammetry water 141
 Combustion coal lime sorbent 1065
 Combustion fluidized bed sorbent review 894
 Combustion plant sulfur detn 437
 Concn sampling trace gas air 557
 Condensate natural gas residue compn 603
 Containment carcinogen soil humus formation 1132
 Continuous steric field flow fractionation 686
 Cooling shale spent wastewater emission 992
 Copper pollution lake sediment transport 356
 Copper water coal tar partition 919
 Creosote sediment polyarom estuary Virginia 597
 Creosote waste groundwater pollution Florida 955
 Cresol reaction nitrogen oxide ozone 968
 Crit flow air flow regulation 1134
 Crystn adsorption ferrihydrate silicon effect 1048
 Cyanide ozonation kinetics aq soln 804
 Cyclodextrin fluorometry PCB identification 155
 Cyclohexene reaction ozone product mechanism 935
 Data analysis estn statistics normal 1201
 DDE benthic nepheloid layer lake 854
 Death air pollutant cause review 764
 Decompn methylphosphonate ac discharge 946
 Degrdn chlorolignin wastewater sporotrichum pulverulentum 1086
 Design expt airborne particulate 121
 Dicarboxylic acid formation humic acid chlorination 512
 Dichlorobenzene biodegrdn river infiltration groundwater 961
 Dichlorobenzene vapor sorption soil Woodburn 1196
 Dichlorobenzidine containment soil ferulic acid 1132
 Dichloroethylene formation trichloroethylene biodegrdn soil 277
 Diesel exhaust particulate mutagenicity chromatogram 270
 Diffusion partitioning hexachlorobiphenyl aquatic sediment 1169
 Diffusion polonium 218 gas 146
 Dimerization phenol chlorine activated carbon 441
 Dimethylbenzene biodegrdn river infiltration groundwater 961
 Dimethylfuran photooxidn water humus sensitization 74
 Dinitrogen pentoxide polycyclic arom hydrocarbon 1115
 Dinitrophenylhydrazine sampling formaldehyde air 70
 Disinfection water chlorolignin mutagen formation 427
 Dispersant oil spill seawater evaluation 454
 Disproportionation bromamine aq ammonia kinetics polemic 286
 Disproportionation bromamine aq ammonia polemic 287
 Drinking water acid deposition review 772
 Drinking water chlorinated polyarom Japan 585
 Dust smelter ferrochrome chromium speciation 345
 Ecotoxicol analysis regression method 747
 Electroredn nitric oxide flue gas 371
 Electrostatic precipitator fly ash org 186
 Engine oil analysis org acid 1082
 Environment aquatic methylation divalent tin 352
 Environment arom natural gas pipeline 603
 Environment mercury shale retorting 316
 Environment pollutant transport multimedia modeling 412
 Environment pollution sewage tocopheryl acetate 282
 Environmental analysis data estn 1201
 Environmental pollution risk assessment uncertainty 662
 Environmental pollution toxicol coal tar 924
 Epidemiol respirable particulate personal exposure 700
 Estn small normal data set 1201
 Estuarine condition methylin compd behavior 1104
 Estuary org matter reaction bromine 1188
 Estuary sediment arom hydrocarbon metab 836
 Estuary sediment polyarom source Virginia 597
 Ethylene plant carbon metab photosynthesis 432
 Exhaust diesel particulate mutagenicity chromatogram 270
 Exhaust gas formaldehyde detn 70
 Exhaust gas particulate compn toxicity 43
 Exhaust methyl nitrite methanol fuel 262
 Exhaust motor analysis org acid 1082
 Exhaust polyarom hydrocarbon sampling detn 695
 Exhaust polyarom hydrocarbon urban air 397
 Ferric hydroxide arsenic removal flotation 538
 Ferrihydrate crystn adsorption silicon effect 1048
 Ferrochrome smelter dust chromium speciation 345
 Ferulic acid dichlorobenzidine containment soil 1132
 Filter alkyl sulfate artifact formation 831
 Filter collector dry deposition atm 721
 Filter water wastewater performance model 497
 Firing coal lime sorbent 1065
 Fish carcinogen water pollution polemic 645 646
 Fish PCB Hudson River US review 656
 Fish sediment org ratio polemic 198 199
 Flocculation kinetics hydrolyzed aluminum modeling 673
 Florisil dinitrophenylhydrazine coated sampler formaldehyde 70
 Flotation arsenic removal geothermal wastewater 538
 Flow hypodermic needle air sampling 1134
 Flue gas fluorine ammonia pollution 1099
 Flue gas fly ash size monitor 458
 Flue gas incinerator PCB US 942
 Flue gas nitric oxide electroredn 371
 Flue gas pollutant transformation cloud 821
 Flue gas polyarom hydrocarbon urban air 397
 Flue gas sampling polyarom hydrocarbon 313
 Fluidized bed combustion sorbent review 894
 Fluorine ammonia pollution flue gas 1099
 Fluoromethylated chlorinated biphenyl water pollution 736
 Fluoromethylbiphenyl Niagara River New York 736
 Fluorometry PCB identification cyclodextrin 155
 Fluoropolymer film fluorocarbon release 361
 Fluoropolymer smog chamber wall loss 1059
 Fly ash coal compn depth 609
 Fly ash coal compn morphol 274
 Fly ash coal org constituent 186
 Fly ash compn particle size 796
 Fly ash size fractionation method 686
 Fly ash size monitor flue gas 458
 Fog water compn California coast 730
 Forest canopy particle dry deposition 238
 Formaldehyde detn air exhaust gas 70
 Fractionation sampler two size 1110
 Fractionation method fly ash size 686
 Freshwater acidification quan model 1144
 Fulvic acid aggregation cation binding 132
 Fulvic acid methyltin removal soln 1104
 Fume coal fly ash compn 796
 Furan reaction nitrate radical kinetics 87
 Gas chromatog mass spectroscopy acid 1082
 Gas flue pollutant transformation cloud 821
 Gas hydrogen peroxide prepn 255
 Gas smog chamber wall loss 1176
 Gasification coal tar water partition 919
 Gasification coal tar water partitioning 924
 Geothermal power wastewater arsenic removal 538
 Glass fiber collector dry deposition 721
 Goethite coagulation kinetics phosphate adsorption 632
 Goethite colloid lead voltammetry water 141
 Groundwater analysis statistics review 1026
 Groundwater infiltration benzene deriv 961
 Groundwater influx seepage lake tracer 405
 Groundwater org pollutant transport review 384
 Groundwater pollution nitrate surface water 781
 Groundwater pollution wood preservative Florida 955
 Group contribution UNIFAC partition arom 960
 Halo hydrocarbon photodegrdn water review 480
 Haloorg bioconcn rainbow trout 842
 Haloorg mixt adsorption active carbon 1037
 Hazardous landfill polychlorinated biphenyl emission 986
 Hazardous waste management academic institution 1150
 Headspace analysis trichloroethylene detn water 1122
 Health drinking water pollution review 772
 Heat transfer thermocline lake modeling 180
 Henrys law biphenyl polychlorinated 590
 Heteroatom atm aerosol particle size 707
 Heterocycle reaction nitrate radical kinetics 87
 Hexachlorobenzene benthic nepheloid layer lake 854
 Hexachlorobiphenyl diffusion partitioning aquatic sediment 1169
 Hexafluoropropylene copolymer fluorocarbon release 361
 Hexenedione reaction hydroxyl radical ozone 265

- Human aquatic chlorination mutagen forma-
tion 422
- Human exposure carbon monoxide measure=
ment 911
- Human total exposure pollutant review 880
- Humic acid aquatic chlorination product of
427
- Humic acid carbon monoxide formation
1165
- Humic acid chlorination chlorinated product
512
- Humic acid complexation tetrachlorobiphe=
nyl water 638
- Humic acid toluene soly water 643
- Humic substance polycyclic arom hydrocar=
bon 1072
- Humus formation carcinogen containment
soil 1132
- Humus photosensitizer pollutant natural
water 74
- Hydrocarbon chloro nepheloid layer lake
854
- Hydrocarbon aliph octanol water partition
628
- Hydrocarbon arom metab benthic organism
836
- Hydrocarbon carbon metab plant 432
- Hydrocarbon halo photodegrdn water review
480
- Hydrocarbon peroxyacetyl nitrate formation
potential 950
- Hydrocarbon polyarom air urban source
397
- Hydrocarbon polyarom photolysis atm par=
ticulate 1004
- Hydrocarbon polycyclic arom humic sub=
stance 1072
- Hydrocarbon polycyclic arom luminescence
spectrometry 695
- Hydrocarbon polycyclic arom natural gas
603
- Hydrocarbon polycyclic arom sampling arti=
fact 313
- Hydrocarbon polycyclic arom scavenging
rain 1044
- Hydrogen peroxide water phase system 255
- Hydrogenolysis polychlorinated biphenyl
gas phase 280
- Hydrophobic compd soly octanol partition
522
- Hydrophobic org partition sediment water
90
- Hydroxy arom methylation 507
- Hydroxyl oxidn isoprene mechanism kinetics
151
- Hydroxyl radical reaction arene kinetics
244
- Hydroxyl reaction chlorobiphenyl kinetics
462
- Hydroxyl reaction hexenedione air pollution
265
- Hydroxyl reaction propene org nitrate 849
- Hydroxylation phenol chlorine activated
carbon 441
- Hypodermic needle flow air sampling 1134
- Ideal adsorbed soln theory 1037
- Incinerator emission polychlorinated biphe=
nyl US 942
- Indicator element air pollutant source 121
- Indoor outdoor exposure respirable particu=
late 700
- Iodomethane methylation tin 352
- Ion chromatog peroxyacetyl nitrate detn
749
- Ionic strength methyltin removal soln 1104
- Ionic strength pH partition chlorophenol
193
- IR spectrophotometry sulfur detn plant 437
- Iron hydroxide methyltin removal water
1104
- Iron oxide crstn adsorption silicon 1048
- Iron oxide particle aggregation kinetics 632
- Iron pollution lake sediment transport 356
- Iron water coal gasification tar 924
- Iron water coal tar partition 919
- Irradn toluene nitrogen oxide mutagenicity
249
- Isoprene oxidn hydroxyl mechanism kinetics
151
- Kinetics bromamine disproportionation aq
ammonia polemic 286 287
- Kinetics bromine reaction org estuary 1188
- Kinetics coagulation goethite phosphate
adsorption 632
- Kinetics flocculation hydrolyzed aluminum
modeling 673
- Kinetics hexenedione reaction hydroxyl
ozone 265
- Kinetics hydroxyl reaction chlorobiphenyl
462
- Kinetics isoprene oxidn hydroxyl 151
- Kinetics methyleneperoxy reaction sulfur
dioxide 815
- Kinetics nitrate radical reaction terpene
159
- Kinetics nitrogen dioxide reaction methanol
262
- Kinetics nitrogen oxide reaction pyrene
1089
- Kinetics ozonation cyanide aq soln 804
- Kinetics ozone decompn water 1206
- Kinetics tetrachlorobiphenyl complexation
humic acid 638
- Krypton 85 Nevada test site 1128
- Lake acid lead cycle aluminum 1182
- Lake acid rain Appalachians US 552
- Lake Adirondack chem characterization
1018
- Lake arsenic cycling New Zealand 231
- Lake calcium chem New York 716
- Lake dissolved oxygen model Ontario 173
- Lake nepheloid layer chloro hydrocarbon
854
- Lake sediment copper pollution transport
356
- Lake sediment water org partitioning 789
- Lake seepage groundwater influx tracer 405
- Lake thermocline oxygen heat transfer 180
- Landfill emission polychlorinated biphenyl
US 942
- Landfill hazardous polychlorinated biphenyl
emission 986
- Lead air pollution urban US 328
- Lead cycle aluminum acid lake 1182
- Lead dissolved particulate detn water 141
- Lead halide aerosol Phoenix Arizona 682
- Lead methylation oxidative methyl transfer
726
- Lichen sulfur detn 437
- Lime sorbent sulfur dioxide 1065
- Lipid water org partition bioconcn 57
- Liq solid partitioning sorbent concn 789
- Luminescence spectrometry polycyclic arom
hydrocarbon 695
- Macrophage alveolar exhaust particulate
effect 43
- Magnesium hydroxide dissoln chrysotile
water 1213
- Magnesium pollution lake sediment trans=
port 356
- Magnesium tracer groundwater influx lake
405
- Manganese air pollution urban US 328
- Manganese dioxide lead voltammetry water
141
- Manganese dioxide tin methylation 352
- Manganese pollution lake sediment transport
356
- Mass spectroscopy gas chromatog acid 1082
- Mass transfer volatile org stripping 164
- Mechanism chlorination organonitrogen
compd chloroamine 810
- Mechanism cyclohexene reaction ozone 935
- Mechanism dibromamine formation polemic
286
- Mechanism ozone decompn water 1206
- Membrane flow cell chlorine dioxide detn
450
- Mercaptan formation groundwater pollution
haloalkane 322
- Mercury film electrode anodic stripping
voltammetry 137
- Mercury oil shale retorting 316
- Metal air pollution urban US 328
- Metal complexation fulvic acid aggregation
132
- Metal water coal tar partition 919
- Methacrolein formation isoprene oxidn hy=
droxyl 151
- Methanol nitrogen dioxide reaction kinetics
262
- Methyl nitrate formation nitrogen dioxide
methanol 262
- Methylation arom hydroxy aldehyde 507
- Methylation divalent tin aquatic environ=
ment 352
- Methylation lead tin aquatic environment
726
- Methylcobalt complex methylation tin 352
- Methyleneperoxy reaction sulfur dioxide
kinetics 815
- Methylfuran formation isoprene oxidn hy=
droxyl 151
- Methylphosphonate decompn ac discharge
946
- Methyltin compd behavior estuarine condi=
tion 1104
- Microbial chem transformation chlorolignin
1219
- Microbial degrdn pulp bleaching wastewater
1086
- Micropteris aluminum 828
- Mining copper lake sediment pollution 356
- Model air pollutant std exceedance 225
- Model dissolved oxygen Lake Ontario 173
- Model filter water wastewater performance
497
- Model quan freshwater acidification 1144
- Model volatile org air stripping 164
- Modeling anion adsorption goethite 544
- Modeling biodegrdn chlorophenol 374
- Modeling kinetics flocculation hydrolyzed
aluminum 673
- Modeling multimedia pollutant transport
environment 412
- Modeling personal exposure respirable par=
ticulate 700
- Modeling solute partitioning sorbent concn
789
- Morphol compn coal fly ash 274
- Mortality air pollution effect review 764
- Mortality environmental pollution assess=
ment uncertainty 662
- Motor exhaust analysis org acid 1082
- Multicomponent adsorption equl calcn
theory 1037
- Mutagen coal gasification tar safety 924
- Mutagen exhaust gas particulate 43
- Mutagen formation aquatic human chlorina=
tion 422
- Mutagen formation chlorolignin chlorination
427
- Mutagen formation propylene photoxidn
620
- Mutagen removal water activated carbon
333
- Mutagen wood smoke transformation 63
- Mutagenicity chromatogram diesel exhaust
particulate 270
- Mutagenicity propylene ozone reactant
1094
- Mutagenicity toluene nitrogen oxide irradi=
tion 249
- Naphthalene groundwater pollution wood
preservative 955
- Naphthalene reaction hydroxyl radical kinet=
ics 244
- Natural gas condensate residue compn 603
- Natural water pollutant humus photosensi=
tizer 74
- Nepheloid layer lake chloro hydrocarbon
854
- Nickel air pollution urban US 328
- Nickel water coal tar partition 919
- Nitrate ammonium sodium atm aerosol 258
- Nitrate dry deposition forest canopy 238
- Nitrate radical reaction kinetics heterocycle
87
- Nitrate radical reaction kinetics terpene
159
- Nitrate radical reaction propene 849
- Nitrate water pollution southern California
781
- Nitric oxide electroredn flue gas 371
- Nitric oxide reaction polyarom hydrocarbon
313
- Nitrification water pollution nitrate 781
- Nitro polycyclic arom hydrocarbon formation
1115
- Nitrocresol reaction nitrogen oxide ozone
968
- Nitrogen dioxide methanol reaction kinetics
262
- Nitrogen dioxide mutagen transformation
smoke 63
- Nitrogen dioxide propylene ozone mutagen=
icity 1094
- Nitrogen dioxide reaction adsorbed pyrene
1089
- Nitrogen dioxide reaction polonium 218 146
- Nitrogen dioxide reaction polyarom hydro=
carbon 313
- Nitrogen formation chlorolignin chlorination
427
- Nitrogen org interference bacteriostasis
chloramine 1192
- Nitrogen oxide detn air chemiluminescence
862
- Nitrogen oxide reaction cresol nitrocresol
968
- Nitrogen oxide toluene irradi mutagenicity
249
- Normal data set small estn 1201
- Nuclear explosion krypton 85 pollution
1128
- Nylon filter collector dry deposition 721
- Occupational exposure airborne polyarom
monitor 997
- Octanol partition aq chlorophenol 193
- Octanol water partition aliph hydrocarbon
628
- Octanol water partition soly relation 522
- Oil engine analysis org acid 1082
- Oil shale retorting mercury 316
- Oil shale spent cooling wastewater emission
992
- Oil spill seawater dispersant evaluation 454

- Oligochaete tubificid pollutant transport sediment 51
 Org acid detn atm exhaust 1082
 Org adsorbed sediment reaction chlorine 340
 Org adsorption chrysotile water 1213
 Org atm aerosol particle size 707
 Org colloidal plutonium adsorption sediment 127
 Org compd soly water calcn 369
 Org compd sorption soil solvent 975
 Org constituent coal fly ash 186
 Org emission shale oil wastewater 992
 Org hydrophobic partition sediment water 90
 Org identification coal gasification wastewater 929
 Org interference nitrogen oxide ozone detn 862
 Org matter estuary reaction bromine 1188
 Org matter soil carbon monoxide formation 1165
 Org nitrate propene hydroxyl nitrate 849
 Org partition lipid water bioconcn 57
 Org partitioning lake sediment water 789
 Org pollutant transport aquifer review 384
 Org ratio fish sediment polemic 198 199
 Org reaction nitrate radical kinetics 159
 Org volatile air stripping model 164
 Organ bass aluminum 828
 Organism benthic arom hydrocarbon metab 836
 Organohalide water pollution bioconcn trout 842
 Organonitrogen compd chlorination chloroa= mine mechanism 810
 Organonitrogen interference bactericidal activity chloramine 1192
 Oxidn phenol chlorine activated carbon 441
 Oxygen dissolved model Lake Ontario 173
 Oxygen reaction polonium 218 ion 146
 Oxygen transport thermocline lake modeling 180
 Ozonation kinetics cyanide aq soln 904
 Ozone aq decompn by promoter inhibitor 1206
 Ozone detn air UV 862
 Ozone mutagen transformation wood smoke 63
 Ozone propylene reactant mutagenicity 1094
 Ozone reaction cresol nitroresol 968
 Ozone reaction cyclohexene product mecha= nism 935
 Ozone reaction hexenedione air pollution 265
 Ozone terpene nighttime troposphere trans= port 364
 Particle airborne size distribution detn 121
 Particle nonsettling water org partition 90
 Particle size atm aerosol org 707
 Particle size fly ash compn 796
 Particle size fly ash property 82
 Particle size monitor optical 458
 Particulate airborne polyarom hydrocarbon photolysis 1004
 Particulate diesel exhaust mutagenicity chromatogram 270
 Particulate dissolved lead detn water 141
 Particulate exhaust gas compn toxicity 43
 Particulate respirable personal exposure epidemiol 700
 Partition arom UNIFAC group contribution 980
 Partition chlorophenol pH ionic strength 193
 Partition coal gasification tar water 919
 Partition hydrophobic org sediment water 90
 Partition octanol water soly relation 522
 Partitioning diffusion hexachlorobiphenyl aquatic sediment 1169
 Partitioning liq solid sorbent concn 789
 Partitioning water coal gasification tar 924
 PCB benthic nepheloid layer lake 854
 PCB complexation humic acid water 638
 PCB emission landfill incinerator US 942
 PCB Hudson River US review 656
 PCB identification cyclodextrin fluorometry 155
 PCB vapor pressure method 500
 Pentachlorophenol waste groundwater pollu= tion Florida 955
 Pentadiene photoisomerization water humus sensitizer 74
 Perfluorodimethylcyclobutane tracer air infiltration building 1225
 Peroxide hydrogen water phase system 255
 Peroxyacetyl nitrate detn method 749
 Peroxyacetyl nitrate formation potential hydrocarbon 950
 Petroleum product sediment estuary Virginia 597
 Petroleum weathering toxicity seawater Arctic 1076
 pH ionic strength partition chlorophenol 193
 Phenanthrene reaction hydroxyl radical kinetics 244
 Phenol adsorption active carbon 690
 Phenol air rain scavenging mechanism 1053
 Phenol carbon monoxide formation 1165
 Phenol chloro partition ionic strength 193
 Phenol groundwater pollution wood preser= vative 955
 Phenol reaction chlorine activated carbon 441
 Phosphate adsorption coagulation kinetics goethite 632
 Phosphate adsorption goethite modeling 544
 Phosphonate decompn ac discharge 946
 Phosphorus zinc Selenastrum growth 417
 Photochem reaction cresol nitroresol 968
 Photochem reaction propene nitrogen oxide 849
 Photodegrdn halo hydrocarbon water review 480
 Photolysis kinetics pyruvic acid biacetyl 968
 Photolysis polyarom hydrocarbon atm par= ticulate 1004
 Photosensitizer pollutant natural water humus 74
 Photosynthesis ethylene plant carbon metab 432
 Photoxidn propylene mutagen formation 620
 Pipeline natural gas residue compn 603
 Plant sulfur detn 437
 Plutonium adsorption sediment org colloidal 127
 Polarg lead dissolved particulate detn 141
 Pollutant air exceedance prediction polemic 866 867
 Pollutant air source indicator element 121
 Pollutant air std exceedance model 225
 Pollutant natural water humus photosens= itizer 74
 Pollutant org transport aquifer review 384
 Pollutant partitioning sediment water model= ing 789
 Pollutant sampling air aq scrubber 557
 Pollutant total human exposure review 880
 Pollutant transport environment multimedia modeling 412
 Pollutant transport sediment tubificid oligo= chaete 51
 Pollutant water toxicity screening polemic 871
 Pollution 1076
 Pollution air effect mortality review 764
 Pollution air hydrocarbon mutagen formation 620
 Pollution air nitro polyarom hydrocarbon 1115
 Pollution air sampling fluoropolymer 361
 Pollution aquatic tin methylation 352
 Pollution arsenic cycling lake 231
 Pollution chlorolignin transformation 1219
 Pollution drinking water health review 772
 Pollution environmental toxicol coal tar 924
 Pollution flue gas fluorine ammonia 1099
 Pollution fog California coast 730
 Pollution groundwater wood preservative Florida 955
 Pollution lake acid rain US 552
 Pollution lake sediment copper transport 356
 Pollution lead aerosol Phoenix Arizona 682
 Pollution migration coal ash disposal 615
 Pollution PCB Hudson River US review 656
 Pollution wall loss smog chamber 1059
 Pollution water chlorinated polyarom Japan 585
 Pollution water chlorolignin transformation 1219
 Pollution water coal gasification 919
 Pollution water fish carcinogen polemic 645 646
 Pollution water fluoromethylated chlorinated biphenyl 736
 Pollution water haloorg trout bioconcn 842
 Pollution water hydrophobic org partition 90
 Pollution water nitrate southern California 781
 Pollution with chlorolignin water purifn 427
 Polonium 218 ion reaction air 146
 Polyarom airborne occupational exposure monitor 997
 Polyarom atm aerosol particle size 707
 Polyarom chlorinated tap water Japan 585
 Polyarom hydrocarbon air urban source 397
 Polyarom hydrocarbon photolysis atm par= ticulate 1004
 Polyarom sampling detn air exhaust 695
 Polychlorinated biphenyl emission hazardous landfill 986
 Polychlorinated biphenyl gas phase hydro= genolysis 280
 Polychlorinated biphenyl Henrys law 590
 Polychlorinated biphenyl removal transform= er oil 740
 Polycyclic arom exhaust gas particulate 43
 Polycyclic arom hydrocarbon dinitrogen pentoxide 1115
 Polycyclic arom hydrocarbon humic sub= stance 1072
 Polycyclic arom hydrocarbon luminescence spectrometry 695
 Polycyclic arom hydrocarbon natural gas 603
 Polycyclic arom hydrocarbon sampling arti= fact 313
 Polycyclic arom hydrocarbon scavenging rain 1044
 Polycyclic arom photolysis airborne particle 1004
 Polyethylene collector dry deposition atm 721
 Polyoxyethylene potassium hydroxide chlo= robiphenyl decompn 740
 Porosity coal fly ash 82
 Potassium dry deposition forest canopy 238
 Potassium hydroxide polyoxyethylene chlo= robiphenyl decompn 740
 Power plant coal air pollution 1099
 Power plant coal ash compn 615
 Pressure vapor PCB method 500
 Product polyarom coal sediment Virginia 597
 Propene hydroxyl nitrate org nitrate 849
 Propylene ozone reactant mutagenicity 1094
 Propylene photoxidn mutagen formation 620
 Public health risk pollution assessment 662
 Pulp bleaching chlorination pollution chlori= nation 427
 Pulp bleaching wastewater microbial degrdn 1086
 Pulping wastewater chlorolignin chem 1219
 Pulverulentum sporotrichum degrdn chlo= lignn wastewater 1086
 Pyrene adsorbed reaction nitrogen dioxide 1089
 Pyridine coal gasification tar 924
 Pyruvic acid photolysis kinetics 968
 Pyrrole reaction nitrate radical kinetics 87
 Quartz fiber collector dry deposition 721
 Radical hydroxyl reaction arene kinetics 244
 Rain acid lake Appalachians US 552
 Rain acid research polemic 646
 Rain polycyclic arom hydrocarbon scavenging 1044
 Rainbow trout bioconcn haloorg 842
 Rainwater pollution phenol scavenging mechanism 1053
 Rayleigh scattering fulvic acid aggregation 132
 Reaction nitrate radical kinetics heterocycle 87
 Redistribution mercury shale retorting 316
 Redn electrochem nitric oxide 371
 Regression method ecotoxicol analysis 747
 Residence perfluorodimethylcyclobutane tracer air infiltration 1225
 Respirable particulate personal exposure epidemiol 700
 Retorting oil shale mercury 316
 Review acid deposition drinking water 772
 Review air pollution effect mortality 764
 Review cancer risk regulation std 473
 Review org pollutant transport aquifer 384
 Review PCB Hudson River US 656
 Review photocatalysis halo hydrocarbon degrdn 480
 Review pollutant total human exposure 880
 Review sorbent fluidized bed combustion 894
 Review statistics groundwater soil analysis 1026
 Risk assessment uncertainty environmental pollution 662
 River infiltration groundwater benzene deriv 961
 River pollution PCB Hudson River review 656
 Safety air pollution std model 225
 Safety arom natural gas pipeline 603
 Safety coal gasification metal water 919
 Safety coal gasification tar mutagen 924
 Sampler aerosol air analysis 1110

- Sampling air hypodermic needle flow 1134
 Sampling air pollution fluoropolymer 361
 Sampling groundwater soil statistics review 1026
 Sampling polyarom hydrocarbon air exhaust 695
 Sampling trace gas air scrubber 557
 Scrubber sampling trace gas air 557
 Seawater oil spill dispersant evaluation 454
 Seawater petroleum weathering toxicity Arctic 1076
 Sediment adsorbed org reaction chlorine 340
 Sediment adsorption plutonium org colloidal 127
 Sediment aquatic hexachlorobiphenyl diffusion partitioning 1169
 Sediment estuary arom hydrocarbon metabolite 836
 Sediment fish org ratio polemic 198 199
 Sediment lake copper pollution transport 356
 Sediment lake water org partitioning 789
 Sediment PCB Hudson River US review 656
 Sediment pollutant transport tubificid oligochaete 51
 Sediment polyarom coal product Virginia 597
 Sediment water hydrophobic org partition 90
 Sediments water arsenic cycling lake 231
 Seepage lake groundwater influx tracer 405
 Selenastrum growth phosphorus zinc 417
 Selenite adsorption goethite modeling 544
 Sewage pollution environment tocopheryl acetate 282
 Shale oil retorting mercury 316
 Shale oil wastewater org emission 992
 Shale spent cooling wastewater emission 992
 Silica adsorbed pyrene reaction nitrogen dioxide 1089
 Silica colloidal lead voltammetry water 141
 Silicon effect ferrihydrate crystal adsorption 1048
 Size exclusion chromatography chlorinated humus 422
 Size fly ash fractionation method 686
 Small normal data set estimate 1201
 Smelter dust ferrochrome chromium specification 345
 Smog chamber pollution wall loss 1059
 Smog chamber Teflon wall loss 1176
 Smoke wood mutagen transformation 63
 Smoking respirable particulate personal exposure 740
 Sodium ammonium nitrate atmosphere aerosol 258
 Soil analysis statistics review 1026
 Soil carcinogen containment humus formation 1132
 Soil neutralization acid input lake 552
 Soil pollutant transport multimedia modeling 412
 Soil trichloroethylene anaerobic biodegradation 277
 Soil vapor sorption org compound 1196
 Solid liquid partitioning sorbent concentration 789
 Solvent org compound sorption soil 975
 Soly org compound water calcium 369
 Soly relation octanol water partition 522
 Sorbent fluidized bed review 894
 Sorbent lime sulfur dioxide 1065
 Sorption org compound soil solvent 975
 Sorption org nonsettling particle water 90
 Sorptive partitioning toluene detrital water 1122
 Speciation chromium ferrochrome smelter dust 345
 Spectrophotometry IR sulfur detrital plant 437
 Sporotrichum pulverulentum degradation chlorolignin wastewater 1086
 Statistical evaluation aquatic toxicity 35
 Statistics groundwater soil analysis review 1026
 Statistics normal data analysis estimate 1201
 Std air pollutant exceedance model 225
 Std air pollution exceedance polemic 866 867
 Std cancer risk regulation review 473
 Steric field flow fractionation continuous 686
 Sulfate adsorption goethite modeling 544
 Sulfate aerosol pollution mortality assessment 662
 Sulfate alkylthoxylated detrital water wastewater 1232
 Sulfate artifact formation filter alkyl 831
 Sulfate deposition redox climatological variability 887
 Sulfate dry deposition forest canopy 238
 Sulfate particulate compound Virginia 529
 Sulfation lime coal firing 1065
 Sulfur coal fly ash compound 274
 Sulfur detrital lichen plant pollution 437
 Sulfur dioxide control climatological variability 887
 Sulfur dioxide reaction methyleneperoxy kinetics 815
 Sulfur dioxide reaction polyarom hydrocarbon 313
 Sulfur dioxide sorbent combustion review 894
 Sulfur dioxide sorbent lime 1065
 Sulfur trioxide reaction polyarom hydrocarbon 313
 Sulfuric acid aerosol detection UV 815
 Surface area coal fly ash 82
 Surface charge reversal chrysotile water 1213
 Surface enrichment element fly ash 609
 Surface structure coal fly ash 82
 Surfactant presence cadmium detrital water 137
 Tar coal gasification water partition 919
 Tar coal gasification water partitioning 924
 Teflon collector dry deposition atmosphere 721
 Teflon smog chamber wall loss 1176
 Terpene nighttime troposphere transport ozone 364
 Terpene reaction kinetics nitrate radical 159
 Tetrachlorobiphenyl complexation humic acid water 638
 Tetrafluoroethylene copolymer fluorocarbon release 361
 Thiophene reaction nitrate radical kinetics 87
 Tin divalent methylation aquatic environment 352
 Tin methylation oxidative methyl transfer 726
 Tocopheryl acetate indicator sewage environment 282
 Toluene detrital water sorptive partitioning 1122
 Toluene humic acid soly water 643
 Toluene nitrogen oxide irradiation mutagenicity 249
 Toxicity oil spill seawater evaluation 454
 Toxicity screening water pollutant polemic 871
 Toxicity weathering petroleum seawater Arctic 1076
 Toxicol coal tar environmental pollution 924
 Trace analysis data estimate 1201
 Trace element airborne remote US 27
 Trace element fine particulate Virginia 529
 Trace gas sampling air scrubber 557
 Tracer air infiltration building perfluorodimethylcyclobutane 1225
 Tracer groundwater influx seepage lake 405
 Transformer oil polychlorinated biphenyl removal 740
 Transport copper pollution lake sediment 356
 Transport model regional sulfate particulate 529
 Transport org pollutant aquifer review 384
 Transport pollutant environment multimedia modeling 412
 Transport pollutant sediment tubificid oligochaete 51
 Transport terpene nighttime troposphere ozone 364
 Transport wood preservative groundwater pollution 955
 Trichlorobenzene vapor sorption soil Woodburn 1196
 Trichloroethylene anaerobic biodegradation soil 277
 Trichloroethylene detrital water headspace analysis 1122
 Trichloroethylene transport environment multimedia modeling 412
 Trihalomethane formation aquatic sediment chlorine 340
 Triolein water partition org compound 57
 Troposphere nighttime terpene transport ozone 364
 Tubificid oligochaete pollutant transport sediment 51
 Ultrafiltration chlorinated humus 422
 Underground shale retorting mercury 316
 UNIFAC group contribution partition arom 980
 Urban metal air pollution US 328
 Urban population exposure carbon monoxide 911
 Vapor pressure PCB method 500
 Vapor sorption org compound soil 1196
 Venturi scrubber fly ash org 186
 Vinyl methyl ketone formation isoprene 151
 Volatile org air stripping model 164
 Voltammery anodic stripping cadmium water 137
 Voltammery lead dissolved particulate detrital 141
 Waste gas acid emission polemic 646
 Waste gas acidic emission polemic 646
 Waste hazardous management academic institution 1150
 Waste mercury oil shale retorting 316
 Wastewater chlorine dioxide detrital chemiluminescence 450
 Wastewater chlorolignin degradation sporotrichum pulverulentum 1086
 Wastewater coal gasification org identification 929
 Wastewater filter water performance model 497
 Wastewater treatment organonitrogen chlorination chloramine 810
 Water chlorination humic acid product 512
 Water collector dry deposition atmosphere 721
 Water disinfection chloramine interference organonitrogen 1192
 Water flocculation aluminum ion kinetics 673
 Water pollutant toxicity screening polemic 871
 Water pollutant transport multimedia modeling 412
 Water pollution fish carcinogen polemic 645 646
 Water pollution fluoromethylated chlorinated biphenyl 736
 Water pollution haloorg trout bioconcentration 842
 Water pollution nitrate southern California 781
 Water purify organonitrogen chlorination chloramine 810
 Water purify photochem haloorg review 480
 Water soly org compound calcium 369
 Water tetrachlorobiphenyl complexation humic acid 638
 Water toluene humic acid soly 643
 Weathering toxicity petroleum seawater Arctic 1076
 Wildfire water pollution nitrate 781
 Wood preservative groundwater pollution Florida 955
 Wood smoke mutagen transformation 63
 X ray analysis lead aerosol 682
 XPS coal fly ash depth 609
 Zinc air pollution urban US 328
 Zinc phosphorus Selenastrum growth 417

Front Section Subject Index

Critical Reviews

Organic contaminants in groundwater, 384
Photochemistry of petroleum in water, 569
Regulating cancer risks, 473

Features

Acid deposition and drinking water, 772
Acid deposition control, 112
Air pollution worldwide, 298
Biodegradation of organic chemicals, 106
Chemical characteristics of Adirondack lakes, 1018
Climatological variability and acid deposition, 887
Coal liquefaction products, 14
Deactivation of hazardous chemical wastes, 215
Hazardous chemical wastes in academia, 1150
Indoor air quality, 305
Monitoring statistics, 1026
Mortality and air pollution, 764
PCBs in the Hudson River, 656
Photocatalytic degradation of water contaminants, 480
Proficiency testing of environmental laboratories, 8
Sorbents for fluidized-bed combustion, 894
Timescales of catchment acidification, 1144
Total human exposure, an emerging science, 880
Uncertainties in risk assessment, 662
Water reuse, 208

Regulatory Focus

Air toxics legislation proposed, 580
CEQ's report on long-term environmental research, 393
Chemicals advisory program, 117
EPA drinking-water proposals: Round one, 1156
EPA's groundwater research, 1031
EPA's regulatory agenda, 669
Groundwater monitoring, 485
Legislative outlook for environmental amendments, 221
RCRA reauthorization, 19
Reagan's EPA budget request, 310

Regulatory reform revisited, 903
Waste management regulations, 777

Views

Acid deposition lectures, 904, 1032, 1157
Bhopal, blind technology transfer, 581
Miami ACS meeting report, 488
Ocean incineration of hazardous wastes, 486

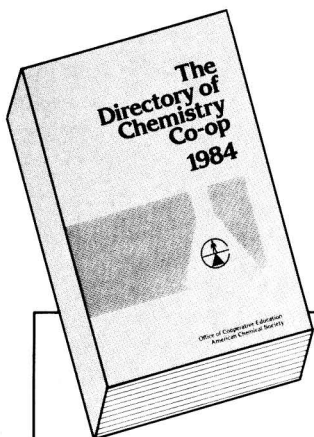
Editorials

A farewell—not a goodbye, guest, 203
Acid deposition in the western U.S., guest, 755
Acid deposition series, 875
Clean shirts and clean water, guest, 1013
Conservation and industry, guest, 380
Drinking water research, is it necessary?, guest, 651
Ethics in scientific publishing, 1139
New features in *ES&T*, 563
Phosphate here, phosphate there, 467
Resolving environmental conflicts, guest, 291
The road not taken, guest, 3
Uncertainty and environmental risk assessment, guest, 99

Letters

Acid rain research, 4
Advertising, 292
Biodegradation of organic chemicals, 379
Cancer risk, 756
Cost-benefit analysis, 1011
Editorial opinion, 4
Environmental achievement prize, 204
Fellowship program, 379
January editorial, 204
Laboratory testing, 204
Ocean incineration, 756
Pesticide residues in humans, 379
Zimmerman award, 4

RECRUITERS ... EDUCATORS ... CHEMISTS ...



SAVE 25%!

This informative, 280-page paperbound volume is available for just \$15.00 a copy (After April 1, 1985, the price will be \$20.00) Order now to take advantage of these special introductory savings.

PHONE TOLL FREE!

Call 1-800-424-6747 (credit card orders only) to order your copy at this special price or mail coupon today!

NOW AVAILABLE FROM ACS

THE DIRECTORY OF CHEMISTRY CO-OP

The indispensable guide to cooperative education programs in the U.S. and Canada.

If you are interested in co-op programs as participant, sponsor, or advisor, take advantage of this unique, authoritative reference! Get practical, accurate information on 265 chemistry, chemical engineering, and chemistry-related cooperative education programs in the U.S. and Canada.

In-depth coverage includes contact names and addresses, program size, typical work schedules, academic requirements, geographical and program indices, and a great deal more.

As a reference, this timely resource is essential for:

- Schools interested in starting co-op
- Employers seeking sources of co-op students
- High school students and advisors wishing to locate co-op schools
- Co-op professionals requiring a convenient source of information

Please send _____ copies of the ACS *Directory of Chemistry Co-op* @ \$15.00 per copy to:

Name _____

Address _____

Check the method of payment: Check or money order enclosed Credit card: Visa MasterCard Barclay Access American Express

Cardholder Name _____

Card No. _____

Exp. Date _____ Interbank No. _____

(MasterCard and Access only)

Signature _____

Amount Enclosed \$ _____
Make checks payable to **ACS Co-op Directory**.
Orders must be prepaid. California residents,
add 6% sales tax.

Return to: **Office of Cooperative Education**
American Chemical Society
1155 Sixteenth St., N.W.
Washington, DC 20036

What Do These Nobel Laureates Have in Common?



They have all published articles
in the journals of the American Chemical Society.

- Analytical Chemistry
- Chemical & Engineering News
- CHEMTECH
- Environmental Science & Technology
- Accounts of Chemical Research
- Biochemistry
- Chemical Reviews
- Industrial & Engineering Chemistry—Process Design and Development
- Industrial & Engineering Chemistry—Product R&D
- Industrial & Engineering Chemistry—Fundamentals
- Inorganic Chemistry
- Journal of Agricultural & Food Chemistry
- Journal of the American Chemical Society
- Journal of Chemical & Engineering Data
- Journal of Chemical Information and Computer Sciences
- Macromolecules
- Journal of Medicinal Chemistry
- The Journal of Organic Chemistry
- The Journal of Physical Chemistry
- ACS Single Article Announcement
- Journal of Physical and Chemical Reference Data
- Organometallics
- Langmuir

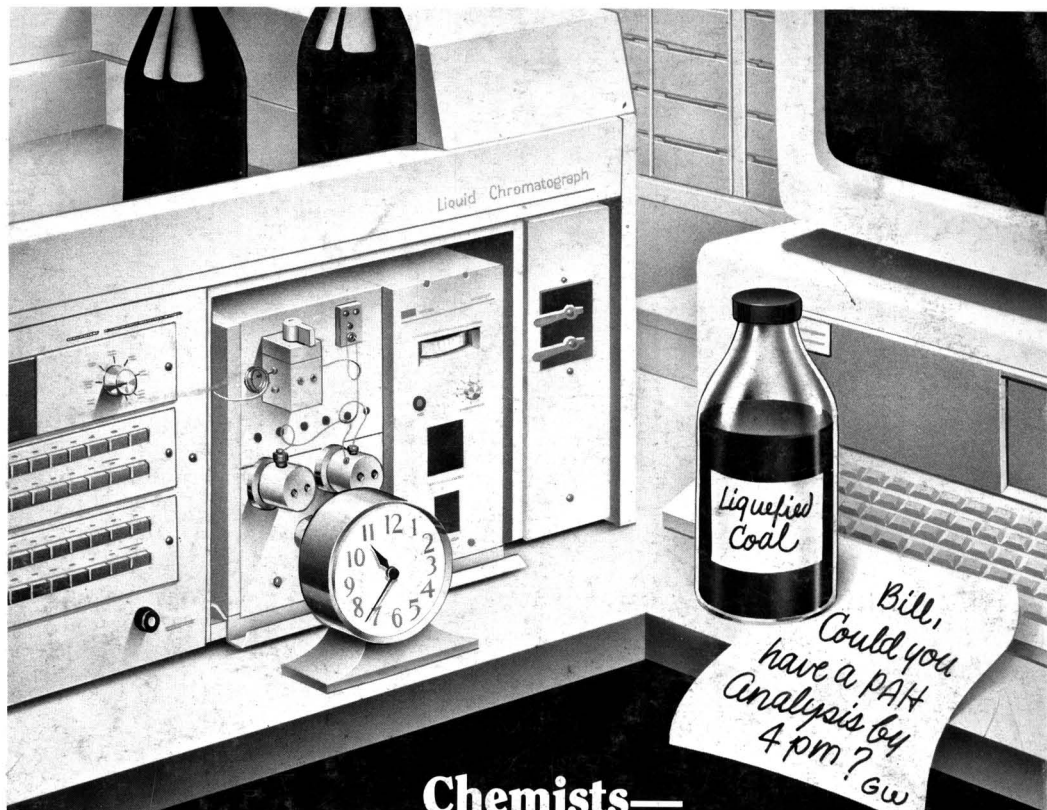
American Chemical Society—
chemical publishers since 1879.



Send orders or inquiries to:
1155 Sixteenth Street, N.W.
Washington, D.C. 20036 U.S.A.

Cable Address: JIECHEM
Telex: 440159 ACSPIJ or
892582 ACS PUBS

U.S.A. Call toll free: 800-424-6747



**Chemists—
How can you quickly find
an analytical procedure
to solve this problem?**

Search ACS JOURNALS ONLINE.

ACS JOURNALS ONLINE is a high-efficiency chemical information search system that can save you hours of searching through chemical journals for an analytical procedure.

You can use it right in your laboratory. Just turn on your computer or terminal.

In minutes you'll be reading about the analytical procedure you need.

In this case, it's a high-performance liquid chromatography procedure for determining polycyclic aromatic hydrocarbons in liquid coal.

And with the touch of a key, you can even zero in on specific paragraphs that contain the data you need.

Find out how you can make this high-efficiency chemical information search system work for you. Call an American Chemical Society sales representative today at 800-424-6747. The call is free.

Or write, Sales Office, American Chemical Society, 1155 Sixteenth Street, N.W., Washington, D.C. 20036.

ACS JOURNALS ONLINE contains: Accounts of Chemical Research, Analytical Chemistry, Biochemistry, Chemical Reviews, Environmental Science & Technology, Industrial & Engineering Chemistry—Fundamentals—Process Design & Development—Product Research & Development, Inorganic Chemistry, Journal of Agricultural and Food Chemistry, Journal of Chemical and Engineering Data, Journal of the American Chemical Society, Journal of Chemical Information and Computer Sciences, Journal of Medicinal Chemistry, The Journal of Organic Chemistry, The Journal of Physical Chemistry, Langmuir, Macromolecules, and Organometallics.

The Computer-Powered
Full-Text Search System
From The American
Chemical Society

ACS JOURNALS
ONLINE



1155 Sixteenth Street, N.W., Washington, D.C. 20036

